UCL SCHOOL OF PHARMACY

BRUNSWICK SQUARE

NOVEL POTENTIAL PEPTIDE THERAPEUTICS FOR TUBERCULOSIS THERAPY

Francesca Scotti

PhD candidate

2017

Supervisors:

Dr John P. Malkinson, UCL School of Pharmacy

Dr Sanjib Bhakta, Birkbeck College, University of London

STATEMENT

I declare that all the work here presented has been conducted by myself, unless where I have acknowledged another person or given a published reference.

Date:

Signed:

Francesca Scotti, PhD Candidate

Department of Pharmaceutical and Biological Chemistry

UCL School of Pharmacy

29-39 Brunswick Square

WC1N 1AX London

And

Department of Biological Sciences

Institute of Structural and Molecular Biology

Birkbeck College, University of London

Malet Street

WC1E 7HX London

Signatures:

Supervisor 1

Supervisor 2

ABSTRACT

Despite the existence of vaccinations, diagnostic tools and treatments, tuberculosis (TB) prevalence is increasing because of the circulation of people and misuse of antibiotics, giving rise to growing numbers of drug resistant strains of *Mycobacterium tuberculosis*. There is therefore a pressing need to look for new strategies against TB, in the hope of finding new drugs with novel mechanisms of anti-tubercular action or ways to potentiate the activity of already existing drugs and reduce treatment duration.

This thesis explores the employment of peptides in anti-tuberculosis therapy. The project was initiated by the identification of a novel therapeutic target in *M. tuberculosis*: murein peptide ligase (Mpl, Rv3712), an enzyme involved in the bacterial peptidoglycan recycling process. The aim is to synthesise its putative natural substrates (peptidoglycan peptide fragments) to characterise its activity and synthesise sequence analogues. These analogues were tested on the whole-cell and will be evaluated for inhibitory activity on the recombinant Mpl enzyme and eventually could be used in combination with existing or new drugs to see whether they increase anti-tubercular potency and thus combat resistance. Attainment of the putative substrate required the synthesis of *m*DAP, an unusual amino acid unique to peptidoglycan. Its synthesis was successfully completed and it was incorporated in the tripeptide Mpl putative substrate.

Solid-phase synthesis has been used successfully and proved effective for rapid synthesis of multiple short peptide analogues in parallel. In addition it was used to synthesise anti-tuberculosis lasso peptides, lariatins A and B, lassomycin and analogues, to evaluate the structural requirements for biological activity.

The method for the heterologous expression and purification of recombinant Mpl from *M. tuberculosis* has been confirmed as successful, and the enzyme is available for future target-based evaluation using the synthesised *m*DAP-containing tripeptide and eventually for other *m*DAP-containing PG fragments and analogues.

TABLE OF CONTENTS

LIST OF SCHEMES

LIST OF FIGURES

LIST OF TABLES

LIST OF ABBREVIATIONS

AG	Arabinogalactan
All	Allyl
AMPs	Antimicrobial peptides
APS	Ammonium persulphate
atm	Atmosphere
AUC	Area Under the Curve
BCG	Bacillus Calmette-Guerin
Bn	Benzyl
Boc	*t*-Butyloxycarbonyl
BSA	Bovine Serum Albumine
BuLi	*n*-Butyllithium
Bzl	Benzyl
CBB	Coomassie Brilliant Blue
Cbz	Carboxybenzyl
CHMP	Committee for Medicinal Products for Human Use
CLPs	Cyclic lipodepsipeptides
CTC	2-Chlorotrityl chloride resin
CV	Column Volume
DAP	Diaminopimelic acid
DCC	*N,N'*-Dicyclohexylcarbodiimide
ddH_2O	Double distilled water
Dha	2,3-Didehydroalanine
Dhb	(*Z*)-2,3-Didehydrobutyrine

DIC	*N,N'*-Diisopropylcarbodiimide
DIEA	*N,N*-Diisopropylethylamine
DKP	Diketopiperazine
Dmab	4-(*N*-[1-(4,4-Dimethyl-2,6-dioxocyclohexylidene)-3-methylbutyl]amino)benzyl
DMAP	4-Dimethylaminopyridine
DMF	Dimethylformamide
DOT	Directly Observed Therapy
DST	Drug Susceptibility Test
EDC	1-Ethyl-3-(3-dimethylaminopropyl)carbodiimide
EMA	European Medicines Agency
Et_3N	Triethylamine
EtOAc	Ethyl acetate
EtOH	Ethanol
FAS I	Fatty acid synthetase I
FDA	Food and Drug Administration
FDAA	1-Fluoro-2,4-nitrophenyl-5-L-alaninamide
Fmoc	9-Fluorenylmethoxycarbonyl
Glc*N*Ac	*N*-Acetylglucosamine
HATU	*O*-(7-azabenzotriazol-1-yl)-1,1,3,3-tetramethyluronium hexafluorophosphate
HBTU	*O*-(benzotriazol-1-yl)-1,1,3,3-tetramethyluronium hexafluorophosphate
HMW	High molecular weight
HOAt	1-Hydroxy-7-azabenzotriazole
HOBt	1-Hydroxybenzotriazole

HPLC	High Performance Liquid Chromatography
IDSA	Infectious Diseases Society of America
iE-DAP	D-Glu(*m*DAP-OH)-OH dipeptide
INH	Isoniazid
IPTG	Isopropylthio-β-D-galactoside
LB	Luria-Bertani
LC-MS	Liquid Chromatography – Mass Spectrometry
MAGP	Mycolil-Arabinogalactan Peptidoglycan Complex
***m*DAP**	*meso*-Diaminopimelic acid
MDR	Multi-Drug Resistant
MeCN	Acetonitrile
MeOH	Methanol
MIC	Minimum Inhibitory Concentration
min	Minutes
mpl	Murein peptide ligase
MRSA	Multi-drug resistant *S. aureus*
MS	Mass Spectrometry
Mtb	*Mycobacterium tuberculosis*
Mur*N*Ac	*N*-Acetylmuramic acid
NaHMDS	Sodium bis(trimethylsilyl)amide
NHS	*N*-hydroxysuccinimide
Ni-NTA	Nickel-Nitrilotriacetic acid
NMR	Nuclear Magnetic Resonance
NOD	Nucleotide-binding Oligomerisation Domain-containing protein

PBP	Penicillin Binding Protein
PDC	Pyridinium dichromate
PG	Peptidoglycan
Ph_3P	Triphenylphosphine
PMA	Phosphomolybdic acid
POA	Pyrazinoic acid (**HPOA** protonated pyrazinoic acid)
***p*-TsOH**	*para*-Toluenesulfonic acid
PyBOP	Benzotriazol-1-yl-oxytripyrrolidinophosphonium hexafluorophosphate
PZA	Pyrazinamide
R&D	Research and Development
RiPPs	Ribosomally-synthesised and post-translationally modified peptides
rpm	Rounds-per-minute
RP-HPLC	Reverse-phase HPLC
RpsA	Rybosomal protein S1
rt	Room temperature
SD	Standard deviation
SDS	Sodium Dodecyl Phopshate
SPPS	Solid-Phase Peptide Synthesis
TB	Tuberculosis
TBS	Tris-Buffered Saline
TBST	Tris-Buffered Saline with Tween
***t*Bu**	*tert*-Butyl
TEMED	Tetramethylethylenediamine
TEMPO	(2,2,6,6-Tetramethylpiperidin-1-yl)oxy or (2,2,6,6-tetramethylpiperidin-1-yl)oxidanyl

TDR	Totally drug-resistant
TFA	Trifluoro acetic acid
THF	Tetrahydrofuran
TIS	Triisopropylsilane
TLC	Thin Layer Chromatography
Tris	Tris(hydroxymethyl)aminomethane
Troc	Trichloroethyl chloroformate
v/v	Volume/volume
WHO	World Health Organisation
XDR	Extensively Drug Resistant

LIST OF PUBLICATIONS ASSOCIATED WITH THIS WORK

Publications

Maitra A, Danquah CA, Scotti F, Francesca Howard TK, Kamil TK,. Bhakta S (2015). *"Tackling tuberculosis: insights from an international TB Summit in London"* Virulence, ISSN 2150-5594.

Conference proceedings

Scotti F, Bhakta S, Malkinson J (2015). *"Lasso peptides and murein peptide ligase inhibitors as novel anti-mycobacterial agents"* Proceedings of the 24th American Peptide Symposium. Ved Srivastava, Andrei Yudin, and Michal Lebl (Editors) American Peptide Society. http://dx.doi.org//10.17952/24APS.2015.193

Abstracts

https://www.ucl.ac.uk/pharmacy/research/doctoral-training-programme/dtp-projects/mur-ligases

Presentations

Bloomsbury Colleges Symposium, London, 6th June 2013 *"Synthesis of Mpl Substrates: a Potential New Strategy to Combat Tuberculosis"*

Bloomsbury Colleges Symposium, London, May 2014 *"Synthesis of Murein Peptide Ligase (Mpl) Substrates: a Potential Strategy to Combat Tuberculosis"*

PhD Research Day, UCL SoP, 15th April 2016 *"Peptide Therapeutics for Tuberculosis (TB) Therapy"*

Posters

TB Summit, London 25th-27th March 2014 *"Substrates and inhibitors of Murein peptide ligase (Mpl): a novel strategy to combat tuberculosis (TB)"*

PhD Research Day, UCL SoP, 19th September 2014 *"Targeting Murein Peptide Ligase (Mpl): a Potential Strategy to Tackle Tuberculosis"*

Bloomsbury Colleges Symposium, London, 2015 *"Synthesis of Murein Peptide Ligase (Mpl) Substrates Analogues: a Potential Strategy to Combat Tuberculosis"*

American Peptide Society Symposium, Orlando, Florida, June 2015 *"Lasso Peptides and Murein Peptide Ligase Inhibitors as Novel Anti-Mycobacterial Agents"*

Royal Society of Chemistry, PPSG Early Stage Researcher Meeting, 13th November 2015 Durham "*Murein Peptide Ligase Inhibitors and Lasso Peptides: New Strategies against an Ancient Disease"*

Bloomsbury Colleges Symposium, London, 2016 "*Synthesis of Murein Peptide Ligase (Mpl) Substrate Analogues for the Treatment of Tuberculosis"*

1. INTRODUCTION

1.1 The burden of infectious diseases

After the onset of the antibiotics golden era, the world witnessed a surge in the discovery and development of such compounds; nonetheless the past couple of decades has seen a decline in antimicrobial production rate (1). Oddly this has coincided with the widespread use and misuse of antibiotics in previous years, which triggered the development of bacterial resistance to those agents. The drugs provided microorganisms with selective pressure, challenging their ability to survive the inhospitable conditions created by the use of antibiotics and rewarding those that evolved accordingly. The rate of appearance of resistant mutants has been steadily increasing, and in this light the unlikelihood of such drugs bringing profit in the long term and especially the financial and time resources needed to bring them to market seems to have driven most major pharmaceutical companies to reduce their investment in antibiotic R&D departments (1). This is counterproductive as the urgent need for new antimicrobial agents has actually increased proportionally. Major infectious diseases such as tuberculosis (TB) and the ones caused by 'ESKAPE' pathogens have become extremely detrimental to human health and wellbeing. This acronym, coined by the Infectious Diseases Society of America (IDSA), refers to *Enterococcus faecium*, *Staphylococcus aureus*, *Klebsiella pneumoniae*, *Acinetobacter baumannii*, *Pseudomonas aeruginosa* and *Enterobacter* spp. (1). These organisms are widespread and common causes of nosocomial infections, but, as they are able to escape antibiotic action and became pan-resistant, they represent a mounting clinical burden for the future, especially for immunocompromised patients (2). *Mycobacterium tuberculosis* also poses a serious threat as it is still one of the major deadly diseases in the world (3). It is in this perspective that the quest for investigating multiple ways of dealing with infections and bacterial resistance becomes fundamental.

1.1.1 Tuberculosis

TB is an ancient disease that, despite an important decrease (47%) in mortality between 1990 and 2014, is still one of the biggest global health threats (3). WHO estimated 9.6 million new cases in 2014 and the yearly death toll is still well above 1 million (3). *M. tuberculosis*, identified as the tuberculosis causative agent in 1882 by Robert Koch, is a slow growing acid-fast bacterium. Despite the absence of an outer membrane, it does not retain the typical crystal violet dye used to differentiate Gram

negative and positive organisms. This happens as a result of a layer of mycolic acids and other complex lipids that covers the outer surface of the bacterium, conferring upon it a waxy consistency. The alternative Ziehl-Neelsen stain is very specific towards mycobacteria (and some Protozoa). The carbol fuchsin component of the stain penetrates and stains red any cell, but after the use of a destaining solution, only the “acid-fast” bacteria are able to retain it due to their mycolic acid layer. The latter is one of the peculiar features of mycobacteria. The extra layer, and the relatively lower peptidoglycan (PG) content (similarly to that found in Gram negative organisms) are characteristics of this bacterium.

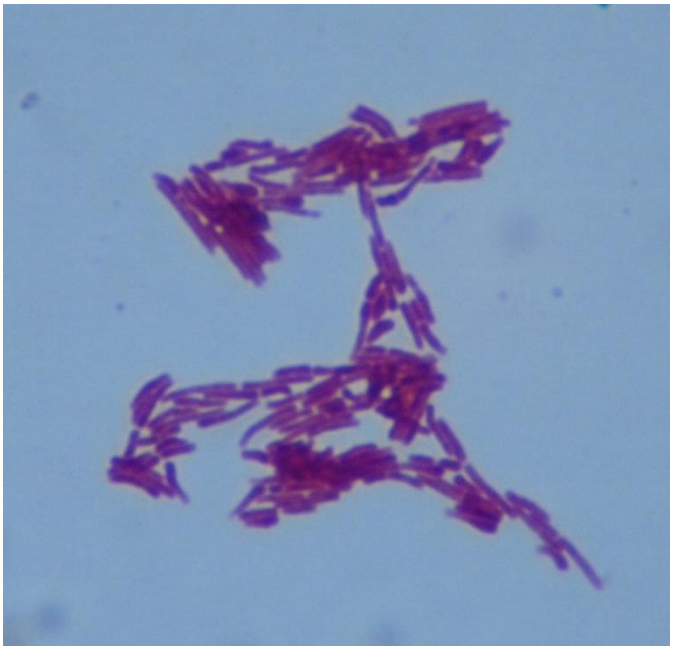

Figure 1.1 *Mycobacterium* sp. (1000x) stained following Ziehl-Neelsen staining protocol

TB is an air-borne disease of bacterial origin, transmitted through the aerosol droplets exhaled by an individual with active pulmonary disease, while sneezing, coughing or talking. There have been a limited number of cases reported in which transmission occurred through infected milk from cattle (4).

After entering the body via the respiratory system the bacteria settle in the lungs, which generally become the primary site of the infection. The bacteria then multiply, causing the initiation of an immune response from the host (5,6). Activated macrophages, deputed to kill and digest pathogens, ingest the bacteria, then fibroblasts are recruited that envelope the phages causing the formation of tubercles. However *M. tuberculosis* is often able to survive and multiply inside the macrophage, resisting the low pH and the oxidative species produced by the

phagocytes (7). This appears to happen as a result of the cell-wall glycolipids, which are able to absorb hydroxyl radicals and superoxide anions. The ability of *M. tuberculosis* to enter a dormant state with a lower metabolic activity, allows it to survive under difficult conditions and reactivate later, making TB a disease particularly prone to relapses. In individuals with a low resistance, such as children, elderly people and immunocompromised patients, therefore, the multiplication of the bacteria is uncontrolled, leading to an acute pulmonary infection that causes extensive destruction of lung tissue and the spread of the infection to other parts of the body (extra-pulmonary TB), typically ending in death. Despite this possibility, generally the infection remains localised and unapparent. In most cases an initial infection is sufficient to cause hypersensitisation of the individual to the bacteria and their products, subsequently altering the response in the case of further post-primary infections by *M. tuberculosis* (5). In general, cell-mediated immunity is a lifelong protection, although there is still the possibility of reinfection from other sources or due to reactivation of dormant bacteria in the lungs' macrophages (6,8,9). The typical clinical symptoms of the disease are chronic cough with blood-tinged sputum, fever, sweats, decreased appetite and weight loss. Given the role played by the immune system it is easy to imagine why immunocompromised patients such those infected with HIV are the biggest risk group. In fact TB is one of the main causes of death among these individuals (3).

If untreated, TB infection can lead to death. It is important to note how almost 90% of new cases occur in South-East Asia, Western Pacific countries and Africa (3) – countries affected by social and geographical (humid tropical weather) conditions that lead to low levels of hygiene, greater difficulties in accessing therapy, poor compliance and support. A larger pool of HIV cases also makes these countries more susceptible to TB burden.

1.1.2 Current treatment of tuberculosis

The current standard treatment for patients that have never been previously treated – and therefore initially assumed to be infected with a susceptible strain – consists of two months' therapy with isoniazid **1** (INH), ethambutol **2**, pyrazinamide **3** (PZA) and rifampicin **4**. The continuation phase consists of four further months of isoniazid, rifampicin and ethambutol treatment. The doses have to conform to international recommendations.

Isoniazid **1**, a prodrug, and ethambutol **2** inhibit cell-wall synthesis, the former by interfering with the biosynthesis of mycolic acids, the latter by inhibiting the enzyme arabinosyl transferase, which contributes to the synthesis of arabinolactan (10).

Rifampicin **4**, an ansamycin, acts differently, inhibiting RNA synthesis by binding to the β-subunit of DNA-dependent RNA polymerase therefore inhibiting the elongation of mRNA (11,12).

Pyrazinamide **3** is a prodrug activated intracellularly by pyrazinamidase PncA, which hydrolyses the primary amide to give the carboxylic acid derivative pyrazinoic acid (POA). It is the only drug active against non-replicating persisters; its effect on the growing bacilli is negligible and it works with maximum efficacy at acidic pH and low metabolic conditions. Its exact mechanism of action is not clear.

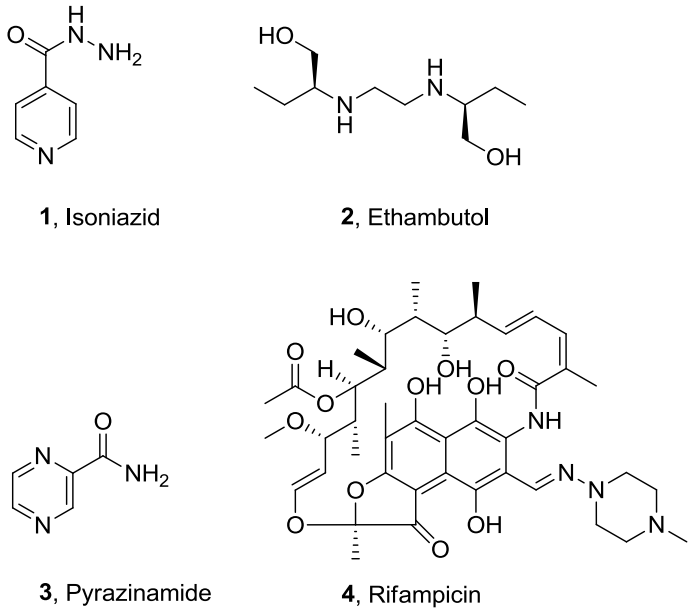

Figure 1.2 First-line anti-TB drugs

One hypothesised mechanism suggested the inhibition of fatty acid synthetase I (FAS I), involved in the elongation of mycolic acids, but this has been recently questioned (13). A model suggested by Zhang *et al.* 2014 (13) considers the main mechanism of action to be the acidification of the cytoplasm leading to the inhibition of the correct functioning of certain cellular enzymes (13,14). In this model, PZA passively enters the cell where PncA activates it to POA, which gets ejected by an efflux system; once outside, at acidic pH, POA gets protonated to HPOA and re-enters the cell. There it releases protons, acidifying the intracellular environment, and being then in anionic form can only be ejected through efflux pumps. The inward permeation rate of HPOA is greater than the efflux of POA, which causes accumulation of the active drug inside the cell. This seems to be rendered possible because of an efflux system deficient in *M. tuberculosis*, this seemingly being the

reason for which other mycobacteria species are not susceptible to PZA (15). The intracellular acidification and accumulation of POA together with the energy expense to fuel the efflux pump, eventually causes cell death, via disruption of the membrane potential and inhibition of essential enzymes (13). This model is supported by the fact that PZA works against *M. tuberculosis* only and other Mycobacteria contain altered forms of PncA (12). Intracellular POA seems to inhibit RpsA (ribosomal protein S1), which regulates trans-translation.

These four compounds in Fig. 1.2 constitute the first-line drugs against TB and they were all discovered in the early days of anti-TB research. Their positive impact on global health, together with the introduction of the BCG vaccine, has been huge and had brought the world close to the eradication of TB. Unfortunately a surge in the number of cases was witnessed throughout the 1980s and then again in the 2000s, especially in those so-called high burden countries and in HIV-positive patients (16). This is due to human movement across countries, low adherence and access to therapy (poor countries) and resistance development.

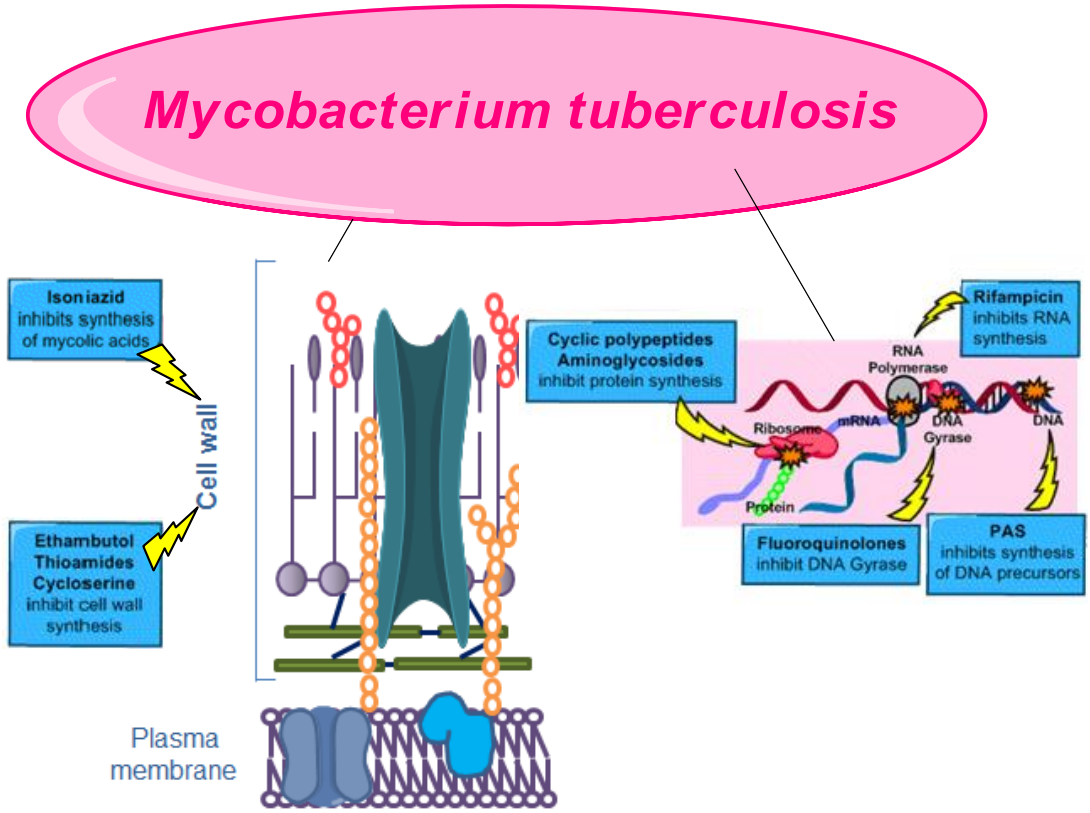

Figure 1.3 Different mechanisms of action of existing anti-TB drugs (modified from (17))

Miscellaneous:

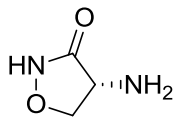

5, D-Cycloserine

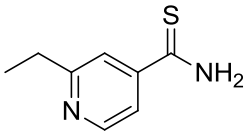

6, Ethionamide

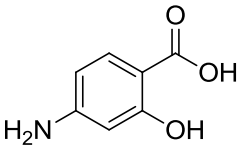

7, *para*-Aminosalicylic acid

Fluoroquinolones:

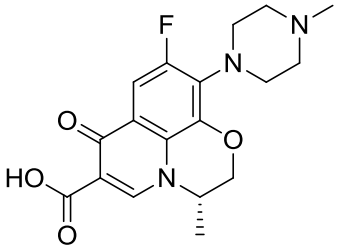

8, Levofloxacin

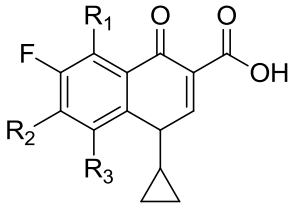

9, Ciprofloxacin (R_1 = H, R_2 = $C_4H_9N_2$, R_3 = H)
10, Moxifloxacin (R_1 = OCH_3, R_2 = $C_7H_{13}N_2$, R_3 = H)
11, Gatifloxacin (R_1 = H, R_2 = $C_4H_9N_2$, R_3 = OCH_3)

Aminoglycosides:

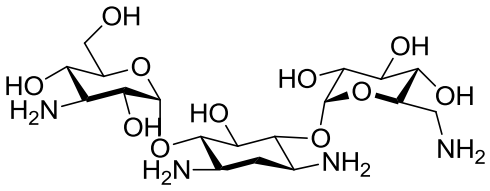

12, Kanamycin

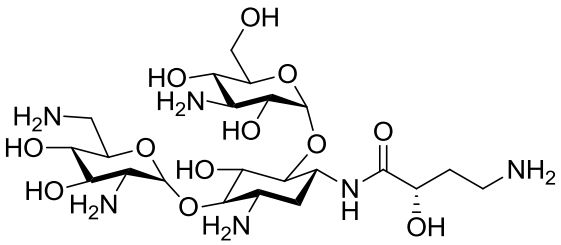

13, Amikacin

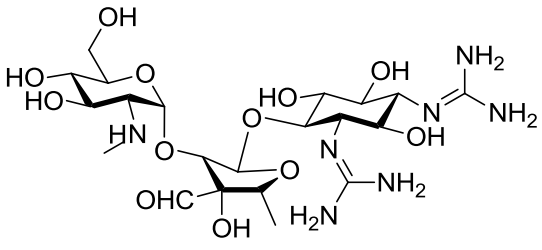

14, Streptomycin

Figure 1.4 Second-line anti-TB drugs

The World Health Organisation has tried to improve the outcome of TB treatment by introducing DOT (Directly Observed Therapy) for the treatment of tuberculosis. This

procedure prescribes that a trained health care professional or other provides a standardised treatment with supervision and patient support. This is especially critical in the case of HIV-positive and drug-resistant patients. The patient is given the medication and has to take it in front of the supervisor (13).

Second-line drugs include molecules with quite different mechanisms of action (Fig. 1.3): D-cycloserine 5 inhibits cell-wall PG synthesis, ethionamide 6, a prodrug, possibly disrupts the mycolic acid layer while another prodrug, *para*-aminosalicylic acid 7, inhibits dihydrofolate reductase (18,19). Fluoroquinolones such as levofloxacin 8 (20,21), ciprofloxacin 9 (22), moxifloxacin 10 and gatifloxacin 11 (23), inhibit DNA gyrase and type II topoisomerase IV therefore interfering with cell division, while aminoglycosides such as kanamycin 12, amikacin 13 and streptomycin 14 are protein synthesis inhibitors.

Since the discovery of the TB aetiological agent in 1882, a number of different anti-TB drugs have been discovered and exploited (Fig. 1.5). Streptomycin was one of the first agents used but resistance soon arose. A few years later the development of INH fuelled great expectations as the molecule was found to be ten times more active than any other previous one and highly selective for mycobacterial cells thus being free of major side effects. Unfortunately resistance rapidly occurred and for this reason nowadays it is used only in combination with the other first-line drugs (24). It is interesting to note that essentially all of the drugs in current routine use were developed within 20 years, but beyond that, little further progress has been made in the subsequent 50 years. Of course those initial 20 years represent the age of pioneering antibiotic research, with many new agents being discovered, and resistance had not at that time developed to the extent that is has now.

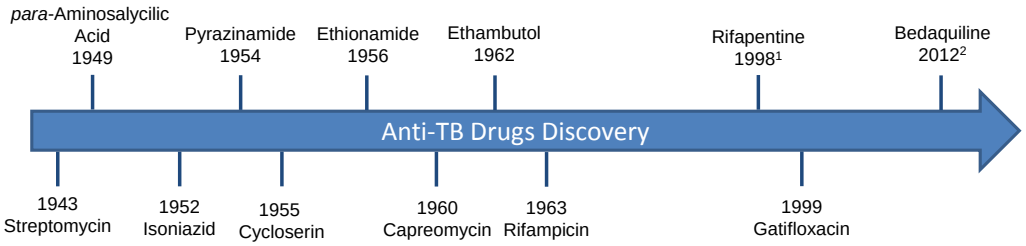

Figure 1.5 TB drugs discovery timeline

[1]approved by FDA for active and latent TB treatment in combination with isoniazid; [2]approved by FDA for treatment of MDR-TB, currently in phase II clinical trials

Furthermore, following the finding that multidrug therapy was effective against susceptible TB, cases decreased impressively and not much effort was invested into finding alternatives. In the light of the current resurgence of TB, it is becoming increasingly evident that looking for better treatment options is necessary. Ideally, more effective drug therapy would be of shorter duration with a lower number of drugs (realistically two drugs would be best, as monotherapy more easily incurs the risk of resistance). This would greatly improve compliance, which would likely result in a reduced need for accessibility and control (DOT), leading to even better compliance and adherence. That would, in turn, limit the spread of the disease and of resistance. The other pillar of the TB fight is prevention, through education, sanitised environments and BCG vaccination. Early detection is also fundamental as undiagnosed cases can be source of contagion.

1.1.3 Resistance

The first line of intrinsic resistance to antibiotics in Mycobacteria is represented by the mycolic acids layer, which naturally confers low permeability to many molecules. *M. tuberculosis* expresses β-lactamases (encoded by *blaC* and *blaS*), conferring resistance to β-lactam antibiotics (25). Furthermore efflux pumps promptly eject tetracycline, fluoroquinolones, aminoglycosides and other antibacterials. Depletion of porins (MspA in *M. smegmatis* (26) and Rv1698 in *M. tuberculosis*), which have been associated with the diffusion of hydrophilic compounds into the bacterial cell, is another general mechanism of resistance in Mycobacteria (12).

Resistance in *M. tuberculosis* typically occurs via single point mutations of chromosomal genes. In the case of INH, the main cause of resistance is due to mutations of *katG*, which encodes for the enzyme responsible for the activation of the prodrug, leading to partial or total loss of katG catalase/peroxidase activity (12). Rifampicin-resistant strains in most cases show mutations of *rpoB*, the gene encoding for the RNA polymerase subunit where the drug binds. The production of a slightly modified target lowers the affinity for the drug, leading to the development of resistance. Interestingly the vast majority of these strains show some degree of resistance against other antibiotics, mainly INH (12). Similarly, pyrazinamide resistance is generally found in strains with mutated *pncA*, the gene encoding for the enzyme responsible for the conversion of the prodrug into its active form (12). It was found that 50% of ethambutol-resistant strains show mutations of *embB*, encoding for an arabinosyl transferase, an enzyme involved in cell-wall assembly. The reasons for resistance in the remaining strains are under investigation and suggest the existence of other mechanisms of action of ethambutol (27).

The term MDR-TB (multi drug-resistant tuberculosis) has been coined to describe the situation in which two of the first-line drugs, generally isoniazid and rifampicin, are no longer effective. MDR-TB is caused by a multi-step process in which the accumulation of mutations on different resistance genes leads to a bacterium better adapted for survival (28). In these cases patients have to be treated with second-line drugs, which take longer to act, are more expensive and present more side effects. When resistance to any fluoroquinolone and to at least one of the second-line injectable drugs also occur, the disease is described as extensively drug-resistant tuberculosis (XDR-TB) (3). In this eventuality, the treatment options are seriously limited. Furthermore, in recent years “totally drug-resistant” (TDR) cases have been reported (29,30). This term, which has not been recognised by the WHO, is used to represent strains that are resistant to all the first-line and second-line drugs *in vitro* (31,32). MDR and XDR tuberculosis strains are not responsive to the standard six-month treatment and generally take two years or more to be treated; cases of TDR are being considered untreatable at the moment, with some cases having been treated for more than four years without any improvement (32). It is therefore of primary importance to develop new anti-TB drugs while controlling the spread of resistant strains of tuberculosis.

1.2 CELL-WALL PEPTIDOGLYCAN

1.2.1 Cell-wall as an antibacterial target

The cell-wall is a unique and essential feature of the bacterial cell providing extra protection from the external environment, therefore being an ideal target for therapy. Its structure is fairly complicated and comprises different molecular components with various functions that can be exploited as targets. All bacteria have a cell-wall but differences in composition are apparent (Fig. 1.6).

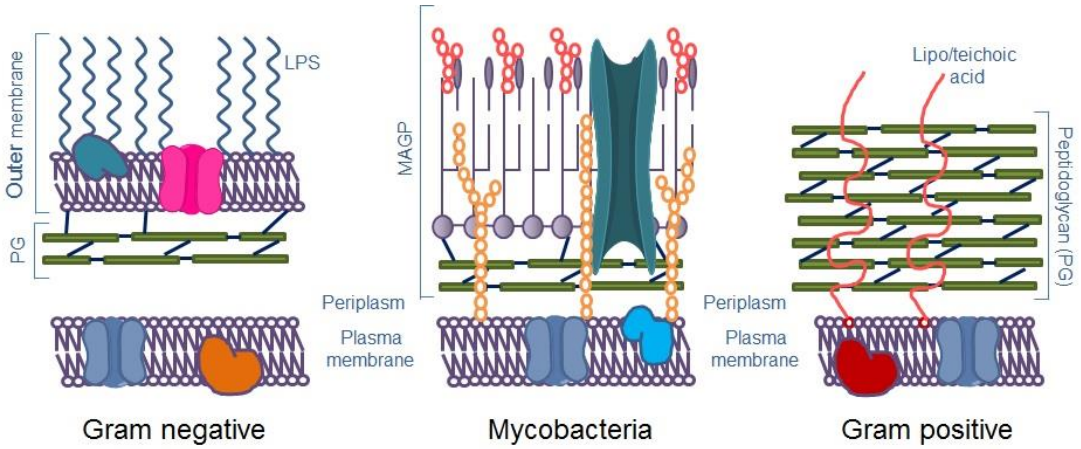

Figure 1.6 Different cell-walls: PG – peptidoglycan; LPS – lipopolysaccharides; MAGP – mycolyl-arabinogalactan-peptidoglycan complex

The mycobacterial cell-wall is comprised of a lower and upper segment. The lower segment lies directly beyond the membrane and it is made of cross-linked peptidoglycan covalently bound to arabinogalactan (AG). This is then esterified by mycolic acids, a group of complex branched-chain hydroxylated lipids, which consist of one long meromycolate and one short alpha-alkyl branch (Fig. 1.7), The meromycolate branch can include cyclopropane, methyl, methoxy and carbonyl groups; unsaturations along the chain have been found in *M. tuberculosis* mycolic acids.

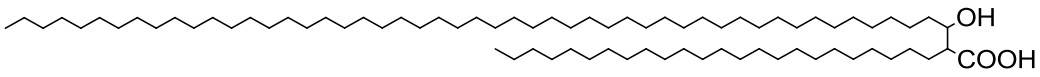

Figure 1.7 Schematic representation of mycolic acid meromycolate and alpha branch

This mycolyl-arabinogalactan-peptidoglycan complex (MAGP) is considered the cell-wall core. This is the portion of the cell-wall that appears to be essential for the viability of the cell. The upper segment, on the other hand, is made of free lipids with variable fatty acid chain length. In between are phthiocerol containing lipids, phosphatidyl inositol mannosides, lipomannan, lipoarabinomannan and cell-wall proteins (33,34) .

PG is a fundamental component of the cell-wall as it gives structural strength to the cell, it counteracts the osmotic pressure and provides anchoring support for other molecules that enrich this structure, and it takes part in cell division (35). It is particularly abundant in Gram positive bacteria, while in Gram negative organisms it constitutes a thinner layer. It is a large polymer made of repeating disaccharide-pentapeptide units (36,37). Each of these is made of alternating β(1→4)-linked *N*-

acetylglucosamine (Glc*N*Ac) and *N*-acetylmuramic acid (Mur*N*Ac) residues, the latter of which has a pentapeptide attached through its D-lactyl moiety. Each strand of the peptidoglycan is predisposed for cross-linking to a maximum of three neighbouring peptidoglycan strands, even though not all strands have to be cross-linked (38).

For most Gram positive bacteria the pentapeptide (**15**) growing sequence is L-Ala, γ-D-Glu, L-Lys, D-Ala, D-Ala, but for Gram negative bacteria and in few Gram positive organisms, including *Mycobacterium tuberculosis*, *meso*-2,6-diaminopimelic acid (*m*DAP) is substituted for L-lysine in the peptide chain of the peptidoglycan (Fig 1.8) (37,39). This type of bacterium also shares the larger intermembrane space found in Gram negative bacteria, but characterised by the presence of mycolic acid lipids, which are found only in mycobacteria and some species belonging to *Corynebacteriales* (40).

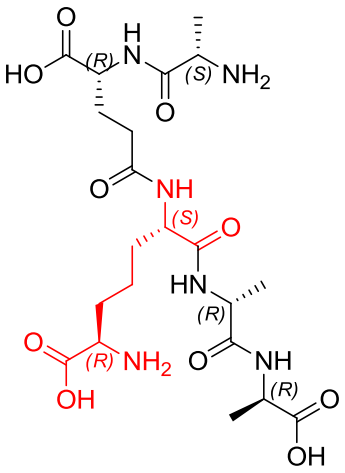

15

Figure 1.8 Structure of the mycobacterial pentapeptide, highlighting the *m*DAP residue (red)

Different bacterial genera and species showcase peculiarities in their PG structures. There is a higher frequency (75%) of cross links in *M. tuberculosis* PG compared to that of *E. coli* (41). These are mainly 4→3 linkages, between D-Ala and *m*DAP, but about one third is constituted of 3→3 linkages, between two *m*DAP residues (41–44). The latter are the result of L,D-transpeptidase activity and are found in *E. coli* solely during the stationary phase under stress conditions, such as nutrient depletion (45). In *M. tuberculosis* they are also present during the growth phase but their content increases up to 80% during the stationary and dormant phases (46,47).

1.2.2 Peptidoglycan: biosynthesis, degradation and recycling

1.2.2.1 Biosynthesis of the peptidoglycan

The building blocks of the peptidoglycan are sequentially assembled in the cytoplasm by Mur ligases (or synthetases). They are a family of bacterial enzymes responsible for the synthesis (and recycling) of peptidoglycan. They have recently become the centre of increasing interest in the potential development of PG inhibitors with activity against different pathogens (*M. tuberculosis*, *M. leprae* (48,49), Chlamydiaceae (50), *H. influenza* (51), *S. pneumoniae, S. aureus* (52)), as they are essential for the survival of the bacterial cell. They are highly specialised enzymes that generally have high substrate specificity. The initial conversion of UDP-Glc*N*Ac to UDP-Mur*N*Ac is performed by MurA and MurB: MurA, a transferase, catalyses the transfer of enolpyruvate from phosphoenolpyruvate to UDP-Glc*N*Ac; MurB, a reductase, transforms enolpyruvate to D-lactate, producing UDP-Mur*N*Ac (Scheme 1.1) (53).

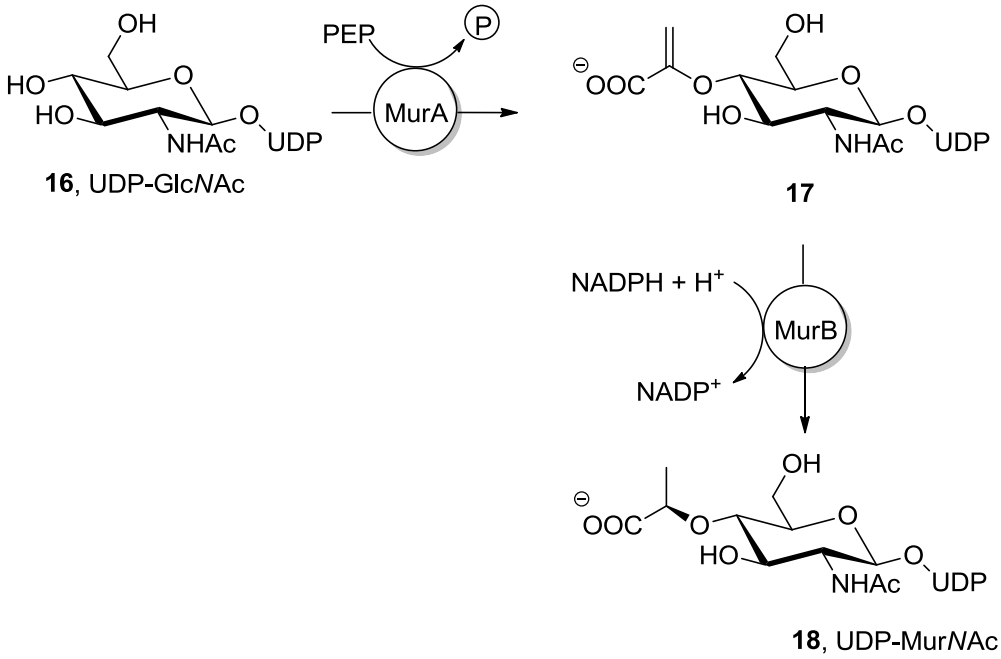

16, UDP-Glc*N*Ac

17

18, UDP-Mur*N*Ac

Scheme 1.1 MurA and MurB convert UDP-Glc*N*Ac to UDP-Mur*N*Ac

Subsequently the addition of the five amino acids of the pentapeptide is catalysed by a series of essential ATP-dependent Mur ligases. Each step requires the hydrolysis of ATP, releasing ADP and inorganic phosphate (39,54); interaction of the UDP-precursor with ATP generates an acyl phosphate. The amino group of the incoming amino acid attacks the carbonyl carbon atom, producing a tetrahedral intermediate, which leads to the elimination of the phosphate group to give a peptide

bond (53,55). These enzymes sequentially attach amino acids to the PG disaccharide formed by UDP-Glc*N*Ac-UDP-Mur*N*Ac to form the peptide stem of the PG monomer. Their activity in *M. tuberculosis* is illustrated in Scheme 1.2. The sequence similarities among these enzymes are limited to the highly conserved regions corresponding to the active site: the ATP-binding pocket, the *N*-terminal domain that accommodates UDP-Mur*N*Ac and the *C*-terminal domain where the amino acid substrate binds (56). MurC generally catalyses the attachment of L-Ala on the carboxylate of UDP-Mur*N*Ac, with some exceptions *e.g. M. tuberculosis* and *leprae* MurC showed substrate affinity also for Gly (48) and L-Ser (54).

MurD catalyses the formation of a peptide bond between the UDP-Mur*N*Ac-L-Ala free carboxyl group and the D-Glu amino group. Its specificity for its substrate D-Glu is particularly high, and this ability seems to make MurD an extremely promising target within the antibacterial drug discovery field (57). In *E. coli*, MurD doesn't show any ligase activity in the presence of L-Glu, and it allows as substrates only the unusual DL-homocysteic acid, D-erythro-3- and 4-methylglutamic acids and 5- or 6-membered cyclic analogues of D-Glu (57). A study on *E.coli* MurD highlighted how UDP-*N*-acetylmuramyl-L-Ala intracellular levels affect the enzyme activity. When its concentration reaches 10 μM it stimulates MurD ligase activity, while when it goes above 15 μM it shows an inhibitory effect on MurD (58). In Gram positive organisms this effect is significantly lower (starting at concentrations of 1-2 mM). Given the different quantity of PG present in the different cell walls, this fact seems to suggest that MurD ligase activity could be the bottleneck regulating the thickness of the PG layer in Gram negative organisms (58).

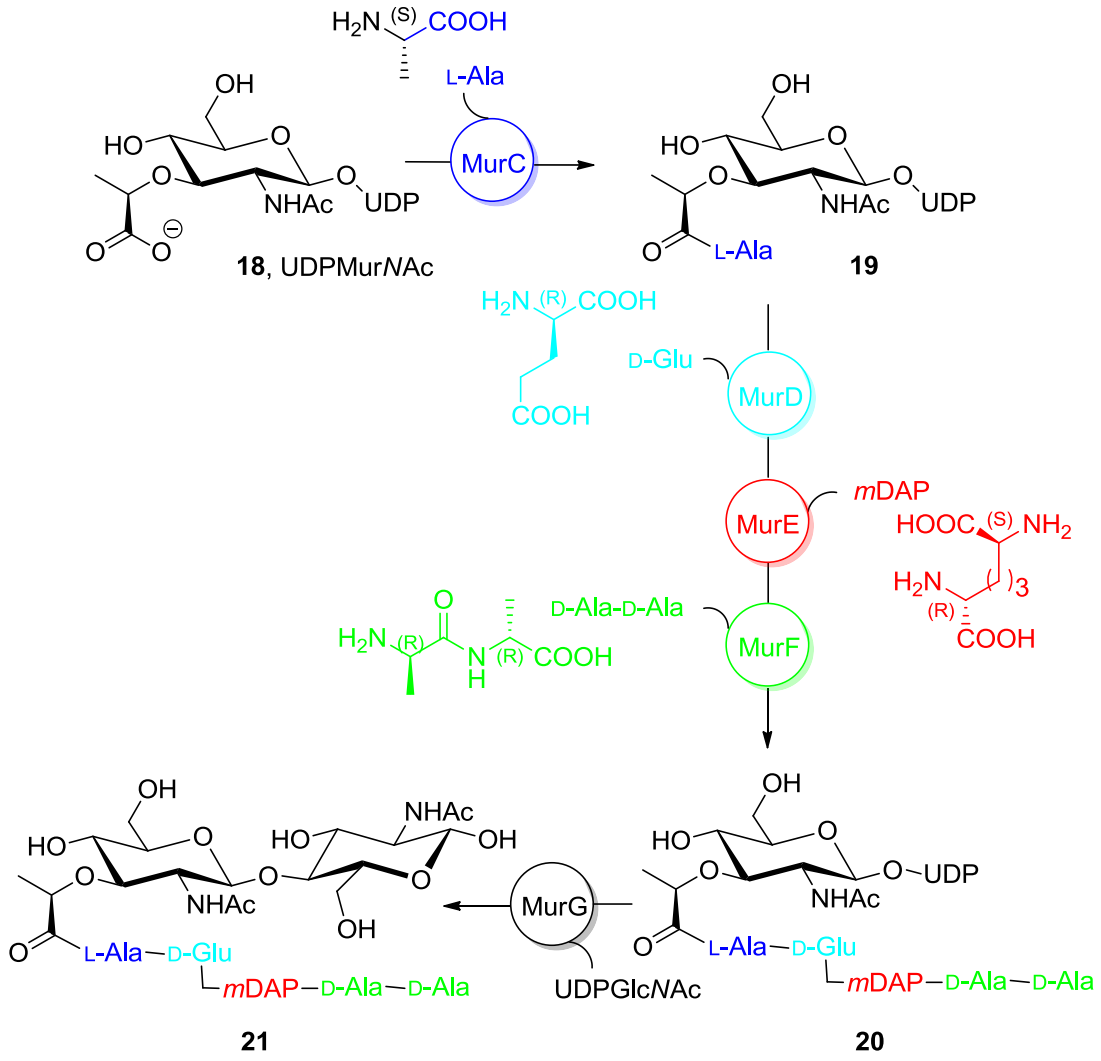

Scheme 1.2 Biosynthesis of the glycopeptide in *Mycobacterium tuberculosis*

MurE has a species-specific selectivity for its substrate: depending on the organism, it will accept *m*DAP or Lys for incorporation into the PG peptide stem. Mis-incorporations lead to irreversible cell damage. *E. coli* overexpressing *S. aureus* MurE starts incorporating only L-Lys, instead of *m*DAP, in its PG leading to cell lysis within 1 h. The enzyme is active only in the presence of UDP-Mur*N*Ac-L-Ala-D-Glu. In *E. coli* MurE has been found to accept L,L DAP and other *m*DAP analogues but not L-Lys (59,60). The species specificity seems to be related to the residue in position 416 of the MurE sequence. In organisms that incorporate *m*DAP into their PG, an Arg residue, able to bind to the free end of *m*DAP, is found, while in those organisms that incorporate Lys into their PG, Ala or Asn is found (39,54,61).

MurF seems to have fair substrate flexibility. It always adds a dipeptide to the growing peptide stem – generally D-Ala-D-Ala – but it has the ability to introduce a

variety of D-amino acids *e.g*. by accepting D-Ala-D-Lac or D-Ala-D-Ser instead of the canonical D-Ala dimer. MurF from *S. aureus* showed an equal ability to add the dimer to the Lys-containing or *m*DAP-containing growing peptide stem (62).

These are the key catalytic drivers of the peptidoglycan monomer assembly, but their actions are dependent on the availability of substrates produced by the activity of a number of corollary enzymes. For example DapF is an epimerase that converts L,L-DAP to *m*DAP – the required MurE substrate (63). The dimer D-Ala-D-Ala (the required substrate of MurF) is the result of the activity of Alr, a racemase that converts L-Ala to D-Ala, and Ddl (D-Ala:D-Ala ligase), which catalyses the formation of the dimer (64). Subsequently in PG assembly, lipid linked precursors are synthesised then translocated by a flippase protein across the membrane to the periplasmic space. This flippase has been identified as FtsW in *E. coli*, in which it has also been found to play an essential role in cell division (65). Similar lipid II flippases have been identified in other bacteria and within the Actinobacterium *Corynebacterium glutamicum* (66). In the periplasmic space, the lipid-linked precursors are substrates for transpeptidases and transglycosylases involved in PG polymerisation. These roles are played by bifunctional penicillin binding proteins (PBPs); they polymerise and cross-link the separate units, forming the final, alternating Glc*N*Ac and Mur*N*Ac, structure of PG, which can finally be bound to the rest of the cell-wall (Fig 1.9) (61). The PBPs involved in PG polymerisation and cross-linking are of high molecular-weight (HMW-PBPs).

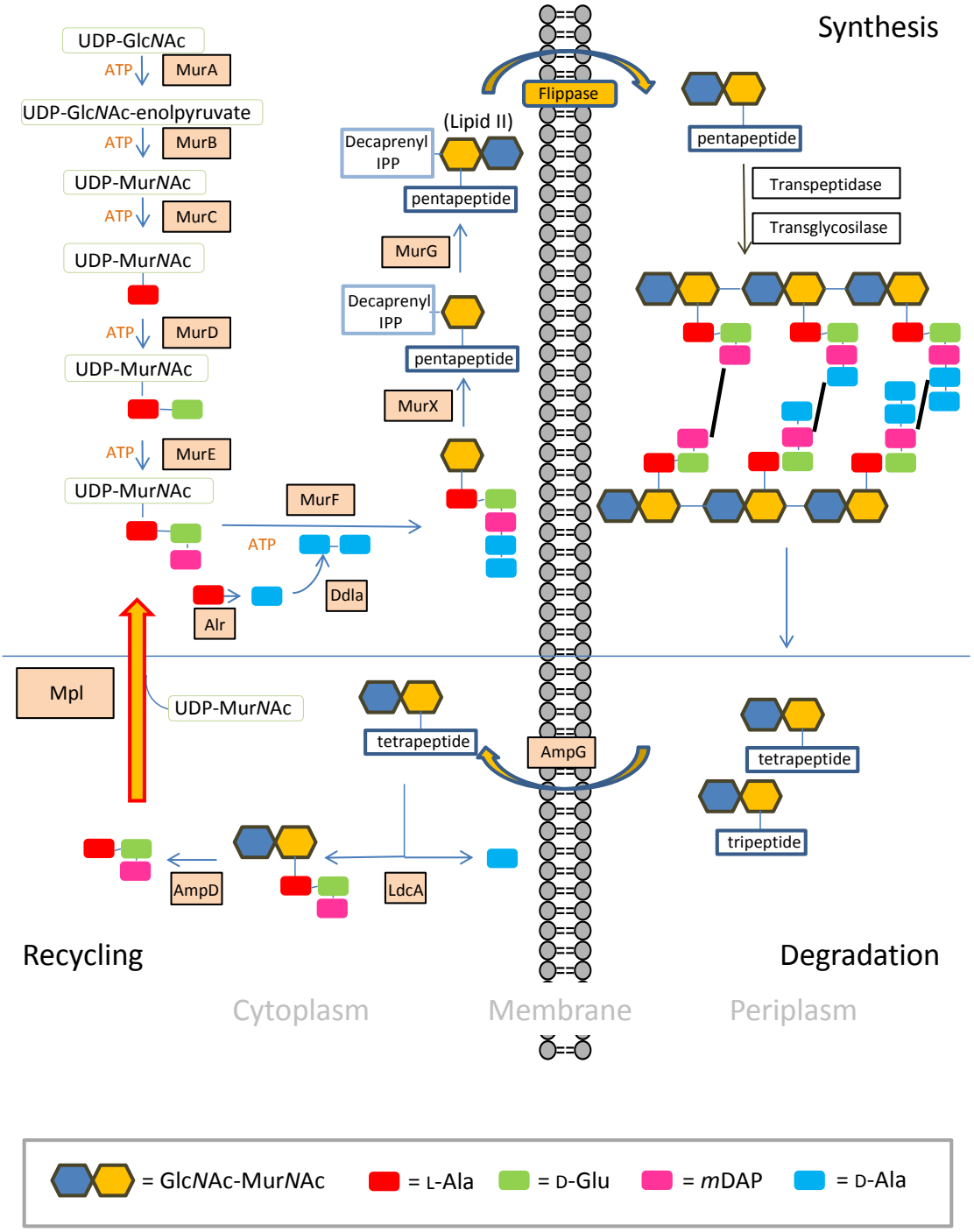

Figure 1.9 Schematic description of the biosynthesis, degradation and recycling of Gram negative bacteria peptidoglycan (modified from (61))

Cross-linking generally involves the third amino acid in one chain and the fourth in another one but in *M. tuberculosis* the cross-linking can also occur between two *m*DAP (third) residues (43). Furthermore, some of the *N*-acetyl groups on Mur*N*Ac can be oxidised to *N*-glycolyl groups causing the incorporation of *N*-glycolylmuramic

acid as the predominant component of the saccharide. In addition, a small percentage of the D-Glu residues are replaced by glycine and the side chain residues of D-Glu and *m*DAP can be amidated. These features, together with the unusual presence (for a Gram positive species) of *m*DAP, make *M. tuberculosis* peptidoglycan unique and can provide specific targets for the development of anti-tuberculosis drugs (61,67).

1.2.2.2 The peptidoglycan can also be synthesised through recycling

Another important issue is the discovery that Gram negative bacteria such as *E. coli* have specific enzymes that are able to recycle components of the cell-wall that are broken down during normal cell-wall turnover (Fig. 1.9) (68). Mpl has been identified in a number of organisms, including *E. coli* (69), *Psychrobacter arcticus* (70) and possibly *Salmonella paratyphi* C (71). It is an enzyme involved in the recycling of peptidoglycan. Its existence has been speculated since the realisation that MurC did not have the ability to utilise the tripeptide H-Ala-D-Glu(*m*DAP-OH)-OH as a substrate to attach to the UDP-Mur*N*Ac; hence, within the recycling context, there had to be another enzyme with said activity (72). Mpl in *E. coli* was found first as a homologue of MurC lacking ligase activity in the presence of L-Ala (48,73). Later on, its activity in *E. coli* was evaluated and it was found to have high substrate affinity for the tripeptide H-Ala-D-Glu(*m*DAP-OH)-OH and it was therefore called UDP-*N*-acetylmuramate:L-alanyl-γ-D-glutamyl-*meso*-diaminopimelate ligase. It was also shown to be able to accept the tetra and pentapeptide with similar efficiency, as well as demonstrating some ligase activity even with the dipeptide H-Ala-D-Glu-OH and L-Ala itself (69). Given that any Mur ligase reaction requires one molecule of ATP, re-introduction of, typically, a tripeptide fragment into the PG strand represents a net saving of two molecules of ATP. This seems to suggest the enzyme's possible involvement in conserving energy during the transition to the dormant state in *M. tuberculosis*, and possibly a role in surviving harsh conditions (antibiotic presence and resistance). Through computational analysis, recent results in our laboratory have identified this enzyme in *M. tuberculosis* as Rv3712, which was initially identified as a MurC homologue.

It has been estimated that in Gram negative organisms, recycling is believed to account for 30 to 60% of PG synthesis (11). It was thought that this phenomenon did not apply to Gram positive bacteria because of their thicker exoskeleton, their inside-to-outside synthesis of peptidoglycan and because of the detection of a significant quantity of PG fragments released in the medium by Gram positive organisms (74). Some Gram positive species, however, turn over up to 50% of their

peptidoglycan during vegetative growth (75). This would mean a massive loss of material, especially in Gram positive bacteria, as peptidoglycan constitutes 20% of their cell-wall mass. Recently, however, the identification in *Bacillus subtilis* of a gene cluster containing 5 orthologues of enzymes involved in recycling in *E. coli* (74,76) suggests that a recycling pathway exists also in Gram positive bacteria. Furthermore in the case of Mycobacteria it is believed that the thick lipid-containing outer wall prevents the fragments from diffusing away, allowing their reuptake for recycling purposes (41). This means that inhibition of the Mur ligases, which build the PG *de novo*, is unlikely to completely inhibit the synthesis of the cell-wall.

A recent study by Borisova *et al.* showed how deletion of genes encoding for recycling enzymes (amgK, MurU, anmK, NagZ) in a fosfomycin-resistant strain restored the MIC of the antibiotic to therapeutic values (a fourfold increase) (77).

In a comparative study on *M. tuberculosis*, the Mur synthetases, even though provided with the appropriate substrates, showed little product formation in the absence of metal ions (54). The presence of divalent cations seemed to greatly improve conversion. In particular, the concentration of Mg^{2+} was found to exert a strong influence on the activities of MurC, MurE and MurF. In the case of MurD, Mg^{2+} and Mn^{2+} proved similarly essential. Other cations such as Co^{2+} and Zn^{2+}, K^{+} and NH_4^{+} exerted less significant effects (54).

1.2.3 Cell-wall synthesis and recycling inhibition perspective: new or adjunct anti-TB therapy for existing drugs

A connection between cell wall recycling and antibiotic resistance has already been suggested. Cell wall-targeting antibiotics, such as β-lactams, act by triggering (or causing) modifications in the cell wall structure, composition or integrity. It was found that detection of unusual quantities of modified or truncated muropeptides in the cytoplasm provided a good indication that something anomalous was happening (74). In the presence of β-lactams, in some Gram negative bacteria the muropeptides trigger the expression of the gene encoding for AmpC β-lactamase therefore initiating a resistance strategy (74). This is one example of how fragments of cell wall can trigger a resistant response from bacteria. In addition, it has been shown that deletion of certain genes encoding for recycling enzymes can increase susceptibility to antibiotics (78). This seems to demonstrate that the combination of cell wall-targeting antibiotics and inhibitors of cell wall recycling could be a highly promising strategy (74).

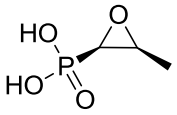

22, Fosfomycin

In addition, as some recycling activities can contribute to intrinsic antibiotic resistance (79), inhibition of said pathways could potentially repurpose old drugs, which were discarded from therapeutic use because of resistance. One important example is the case of fosfomycin, **22**. This drug blocks the formation of UDP-Mur*N*Ac by interfering with the activity of MurA. Pseudomonads can easily acquire resistance to its action. It was found by Borisova *et al.* (77) and Gisin *et al.* (79) that, in *P. aeruginosa* and *P. putida* respectively, a recycling pathway exists that bypasses the activity of MurA and MurB. This pathway is not found in Enterobacteria, *E.coli* included. In this way the bacterium is able to utilise the anhydro version of Mur*N*Ac (AnhMur*N*Ac) product of the degradation of PG through a series of steps (involving AnmK, AgmK, MurU) to re-enter the synthetic cycle through UDP-Mur*N*Ac provision (79). The importance of this finding lies in the fact that when the salvage pathway was blocked, it was found that the susceptibility of *P. aeruginosa* specifically to fosfomycin increased 4- to 8-fold, bringing the MIC of this antibacterial agent back to therapeutic levels.

These findings highlight the new perspective in antibacterial therapy provided by the inhibition of the recycling pathways. Interference with PG salvage routes could help in overcoming antibiotic resistance (to antibiotics that are no longer active because they directly target a biosynthetic step that can be bypassed through recycling).

1.3 Antibacterial peptide drugs

The use of peptides in therapy has increased since penicillin was discovered in the 1920s. Following that serendipitous finding, scientists have been searching for new antibiotic agents. Bacterial and fungal species have been tested extensively and, as a result, many antibiotics still used these days are, in fact, natural products. Naturally produced peptides can be classified as either non-ribosomally or ribosomally synthesised peptides. The latter, also abbreviated RiPPs (ribosomally-synthesised and post-translationally modified peptides) are synthesised as precursor peptides and then sequentially modified post-translation, followed by proteolysis which removes non-core portions to release the actual mature peptide (80).

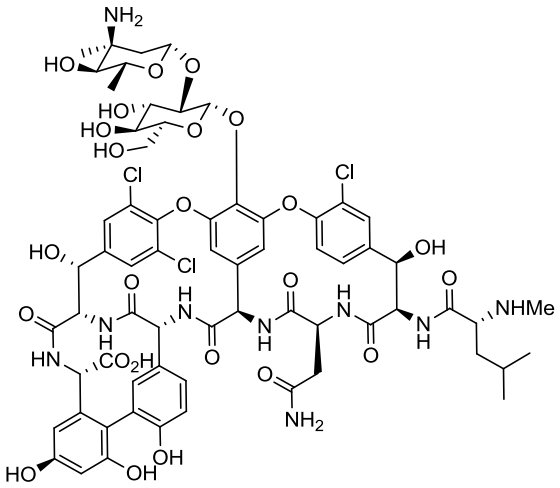

23, Vancomycin

Many display potent bioactivity. Furthermore, more recently, non-ribosomally synthesised AMPs (antimicrobial peptides), such as vancomycin, **23,** have increasingly become the focus for research. These are produced by peptide synthetases in all organisms as part of their innate immune system. This attention on peptides is because they are readily accessible; methodology for their effective synthesis has greatly improved from solution-phase to the use of solid supports, which allow the removal of soluble reagents from preceding steps, therefore yielding purer crude products. More recently the development of automated solid-phase synthesis has rendered this process even more convenient. In addition, peptides are easily modifiable and their building blocks are generally commercially available. This ease of production allows preparation of carefully designed peptides to suit the interaction with a desired target, if its structure is known and if its activity has been previously entirely or partially elucidated. In this way substrate analogues or tailored peptides capable of specific drug-target interactions can be inhibitors or enhancers able to interact with the active or collateral sites of the targets, resulting in modulation of their effects.

1.3.1 β-lactam antibiotics target the cell-wall

β-Lactams represent the oldest class of antibiotics discovered, penicillin G (Fig 1.10) being the first in 1929 (81). Penicillins, cephalosporins, cephamycins, carbapenems and monobactams all belong to the β-lactam antibiotic group; they are potent compounds and they are still the most prescribed antibacterial drugs around the world (82). Resistance however has arisen, mainly thanks to the horizontal transfer of genes encoding for β-lactamases – enzymes able to hydrolyse the β-lactam ring responsible for the antibacterial activity (82).

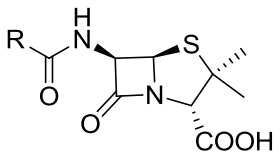

Figure 1.10 General structure of penicillins, substituents R vary largely; in penicillin G R = $CH_2C_6H_5$

The main known target of β-lactams are PBPs, which are D,D-transpeptidases responsible for a specific type of cross-linking between two D-Ala residues on adjacent PG peptide stems. The antibiotics bind selectively and irreversibly to the main active site of the PBPs and form adducts, which therefore inhibit the enzyme's activity. This is due to the fact that β-lactams mimic the D,D-transpeptidase substrate (83). In the case of penicillin and cephalosporins, their structure resembles that of the natural substrate of PBPs, D-Ala-D-Ala (82,83). Carbapenems, have opposite configurations of the two chiral carbon atoms on the lactam ring and their resemblance is more similar to that of *m*DAP-D-Ala which is the substrate of the L,D-transpeptidase (Ldt_{Mt2}), responsible for the 3→3 cross-linking of the PG, which represent around 80% of the non-replicating TB bacillus PG links. In *M. tuberculosis*, β-lactams are not used widely because of the intrinsic resistance of the bacillus to them. The mycolic acid layer in this case does not seem to represent a significant obstacle to the penetration of the antibiotics (82). This natural resistance is mainly due to a strong β-lactamase activity in this species, mediated by BlaC – the only β-lactamase found in the *M.tuberculosis* genome, which has very broad substrate specificity and is therefore able to act against the different β-lactams (82,84,85). Luckily the discovery and development of β-lactamase inhibitors has possibly provided the opportunity to overcome this problem (85,86). The combination of meropenem (a carbapenem) and clavulanic acid (β-lactamase inhibitor) has been shown to not only inhibit the lactamase but also Ldt_{Mt2} (87). This strategy combines different mechanisms of inhibition resulting in a higher, synergistic antibiotic effect. Meropenem alone is already a poor substrate for BlaC, contrary to other β-lactams, and clavulanate is the only FDA-approved β-lactamase inhibitor able to irreversibly inhibit BlaC activity (84). These two drugs together have shown high inhibitory activity on many XDR strains, on aerobically- and anaerobically-grown cultures of *M. tuberculosis* and exceedingly good results with the customary laboratory strains (84). These recent developments reinforce the continued importance of β-lactams in antibiotic treatments.

1.3.2 Current antibacterial peptides

Among current antibacterials, many are of peptide origin. They might be unmodified natural products (as in most successful cases), such as those produced by bacteria themselves to compete against each other for survival, they can be of natural inspiration then modified to improve their activity or toxicity profile, or they can be totally synthetic. Gramicidin D, **24**, is a mixture of hydrophobic linear peptides (where R_1 could be Val or Ile and R_2 Trp, Phe or Tyr) produced by *Bacillus brevis,* active mainly against Gram positive bacteria (88–90). They are ionophore molecules, able to make channels across the phospholipid membrane, increasing its permeability to inorganic monovalent cations (88). It is marketed in combination with dexamethasone and framycetin sulfate as a topical treatment of ear and eye inflammation (91).

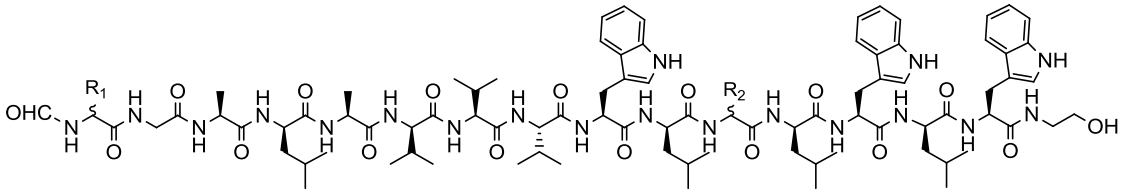

24, Gramicidin D

Vancomycin, **23,** is a glycosylated hexapeptide active against Gram positive bacteria and it is generally used against organisms that have demonstrated resistance to β-lactams. It inhibits cell wall synthesis, specifically the peptidoglycan assembly, by inhibiting transglycosylases (responsible for linking muramic acid and acetyl glucosamine) and transpeptidase (a cross-linking enzyme). It is active in the presence of UDP-Mur*N*Ac-pentapeptide and binds non-covalently to the D-Ala-D-Ala terminus of the peptide (92) blocking the cross-linking between monomers of the PG because of steric hindrance (93).

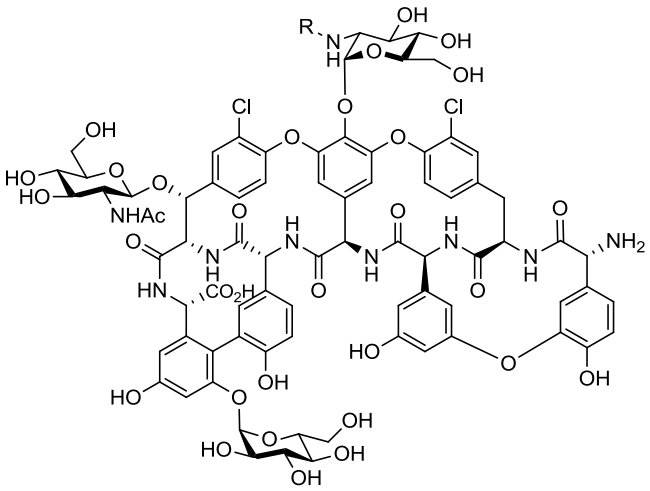

25, Teicoplanin

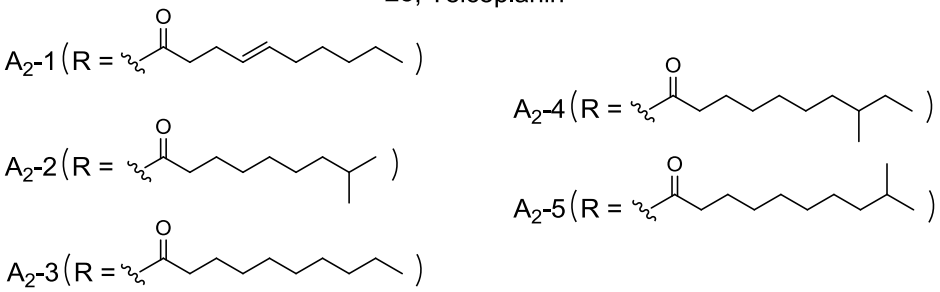

Vancomycin belongs to a family of glycopeptide antibiotics including teicoplanin, **25**, (94). The latter is a complex of natural products produced by *Actinoplanes teichomyceticus*; they are cyclic glycopeptides that inhibit PG polymerisation. Teicoplanin is generally used against MRSA and some enterococci, especially in patients allergic to β-lactams (94,95). The structures of its constituent glycopeptides are similar to that of vancomycin but with an additional fatty acid chain (10-11 carbon atoms), which is the variable component among the five different molecules belonging to this complex.

Pexiganan, **26**, is a linear cationic peptide of 22 amino acids and an analogue of magainin, a peptide isolated from the skin of the *Xenopus laevis* frog (96,97). It is currently in Stage 3 clinical trials for the treatment of diabetic foot ulcers. The product Locilex, a topical foot cream containing 0.8% pexiganan was rejected for FDA approval but the producing company is currently awaiting EMA (European Medicines Agency) Committee for Medicinal Products for Human Use (CHMP) approval through the submission of a Marketing Authorisation Application (MAA) for launch in the European Union (as of 2015, (98)).

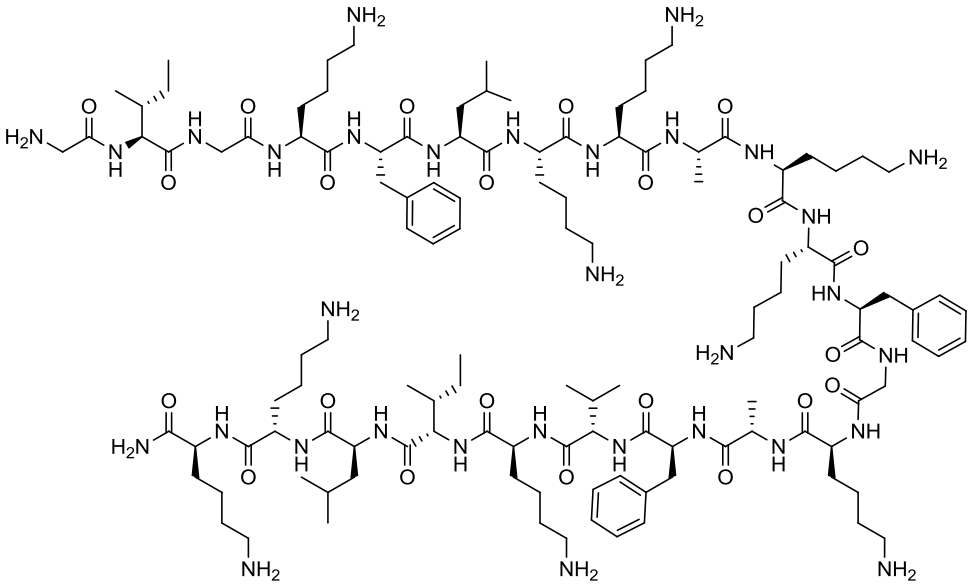

26, Pexiganan

1.3.3 Cyclic antibacterial peptides

Bacitracin A, **27**, is a cyclic polypeptide produced by *Bacillus licheniformis*. It is active against Gram positive bacteria (99) and works by inhibiting the dephosphorylation of undecaprenyl pyrophosphate, a reaction that leads to the regeneration of the lipid carrier involved in PG synthesis (99).

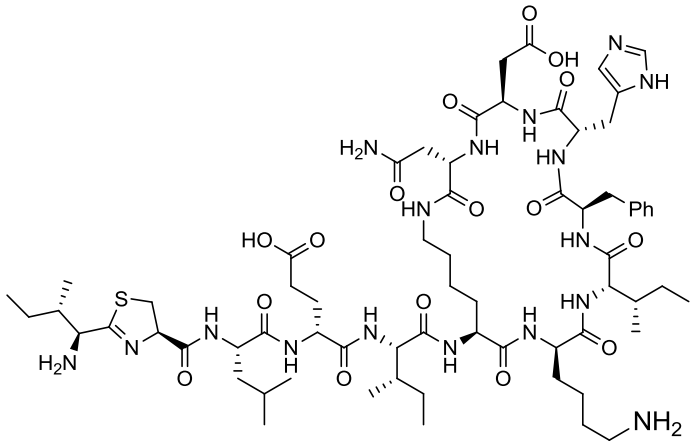

27, Bacitracin A

Bacitracin sequesters the lipid-bound intermediate, via the formation of a ternary complex with a divalent cation, resulting in the reduction of PG precursor availability for cell wall synthesis (100). It is used mainly as a topical remedy in the form of antibiotic ointment for minor skin injuries. In the UK (91) it is marketed as a combination preparation with polymixin B, but the FDA approves its prescription-only

use also via intramuscular injection (101).A depsipeptide is a peptide in which at least one of the amide bonds generally involved in the peptide backbone is replaced by an ester.

Lipodepsipeptides are molecules produced by a variety of bacteria and fungi, with a diverse range of activities. They feature an oligopeptide to which is attached a fatty acid chain of varying length (102). In cyclic lipodepsipeptides (CLPs), part of the peptide portion is condensed to form a lactone ring (102). The general mechanism of action of this class of agents seems to mediate cell death through the formation of pores and the subsequent depolarisation of the membrane (102–104). Among the CLPs daptomycin, **28**, is probably the most well-known; it is licensed for intravenous administration in skin and soft tissue infections caused by Gram positive bacteria, including MRSA, and in endocarditis (91). It is a non-ribosomally synthesised peptide produced by *Streptomyces roseosporus* and is not active against Gram negative bacteria (104).

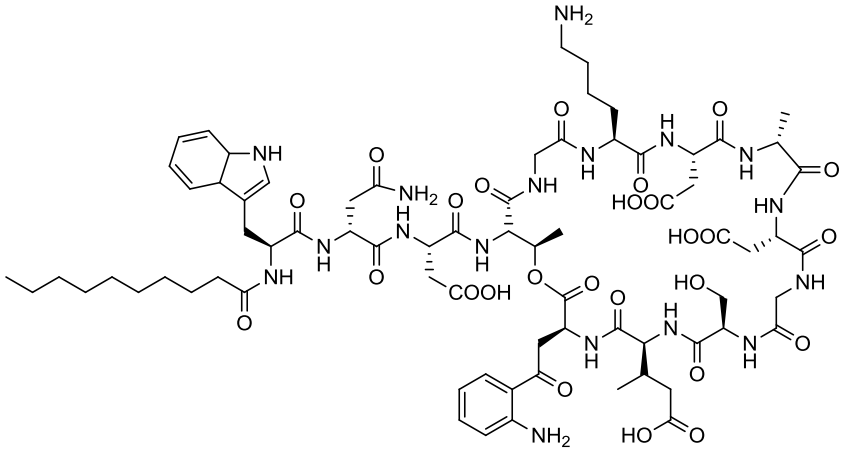

28, Daptomycin

Lantibiotics (105,106) are a group of antibacterial polycyclic peptides that characteristically contain at least one lanthionine (a diamino acid) residue. They are post-translationally modified from a protopeptide via dehydration of Ser or Thr to produce Dha (2,3-didehydroalanine) or Dhb ((*Z*)-2,3-didehydrobutyrine) respectively, which are cyclised via a Michael-type addition of a Cys across the double bond, forming a thioether bridge (106). They have potent antibacterial activity against Gram positive organisms and some of them also possess other types of biological activity (106). They are very promising molecules as they generally combine more than one antibacterial mechanism of action. This feature can become very important when trying to avoid resistance (105).

Another example of cyclic peptides with antibacterial activity is represented by the lasso peptides. These compounds are produced by bacteria and have a broad range of activities, including acting as antimicrobials. They are classified as RiPPs, ribosomally synthesised and post-translationally modified peptides; the polypeptide chain forms a head-to-side chain loop through which the *C*-terminal sequence is threaded. This constrained entropically-disfavoured topology is at the core of their extreme resistance to enzymatic activity (107). The first lasso peptide discovered, Microcin J25 (MccJ25), was isolated from *E. coli* and showed activity against *Escherichia* and *Salmonella* species (107,108). None of lasso peptides are at an advanced stage of research, but they all show promising activities.

Cyclotides are ribosomally-synthesised head-to-tail cyclic peptides found in plants (mainly from *Violaceae* and *Fabaceae*, but also from *Rubiaceae*). These molecules generally comprise 28-37 amino acid residues and they feature several disulfide bridges, resulting in a characteristic cysteine knot structure (109). They have a broad range of activities, including antibacterial activity. As seen for the lasso peptides, their knotted topology confers upon them unusual resistance to enzymatic activity, physical and chemical stress (109,110). These peptides are not yet in clinical trials but there are great expectations for their ability to be scaffolds for the grafting of therapeutic peptides (110).

1.3.4 Anti-tuberculosis peptides

Teixobactin**, 29**, is a recently-discovered and very promising antibiotic of bacterial origin. It is an unusual depsipeptide produced by *Eleftheria terrae* and is active mainly against Gram positive bacteria, including *M. tuberculosis* (111). The MIC found for the susceptible *M. tuberculosis* strain H37Rv was 0.125 μg/mL. The mechanism of action has not yet been identified but intracellular accumulation of UDP-Mur*N*Ac-pentapeptide (in *Staphylococcus aureus*) seems to suggest a link to PG synthesis, more specifically the inhibition of membrane-bound steps. This fact and the observation that no resistant mutants arose in *S. aureus* and *M. tuberculosis* seem to suggest that the mechanism of action is non-specific (111).

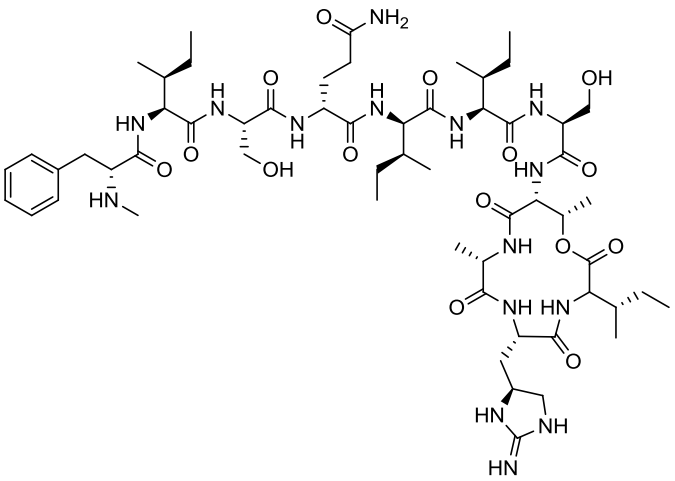

29, Teixobactin

Capreomycin, **30**, is a polypeptide antibiotic first isolated from *Streptomyces capreolus*. It is currently clinically available and it is used as an injectable second-line drug against TB in multidrug-resistant cases (112,113). It binds to the 70s ribosome subunit and inhibits protein synthesis. It actually consists of a mixture of 4 active isoforms, all containing a cyclic pentapeptide core containing L-Ser, 2,3-diaminopropionate, β-ureidodehydroalanine and L-capreomycidine. In two isoforms (IA and IB) a Ser side chain is modified with β-Lys, and in IB the second Ser is replaced by Ala (112).

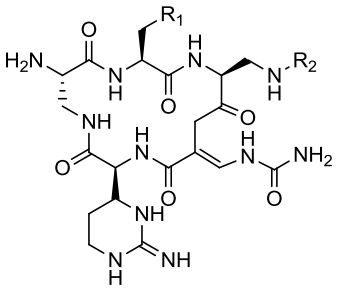

30, Capreomycin
30a, IA (R_1 = OH R_2 = H)
30b, IB (R_1 = H R_2 = H)
30c, IIA (R_1 = OH R_2 = β-Lys)
30c, IIB (R_1 = H R_2 = β-Lys)

Among the already mentioned (Chapter 1.3.3) lasso peptides are the lariatins (A **31** and B **32**), which have shown specific activity against Mycobacteria (114). Furthermore lassomycin, **33**, is a recently discovered cyclic peptide with anti-tuberculosis activity, which might also be classified as a lasso peptide (115,116). Lasso peptides are a heterogeneous group of compounds of bacterial origin. They are all ribosomally synthesised and post-translationally modified by specific

enzymes. These modifications in mature RiPPs generally confer higher stability to the molecules. Within the lasso peptides such modifications include topological remodelling that leads to the formation of the actual “lasso” structure, also known as a lariat (114). This alteration brings the *C*-terminal tail through the ring (generally comprised of 7-9 residues) formed by an amide bond between the *N*-terminal amino group and the side chain carboxy group of an aspartate or glutamate residue, resulting in a structure that resembles a lasso. The direction in which the *N*-terminal cyclic sequence circles around the *C*-terminal tail defines whether the structure is left- or right-handed (107); so far only right-handed molecules have been discovered. This “entropically disfavoured fold” (114) confers exceptional stability, for a peptide, to the molecule. It is clear that such a structure is difficult to recreate. The steps involved require the assistance of specialised bacterial enzymes (114). In fact the tail cannot be threaded through after ring closure because its passage would be impeded by the steric bulk of certain ring and tail residues (114). At the same time the tail needs to be somehow anchored to the ring to maintain the energetically unfavourable conformation. These molecules generally feature disulfide bonds as braces holding the tail in the loop.

The current classification system for lasso peptides is based on the type and number of said constraints. Compounds belonging to class I have two disulfide bonds between the tail and the ring, one of which involves an *N*-terminal cysteine residue. Class II lasso peptides, on the other hand, have no disulfide bond but bulky side chains, that act as “steric traps” (107,114). The only compound so far assigned to class III has one single disulfide bond. As extremely stable peptides that are mostly non-immunogenic, these molecules provide great potential as possible scaffolds for the delivery of drugs (117). Their unique folded conformations, however, present great challenges in being duplicated synthetically.

These peptides generally have intrinsic antibacterial or antiviral activities through a variety of mechanisms of action (114,117). They seem to be produced mainly by Actinobacteria and Proteobacteria (114). Among them, interestingly, two lasso peptides, lariatin A, **31,** and B, **32,** have shown antimycobacterial activity (118–120).

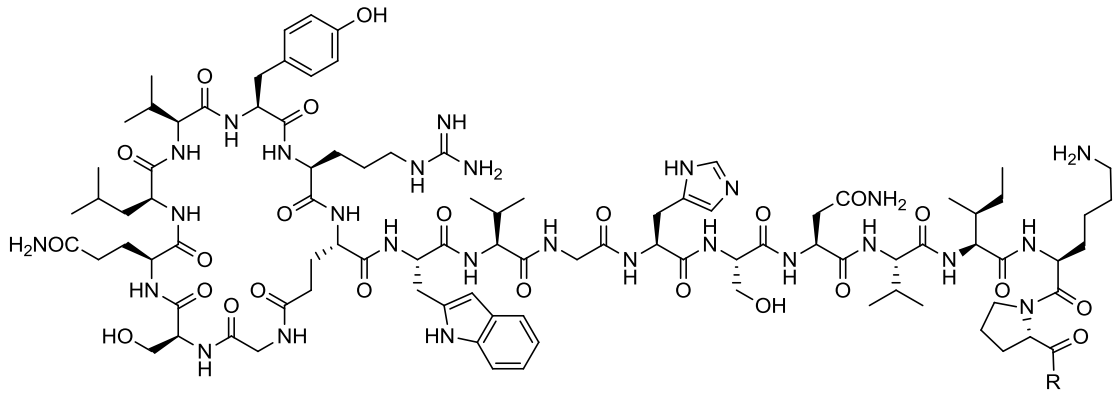

31, Lariatin A (R = OH)
32, Lariatin B (R = Gly-Pro-OH)

They are produced by *Rhodococcus jostii* sp. K01-B0171, an Actinobacterium, and belong to class II, having no disulfide bridges. Lariatin A (18 residues) is a *C*-terminally truncated analogue of lariatin B (20 residues) (118,120). The latter is active against *M. smegmatis* while lariatin A also shows significant bactericidal activity against *M. tuberculosis*.

Lassomycin **33**, is a molecule isolated from a *Lentzea kentuckiensis* sp., an Actinobacterium (115).

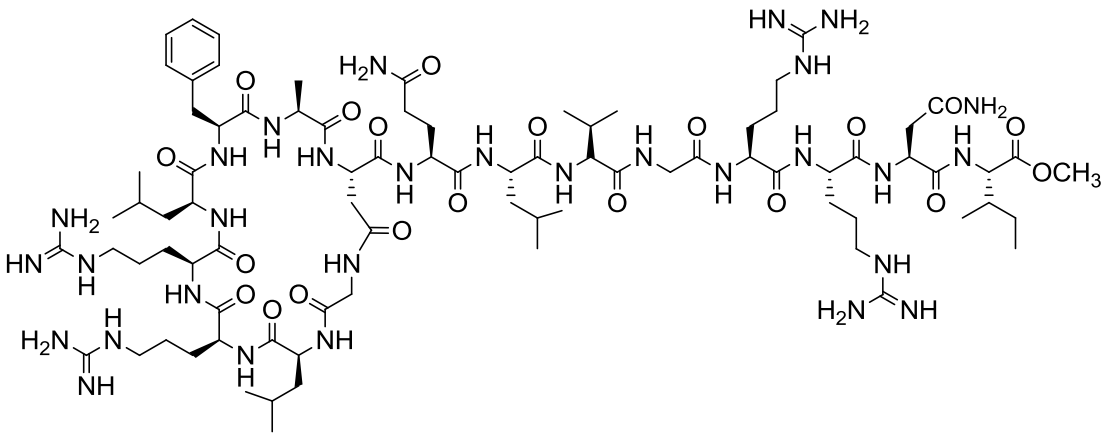

33, Lassomycin

The stability profile of lassomycin, discovered in 2014 (115), matches that of other lasso peptides, but X-ray analysis and structure elucidation studies suggested a non-threaded lasso structure, therefore putting it outside of the standard lasso peptide classifications. Subsequently Lear *et al.* (116) reported the synthesis of lassomycin with this suggested open topology and found out that it had no biological activity against *M. tuberculosis*. This finding may imply that the tail might actually be

threaded through the loop in a manner similar to that of other lasso peptides. This supposition seems to better match the extreme stability of this peptide. An open structure would be more likely to be attacked and degraded by enzymes. At the time this project was conducted, the available literature suggested the unthreaded structure, therefore the synthetic efforts here described were directed towards what was believed to be the peptide in its correct folding.

1.3.5 Peptide synthesis

The production of peptides is based on the formation of the amide bond between two amino acids, an operation called “coupling”.

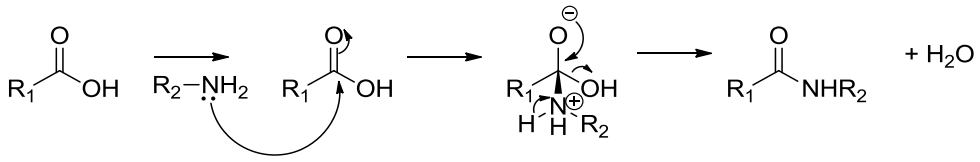

Scheme 1.3 General scheme of peptide bond formation

As carboxylic acids normally react with amines to give salts, in order to obtain the peptide bond, the carboxyl group must be activated, so that it is more susceptible to attack by the amino group of the second amino acid. This means that a leaving group has to be attached to the acyl carbon of the carboxyl group. Activation can be achieved either in a separate step, then adding the amino component, or the acylating intermediate can be formed in the presence of the amino component helped by the introduction of an activating agent. It is even possible to generate the acylating agent separately and eventually purify it before adding it to the reaction. In any case the amino group of the first amino acid has to be temporarily protected, while in the second amino acid the amino group must be free and any other exposed reactive group must be protected. Protection makes these groups unreactive, and permits the carboxyl group to react only with the amino group of the other amino acid (121). For every subsequent coupling step, the amino group of the growing peptide needs first to be deprotected in order to react with the activated carboxyl group of the next amino acid added.

The choice of the protecting groups is extremely important. They should provide orthogonal protection: the permanent protecting groups should be resistant to the deprotecting conditions used to remove the temporary ones. Furthermore all of the protecting groups should be easily removable, without either causing fragmentation of the peptide or modification of any side chain functional groups, at the completion of synthesis. However it has to be taken into account that certain fully-protected building blocks may have poor solubility in the solvent used for coupling.

α-Amino protecting groups

The aim of protecting α-amino groups is to suppress their nucleophilic reactivity either by adding a substituent that draws the electron density away from the nitrogen

atom or that shields it through steric hindrance. Ideally it should be easy to both add and remove the protecting group without compromising either the assembled structure or its configuration. A good option is given by alkoxycarbonyl protecting groups, which are able to transform the amino function into a carbamate, therefore lowering the nucleophilic reactivity of the nitrogen atom. Furthermore these protecting groups can be easily removed by alkyl-oxygen fission, generating the corresponding carbamic acids which will spontaneously decarboxylate to regenerate the amine (121).

The most commonly used alkoxycarbonyl α-amino protecting groups are Boc (*t*-butyloxycarbonyl) and Fmoc (9-fluorenylmethoxycarbonyl).

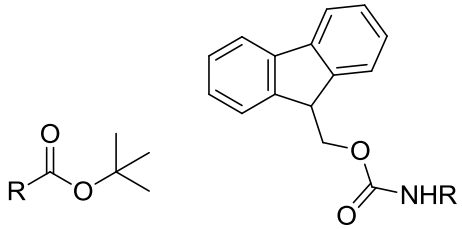

34 **35**

Boc, **34**, introduced into peptide synthesis in 1957, by Anderson and McGregor (122), is widely used both in solution phase and solid phase synthesis (Merrifield type SPPS). It is stable to bases and most nucleophiles and is unaffected by catalytic hydrogenation. In addition, Boc can be introduced and deprotected in good yields and Boc-protected amino acids can be stored in the fridge even for long periods without incurring any deterioration. It can be removed by acidolysis using aqueous HCl or trifluoroacetic acid (TFA) at room temperature (Scheme 1.4). Deprotection via dissolution in TFA, either pure or diluted in dichloromethane, followed by flooding with ether or evaporation, is a fairly common procedure as it involves mild and reliable conditions. TFA protonates the carbonyl oxygen, resulting in the subsequent loss of a stable *tert*-butyl carbocation and the formation of the corresponding carbamic acid. The carbamic acid then spontaneously decarboxylates to give the deprotected amine. The *tert*-butyl carbocation can either be converted to isobutene or be quenched by an available nucleophile (121,123).

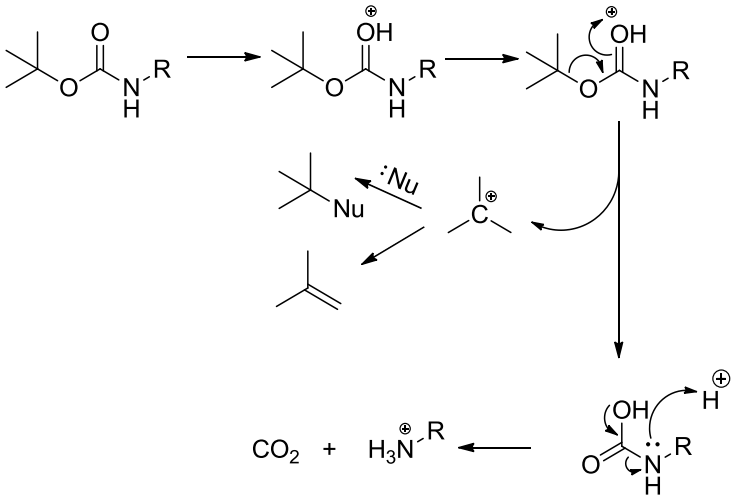

Scheme 1.4 Acid-mediated removal of the Boc group

Fmoc, **35**, is generally and widely used in SPPS, preferably in conjunction with *t*-butyl side chain protecting groups because Fmoc is removed under mild basic conditions, allowing acid-labile groups (e.g. *t*Bu and Boc) to be used for side chain protection. This means that its removal does not affect the stability of other groups, therefore offering true orthogonality. Generally Fmoc is not used in solution phase synthesis because the by-products of its deprotection are non-volatile (121).

When preparing N^{α}-Fmoc-amino acids the use of the hydroxysuccinimide carbonate of Fmoc (Fmoc-OSu) for acylation is preferred because the use of Fmoc chloride can lead to the formation of dipeptide by-products (124).

One drawback of some carbamates is that their cleavage generates a transient carbocation that could eventually modify the product by alkylation. Fmoc deprotection (Scheme 1.5), on the other hand, follows an E1cb β-elimination mechanism. The acidity of H9 on the fluorenyl system allows its removal by weak bases like piperidine, forming a resonance stabilised carbanion. This then eliminates to form the carbamic acid, which subsequently undergoes spontaneous decarboxylation to yield the free amine (rather than the ammonium cation) and the dibenzofulvene by-product (125).

Fmoc is typically removed with a 20-25% *v/v* solution of piperidine in DMF, with the reaction generally complete in approximately 20 min (126).

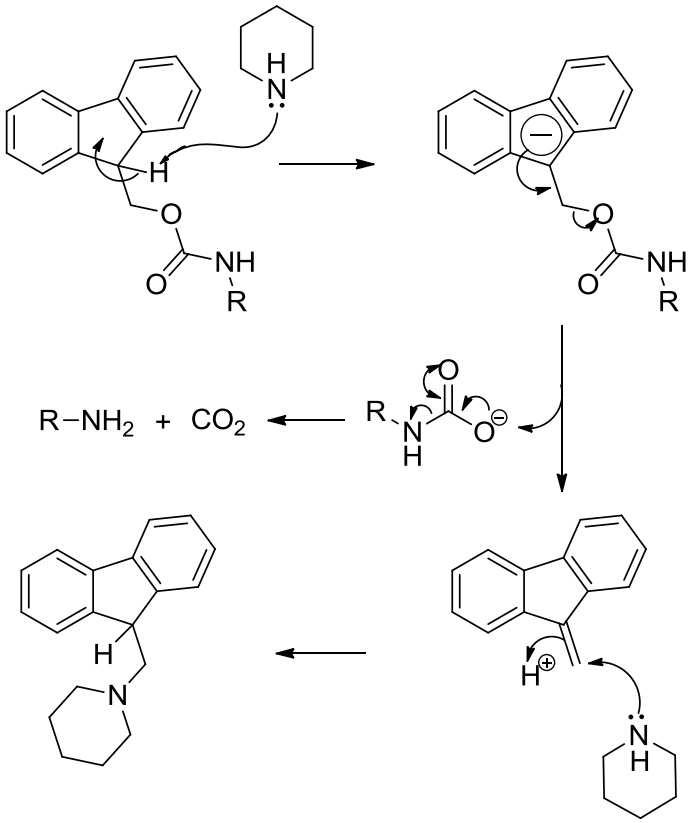

Scheme 1.5 Deprotection of the Fmoc group using piperidine

Side chain protecting groups

Typically the protection of a carboxyl group is easily achieved via esterification. Methyl esters provide good protection – they are stable to HBr/CH_3COOH or TFA treatment at room temperature, they are not affected by catalytic hydrogenolysis conditions, or by thiols or amines in organic solvents (121). On one hand, this means that the amino-protecting groups can be selectively removed; on the other hand, methyl esters tend to be difficult to remove in the final step, often requiring harsh conditions. *t*-Butyl esters are usually inert to nucleophilic and basic attack. Treatment with TFA cleaves any *t*-butanol-based protecting group (generally *t*Bu ester for Glu, *t*Bu ether for Ser and *t*Bu carbamate for Lys), though under milder conditions, when carefully controlled, it is possible to cleave Boc groups and leave *t*-Bu esters in place (121). Benzyl esters, on the other hand, cannot be removed with TFA. They are cleaved by saponification or hydrazinolysis, by treatment with very strong acids such as HBr/CH_3COOH or hydrofluoric acid, or by catalytic hydrogenolysis and they are often unstable as their free bases (121). For these reasons in Fmoc SPPS the preferred side chain protection strategy involves *t*Bu-based groups, while generally when using Boc, benzyl esters are recommended.

Other protecting groups can be selected as long as orthogonality is maintained, therefore side chain protection in Fmoc strategy is chosen to be stable to mild bases, like piperidine and removable by acidolysis with TFA after peptide synthesis is complete.

Coupling reagents

To activate the carboxylic acid group of an amino acid in order to enable the formation of the peptide bond, the presence of an electron withdrawing group that will promote the nucleophilic attack by the amino group of the other amino acid is necessary. Common examples of coupling reagents are carbodiimides and the phosphonium and uronium derivatives (126).

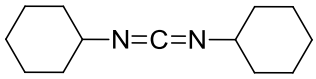

36, DCC

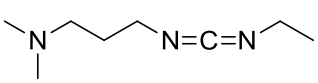

37, EDC

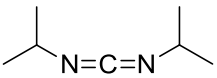

38, DIC

Carbodiimides include *N,N'*-dicyclohexylcarbodiimide **36** (DCC), *N*-(3-dimethylaminopropyl)-*N'*-ethylcarbodiimide **37** (EDC) and *N,N'*-diisopropylcarbodiimide **38** (DIC). The most widely known is DCC, which was introduced in peptide synthesis by Sheehan and Hess in 1955 (127). By addition of the carboxylic acid to the carbodiimide, an *O*-acylisourea (**39**) is formed, which can then be attacked by the nucleophilic amino group of the amino acid (Scheme 1.6). It is also possible that the *O*-acylisourea rearranges via *O*→*N* acyl shift to form the *N*-acylisourea which, on the other hand, is unreactive. This eventuality can be prevented by adding a second equivalent of the carboxyl component that can attack the *O*-acylisourea and form a symmetrical anhydride, which can then react with the amine. The addition of appropriate additives, such as HOBt (1-hydroxybenzotriazole), promotes the formation of an active ester (128), which also serves to reduce the occurrence of side reactions. Carbodiimides in general can demonstrate a propensity to cause racemisation of the activated amino acid as the high reactivity of the *O*-acylisourea can cause its intramolecular cyclisation, leading to the formation of a 5(*4H*)-oxazolone.

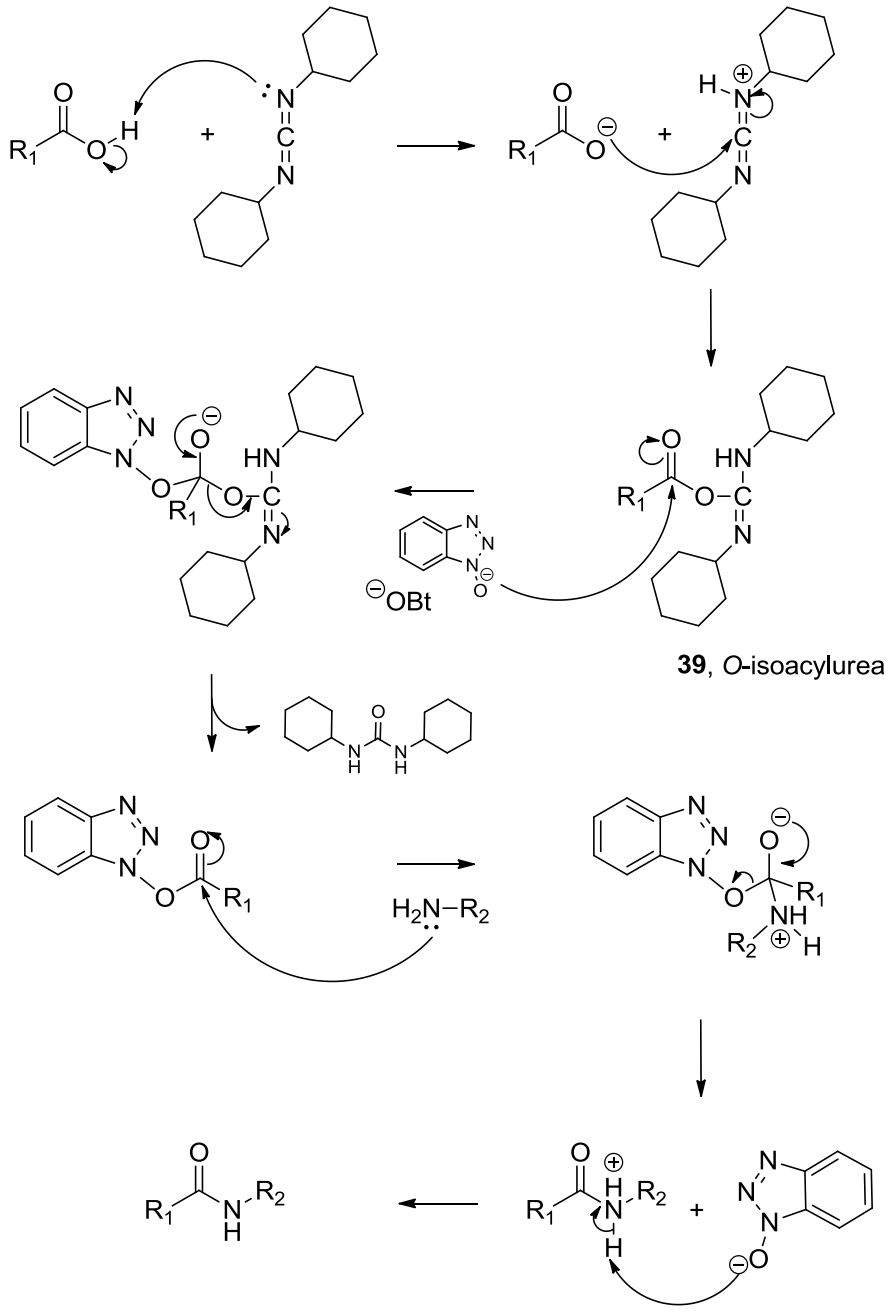

Scheme 1.6 Mechanism of DCC-mediated coupling in the presence of HOBt

Auxiliary nucleophiles like HOBt or NHS (*N*-hydroxysuccinimide) can also help to minimise racemisation, as the active ester formed by reaction with the *O*-acylisourea (or symmetrical anhydride) is less reactive and less prone to oxazolone formation (121).

Another issue is that carbodiimides are not completely selective and they can react with amines to form guanidines. In order to avoid the formation of this unwanted product, the carbodiimide should be added first to the carboxyl component in order

to form the *O*-acylisourea, followed by the addition of the amino component (128). Furthermore it is important that the amount of carbodiimide does not exceed the amount of the carboxylic acid

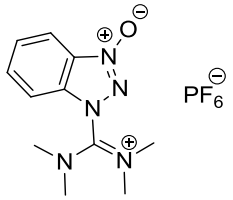

40, HBTU

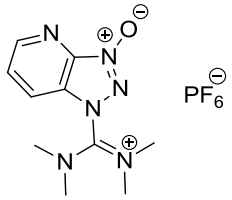

42, HATU

The first aminium/uronium coupling reagent to be used, in 1978, was *O*-(benzotriazol-1-yl)-1,1,3,3 tetramethyluronium hexafluorophosphate (HBTU, **40**) (129); it reacts with the carboxyl component giving an active intermediate and one equivalent of an auxiliary nucleophile (HOBt, **41**), which will subsequently react with the intermediate generating the active ester (Scheme 1.7). Many modifications have been made to the scaffold of HBTU, leading to different analogues with different levels of efficiency, like HATU, **42**, *O*-(7-azabenzotriazol-1-yl)-1,1,3,3 tetramethyluronium hexafluorophosphate (126). Nevertheless HBTU is still widely used. When first described HBTU, and subsequently HATU, was assigned a uronium structure but later X-ray crystallography revealed that it actually was an aminium (or guanidinium) salt (130). The original names though were kept as they were already well-known and widely used.

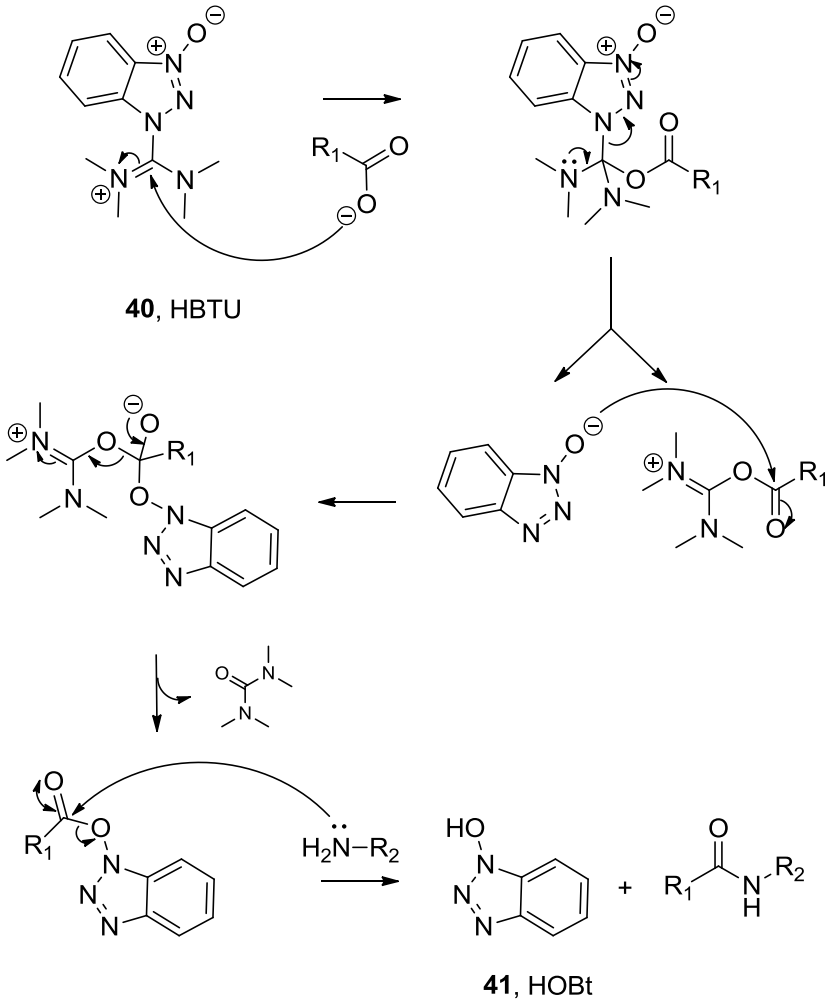

Scheme 1.7 Mechanism of HBTU-mediated coupling

Solid-Phase Peptide Synthesis (SPPS)

The concept of solid phase peptide synthesis was formulated in 1959 by R. Bruce Merrifield, the father of SPPS, when trying to find an easier way to synthesise peptides in higher yields than traditional solution-phase synthesis. The intent was to introduce an insoluble polymer as a solid support for a growing peptide chain covalently linked to it. In 1963 he achieved the first solid phase synthesis of the tetrapeptide H-Leu-Ala-Gly-Val-OH (131). He later optimised the technique by choosing increasingly appropriate matrices, protecting groups and deprotection systems.

The α-amino group of the initial amino acid is masked with a protecting group, while its carboxyl group is attached to the solid support, usually a polystyrene resin, through a linker. Any functional groups on the side chains must be masked with orthogonal protecting groups, which are able to resist the conditions of the reactions in the different following steps. Subsequently the temporary α-amino protecting

group is removed. The coupling of the next amino acid, protected at its α-amino functionality with an appropriate temporary protecting group, is achieved by activating its carboxyl group in order to allow the formation of the amide bond. This usually happens through the generation of an active ester, typically obtained by reaction with a coupling reagent. After coupling, the peptide-resin is washed thoroughly to remove any excess reagents and/or any by-products, and the α-amino protecting group of the dipeptide is removed. The procedures for the coupling and deprotection are then repeated until the target peptide sequence is completed. In the final step, the desired peptide is cleaved from the support and the side chain protecting groups are removed (126).

The development of the SPPS method improved the efficiency of peptide synthesis, allowing savings in time and labour. It became easier to separate the intermediate peptides from soluble reagents and solvents through simple filtration and washing, without the need for extraction, purification and characterisation of the intermediates. This also allows the use of excess of reagents to drive the reaction to completion and minimises physical losses. Furthermore it is a technique feasible for automation, as witnessed by the development of automated peptide synthesisers, leading to a drastic decrease in the time and effort necessary to obtain a peptide.
A potential disadvantage, however, is that incomplete reactions, side reactions and impure reactants can generate by-products that, in the case of SPPS, are resin-bound and can accumulate on the resin to contaminate the final product. Moreover these impurities will have very similar characteristics to the desired compound, making the separation potentially difficult (121). The original Merrifield SPPS strategy used Boc α-amino protection in conjunction with benzyl (Bn) side chain protection. A Merrifield resin can be attached to the *C*-terminal residue of the target peptide by nucleophilic displacement (121). The deprotection and neutralisation leave a free amino group that can readily react with the second, appropriately protected, amino acid using DCC. Unfortunately this combination of protecting groups is not entirely orthogonal, as Boc is removed with a mild acid such as TFA, whereas Bn removal and cleavage from the resin requires a stronger acid, such as hydrogen fluoride. There remains the risk that the repeated use of TFA may result in gradual cleavage of the peptide and/or side-chain deprotection, even though these groups are less acid-labile. Furthermore the reactions are not necessarily quantitative, with the formation of incomplete peptides at each step potentially resulting in significant percentages of contamination. This problem can be partially solved with the use of an excess of acylating agent, or by repeating the coupling

step more times while monitoring the completeness of the reaction with an appropriate method like the Kaiser test (132), able to detect any residual free amino groups. In the event that the coupling reaction still remains incomplete, it is still possible to limit the consequences by "capping" any uncoupled α-amino groups. Acetic anhydride is added to react with the unreacted amino groups. This *N*-acetylation prevents the elongation of these unreacted reactive amino groups, therefore avoiding the formation of deletion peptides (133).

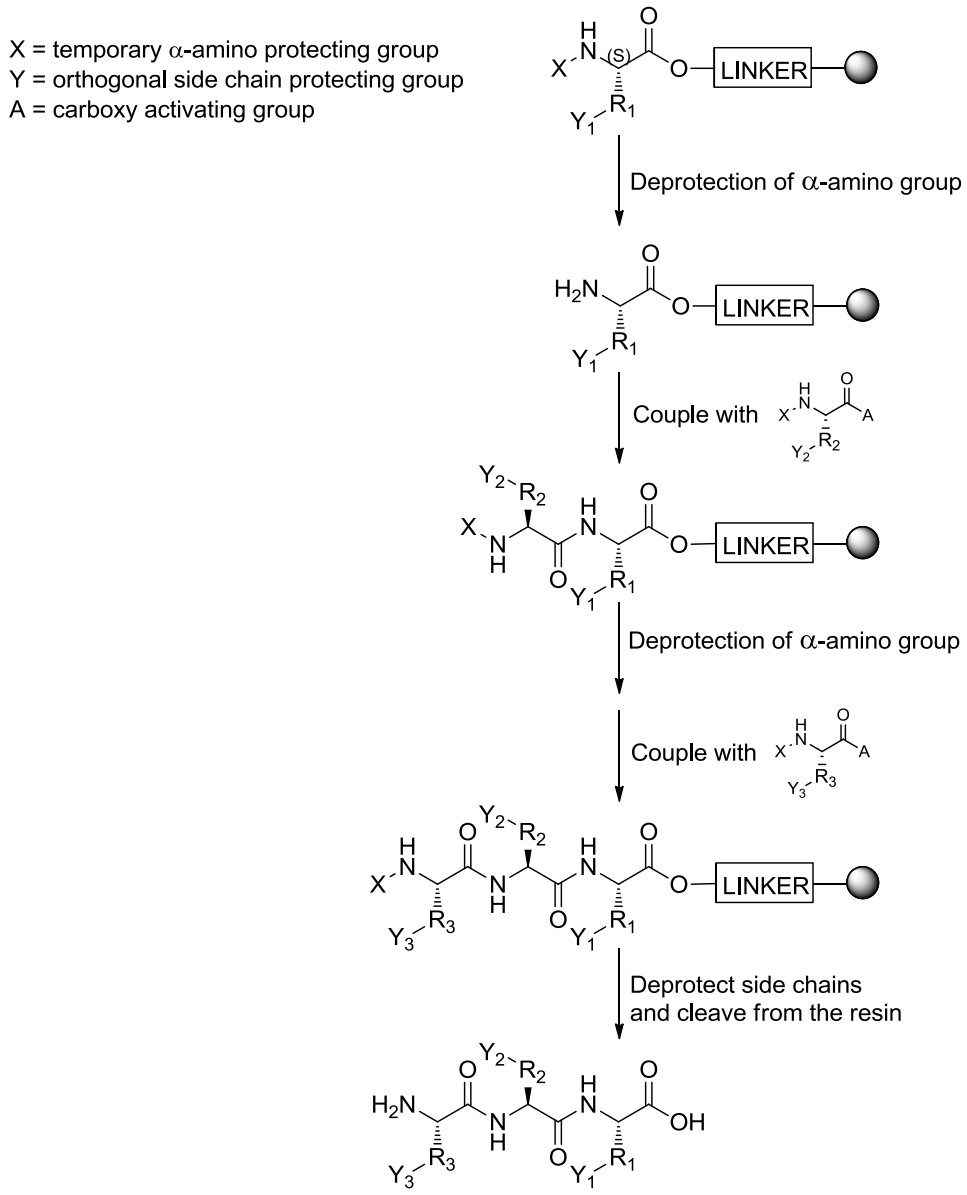

Scheme 1.8 Schematic representation of solid phase peptide synthesis

Modern separation techniques have reached a high level of purification potential and the use of "hyphenated" techniques, for example LC-MS, allows the identification of

the peptides as they emerge. The desired peptide can thus be separated even from complex mixtures.

Sheppard type SPPS, on the other hand, is based on the idea that the polymeric support should have a similar structure to the growing peptide chain and this led to the development of polyamide resins. This strategy usually combines this type of polymeric matrix with Fmoc α-protection and side chain protecting groups that are labile to mild acid. This approach offers complete orthogonality as the repeated removal of the temporary α-amino protecting groups is achieved under basic conditions, while the final side-chain deprotection and resin cleavage are achieved under much milder acidolysis conditions than that used for the Merrifield strategy (126). The milder nature of the reaction conditions used for Fmoc-based SPPS also lends itself to the construction of more complex peptides including glycopeptides and depsipeptides.

Resins

Polystyrene is the most widely used core resin in SPPS and it is generally prepared in the form of spherical beads. Linear polystyrene dissolves in hydrophobic solvents and precipitates in protic solvents, while cross-linked polystyrene is insoluble in almost all common solvents (11). An aprotic solvent will solvate cross-linked polystyrene resulting in swelling, which is important in order to facilitate the diffusion of the reagents into the core of the matrix, shortening reaction times as the resin-bound intermediates behave more like they are in solution.

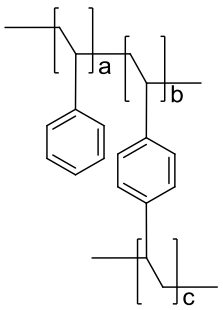

43

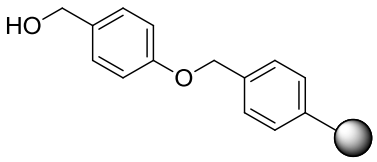

44

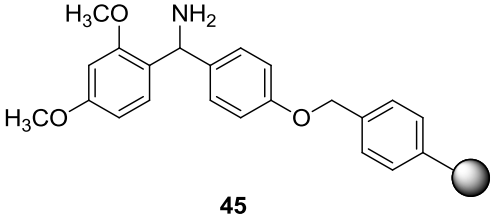

45

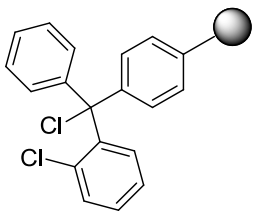

46

Resin linkers can be distinguished between integral, like the Merrifield resin (chloromethylstyrene-divinylbenzene, **43**), in which the linker is part of the matrix itself, and non-integral resins, like the Wang resin **44**, in which the linker is a separate entity attached to the polymer.

The Wang resin **44**, is widely used and incorporates a 4-hydroxybenzyl alcohol moiety attached to the polystyrene core through a phenyl ether bond. It is coupled to the desired amino acid with good stability through the formation of a benzylic ester bond that can be cleaved with moderate acid treatment. Another widely used resin is the Rink amide resin **45,** which has a benzylhydrylamine attached through a benzylic ether bond to the polystyrene core. As with the Wang resin, it can be cleaved using moderate acidic conditions, usually with TFA (121) but, as the Rink amide resin is linked to the peptide through an amide bond, cleavage yields an α-carboxamide. Trityl (triphenylmethyl) resins, specifically the 2-chlorotrityl chloride resin (CTC **46**), are particularly acid-labile (due to the high stability of the trityl cation generated) and can be cleaved with acetic acid. This characteristic becomes useful when less acid-labile protecting groups need to left in place on the peptide. Furthermore, these resins are good for suppressing *C*-terminal racemisation, as their loading doesn't require carboxyl activation. In addition, the steric hindrance of the triphenylmethyl group minimises diketopiperazine (DKP, piperazidinedione) formation (Scheme 1.9).

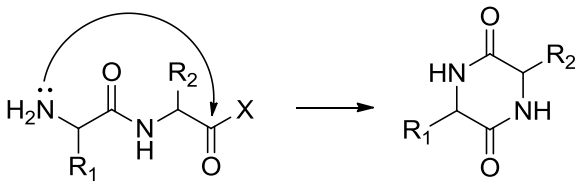

Scheme 1.9 Diketopiperazine formation

The formation of diketopiperazines, **48**, is a common side reaction that can spontaneously occur at the dipeptide stage in peptide synthesis. It is an aminolysis reaction and is triggered generally by basic conditions, even though it has been reported that acidic conditions can also promote it, to a certain extent (134). After deprotection, the free amino group of the resin-bound dipeptide can cleave the resin ester link while forming a DKP. Numerous authors reported unwanted cyclisation and examined the problem. It seems that certain *C*-terminal residues are more prone to DKP cyclisation, Gly and Pro being the most cited ones, but also *N*-methyl

amino acids, Val, Ile and iminoacids. Furthermore it appears that DKP formation is particularly common when dealing with L,D-dipeptides (134,135). According to Bodanszky (135) the tendency towards cyclisation is enhanced in the latter case because the side chains are on opposite sides of the plane of the DKP ring. Bodansky (135) also reported a higher predisposition for cyclisation in Ala-containing dipeptides when compared to the ones containing other lipophilic amino acids. The reaction is well-known in Fmoc-based solid-phase synthesis because of the need for basic conditions (piperidine) to bring about deprotection. The presence of a benzyl ester linkage to the resin also seems to be a common feature for the undesired DKP formation.

1.4 Aims and objectives

In the light of the general quest for better antibiotic therapies able to eradicate increasingly threatening infectious diseases, there are a number of different specific strategies. With tuberculosis there is a growing need to tackle antibiotic resistance and to provide a shorter duration of therapy for susceptible TB that is more likely to be complied with by patients. The search for effective treatments should involve discovery or development of new lead compounds, repurposing of already known ones and also a search for compounds able to enhance the effect of the already available drugs. The latter strategy becomes particularly important in tackling resistance, when effective drugs are rendered useless by acquired resistance mechanisms. Knowledge of said mechanisms will lead to the identification of potential new targets which by themselves might not be essential but become fundamental for the cell survival when fighting against antibiotic attack. Elucidation of a target structure and evaluation of its activity allows the design of molecules able to selectively interact and possibly interfere with it, opening the opportunity for the production of inhibitors. New lead compounds can be obtained as classically done by exploring the activity of antibiotics of bacterial origin and other molecules naturally produced by different organisms as part of their immune response to bacterial attack.

The project will examine a number of different strategies.
The identification in *M. tuberculosis* of a potential antibacterial target, Rv3712, possibly encoding for Mpl, highlights the need to evaluate its activity utilising its possible substrates. This implied:

- The synthesis of suitably-protected D-allylglycine **49** and L-vinylglycine **50** olefin building blocks (Chapter 2.2.3)
- The synthesis, via cross-metathesis of these olefin building blocks, of the unusual amino acid *m*DAP in an appropriately protected form, **51**, to provide the orthogonality necessary for its employment in solid-phase peptide synthesis (Scheme 1.10) (Chapter 2.2.4)
- The solid-phase synthesis of the *m*DAP-containing tripeptide H-Ala-D-Glu(*m*DAP-OH)-OH, which is the putative Mpl natural substrate (Scheme 1.10) (Chapter 2.3)
- The heterologous expression and purification of recombinant Mpl (Rv3712) in *E.coli* using plasmid pCDFDuet-1 carrying the gene of interest (*rv3712*).

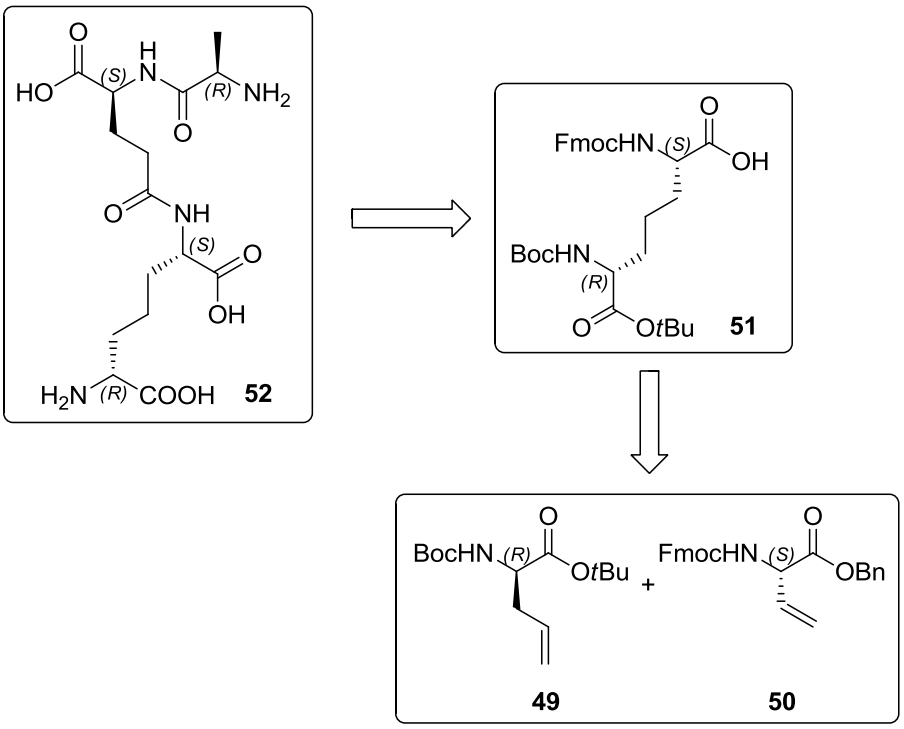

Scheme 1.10 Retrosynthesis of the putative H-Ala-D-Glu(*m*DAP-OH)-OH tripeptide substrate of Mpl

Furthermore, structural analogues of the putative substrate would be a logical starting point for the production of possible inhibitors of the Mpl target. This would require:

- Optimisation of automated solid-phase synthesis methodology (Chapter 2.1.3)
- The manual and/or automated synthesis of Lys-containing PG fragments (Chapter 2.1)
- Testing of the inhibitory activity of the PG fragments on a whole-cell assay, using *Mycobacterium smegmatis*, *M. aurum* and *M. bovis* BCG, and *E. coli* (Chapter 2.1.5.2)

Following on from the general aim, the discovery of anti-TB naturally-occurring lasso peptides inspired a different approach, with the purpose of evaluating if simplified analogues and the non-threaded precursors might retain any level of antibacterial activity. This would require:

- The synthesis of the linear analogues of lariatins A and B (Chapter 2.4.1)
- The synthesis of the linear analogue of lassomycin, and its *C*-terminal free acid derivative (Chapter 2.4.1)

- The synthesis of the cyclic natural products lassomycin and lariatins A and B (Chapters 2.4.1 and 2.4.2)
- Evaluation of the antibacterial activity of the synthesised lasso peptides using a whole-cell assay, using *Mycobacterium aurum*, *Mycobacterium smegmatis* and *Mycobacterium bovis* BCG (Chapter 2.4.4)

2. RESULTS AND DISCUSSION

2.1 *C*-Terminal truncated fragments of PG pentapeptide H-Ala-D-Glu(Lys-D-Ala-D-Ala-OH)-OH

We first sought to synthesise a series of truncated peptides based upon the pentapeptide **53** found in the peptidoglycan of Gram positive organisms. The peptides were truncated from the *C*-terminus, giving the di-, tri- and tetrapeptide (as well as the complete pentapeptide), all starting with the *N*-terminal L-alanine residue. As the *C*-terminal residues of the peptides were different, each synthesis had to be performed independently.

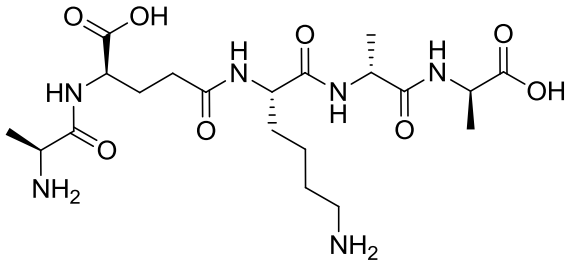

53

2.1.1 Manual synthesis of lysine-containing peptides

While a strategy for the synthesis of *m*DAP was being devised, the H-Ala-D-Glu-OH dipeptide and Lys-containing peptidoglycan peptide fragments were synthesised. These fragments could possibly act as inhibitors of the Mur ligases of organisms generally incorporating *m*DAP in their PG. In addition, they are the natural substrates of Gram positive bacterial Mur ligases, and are therefore also useful to evaluate the ligase activity in such organisms.

The manual synthesis of the tripeptide **54** started from Fmoc-Lys(Boc)-Wang resin. Coupling between the D-Glu and Lys residues required the reaction between the side chain γ-carboxyl group of D-Glu and the α-amino group of Lys. After N^{α}-Fmoc deprotection, coupling of Fmoc-D-Glu-O*t*Bu gave the desired linkage and the tripeptide was completed using standard SPPS, through deprotection followed by coupling of the Ala residue (Scheme 2.1).

The manual synthesis of tripeptide **54** required triple coupling with Fmoc-D-Glu-O*t*Bu in order to obtain a negative Kaiser test result and yielded a product with a crude purity of 42%.

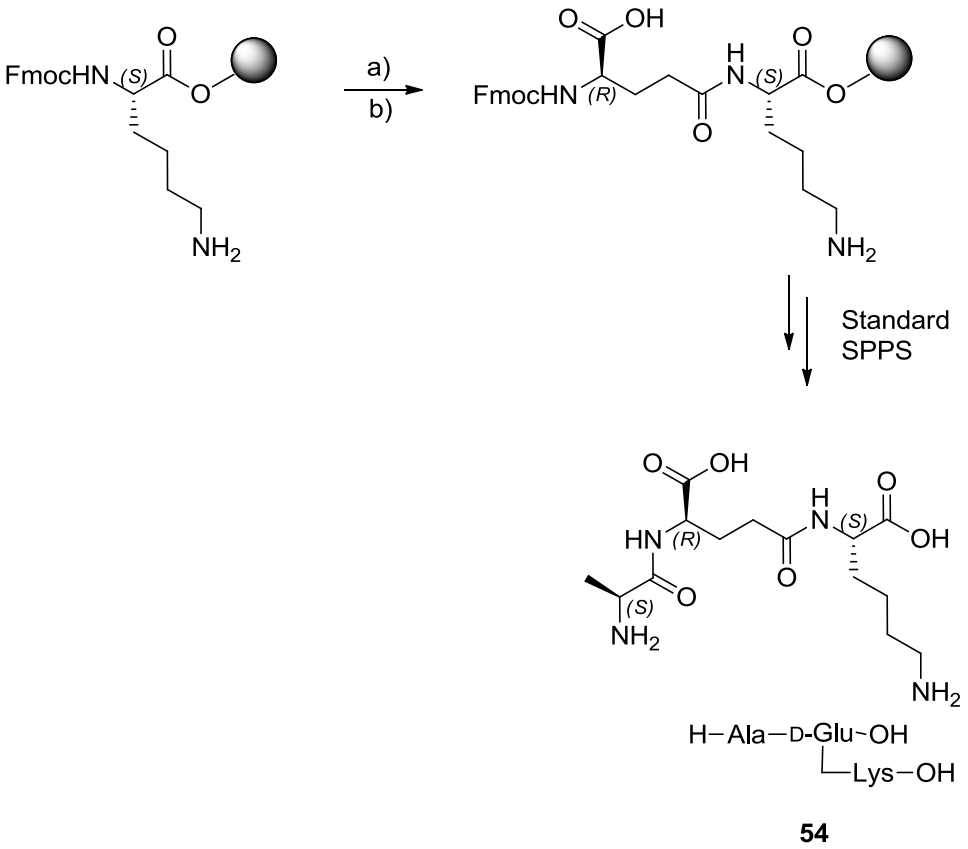

Scheme 2.1 Solid-phase synthesis of tripeptide **54**

Reagents and conditions: a) 20% piperidine in DMF, 2 x 15 min; b) Fmoc-D-Glu-O*t*Bu, HBTU, HOBt, DIEA, DMF, 2 x 30 min.

The manual synthesis of tetrapeptide **55**, starting from Fmoc-D-Ala-Wang, required three cycles with Fmoc-Lys(Boc)-OH to achieve successful coupling and yielded a crude product with a 34% purity. Synthesis was otherwise generally carried out as described for the tripeptide **54**.

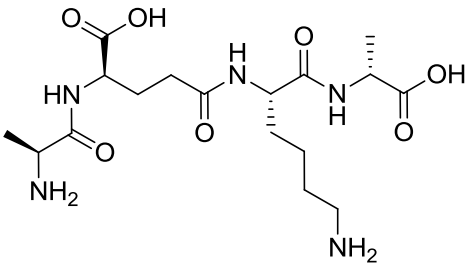

H–Ala–D-Glu~OH
└Lys–D-Ala~OH

55

The manual synthesis of pentapeptide **53,** starting from Fmoc-D-Ala-Wang resin**,** required three couplings with Fmoc-Lys(Boc)-OH and Fmoc-D-Glu-O*t*Bu, and four couplings with Fmoc-Ala-OH to give a crude product with a 36% purity.

Dipeptide **56**, which is one of the naturally occurring substrates for Mpl and MurC both in Gram negative and Gram positive bacteria, was first synthesised manually starting from pre-loaded Fmoc-D-Glu(O*t*Bu)-Wang resin. HPLC analysis showed a disappointingly low 18% purity of the crude product. The analytical HPLC chromatogram showed two substantial secondary peaks (R_t = 7.80 and 10.10 min) eluting after the desired peptide (R_t = 5.68 min). It was suspected that one could be due to the formation of a diketopiperazine (DKP, piperazinedione). Unfortunately it was not possible to efficiently separate the closely-eluting components by preparative HPLC in order to collect a sample of sufficient mass for full characterisation.

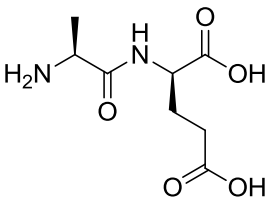

H–Ala–D-Glu~OH

56

As discussed above, the formation of diketopiperazines is a known side reaction, generally triggered by basic conditions, which can spontaneously take place after deprotection of the resin-bound dipeptide in peptide synthesis. In this case the dipeptide is pre-disposed to DKP formation as the two constituent amino acids are of opposite configuration (Scheme 2.2).

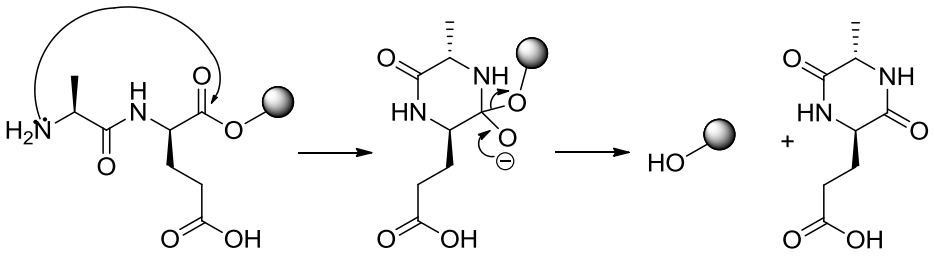

57

Scheme 2.2 The eventual cyclisation of deprotected H-Ala-D-Glu-OH would lead to the formation of a diketopiperazine, 3-(5-methyl-3,6-dioxopiperazine-2-yl)propanoic acid **57**

We therefore attempted to minimise the chances of DKP formation by using a 2-chlorotrityl chloride resin (CTC), which has been shown to protect from undesired early cleavage through the steric hindrance of the bulky triphenylmethyl group close to the esterification site (136).

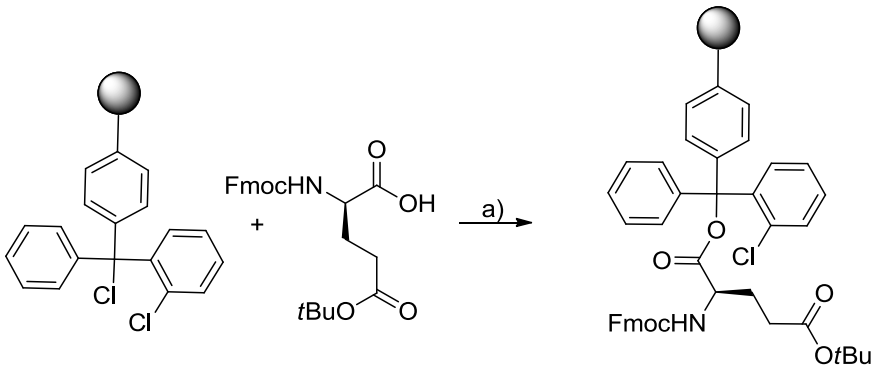

58 **59** **60**

Scheme 2.3 Fmoc-D-Glu(O*t*Bu)-OH loading onto CTC resin
Reagents and conditions: a) dry CH_2Cl_2, DIEA, N_2, 120 min.

Protected D-Glu first had to be loaded onto the resin as shown in Scheme 2.3. CTC resin is very sensitive to moisture and therefore the amount required was thoroughly dried in a desiccator prior to use and the loading procedure was carried out in anhydrous conditions under a nitrogen atmosphere. The dipeptide was completed by Fmoc deprotection and coupling of L-Ala in the normal manner, followed by cleavage. Preparative HPLC led to the successful isolation of the pure dipeptide in 47% yield, the identity of which was confirmed by MS analysis. The analytical HPLC chromatogram highlighted the presence of one single secondary peak, which remains unidentified. This approach represents an improvement over the Wang

resin-based attempt, as the yield recovered is more than double compared to that extrapolated from the HPLC (18%) of the Wang attempt.

2.1.2 Automatic synthesis of lysine-containing peptides

Synthesis of the peptides was repeated using a Biotage Syro I automatic synthesiser. The intention was to compare crude yields and purities obtained manually and automatically to find the best approach for the production of a series of analogues. For ease of comparison the synthesiser was programmed to mimic as closely as possible, given the machine limitations, the standard approach utilised for the manual synthesis (two couplings of 30 min per residue, including initial swelling of the resin in DMF for 1 h). On the other hand, it should be considered that the machine system performs deprotection using 40% piperidine for 3 min, followed by a longer reaction with 20% piperidine, while manually the two deprotection repetitions both consist of 15 min reactions with 20% piperidine. Furthermore automatic coupling was carried out without the addition of HOBt to the coupling mixture. It should also be taken into consideration that some of the manual synthesis required more than two couplings per residue to obtain a negative Kaiser test, while altering the programmed cycles based on the completeness of the coupling reactions would lose the principal advantage of no need for user intervention, provided by automatic synthesisers.

Description	Manual (%)	Automatic (%)	Combined yield (%)
Pentapeptide 53	36	41	43
Tetrapeptide 55	34	59	20
Tripeptide 54	42	61	41
Dipeptide 56 (Wang)	18	37	-
Dipeptide 56 (CTC)	43	-	47

Table 2.1 Comparison between manual and automated syntheses of **53**, **54**, **55** and **56.** The values reported as “manual” and “automatic” represent the percentages of the desired peptide AUC compared to total AUC in the HPLC chromatogram. “Combined yield” represents the yield obtained after purification (System P3) of the combined crude samples obtained from manual and automatic syntheses.

All the *C*-terminal truncated Lys-contaning PG fragments were therefore synthesised again using the automated system mentioned above. The comparison of the crude purities (percentage of total chromatogram AUC represented by the desired peak)

obtained from HPLC analyses of the manually and automatically synthesised samples is shown in Table 2.1.

The crude product purities extrapolated from HPLC chromatograms were deemed sufficient for comparison purposes but in order to be able to utilise the peptides for evaluation of biological activity it was necessary to purify them, therefore the manually and automatically obtained samples were combined prior to purification. The yields of the combined syntheses are shown in Table 2.1.

As the manual synthesis can be tightly controlled, monitoring couplings through the use of the ninhydrin test, and couplings repeated if incomplete, it would have been expected to observe a better purity profile in samples obtained manually. The results, however, indicated the contrary as the automatically synthesised peptides showed higher purities.

For pentapeptide H-Ala-D-Glu(Lys-D-Ala-D-Ala-OH)-OH **53,** manual and automatic syntheses did not differ significantly in terms of purity, though it should be taken into account that three additional coupling steps were performed for the manual synthesis. The automated synthesis was therefore more efficient than the manual one, allowing a saving in material and time.

Repetition of the tetrapeptide H-Ala-D-Glu(Lys-D-Ala-OH)-OH synthesis with the automatic system gave a much purer crude product (59% purity) when compared to the manually synthesised one (34%).

Automatic synthesis of tripeptide H-Ala-D-Glu(Lys-OH)-OH **54** set up with double coupling also significantly improved the purity of the crude product (61%) in comparison with the product from the manual synthesis. A second automated synthesis of **54** gave similar results (55% crude purity) and purification of this sample via preparative HPLC gave the desired peptide in 49% yield.

The synthesis of the dipeptide H-Ala-D-Glu-OH **56** was attempted on the automatic synthesiser starting as before with Fmoc-D-Glu(O*t*Bu)-Wang resin. HPLC analysis of the crude product indicated a crude purity of 37%. Two later-eluting peaks of unknown identity were visible on the HPLC chromatogram, as was the case for the manual synthesis The crude sample was combined with the crude dipeptides from two Wang resin-based manual syntheses for preparative HPLC. Unfortunately, instrumental problems during the purification led to sample loss meaning that the overall combined yields of dipeptide cannot be reliably stated. It is still possible to compare the purities extrapolated from the HPLCs of the crude products. According

to these data the automated synthesis on the Wang resin gave a much better quality product than the manual one. The CTC approach, meant to reduce DKP formation, was the most successful resulting in a greater proportion of desired product (47%) compared to the manual and automated Wang resin samples extrapolated purities (18% and 37% respectively).

It is apparent that the automated syntheses, in general, resulted in crude peptides of better quality than the same peptides synthesised manually. Considering that each manual synthesis required a number of additional couplings to obtain a negative Kaiser test at each cycle, this is perhaps surprising as it might be expected that reactions would proceed similarly during automated synthesis. One possible reason for this could be the consistency of the automated repeated task performance, particularly the efficiency of the mixing and washing steps, which may help to avoid the “operator error”. The use of the synthesiser also reduced the time and the material necessary for the obtainment of the products and required considerably less “operator time” than manual synthesis.

The use of the automated system is therefore advisable even though it might be appropriate, when dealing with expensive or unusual amino acids, to investigate the optimum protocols first manually, in order to avoid excessive loss of precious material.

2.1.3 Syro I optimisation

Automated solid-phase peptide synthesisers are very useful tools for saving time and labour. The question is whether they are as reliable (giving the best chance of a high-quality product) and flexible (able to manage a variety of synthetic steps) as a manually operated synthesis. The laboratory is equipped with a Biotage Syro I synthesiser. This is a programmable single-channel synthesiser with a robotic arm capable of dispensing accurate volumes of liquid reagents and solutions (amino acids, coupling agents) into multiple reaction vessels. Other liquid handling processes (washing, filtration) and mixing are controlled automatically. Up to 24 peptides can be synthesised simultaneously. The instrument has a default SPPS protocol that can be easily customised as preferred. There is a lack of published literature on the rationale for the selection of standard automated protocols used for coupling and deprotection, and typically no indication as to why instrument manufacturers pre-program certain protocols for SPPS. Therefore it was thought that a comparative study would be useful in order to investigate the optimal coupling protocol to be used and to verify how efficient the automated system is. The default

coupling protocol that is pre-programmed on the system utilises a four-fold excess (over resin substitution) of amino acid and HBTU and a two-fold excess (over amino acid residue amount) of DIEA in a single coupling step of 40 minutes. When working manually, the protocol adopted in our laboratory consists of a minimum of two couplings of 30 min each with 2.5 equivalents of amino acid, HBTU and HOBt and 5 equivalents of DIEA. As a starting point, we first evaluated the use of this coupling protocol on the Syro I, but without using HOBt, followed by a series of protocols differing in the number and duration of couplings and the molar excess of activated amino acids used.

Initially a biologically relevant test peptide, Leu-enkephalin **61**, was used throughout the study.*

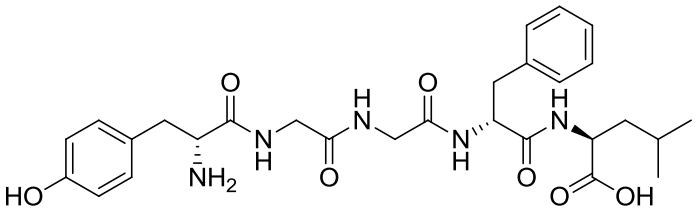

61

In the initial investigation, an identical mass of Fmoc-Leu-Wang resin was used for each synthesis. The automated SPPS coupling protocol was varied from the pre-programmed Syro protocol (entry #1, Table 2.2) to examine the effect on the yield obtained using a different number of couplings with the same individual duration (entries #2 and #5, #4 and #8, Table 2.2) and with different durations but adding up to the same overall coupling time, 60 min (entries #2, #3 and #4, Table 2.2). The duration of the repeated couplings (entries #2 and #8, #3 and #7, Table 2.2) and the number of amino acid equivalents used (entries #2 and #6) were also varied. One further investigation was carried out to evaluate a different work-up procedure to isolate the crude peptide after cleavage. Rather than the standard procedure in our laboratory of filtration after precipitation of the peptide in cold diethyl ether, we examined the use of a centrifuge to sediment the peptide after precipitation with (less volatile) *tert*-butyl ether (entry #9, Table 2.2). All syntheses were repeated in quadruplicate and the mean percentage yield calculated. The maximum expected yield of pure peptide was calculated by multiplying the percentage purity of the crude product (AUC of target Leu-enkephalin peak divided by total chromatogram

* Some aspects of these preliminary studies were contributed to by MPharm project students, Ambica Bhambra and Min Tan, under my supervision.

peak area) by the mass of crude peptide. This method was adopted to remove the recovery from HPLC purification as a factor that might affect the yield. The retention time of **61** was known as an analytical standard was synthesised, purified and analysed.

Entry	Equivalents	Couplings	Time (min)	Crude Purity (%)	SD	Notes
1	4.0	1	40	60	3.5	Syro default method
2	2.5	2	30	69	2.6	
3	2.5	3	20	70	2.5	
4	2.5	1	60	41	1.7	
5	2.5	1	30	66	5.8	
6	4.0	2	30	32	10.8	
7	2.5	3	10	54	3.3	
8	2.5	2	60	35	3.7	
9	2.5	2	30	71	2.7	Centrifuge

Table 2.2 Percentage yields obtained using different protocols for the automatic synthesis of Leu-enkephalin on a Biotage Syro I instrument. Each protocol was carried out 4 times and the percentage yield shown is the mean. The equivalents mentioned in the column title refer to the amino acids and HBTU.

The results obtained were statistically analysed using one-way ANOVA and the test showed that they are not to be considered statistically different. This outcome suggests that different number of couplings do not significantly affect the yield; one coupling of 30 min (#5) gave very similar results to two couplings of 30 min (#2). It also seems that increasing the duration of the coupling reaction may even produce a decrease in yield, as shown by the comparison between entries #4 and #5, involving individual couplings of 60 min, and their correspondent entries #2 and #8, involving double couplings of 30 min. This can possibly be due to the fact that longer reaction time allows an increase in the formation of side products, which will reduce the yield of the desired product. In addition it seems that using a higher number of amino acid equivalents does not necessarily result in an improved outcome; on the contrary, as noticeable by comparing #2 and #6, it appears to have reduced the percentage yield. A possible reason for this result could be that, given that increasing the equivalents produces a higher concentration of reactants is likely to increase the rate of by-product formation, as well as the desired product formation. The use of

centrifugation during the peptide work up seems to not significantly affect the outcome (#2 and #9), which confirms this as a promising method that could be potentially less time-consuming and labour intensive, as well as being more consistent and suitable for higher throughput. A disadvantage is that access to appropriate equipment is required.

A second attempt at the evaluation of the optimal automated synthesis involved the use of an HPLC calibration curve to more reliably calculate the mass of pure peptide obtained from each trial. The calibration curve was obtained by analysing known concentrations of a manually synthesised and purified Leu-enkephalin standard (see Chapter 4.7). The mass extrapolated this way will be more accurate because it won't be influenced by any residual solvent present after freeze-drying or fluctuation in mass due to external factors. The crude product obtained through the Syro I could, once dissolved to make a fixed volume of solution, be analysed via HPLC and the concentration determined from the peptide AUC by interpolation on the calibration curve. At this point, knowing the solution volume, the mass of pure peptide in the crude sample can easily be calculated, avoiding the problem of recovery from preparative HPLC, but in a more accurate manner than the gravimetric method used before.

Entry	Equivalents	Couplings	Time (min)	Crude Purity (%)	SD	Notes
1	2.5	1	40	52	4.5	
2	2.5	1	30	56	1.0	
3	2.5	3	30	57	1.0	
4	2.5	2	30	46	1.5	
5	2.5	1	60	54	0.4	
6	2.5	3	20	61	1.9	
7	2.5	2	15	57	1.8	
8	2.5	2	45	60	0.6	
9	2.5	2	30	55	1.2	No swelling
10	2.5	2	30	66	0.6	Centrifuge
11	4.0	2	30	60	0.2	
12	5.0	2	30	57	2.1	

Table 2.3 Percentage yields obtained using different protocols for the automatic synthesis of Leu-enkephalin (calibration curve method) on a Biotage Syro I instrument. Each protocol was carried out 3 times and the percentage yield shown is the mean.

When performing routine solid-phase synthesis it is conventional to allow the resin to swell in the appropriate solvent before starting the first synthetic step. This ensures solvation of the polymer and aids penetration of reactants and reagents. Each synthesis was therefore preceded by one hour swelling of the resin in DMF, except for one, in order examine the effect, if any, that this step may have on the yield. The experiment involving the use of a centrifuge during work up was also reproduced and evaluated using the current method. Each protocol was repeated in triplicate and the mean percentage yields obtained are shown in Table 2.3.

Statistical analysis of the results using one-way ANOVA showed that the variation between the yields obtained through different protocols are not to be considered significantly different (the centrifuge experiment was not included in the statistical analysis because its outcome is to be considered a result of the different treatment after cleavage). The experiment with the standard conditions used for manual synthesis (entry #4, Table 2.3) gave an unexpectedly low mean yield (46%), which was the result of a quite high standard deviation of the three repeats; the corresponding experiment without pre-swelling (entry #9, Table 2.3) gave a mean yield of 55%. In the light of other results it would seem beneficial to repeat that individual trial (entry #4, Table 2.3) but technical issues at the time made it impossible. For the purpose of comparing yields, when the variable is the duration of each coupling (entries #7 and #8, Table 2.3), a more reliable comparison might be made with the result obtained without swelling (entry #9, Table 2.3). It might be expected that a longer coupling time would improve the yield, but the results obtained with 15, 30 and 45 min couplings are not statistically different. This finding actually agrees with the findings of Fields (137) that most coupling reactions reach a plateau, in terms of percentage completion, in less than 30 minutes and cannot be pushed any further forward by extending the reaction time. In addition, long reaction times may favour kinetically slower side reactions leading to an increased percentage of undesired side products. The duration of the reaction therefore seems not to play a significant role in the yield obtained when performed for longer than 30 minutes. The lack of improvement with increase coupling duration agrees with the results of the first study. Varying the number of couplings also did not result in a significant difference in percentage yield, according with the results of entries #2, #3 and #9, as also found through the previous Leu-enkephalin protocol evaluation (Table 2.2). Partly in contrast to the previous study, the employment of higher amino acid equivalents per coupling (#9, #11 and #12) did not appear cause any significant variation in the percentage yield. The results in this study do not seem to indicate

that increasing the number of equivalents is as detrimental as suggested in the first study.

Collectively, these outcomes likely suggest that the chosen peptide sequence is insufficiently challenging to synthesise, therefore it was deemed necessary to re-evaluate the series of protocols using a more challenging sequence.
Still, it is clear that eliminating the swelling step does not appear to significantly influence the product yield for this sequence (in which the first synthetic step is deprotection). This means that the overall SPPS process can potentially be speeded up by eliminating or reducing the duration of this step as sufficient swelling may occur during deprotection. Furthermore the use of the centrifuge to facilitate isolation of the peptide after cleavage and precipitation has been demonstrated to be at least comparable to, if not slightly better than, the normal filtration-based manual work-up typically employed in our laboratory, from a quantitative point of view. As mentioned above, the use of a centrifuge, depending on its capacity, can allow the post-cleavage work-up of multiple samples at the same time. This is ideally suited for use in conjunction with an automatic synthesiser if several peptides are synthesised simultaneously.

In the light of the outcomes with Leu-enkephalin, the acyl carrier protein fragment ACP 65-74 (**62**) Val-Gln-Ala-Ala-Ile-Asp-Tyr-Ile-Asn-Gly) was selected as an appropriately challenging sequence (138). This peptide has been extensively used as a model to evaluate different aspects of peptide synthesis, due to the difficulties commonly encountered in the coupling reactions and in its purification (138). The progressive elongation results in folding of the peptide and the steric hindrance of side chains reduces peptide-polystyrene solvation which usually renders reactive sites increasingly inaccessible resulting in lower yields (139).

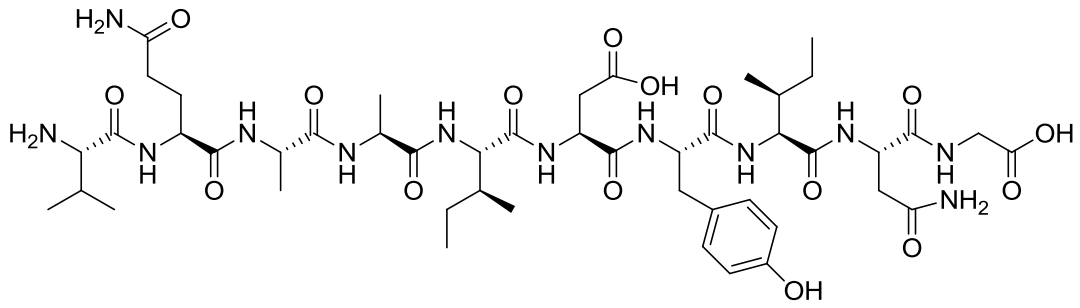

62

In order to prepare a calibration curve, a pure analytical standard of ACP 65-74 needed to be synthesised. Firstly manual synthesis was performed starting from

Fmoc-Gly-Wang resin. Most amino acids required three (or even four) couplings of 30 min (using a 2.5-fold molar excess of amino acid, HBTU and HOBt in the presence of a 5-fold excess of DIEA) for the Kaiser test to be negative. Coupling of the last amino acid, Fmoc-Val-OH, was not complete after five attempts. An extended 4 h coupling using double amounts of reagents, still failed to bring the reaction to completion, therefore a further 4 h coupling, using DIC activation in the presence of catalytic DMAP, was conducted. As the Kaiser test result was still not completely satisfactory, the remaining free amino groups were capped using acetic anhydride. These difficulties agree with previous findings, in which the ACP sequence folds into a β-sheet conformation after coupling of the penultimate Gln residue. This folding makes it very difficult for the activated Fmoc-Val-OH to approach the free *N*-terminal amino group in such a way as to result in acylation (138). Unfortunately preparative HPLC separation of the crude mixture failed to yield any completely pure product, even after a further HPLC purification of the fractions containing the peptide of interest. An automated synthesis on Wang resin utilising double-couplings of 30 min duration for every residue was subsequently programmed. Careful purifications of the crude product obtained led to the isolation of a small quantity of pure ACP 65-74. Serial two-fold dilutions of a standard solution of the peptide and analysis of the resulting diluted solutions via HPLC allowed the construction of the calibration curve. The peptide was synthesised following the different coupling protocols previously evaluated with Leu-enkephalin, with the inclusion of an experiment involving the addition of HOBt to the coupling mixture. This coupling reagent is used, in combination with HBTU, in the standard manual protocol used in our laboratory and, as it is not included in the pre-loaded default automated protocol of the synthesiser, it seemed appropriate to evaluate whether its use affects the outcome. The centrifuge-based work-up was not further examined as its use would not be dependent on the sequence chosen, therefore the results so far obtained were deemed sufficient for its evaluation. Each experiment was performed in triplicate; the samples were analysed and data collected as described previously with Leu-enkephalin. The resulting percentage yields are shown in Table 2.4.

Statistical evaluation using one-way ANOVA shows that the mean yields are not significantly different from each other except for protocol #4. This lack of significance is likely due to the small number of repeats (three) for each experiment. However it appears that, in general, coupling times longer than 30 min do not necessarily offer any improvement (entries #1, #2 and #5, Table 2.4), and that increasing the number of couplings from one to two brings a modest yield improvement (entries #2 and #4)

but further increasing to three couplings has very little, if any, effect (entries #3 and #4, entries #6 and #8). Increasing the molar excess of reactants per coupling does not seem to significantly improve the yield. In contrast to the Leu-enkephalin results, swelling the resin prior to SPPS seemed to have a beneficial effect on this sequence, but the addition of HOBt to the reaction mixture did not seem to offer any significant advantage.

Entry	Equivalents	Couplings	Time (min)	Crude purity (%)	SD	Notes
1	2.5	1	40	21	1.5	
2	2.5	1	30	25	0.5	
3	2.5	3	30	33	1.7	
4	2.5	2	30	39	1.2	
5	2.5	1	60	27	0.3	
6	2.5	3	20	29	2.0	
7	2.5	2	10	27	0.6	
8	2.5	2	20	25	2.2	
9	2.5	2	30	27	1.5	No swelling
10	2.5	2	30	26	1.4	HOBt
11	4.0	2	30	28	2.6	
12	5.0	2	30	32	0.2	

Table 2.4 Percentage yields obtained using different protocols for the automatic synthesis of ACP 65-74 on a Biotage Syro I instrument. Each protocol was carried out 3 times and the percentage yield shown as the mean. One-way ANOVA with Bonferroni correction showed that protocol #4 is significantly different from protocol #1 ($P<0.001$), #2 ($P<0.01$), #5 ($P<0.05$), #7 ($P<0.05$), #8 ($P<0.01$), #9 ($P<0.05$), #10 ($P<0.05$).

Given these results, the protocol analogous to that used for manual SPPS (2 couplings of 30 min employing 2.5 amino acid equivalents per coupling, entry #4) was adopted for subsequent syntheses, because it seems a good compromise between coupling repetitions, duration and material usage especially when compared to the other protocols whose running time adds up to 1 h (entries #5 and #6).

2.1.4 Automatic synthesis of analogues of Gram positive bacterial PG fragments†

After the optimisation of the automatic synthesis, the chosen protocol was used to synthesise a number of structural analogues of the previously synthesised Gram positive bacterial PG fragments. A series of tripeptide sequence analogues was synthesised replacing the L-Ala residue with similar small, lipophilic amino acid residues: L-Val, L-Leu and L-Ile (**63**, **64** and **65** respectively), or replacing the basic Lys residue with an Arg residue (**66**). Similarly, the pentapeptide sequence analogue H-Ala-D-Glu(Lys-Gly-Gly-OH)-OH (**67**), in which both D-Ala residues were substituted by Gly residues, was prepared.

These peptides were each synthesised on 25 μmol scale. Each of the crude peptides was of sufficient quality (judged by their HPLC profiles, >90% purity) to be used for preliminary biological evaluation without further purification.

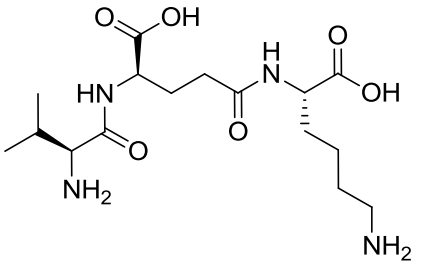

63

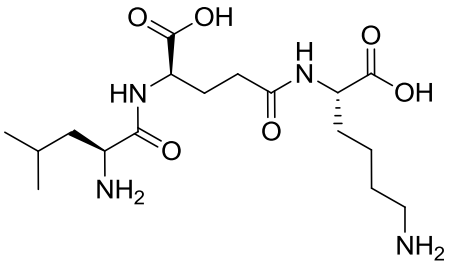

64

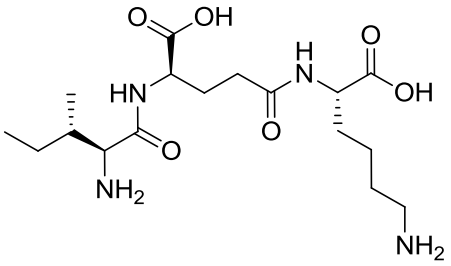

65

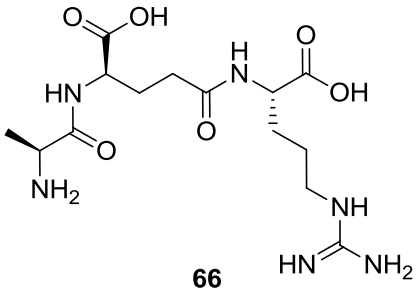

66

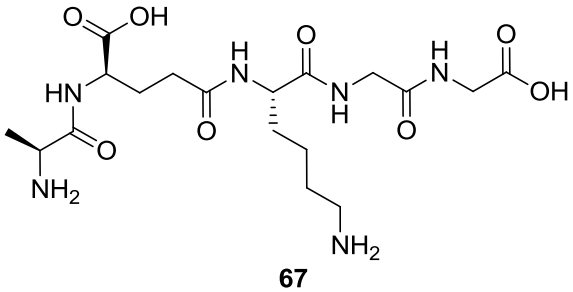

67

† Some aspects of this study were contributed to by a Doctoral Training Programme rotation project student, Yuen Tin Lui, under my supervision.

2.1.5 Biological evaluation

2.1.5.1 Target-based evaluation

Ideally the peptide fragments and analogues were intended to be tested on the heterologously expressed and purified *M. tuberculosis* Mpl, in order to evaluate whether the molecules interact with the target protein and if they exert any type of activity. They were also supposed to be tested on Gram positive bacteria Mur ligases. Unfortunately, due to time restrictions, this testing has yet to be performed.

2.1.5.2 Whole-cell evaluation

The antibacterial activities of the peptide fragments were evaluated using the whole-cell SPOTi assay (as described in Chapter 4.6.5.13), while the isolation of the pure Mpl enzyme was being optimised. The mycobacteria chosen for testing are *M. aurum*, *M. smegmatis* and *M. bovis* BCG. The Gram negative organism used was *E.coli* DH5α. The bacteria were grown as described in Chapter 4.6.5.6. These experiments were intended to demonstrate any degree of growth inhibition by these compounds which could be misincorporated into the peptidoglycan by Mur ligases. Tripeptides **54**, **63**, **64**, **65** and **66** have the potential to specifically interact with MurE and Mpl, while tetrapeptide **55** would be expected to interact with Mpl only, and pentapeptides **53** and **67** with MurF, as they most closely resemble the natural substrates of those enzymes.

The 96-well plate SPOTi method, developed at Birkbeck College (140), is ideal for rapid evaluation of potential antibacterial drugs against the whole cells. Dilutions of the compounds are transferred to a 96-well plate, the plate is filled up with agar, and shaken to achieve a homogeneous dispersion. After drying the plate, bacteria are inoculated on top of the solidified agar and the plate is incubated for the appropriate time. The outcome of the assay is determined by observation of growth, tipically in the form of a spot, and the MIC is assigned based on the lowest concentration of the compound where no growth is visible. Two-fold serial dilutions in water of every peptide were prepared starting from a concentration of 50 mg/mL. Isoniazidwas used as a positive control, with serial dilutions from 5 mg/mL.

The drug dilutions were transferred onto a 96-well plate, followed by addition of agar directly on the plate. Water was used as the negative control. The bacterial liquid culture was then inoculated and the plate incubated at a temperature and for a duration suitable to the organism against which activity was tested (as described in Chapter 4.6.5.13). In the case of *E.coli* the structural analogues of the Lys-

containing PG fragments (**63-67**) were not evaluated because of a lack of material available.

Unfortunately none of the peptides tested showed any inhibition on the whole-cell assay, while the positive control isoniazid showed its characteristic MICs.

This outcome could either be due to the inability of the peptides to reach their target sites or to exert an action on them. In the first case, possibly, the layer of mycolic acids, or the outer membrane in the case of *E.coli*, might be the barrier stopping them from entering the cytosolic space. A previous study on *E.coli* found that the Lys-containing tripeptide was not being accepted as a substrate by Mpl (141). As there are no studies on the permeability of these layers to these compounds it is not possible to draw definitive conclusions from these results regarding their apparent lack of activity in this assay. This is why a target-based assay would be more appropriate.

Furthermore it is not currently known whether these other mycobacteria species possess a gene encoding for Mpl. An ortholog, MSMEG_6276, of the putative *M.tuberculosis* Rv3712, showing 81% sequence homology has been identified in *M. smegmatis* in our group, using bionformatic methods, but has yet to be fully investigated.

2.2 *m*DAP: Access to the putative substrates

2.2.1 The challenges

The main issue that needed to be addressed in order to approach the synthesis of the substrates was how to obtain *m*DAP in a protected form suitable for solid-phase synthesis. *m*DAP is a stereoisomer of 2,6-diaminoheptanedioic acid (Fig. 2.1) in which the two chiral centres (C2 and C6) are of opposite configuration.

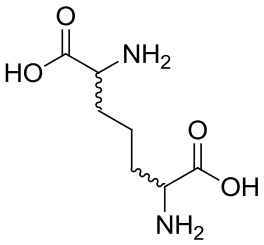

Figure 2.1 2,6-diaminoheptanedioic acid

In a symmetrical molecule with n = 2 chiral centres, like *m*DAP, the number of possible stereoisomers is not 2^n because two of the four possible configurations are superimposable (and therefore identical), as shown in Fig. 2.2. Such a molecule can therefore exist as only three different isomers – (*R*,*R*), (*S*,*S*) and *meso*. The *meso* isomer has opposite absolute configuration (*R* and *S*) at each chiral centre. For this reason DAP can exist as a mixture of three different molecules that are indistinguishable via mass spectrometry.

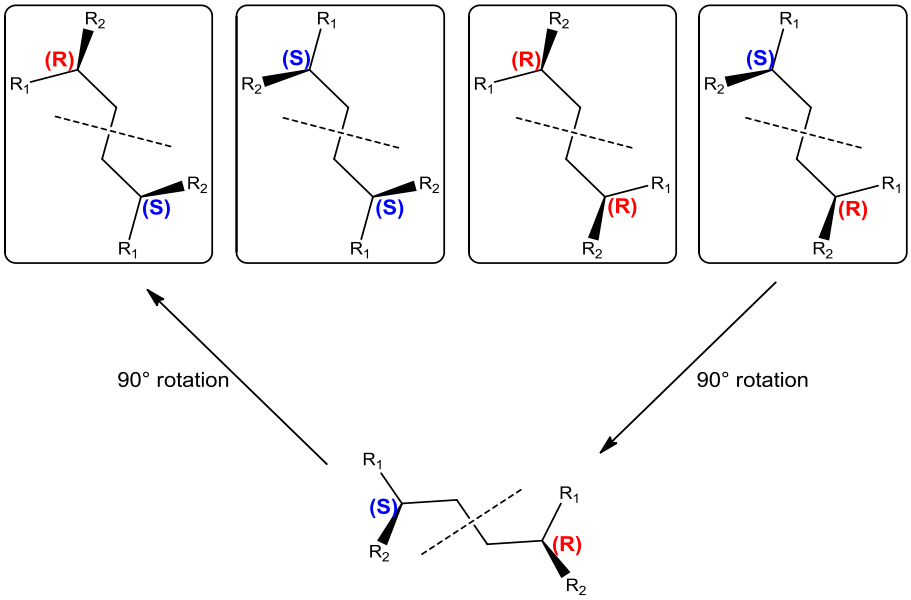

Figure 2.2 Possible configurations of a symmetrical molecule with two chiral centres. The (*R*,*S*) and (*S*,*R*) isomers can be superimposed through a 180° rotation.

The *meso* form could be distinguished from both the (*R*,*R*) and (*S*,*S*) isomers via NMR spectroscopy and liquid chromatography; the (*R*,*R*) and (*S*,*S*) enantiomers would have identical NMR spectra and retention times. Separation of the *meso* form from the other two DAP stereoisomers using a standard reversed-phase HPLC column would not be possible as the molecule is small and the differences in polarity are minimal; a chiral stationary phase would be beneficial.
Isolating the correct isomer would be followed by the issue of finding a protection strategy suitable for solid-phase synthesis. Mycobacterial PGN contains a *meso*-DAP residue, incorporated into the pentapeptide chain through its (*S*)-configuration centre, while the (*R*)-configuration centre forms the free side chain. When incorporated into the peptide backbone, the symmetry is thus lost and the amino acid residue strictly no longer fulfils the conditions of a *meso* compound. Consequently the amino group of the (*S*) centre is the one that needs to be Fmoc-protected and its carboxylic acid group needs to remain unprotected to participate in the solid-phase coupling reaction. For the same reason the (*R*) centre amino and carboxyl groups have to be protected differently, such that the protecting groups remain in place until cleavage of the completed peptide from the resin.

The fact that selectively-protected *m*DAP is not available on the market presents a challenge. *m*DAP can only be purchased in its unprotected form and it is very expensive (£724 for 250 mg from one source). Even if purchased, this would still present the problem of how to differentiate between the identical carboxyl and amino groups. A cheaper (long-term) option available would be the purchase of DAP, followed by isolation of the *meso* isomer on a preparative HPLC chiral column, but still leaving the issue of protection. The most viable option left to access selectively-protected *m*DAP is its synthesis.

2.2.1.1 Stereoselective approaches to *m*DAP and PG fragments

Given the limitations of separating and selectively protecting isomers, the synthetic route of choice should be stereoselective, aiming to obtain the protected *meso* form alone.

Solution-phase synthesis of *m*DAP has been reported through a number of lengthy or inconvenient procedures.

Gao *et al*. (142) tried four different methods: the olefin metathesis skeleton assembly proved unsuccessful due to the propensity of the vinylglycine to isomerise. On the other hand they obtained the desired DAP derivatives following three different routes: an ene reaction employing chiral 2-cyclohexyl auxiliaries gave a

dissatisfying isomer ratio, while the stereospecific reduction of 2-keto-6-aminopimelic derivatives with Binap-ruthenium catalyst and the ene reaction catalysed by a chiral copper oxazoline were more successful yield-wise but nonetheless produced mixtures of the desired DAP diastereoisomers (*meso*- and *S*,*S*-DAP), meaning that separation was still needed (Scheme 2.4). The products obtained with these strategies still contained unprotected carboxyl moieties, leaving the additional problem of how to protect them separately. One further disadvantage of these methods is that they involve a large number of steps.

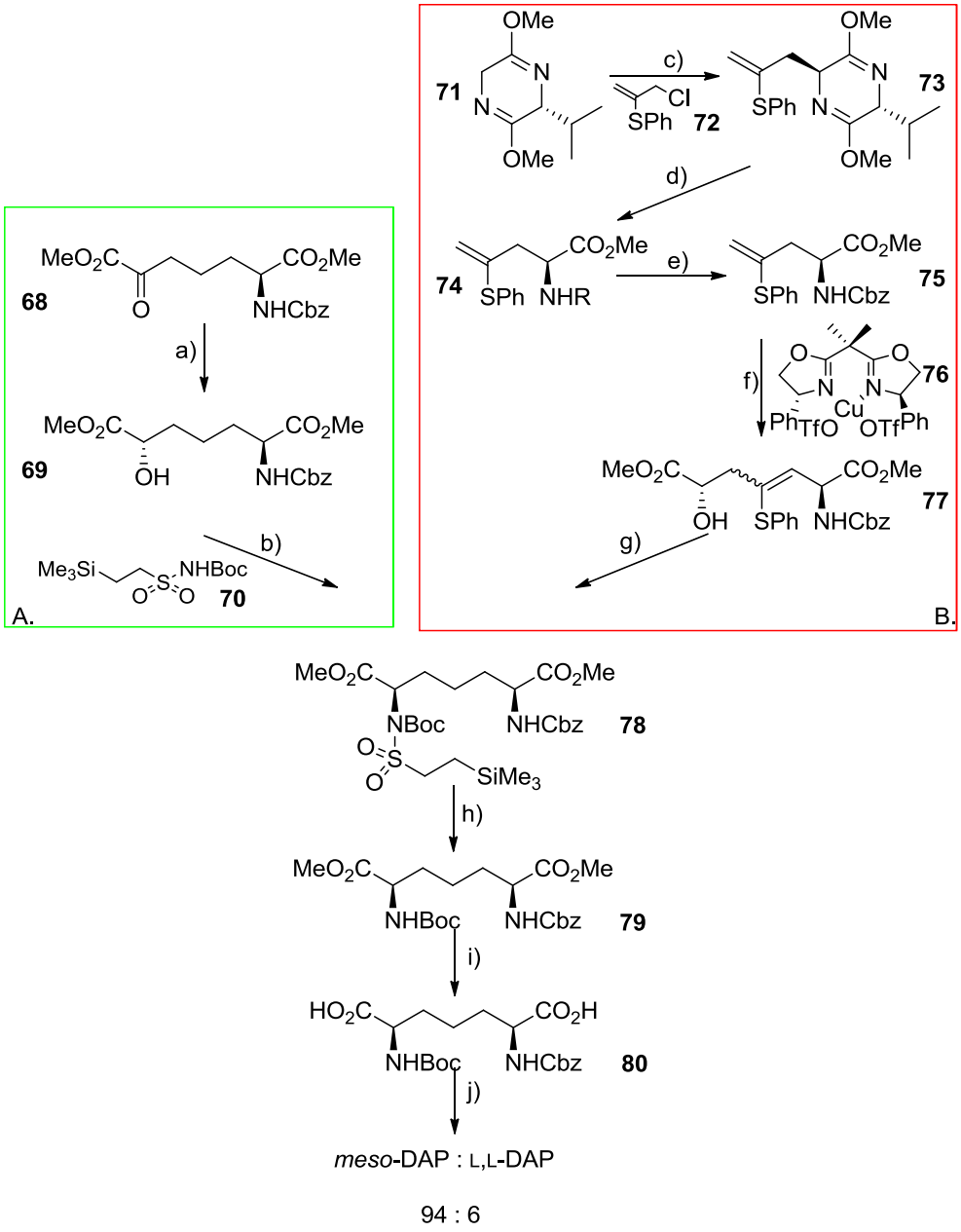

Scheme 2.4 Synthesis of *m*DAP by Gao *et al.* (142)

Reagents and conditions: a) H_2, MeOH, (*S*)-Binap-Ru (II), 4 atm, 100 °C, 4 h, 90%; b) Ph_3P, THF, diethyl azodicarboxylate, 5 h, 79%; c) THF, BuLi, -78 °C, 10 min, sulfonyl chloride, -60 °C, 4 h, 90%; d)

CF_3COOH, THF, 4 h, 79%; e) benzyl chloroformate, CH_2Cl_2, pyridine, 4 h, 98%; f) MeO_2CCHO, (*R*)-2,2′-isopropylidenebis-(4-phenyl-2-oxazoline), Ar, 2 h, 42%; g) $NaBH_4$, $NiCl_2$, 15 min, 42%; h) Bu_4NF, THF, 15 min, 99%; i) NaOH, 4 h, 94%; j) H_2/Pd-C, glacial acetic acid, 14 h; CF_3COOH, CH_2Cl_2, 64%.

In 2007 Inamura *et al*. (143,144) reported the synthesis of derivatives of iE-DAP (H-D-Glu(*m*DAP-OH)-OH) dipeptide **85** from a DAP isomeric mixture, with homoprotected carboxylic groups via solid phase synthesis (Scheme 2.5).

DAP dibenzyl ester was loaded through an amino group onto a 2-chlorotrityl resin, and the remaining free amino group was then acylated with the γ-carboxyl group of Fmoc-D-Glu-OBn. After Fmoc deprotection, the amino group was derivatised with one of a number of acyl substituents using octanoic acid, tridecanoic acid, tetradecanoic acid, pentadecanoic acid, palmitic acid, 4-cyclohexylbenzoic acid, 4-propylbenzoic acid, 4-fluorobenzoic acid, 3-(4-aminocyclohexyl)propionic acid or tetrahydrofuran-2-carboxylic acid (Scheme 2.5).

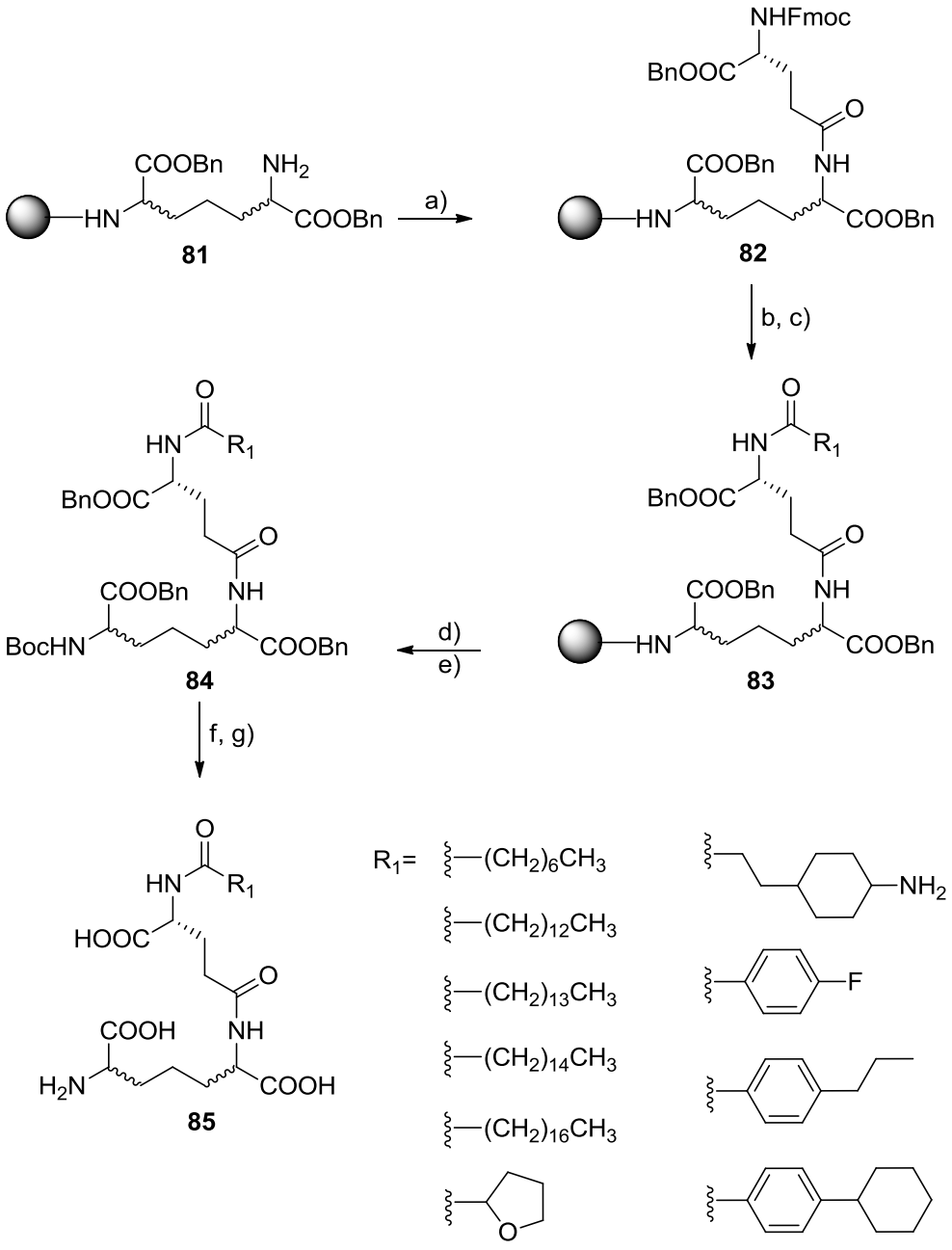

Scheme 2.5 Synthesis of D-Glu(DAP) dipeptide (143)

Reagents and conditions: a) Fmoc-D-Glu-OBn, DIC, HOBt, DMF; b) 20% piperidine/DMF; c) R_1COCl , Et_3N; d) 10% TFA/CH_2Cl_2; e) Boc_2O, Et_3N; f) H_2, $Pd(OH)_2$; g) TFA. Yields vary, depending on R_1, between 24 and 33%, except for the dipeptide bearing the fluorophenol substituent where a 40% yield was reported.

Separation of the different iE-DAP isomers was achieved using a chiral column. The analogues synthesised were used to evaluate the specificity of the interaction with NOD1 (nucleotide-binding oligomerisation domain-containing protein 1), a protein

able to recognise bacterial peptidoglycan products, specifically H-D-Glu(*m*DAP-OH)-OH (143,144) and mediate immune responses.

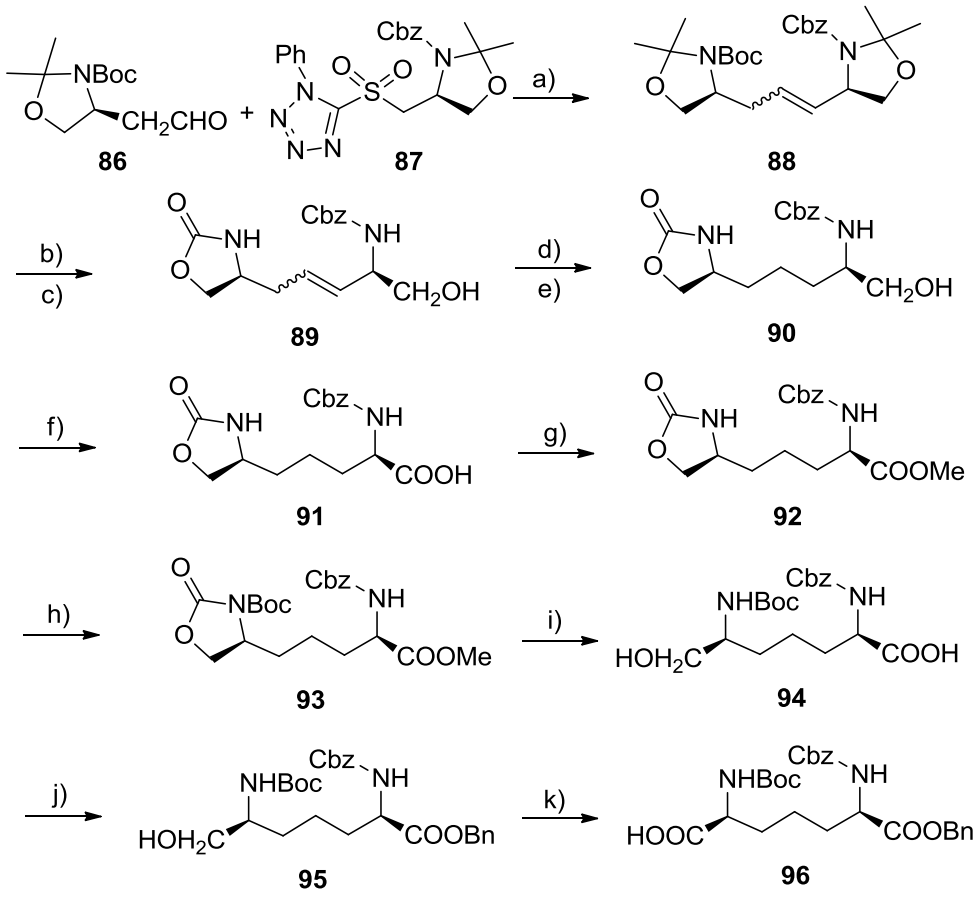

Scheme 2.6 Kocienski-modified Julia olefination (145)

Reagents and conditions: a) NaHMDS, THF, -70 °C, 71%; b) 1 N HCl in MeOH; c) triphosgene, Et_3N, CH_2Cl_2, 22% (over two steps); d) Pd/C, H_2, MeOH; e) CbzCl, $NaHCO_3$, 1,4-dioxane/H_2O 1:1, 82% (over two steps); f) $RuCl_3 \cdot nH_2O$, $NaIO_4$, acetone/H_2O 1:1, 66%; g) AcCl, MeOH, 89%; h) Boc_2O, DMAP, Et_3N, THF, 86%; i) LiOH, THF/H_2O 3:1; j) 1) Cs_2CO_3, MeOH; 2) BnBr, DMF, 83% (over two steps); k) PDC, DMF, 86%.

The same research group successfully synthesised protected *m*DAP starting from an aldehyde, **86**, and a sulfone, **87**, via a Kocienski-modified Julia olefination (Scheme 2.6) (145). Acidolysis of the resulting protected alkene **88**, then treatment with triphosgene to give the cyclic carbamate **89** was followed by alkene reduction and Cbz protection to yield an *N*-Cbz-protected amino alcohol at the *R* configuration centre **90**. Oxidation and protecting group manipulation followed by hydrolysis at the oxazolidinone on the second chiral centre yielded (after Boc re-protection) an *N*-Boc-protected amino alcohol at the *S* configuration chiral centre (**94**). Finally benzyl ester protection and oxidation of the primary alcohol group gave the *N*-protected *m*DAP derivative **96**. The final *m*DAP derivative obtained in this manner displayed

two differently-protected amino groups, one protected carboxyl group and one free carboxyl group. The protecting groups utilised in this approach are not suitable for Fmoc-based solid-phase synthesis and this synthetic route requires a significant number of steps. It was nonetheless successful in obtaining an orthogonally-protected *m*DAP, which was subsequently incorporated in dipeptide and tripeptide fragments (and those conjugated to anhydro Mur*N*Ac) that were used for the purpose of evaluating the stimulation of NOD1 (143,144).

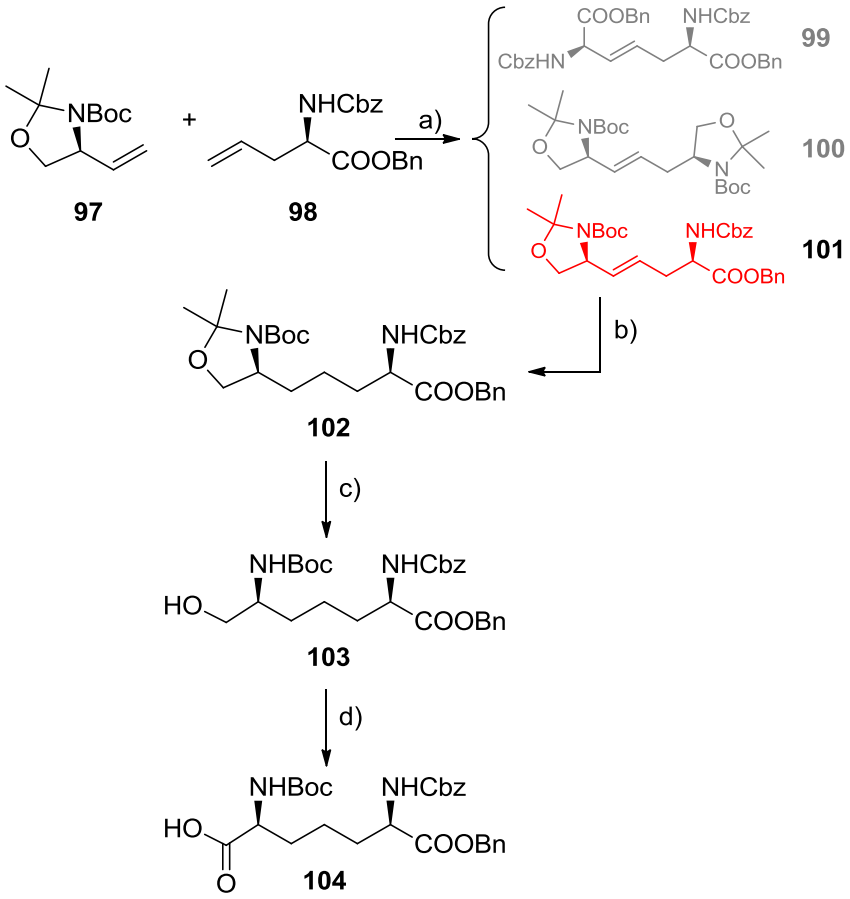

Scheme 2.7 Cross-metathesis of Garner aldehyde-derived vinylglycine derivative and protected allylglycine. Isolation of the desired product is followed by further elaboration to give a partially protected *m*DAP (146)

Reagents and conditions: a) toluene, Grubbs 2nd gen. catalyst, reflux 4 h, 76%; chromatographic separation; b) H_2/cat. PtO_2, EtOAc, 14 h, 97%; c) *p*-TsOH/H_2O, MeOH, H_2O, 36 h, 81%; d) TEMPO, $NaClO_2$, MeCN, H_2O, bleach, 40 °C, 18 h, 94%.

In 2013 Saito *et al.* (146) also reported a method for the synthesis of orthogonally-protected *m*DAP. It was obtained by cross-metathesis between a Garner aldehyde-derived vinylglycine derivative **97** and a Cbz/Bn protected D-allylglycine **98** in the presence of a second-generation Grubbs catalyst (Scheme 2.7).

The cross-metathesis produced three alkenes that could be separated through chromatography. The heterodimer was the required product. Selective reduction of the double bond and hydrolysis of the amino acetal produced yielded amino alcohol **103**. Subsequently the alcoholic group was converted to the carboxylic acid using TEMPO (Scheme 2.7). The protected *m*DAP **104** was then coupled with D-Glu, in order to obtain iE-DAP. This protection strategy could possibly be modified to yield an Fmoc-protected *m*DAP starting from N^{α}-Fmoc-protected D-allylglycine benzyl ester.

2.2.2 Cross-metathesis approach

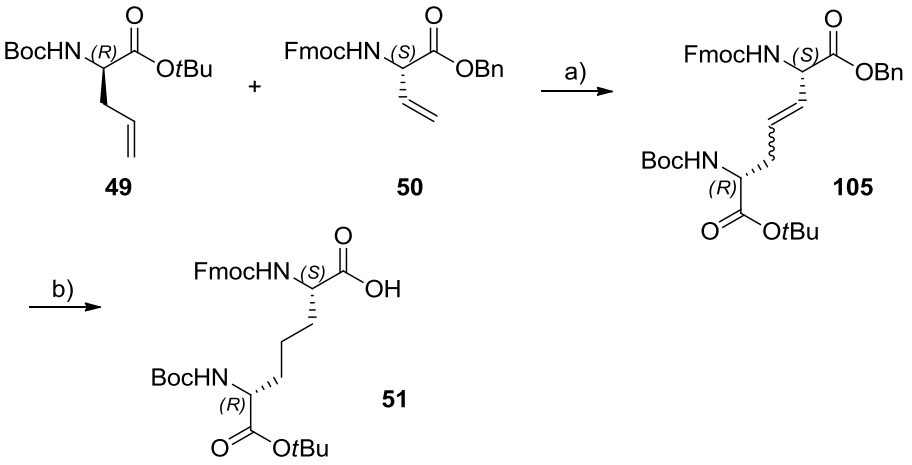

Scheme 2.8 *m*DAP synthesis via cross metathesis (36)
Reagents and conditions: a) Grubbs II gen. catalyst, CH_2Cl_2, 59%; b) Pd/C, H_2, EtOH, CH_2Cl_2, H_2O, >90%.

A simpler stereoselective synthesis of appropriately-protected *m*DAP was successfully achieved by Roychowdhury and co-workers (36,147). The method involved an olefin cross metathesis in the presence of Grubbs second-generation catalyst, and reduction of the β-γ double bond through hydrogenation over a Pd-C catalyst (Scheme 2.8). The reported method was performed starting from D-allylglycine and L-vinylglycine with different combinations of protecting groups. In the reported synthesis (36), the combination of Fmoc-vinylglycine and benzyl protecting groups gave the best yield when combined with Boc- and *t*Bu-protection of the allylglycine fragment. Subsequently *m*DAP-containing fragments of the peptidoglycan peptide strand were synthesised on a solid support using this approach.

2.2.3 Building block synthesis

Roychowdhury *et al.* (36) started the synthesis of *m*DAP from two building blocks: D-allylglycine, which was purchased as the N^{α}-Boc protected *t*Bu ester, and L-vinylglycine, which was obtained according to the procedure described by Pellicciari *et al.* (148) and Salituro *et al.* (149).

In order to access sufficient quantities of these building blocks to attempt a large-scale synthesis of protected *m*DAP, we decided to investigate their *de novo* synthesis.

2.2.3.1 Boc-D-allylglycine-O*t*Bu efforts

2.2.3.1.1 *De novo* synthesis of Boc-D-allylglycine-O*t*Bu

At first we sought to synthesise appropriately protected D-allylglycine *de novo*, obtaining a racemic mixture of N^{α}-acetylated amino acid. This would then be resolved using acylase I from *Aspergillus melleus*, an enzyme able to remove N^{α}-acetyl groups selectively from amino acids with L relative configuration (150).

In the first step, diethylacetamidomalonate **106** reacted with allyl bromide **107**. Different attempts, aimed at improving the recovery, yielded the alkylated intermediate **108** in 31-47% yield.

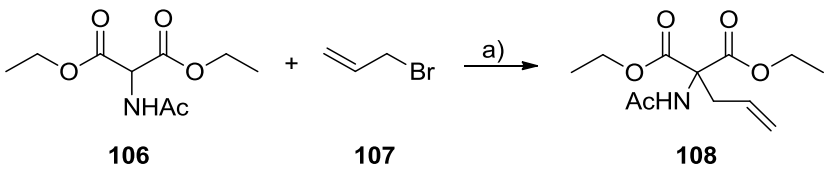

106 **107** **108**

Scheme 2.9 Alkylation of diethylacetamidomalonate
Reagents and conditions: a) Na (solid), abs. EtOH, 24 h, 110 °C, 47%.

After the reaction, ice-water was used to promote precipitation of the waxy product, which was separated from the inorganic salts and excess allyl bromide (liquid) via filtration. The highest yield was achieved by extraction into $CHCl_3$ and concentration under reduced pressure prior to precipitation.

The following step required the removal of one ethoxycarbonyl group and hydrolysis of the other ethyl ester to give the racemic N^{α}-acetylated allylglycine. An initial attempt at complete decarboxylation and hydrolysis (to yield the free amino acid) using HCl was unsuccessful. NMR analysis showed that this attempt resulted in the electrophilic addition of HCl across the double bond. The reaction resulted in four

possible diastereoisomers, **109**, **110**, **111**, **112**, as two pairs of enantiomers in the ratio 79% to 21%, with ^{1}H-NMR signals for γCH at 4.91 and 5.11 ppm. This outcome was anticipated despite a report (151) that suggested the transformation could be carried out without competing electrophilic addition.

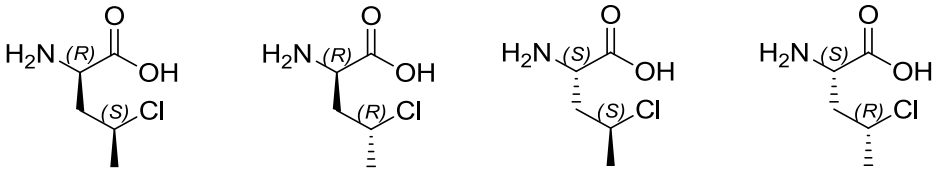

109 **110** **111** **112**

As a result, partial hydrolysis was pursued by refluxing alkylated malonate derivative **108** with NaOH as performed by Lin and Chalker (152). *N*$^{\alpha}$-Acetyl-D,L-allylglycine **113** was obtained with 73% yield and the identity of the molecule confirmed by ^{1}H and ^{13}C NMR.

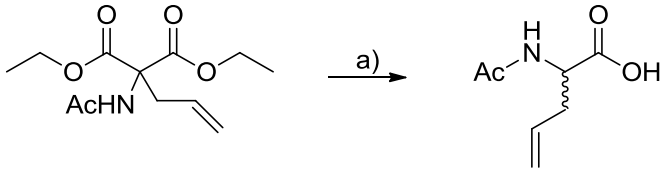

108 **113**

Scheme 2.10 Partial hydrolysis and decarboxylation of diethyl 2-acetamido-2-allylmalonate
Reagents and conditions: a) NaOH, EtOH, 105 °C, 16 h, neutralisation with 2 M HCl, 73%.

The resolution of *N*$^{\alpha}$-acetyl-D-allylglycine and *N*$^{\alpha}$-acetyl-L-allylglycine was attempted through the use of the enzyme acylase I from *Aspergillus melleus.*

As mentioned above, this enzyme selectively removes *N*$^{\alpha}$-acetyl groups from L amino acids leaving a mixture of free L-amino acid and *N*$^{\alpha}$-acetyl-D-amino acid (150). These two molecules should then be separable on the basis of their polarities. The use of a preparative HPLC column would have been ideal and would have allowed the separation and isolation of both pure compounds, but was not suitable given the reaction scale (the crude product masses recovered were 10-20 g). Alternatively, extraction using ethyl acetate was performed. Sequential extractions showed, as expected, that a diminishing mass of *N*$^{\alpha}$-acetyl-D-allylglycine **114** was extracted from the mixture with each further extraction.

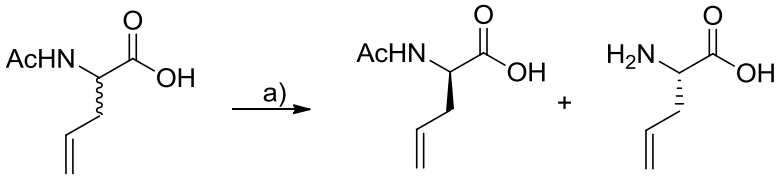

113 **114** **115**

Scheme 2.11 Resolution of the N^{α}-acetylallylglycine racemic mixture
Reagents and conditions: a) acylase I, LiOH, 72 h, 87% (**114**).

The optimised procedure involved two extractions with equal volumes, compared to that of the aqueous solution, of ethyl acetate (recovering 61% of the final mass) then two extractions with an excess of ethyl acetate (1.67 volume equivalents, recovering 24% of the final mass) followed by concentration of the volume of the aqueous phase and one further extraction with a double volume equivalent of ethyl acetate (a further 15% of the final mass). The organic fractions were combined and concentrated to give a mass corresponding to 86% of the theoretical yield. NMR analysis of the organic phase showed a single, acetylated product, therefore believed to be N^{α}-acetyl-D-allylglycine.

The L-allylglycine product **115** needed to be separated from the inorganic salts present in the aqueous phase. Removal of the water and extraction with hot ethanol also resulted in some dissolution of the salts and hence the yield of L-allylglycine could not be reliably measured. This could be an issue that needs to be resolved if the L-isomer has to be recovered. NMR analysis seemed to indicate the absence of any secondary product in the aqueous phase.

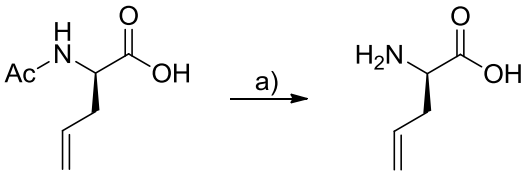

114 **116**

Scheme 2.12 Hydrolysis of N^{α}-acetyl-D-allylglycine
Reagents and conditions: a) 2.5 M NaOH, 60 °C, 24 h; neutralisation with 5 M HCl.

In order to determine the enantiomeric ratio of the products derived from the aqueous and organic phases, Marfey's advanced method was used (153). Firstly a small sample of the organic phase residue was hydrolysed to obtain the free amino acid (Scheme 2.12).

The hydrolysis product **116** was derivatised with 1-fluoro-2,4-nitrophenyl-5-L-alaninamide (FDAA, **117**). This reagent has one chiral center (L relative configuration in this case) and it forms adducts by reacting with the amino group of amino acids. If FDAA is used to derivatise a racemic mixture of amino acids, two diastereoisomers, L,L and L,D, will be formed. As diastereoisomers, the derivatised D-amino acids interact differently with chromatographic stationary phases compared to the derivatised L-amino acids. This difference allows the separation of the two adducts by reverse-phase HPLC, and the L-derivative (in this case) elutes earlier. With a small molecule like allylglycine, a chiral column was beneficial to improve the resolution of the FDAA derivatives.

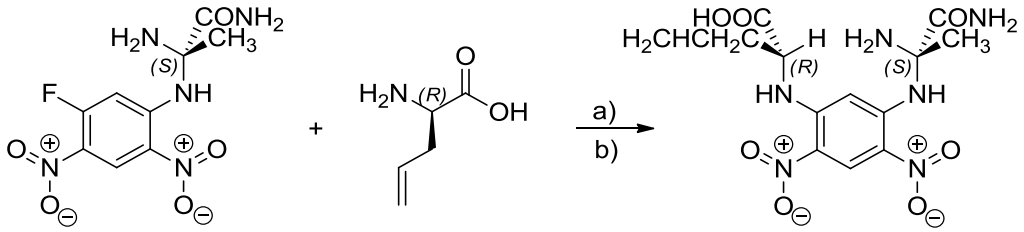

117 **116** **118**

Scheme 2.13 FDAA derivatisation of D-allylglycine
Reagents and conditions: a) $NaHCO_3$ 1 M, 1% FDAA/acetone, 45 °C, 1 h; b) HCl 1 M

The HPLC chromatogram of the derivatised organic phase shows three peaks, corresponding to the free FDAA and the two derivatised allylglycine stereoisomers. Their elution order was determined by overlapping the results obtained from a pure FDAA control and the one from the FDAA derivatisation of the aqueous phase residue, assuming it contains primarily the L-isomer. Hence it was determined that the first component to elute was the residual FDAA, the second one was the L-amino acid derivative and the third was the D-amino acid derivative (Fig. 2.2).

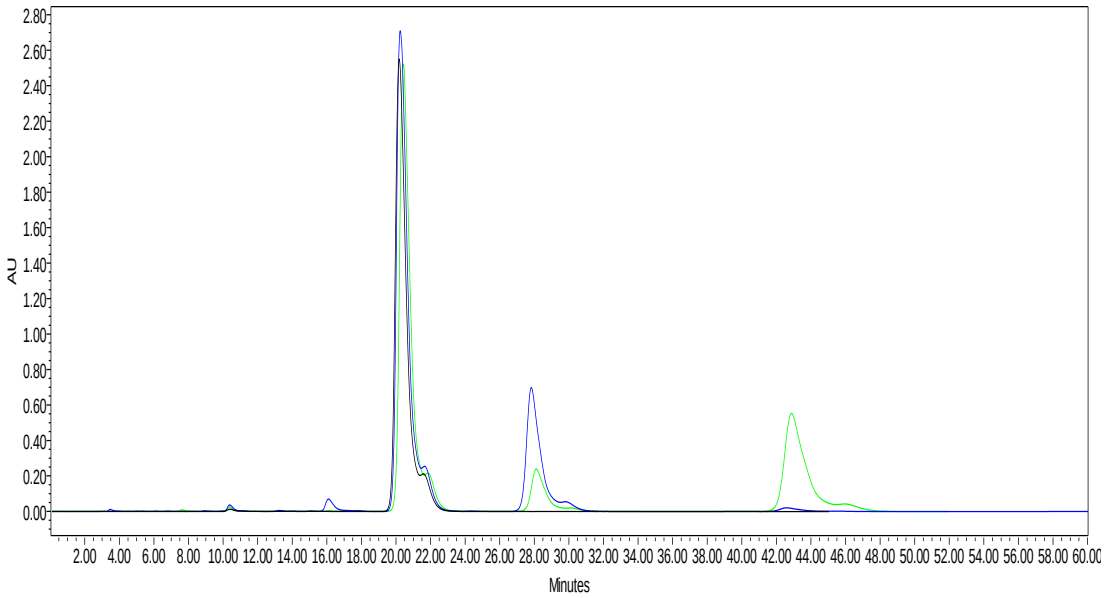

Figure 2.3 Overlapping Marfey's HPLC chromatograms, (black line for pure FDAA, blue for aqueous phase FDAA-derivatised sample, green for organic phase FDAA-derivatised sample)

The crude products of different attempts were hydrolysed and derivatised with FDAA and HPLC analysis showed similar outcomes. The results for the products obtained from the most thorough extraction are presented here and discussed.

The chromatograms from FDAA derivatisation of both the aqueous and organic phases were compared (Fig. 2.3). Integration of the peak areas indicated that the hydrolysed organic phase contains 78% of the expected D-isomer and 22% of the L-isomer, while the hydrolysed aqueous phase showed the presence of 3% D-allylglycine versus 97% L-amino acid. This seems to indicate that the extraction was not fully complete, but that only 3% of N^{α}-acetylated allylglycine was left behind in the aqueous phase. In the light of the results from the organic phase it is likely that the enzymatic resolution failed to hydrolyse all of the L-enantiomer. This would mean that there would be a mixture of N^{α}-acetyl-L-allylglycine, N^{α}-acetyl-D-allylglycine and L-allylglycine in the reaction mixture. Therefore, after the extraction, in the organic phase there would be a mixture of L and D acetylated amino acids and hydrolysis (prior to FDAA derivatisation) would lead to both L and D free amino acids. This explanation is consistent with the NMR spectrum of the product from the organic phase as N^{α}-acetyl-L-allylglycine and N^{α}-acetyl-D-allylglycine would be indistinguishable.

Analysis of a sample of hydrolysed organic phase using a polarimeter measured an $[\alpha]_D$ = +20.0°. Calculation of the expected specific rotation, based on a published

value of +35.0° for pure D-allylglycine (154) and on the 78:22 ratio (D:L) found from the FDAA derivatisation, gives $[\alpha]_D$ = +19.6°. These findings seem to support the enantiomeric ratio found with the FDAA method.

In order to improve the enantiomeric purity of the N^{α}-acetyl-D-allylglycine, the residue from the organic phase obtained in a separate experiment was processed a second time with the acylase. In this way any acetylated L-amino acid that might be left over would be hydrolysed and therefore could be separated through a new extraction. The EtOAc extract from this reprocessed reaction was then chemically hydrolysed with NaOH, refluxing for 24 h at 110 °C to ensure complete reaction. After neutralisation, the isolated crude product was extracted into hot EtOH as described above. Some NaCl (produced during neutralisation) was again present in the mixture after extractions with hot EtOH, but derivatisation with FDAA indicated a composition of 17% L-allylglycine and 83% D-allylglycine.

This enantiomeric purity was not considered sufficient to use the product for the cross-metathesis. The presence of both L- and D-allylglycine in the mixture would lead to the formation of both L,L- and *meso*-DAP. This outcome would jeopardise the enzyme activity assay accuracy in determining the affinity for the substrate, as the substrate composition would be only approximate.

Unfortunately the separation proved itself a challenging step and our experience of the results of the enzymatic reaction proved different to those of the study's authors with this amino acid (150). As a consequence it was decided to set this strategy aside with the intent of investigating the optimal conditions for the acylase reaction in the future, particularly given the commercial availability of D-allylglycine.

2.2.3.1.2 Purchased and protected D-allylglycine

As the enzymatic resolution outcome was not satisfactory and because of the lack of time for further optimisation it was decided to purchase commercial Boc-D-allylglycine, protect its carboxylic moiety as the *t*Bu ester, then to proceed to the cross-metathesis.

2-Allyl-*N*-Boc-D-glycine (Boc-D-allylglycine), purchased from Alfa-Aesar, is commercially available as the dicyclohexylamine (DCHA) salt. Neutralisation of the salt is desirable to avoid any by-products formed by reaction with DCHA. As a secondary amine, DCHA can react with an activated carboxylic acid to give an amide. As many *t*Bu ester protection methods involve activation of the acid, *e.g.* with DCC, it is important to prevent the possibility of reaction with DCHA. With this

purpose the neutralisation is ideally carried out prior to the *t*Bu protection reaction, rather than during. The neutralisation of the salt was achieved through partitioning between ethyl acetate and aqueous potassium hydrogen sulfate, giving pure Boc-D-allylglycine free acid in high yields (> 95%).

Three different methods were evaluated for the the *tert*-butyl protection: first it was attempted (with the DCHA salt) using Boc_2O in combination with DMAP (155), then (with the free acid) with DCC, or DIC, and *t*BuOH with DMAP (Scheme 2.14 a, b and c) (156).

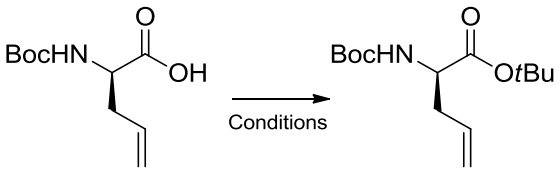

119 **49**

Scheme 2.14 *t*Bu protection of Boc-D-allylglycine
Reagents and conditions: a) Boc_2O, DMAP, *t*BuOH, rt, 24 h or b) DCC, DMAP, *t*BuOH, dry CH_2Cl_2, rt, 18 h, 43% or c) DIC, DMAP, anhydrous *t*BuOH, dry CH_2Cl_2, Ar, 18 h, 60%.

During the first attempt to synthesise Boc/O*t*Bu protected D-allylglycine using Boc_2O and DMAP in *t*BuOH (Scheme 2.14 a) (155)the reaction failed to reach completion after 30 min, which was the reaction time suggested by the original report (157) of this method. As in this case the Boc-D-allylglycine had been used directly as the DCHA salt, one further equivalent Boc_2O was added and the reaction continued up to 24 h. The excess of Boc_2O should have reacted with the DCHA then proceeded to react with the allylglycine. Unfortunately no improvement was observed; TLC analysis throughout the reaction time showed remaining starting material.

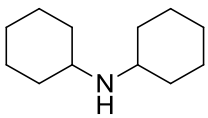

Figure 2. 4 DCHA, dicyclohexylamine

As a consequence, another method using DCC, DMAP and *t*BuOH (Scheme 2.14 b) to protect the carboxyl group as the *t*Bu ester was followed, in the hope of improving the outcome.

In this case the Boc-D-allylglycine·DCHA was first neutralised as described above to allow isolation of the free acid. As the article from Rees *et al.* (158) did not provide full experimental details for this reaction, DCC was first added to the amino acid and the mixture left to stir in CH_2Cl_2 for 30 min, prior to the addition of the DMAP and *t*BuOH, in the attempt to maximise the yield. Again the reaction failed to reach completion but purification afforded the *tert*-butyl ester **49** in disappointing but acceptable 43% yield. NMR spectroscopy confirmed the successful synthesis of compound **49**, showing the typical *t*Bu and Boc singlets at 1.44 and 1.46 ppm respectively.

The third attempt (Scheme 2.14 c) utilised DIC instead of DCC, as the urea by-product derived from DIC is more soluble in CH_2Cl_2 than the one from DCC, which needs to be removed by thorough and repeated filtration prior to the purification, making DIC easier to handle in comparison. The whole procedure was conducted under dry conditions, including the use of anhydrous *t*BuOH, in order to limit the hydrolysis of active intermediates. Even in this case, residual starting material was evident on the TLC plate after 18 h, however the conversion was considered sufficient to proceed to the purification. Significant improvements were obtained by observing strictly dry conditions, using anhydrous *t*BuOH and keeping the reaction under argon. The substitution of DCC with DIC did not hinder the efficiency of the reaction. Given the fact that this reaction was the one that gave the highest yield (60%), it was chosen as the most suitable method for the *t*Bu protection of readily available Boc protected D-allylglycine.

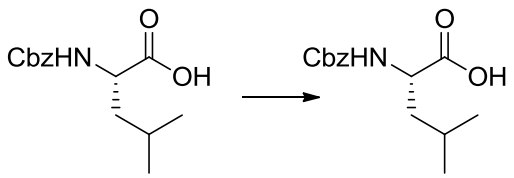

120 **121**

Scheme 2.15 *t*Bu protection of Cbz-Leu-OH
Reagents and conditions: *tert*-butyltrichloroacetimidate, $BF_3{\cdot}Et_2O$, dry CH_2Cl_2, N_2, rt, 16 h.

Another attempt to find a more suitable method for *t*Bu protection was performed using Cbz-Leu-OH – a different and less expensive amino acid – that also has the advantage of being Cbz-protected, making it UV active and easily visualised on TLC. The supplied DCHA salt was first neutralised and the free Cbz-Leu-OH was dissolved in dry CH_2Cl_2. *t*-Butyl trichloroacetimidate (**122**) and the Lewis acid boron trifluoride diethyl etherate (**123**) were added to the mixture and the reaction allowed

to proceed overnight (Scheme 2.15). Unfortunately TLC analysis showed residual starting material in this case; addition of more *t*-butyl trichloroacetimidate and BF_3 and prolonging the reaction time failed to drive the reaction any further towards completion. This approach was not pursued further with the Boc-D-allylglycine.

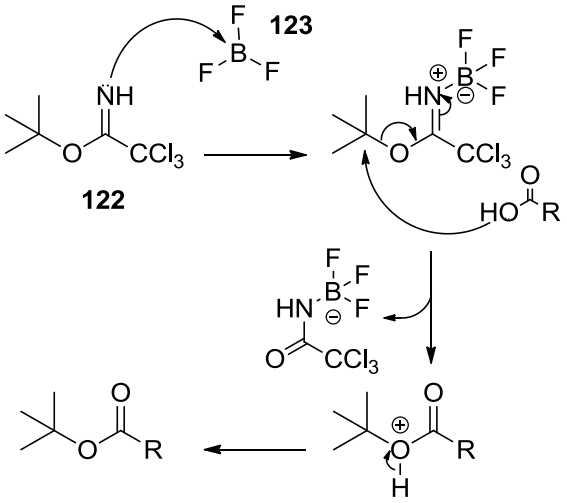

Scheme 2.16 Mechanism of *t*Bu protection with *tert*-butyl trichloroacetimidate and $BF_3 \cdot Et_2O$

2.2.3.2 Fmoc-vinylglycine-OBn synthesis

The second building block required for the cross-metathesis reaction is an appropriately-protected L-vinylglycine, the synthesis of which was attempted through decarboxylative elimination of an appropriately-protected glutamate derivative (159), and alternatively via elimination of the primary alcohol, via a selenide intermediate, from an appropriately-protected homoserine derivative (148).

The reaction published by Hanessian and Sahoo (159) describes a decarboxylative elimination with lead (IV) acetate, catalysed by copper (II) acetate, of N^{α}-Cbz-protected glutamic acid α-methyl ester. This combination of protecting groups is not suitable for this project's intention to synthesise appropriately protected *m*DAP.

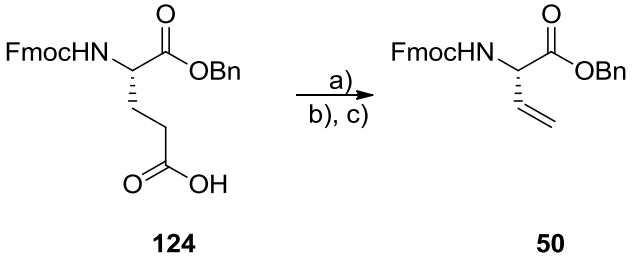

Scheme 2.17 Synthesis of protected vinylglycine from protected glutamate

Reagents and conditions: a) copper (II) acetate, benzene, Ar, 1 h, rt; b) lead (IV) acetate, benzene, Ar, 1 h, rt; c) benzene, reflux 90 °C, 42 h, 2% (over three steps).

A suitable derivative for the intended cross-metathesis requires an L-vinylglycine derivative with Fmoc as the amino-protecting group and a benzyl ester as the α-carboxyl protecting group. This combination of protecting groups will eventually be required for the *S*-configuration centre of the protected *m*DAP precursor (Scheme 2.8). The initial attempt involved the use of commercially available Fmoc-Glu-OBn but since Fmoc-Glu(O*t*Bu)-OH is considerably (*ca*. 25 times) less expensive it was decided to utilise the latter as a precursor for the required substrate. Reaction of the caesium salt of the α-carboxylate with benzyl bromide gave the corresponding benzyl ester, followed by selective acidolysis of the side chain *tert*-butyl ester (Scheme 2.18).

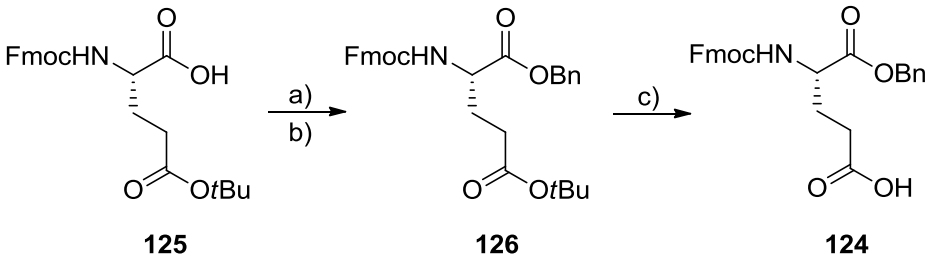

125 **126** **124**

Scheme 2.18 Synthesis of Fmoc-Glu-OBn

Reagents and conditions: a) Cs_2CO_3, MeOH, 0 °C to rt, 20 min; b) BnBr, dry DMF, rt, Ar, o/n, 72% (over two steps); c) 50% CH_2Cl_2/TFA, N_2, 2h, 87%.

One further modification to the conditions used by Hanessian and Sahoo (159) was the length of the reflux. After the prescribed 15 h, the TLC still showed a significant amount of starting material. The reaction was continued for several days, up to one week, to check whether longer reaction times might improve the yield. Increased reaction time seemed initially to improve conversion to the desired product but only up until around 42-65 h, at which time an optimum point in terms of conversion and by-product production seemed to be reached.

Purification by flash chromatography afforded the desired building block in a disappointing yield of 12% and NMR indicated the persistence of a minor contaminant, not detected by TLC.

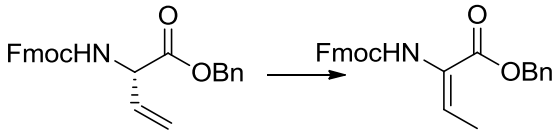

50 **127**

Scheme 2.19 Isomerisation of vinylglycine

There is evidence (160) to suggest that prolonged contact with silica may promote isomerisation of the vinylglycine **50** to the corresponding dehydrobutyrine derivative **127** (Scheme 2.19), which further complicates its isolation and purification.

The other products of the reaction do not correspond to any of the reactants. Hanessian reported only three products from their reaction, but it is important to bear in mind that they used a differently-protected substrate. A subsequent purification allowed the isolation of the pure desired protected vinylglycine, but the yield corresponded to only 1% of the theoretical yield. The mass of the product was not useful for further synthesis but served as a pure standard for the further methods developed.

Further attempts were made to try to improve the yield using the Hanessian method (159). Based upon the time course of the reaction from the first trial, in the following attempts to obtain vinylglycine, the reaction mixture was allowed to reflux for 48 h. Unfortunately after purification the yield obtained was essentially unchanged at a disappointingly low 2%. Therefore it was deemed necessary to find another strategy.

Pellicciari *et al.* (148) accomplished the synthesis of vinylglycine starting from appropriately-protected homoserine. This methodology was investigated as well.

This reaction was first attempted starting from purchased L-homoserine **128**. The amino acid was N^{α}-Fmoc and benzyl protected as shown in Scheme 2.20.

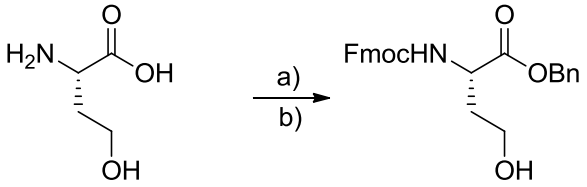

128 **129**

Scheme 2.20 Protection of L-homoserine

Reagents and conditions: a) Fmoc-OSu, $NaHCO_3$, water, acetone, 18 h; b) benzyl bromide, DMF dry, 0° C for 3 h, rt for 18 h; 64% over two steps.

Alternatively the protected homoserine derivative could be obtained from aspartic acid. The published reaction (148) involved carboxybenzyl amino protection and isopropyl carboxylic protection, which did not comply with the protection strategy selected for this project. Conveniently Fmoc-Asp(O*t*Bu)-OH is commercially available and cheap. Therefore (as for Glu above) reaction with benzyl bromide was used to protect the α-carboxyl group, followed by acidolysis of the *t*Bu protecting group on the γ-carboxyl group to yield Fmoc-Asp-OBn **132** (Scheme 2.21).

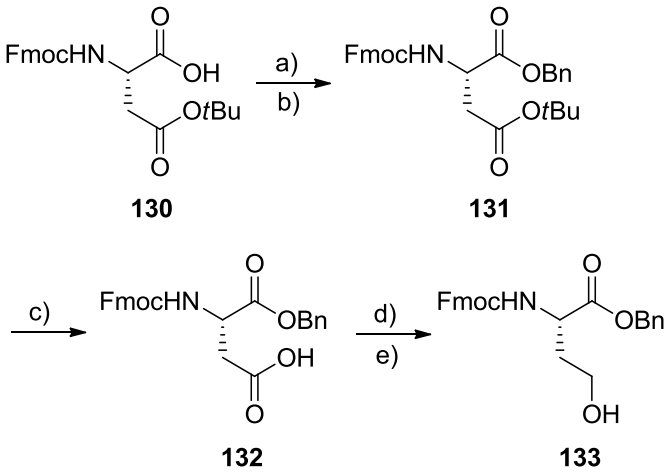

Scheme 2.21 Synthesis of homoserine from protected aspartic acid

Reagents and conditions: a) Cs_2CO_3, MeOH, 0 °C to rt, 20 min; b) BnBr, dry DMF, rt, Ar, o/n, 82% (over two steps); c) CH_2Cl_2, TFA, Ar, 2 h, 89%; d) *N*-methylmorpholine, isobutyl chloroformate, dry THF, -10 °C, Ar; 30 min, e) $NaBH_4$, 2 h, 55% (over two steps).

Vinylglycine was obtained via a Grieco-modified Mitsunobu protocol (148) for the primary alcohol elimination using *o*-nitrophenylselenocyanate and tributyl phosphine, resulting in the desired terminal alkene **50** (Scheme 2.22).

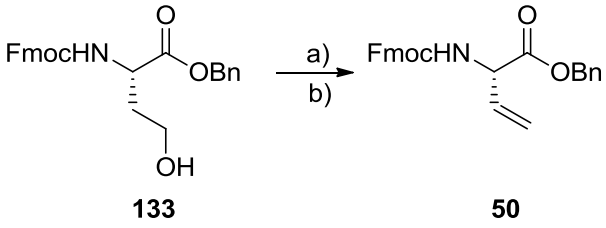

Scheme 2.22 Synthesis of Fmoc-vinylglycine-OBn from appropriately-protected homoserine, via elimination of the primary alcohol

Reagents and conditions: a) tributyl phosphine, 2-nitrophenylselenocyanate, THF, rt, 3 h; b) 30% H_2O_2, rt, 18 h, 45% (over two steps).

In this reaction (Scheme 2.23), the alcoholic oxygen is converted into a good leaving group leading the formation of selenide **134**, which is subsequently oxidised to a selenoxide **135** and eliminated to release the terminal alkene (161).

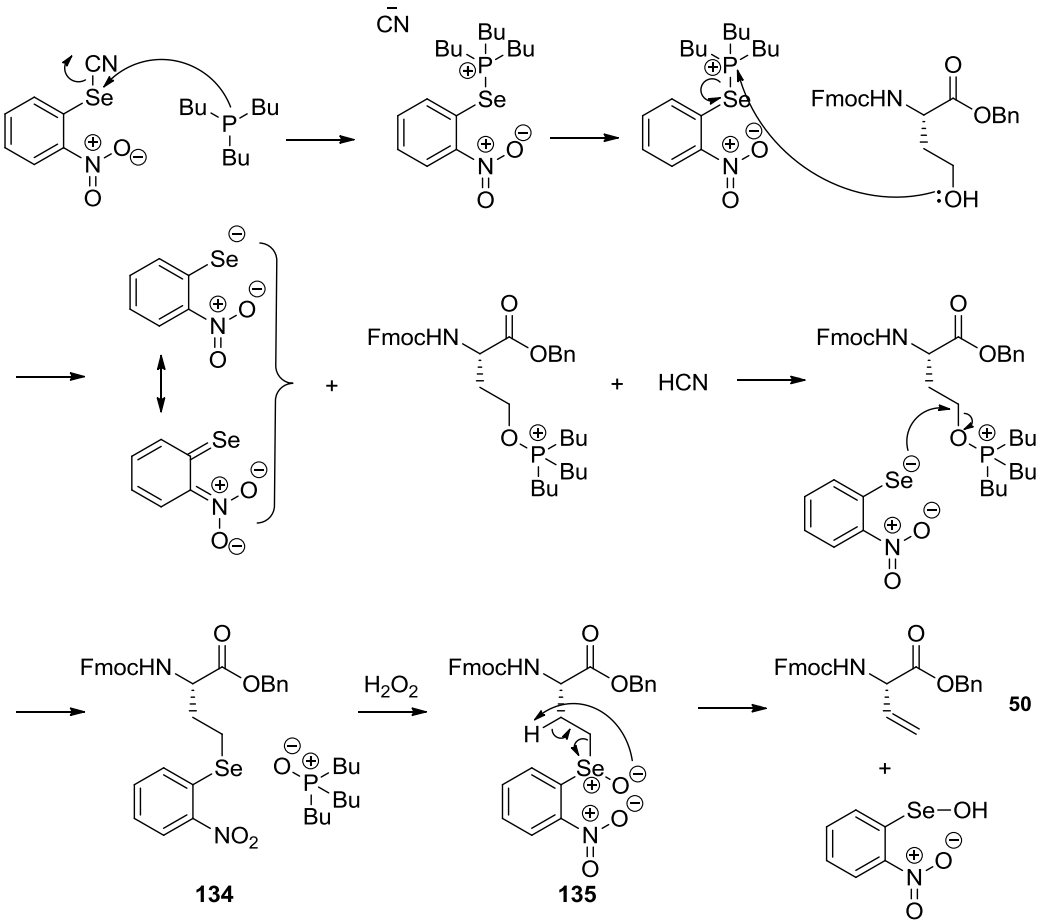

Scheme 2.23 Mechanism of the Grieco elimination (reaction between *o*NO_2SeCN and PBu_3 in presence of a primary alcohol)

The initial attempt at conversion of protected homoserine derivative **133** into vinylglycine via the Grieco elimination (Scheme 2.22), was unsuccessful; the TLC plate showed two spots, one corresponding to the protected L-homoserine and another that was identified as the 2-nitrophenyl selenocyanate.

In the second attempt THF, which is more difficult to dry exhaustively, was substituted with dry CH_2Cl_2 and the tributylphosphine was freshly distilled, as the original paper prescribed. Although the tributylphosphine appeared unusually turbid, the reaction was carried out, but TLC analysis showed that the starting material appeared not to have reacted.

A further attempt, using newly purchased tributylphosphine and again using dry CH_2Cl_2, was made. In this case the TLC plate showed the formation of three products, including Fmoc-vinylglycine-OBn. The first analytical TLC mobile phase (hexane/EtOAc 1:2) unexpectedly had a different elution order compared to the flash chromatography mobile phase (petroleum ether/Et_2O 4:1) so the first isolated

product was not the desired one. The post-purification TLC plate revealed this error, and further fractions were collected. Unfortunately, during the lengthy purification, a new spot appeared with a very similar R_f to the desired product, making its purification impossible, as the desired product and the by-product co-eluted in the system used. It is very likely that the by-product was the rearranged dehydrobutyrine isomer (**127**) of the desired product.

The reaction was repeated once more (in THF) and the crude product quickly purified, minimising contact time with silica, and Fmoc-vinylglycine-OBn was successfully obtained (Scheme 2.22) in acceptable yield (45%).

2.2.4 Cross-metathesis between Boc-D-allylglycine-O*t*Bu and Fmoc-vinylglycine-OBn

Firstly the cross-metathesis was attempted following a method based on that of Roychowdury and Boons (36) at room temperature (Scheme 2.24).
The first attempt at the cross-metathesis, using a 1.8-fold molar excess of vinylglycine **50** over allylglycine derivative **49** (0.28 mmol) for 24 h at room temperature, followed the literature procedure (36).

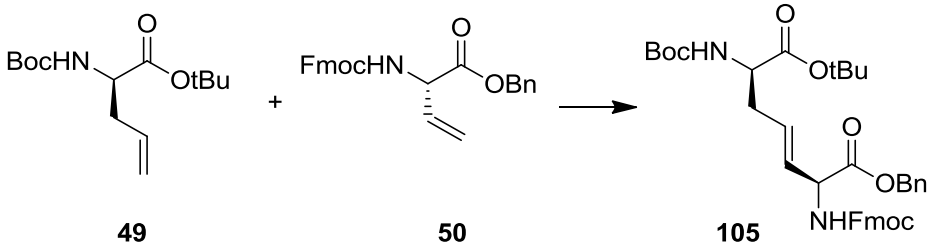

49 **50** **105**

Scheme 2.24 Cross-metathesis between appropriately protected D-allylglycine and L-vinylglycine (36) Reagents and conditions: Grubbs 2nd gen. catalyst, dry CH_2Cl_2, rt, Ar, 24 h, 64%.

TLC analysis showed a significant amount of residual starting materials, an additional non-UV-visible spot most likely to correspond to the D-allylglycine homodimer and one new UV-visible one, which was assumed to be the desired product. Three fractions were isolated via flash chromatography and analysed by NMR. The least polar component was confirmed to be the unreacted Boc/*t*Bu protected D-allylglycine, as its NMR spectrum matched that of the starting material. The second fraction contained a mixture of two more polar components, corresponding to the D-allylglycine homodimer and Fmoc-vinylglycine-OBn; it was not possible to fully separate these two components through flash chromatography but ^{1}H-NMR spectra highlighted the presence of all the characteristic signals corresponding to Fmoc-vinylglycine-OBn: Fmoc aromatic protons at 7.23 to 7.29,

benzyl methylene at 5.20, alkene protons at 5.25 to 5.40 and 5.89 to 6.00. The NMR of this fraction also confirmed the presence of Boc and *t*Bu groups (singlets at 1.44 and 1.46). This is consistent with the allyglycine homodimer (a fact that was later confirmed by comparison with the R_f of a synthesised analytical standard of the homodimer.

The ^{1}H-NMR spectrum of the final fraction, containing the most polar (lowest R_f) component, showed again the typical singlets for Boc and *t*Bu protecting groups, together with a singlet at 5.20, consistent with a Bn methylene, and signals characteristic of an Fmoc group. The expected signal corresponding to the α-CH adjacent to the benzyl ester and those for the alkene protons were not seen.

On this evidence the desired compound **105** seemed not to be present in any of the fractions isolated therefore the possibility of utilising microwave technology was considered.

A first attempt under microwave heating was performed on a small scale (0.01 mmol) and monitored via TLC. The objective was to quickly identify the best conditions for the reaction as this was a departure from the methodology reported in the literature.

First a cross-metathesis to obtain a Boc-D-allylglycine-O*t*Bu homodimer **136** was performed with the intention of isolating an analytical standard to be able to identify this as an expected side product (Scheme 2.25).

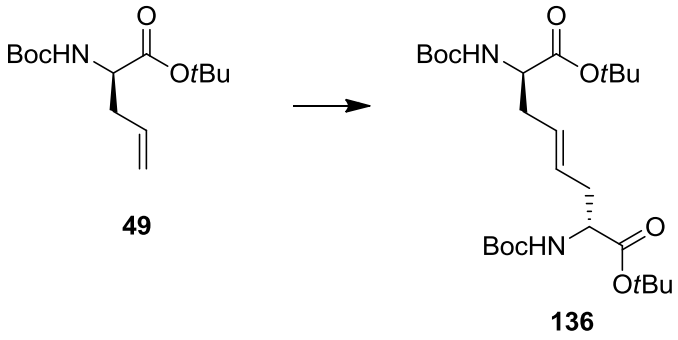

Scheme 2.25 Synthesis of Boc-D-allylglycine-O*t*Bu homodimer

Reagents and conditions: dry CH_2Cl_2, 5% Grubbs 2nd gen. catalyst, times and temperatures as detailed in Table 2.5.

For the homomeric cross-metathesis, the reaction was allowed to proceed under microwave heating at increasing temperatures (40 to 130 °C) and monitored via TLC. At 10-minute intervals the sample was analysed and then the reaction continued at a higher temperature for another 10 min, for a total of 40 min (Table 2.5).

Reaction time (min)	Temperature (°C)
0	40
10	65
20	120
30	130

Table 2.5 Range of temperatures applied during the homodimeric and heterodimeric cross-metathesis reactions (Scheme 2.24 and 2.25)

TLC analysis indicated a decreasing concentration of the starting material and increasing conversion to the homodimer over time. The homodimer was easily distinguished (TLC) from the monomer and catalyst as a non-UV-active spot of lower R_f. The isolated sample was kept as a TLC standard.

2.2.4.1 Investigation of microwave-assisted reaction conditions

The first small scale attempt at the cross-metathesis of the protected vinylglycine **50** and D-allylglycine **49** derivatives was also performed with the temperature settings described in Table 2.5; each time the vial was removed from the microwave, a small sample was taken for TLC, the vial repositioned and a higher temperature used for the next 10 min.

The TLC profile of the samples taken showed the presence of 5-8 components in the reaction mixture, including the homodimer and the two starting materials. UV activity was fundamental to exclude spots corresponding to compounds without Fmoc protection. Two new UV-visible spots were identified, one of which was likely to be the desired product. Higher temperatures seemed to increase the concentration of non UV-visible products.

The literature seems to suggest, in order to avoid isomerisation of olefins, to mantain low temperatures and use short reaction times (162–164). As a consequence, a larger scale microwave-assisted cross-metathesis was attempted with stirring at 55 °C for 1 h (Scheme 2.26). TLC analysis of the crude product showed 3 major UV-visible products.

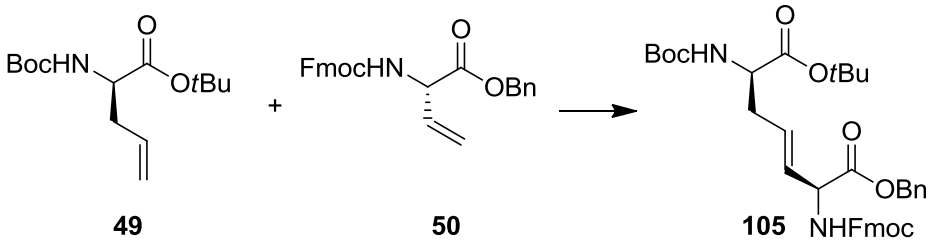

Scheme 2.26 Cross-metathesis between Boc-D-allylglycine-O*t*Bu and Fmoc-vinylglycine-OBn Reagents and conditions: dry CH_2Cl_2, Grubbs 2nd gen. catalyst, microwave 55 °C, 1 h, 8%.

Preparative TLC permitted the isolation of sufficient masses of the individual compounds to send for MS analysis. This analysis confirmed the presence of the desired product among the samples sent (though the sample was not completely pure). Further preparative TLC of the sample allowed isolation of a sufficient quantity of the desired product **105** for HPLC analysis, enabling identification of the peak corresponding to **105** in the crude HPLC chromatogram.

The HPLC profile of the crude cross-metathesis product promisingly showed well-resolved peaks (Fig. 2.5). The peak eluting at 22.95 min corresponds to the desired cross-metathesis product **105**.

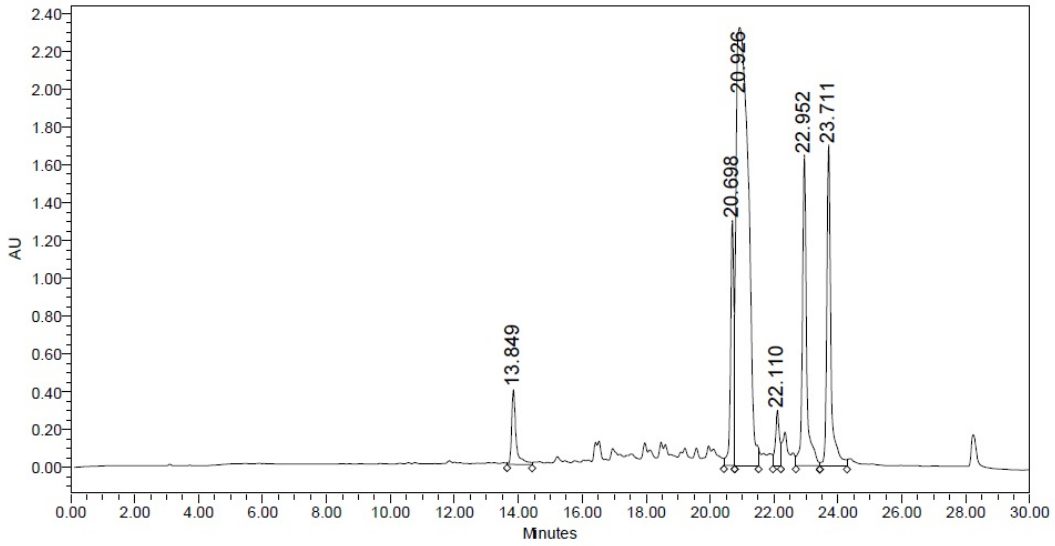

Figure 2.5 HPLC profile of the cross-metathesis crude product (detection at 214 nm, see Chapter 4.2).

A comparison with the profiles of the two starting amino acids showed the complete disappearance of Boc-D-allylglycine-O*t*Bu but the persistence of Fmoc-vinylglycine-OBn (R_t = 20.93 min), as expected, given the use of a 1.8-fold molar excess of the latter. One minor peak (R_t = 13.85 min) appeared to correspond to Grubbs 2nd gen. catalyst and two novel peaks (R_t = 22.95 and 23.71 min) were present with similar retention times. In order to identify the peak belonging to the desired product, the

crude chromatogram was overlapped with the one obtained from the compound isolated via preparative TLC. This fraction contains two peaks, one of which, according to the MS results obtained, belongs to the desired cross-metathesis product. The overlap identified the desired product peak as the one eluting at 22.95 min in Fig. 2.3. The fourth peak (R_t = 23.71 min) was not identified. It was initially suspected to be the Boc-D-allylglycine homodimer but its absorption at 254 nm seems to suggest that this by-product contains an Fmoc and/or benzyl group.
The HPLC chromatogram showed good baseline resolution between the desired product and said by-product (R_t = 23.71 min), therefore small aliquots of the crude product mixture were dissolved in *ca.* 50% aqueous MeCN and used to develop a gradient system suitable for preparative HPLC. The pure product was successfully isolated in a disappointing 8% yield and its identity confirmed by MS and NMR analyses. HPLC was used for purification of all subsequent reaction mixtures.

The cross-metathesis reaction was then repeated several times in order to obtain a greater quantity of product. Unexpectedly, HPLC analysis of early larger-scale trials (see comments below in Chapter 2.2.4.3) indicated either the absence or considerably reduced concentration of the desired product. It was possible that proportionally increasing the amount of catalyst could trigger further side reactions including breakage of the very bond formed in the cross-metathesis, as it is known that cross-metathesis is a reversible reaction (165). Consequently, repetition of the reaction was kept on a small scale and the crude products were combined for purification. Occasionally, despite the same conditions and quantities being used, the desired product was not present, according to analytical HPLC results. Adding more catalyst and repeating the microwave heating occasionally lead to the production of some desired product. The apparent variability of outcomes in this reaction under essentially identical conditions and its lack of scalability proved frustrating. It is currently unlikely to be viable for the large-scale production of protected *m*DAP without much more optimisation, probably at each scale used. The number of variables in the reaction – relative quantities of reactants, concentration, type and quantity of catalyst, time and temperature – make this challenging.

Later on, a smaller-scale cross-metathesis at room temperature for 24 h was attempted in order to quickly compare its results against the ones from the microwave-assisted reactions. TLC analysis of the crude product showed no significant difference from the profile of the microwave-assisted crude product. The D-allylglycine seemed to have been completely consumed, while the vinylglycine (in excess) was still visible. Four additional by-products were observable, one of which

was not UV-active. Given the similarity of the results, it was decided that microwave heating was the most suitable option for the subsequent cross-metathesis reactions as it seemed to drastically reduce the reaction time.

2.2.4.2 Comparison of Hoveyda-Grubbs and Grubbs 2nd gen. catalyst activity

Two parallel microwave-assisted experiments were run with the same molar equivalents of starting materials and amount of catalyst but different types of catalyst. This was done to evaluate whether Hoveyda-Grubbs 2nd gen. would lead to better results than Grubbs 2nd gen. catalyst, the latter being used in the literature (36,147). The crude products were analysed by HPLC and the peak area for the desired product was similar for both - 19.7% for Grubbs *vs.* 23.3% for Hoveyda (measured as percentage of total chromatogram peak area). As no significant difference was detected, it was decided to favour the use of Grubbs 2nd gen. catalyst, as suggested by the literature (36,147).

2.2.4.3 Larger-scale cross-metathesis investigations

Early preliminary attempts at scale-up had proved unsuccessful (see above). Attempting to scale-up the cross-metathesis from the initial 0.088 mmol (24 mg of the allylglycine component), the reaction was repeated with 100 mg (0.370 mmol) of allylglycine under the same conditions (including 5 mol % catalyst quantity). Analytical HPLC of the crude product showed only an extremely small, almost negligible peak consistent with the desired product. The crude product was thus evaporated and a further 5 mol % catalyst was added before repeating the cross-metathesis step. After this treatment the expected peak was detectable via HPLC and therefore purification was carried out leading to the isolation of the desired product in 6% yield. It seemed that increasing the quantity of catalyst might have negatively influenced the outcome, possibly pushing the reaction back to the starting material rather than the products or catalysing alternative side reactions. Given these issues, it was deemed sensible to only slightly increase the quantity of starting material and to avoid scaling up the catalyst quantity.

The following attempts therefore employed the use of 0.175 mmol of Boc-D-allylglycine-O*t*Bu and a quantity of catalyst corresponding to the one used for the initial attempt (3.6 µg). The crude products of several identical reactions were combined prior to purification. The yields recovered from each of these reactions frustratingly varied between 4 and 6% and were considered acceptable given the impracticality of conducting a proper study for the optimisation of scale-up.

2.2.4.4 Hydrogenation step

The final step in the synthesis of the suitably-protected *m*DAP derivative was the reduction of the alkene resulting from the cross-metathesis, with simultaneous removal of the benzyl ester (Scheme 2.27). Roychowdhury *et al.* (36) suggested the use of 3% Pt/C catalyst, while Kastrinsky *et al.* (166) used 10% Pd/C to reduce the alkene in a differently-protected *m*DAP, still bearing the Fmoc amino protecting group. Some reported a risk of possible Fmoc removal with 10% Pd/C during benzyl deprotection (167–169,155) contrasting with Kastrinsky's outcome and statements of its supposed stability to hydrogenation conditions (155,170,171). A small-scale test was performed on Fmoc-Glu(O*t*Bu)-OH to evaluate the effect of the two catalysts on Fmoc stability. A solution of the amino acid in a mixture of MeOH, H_2O and CH_2Cl_2 (the intended eventual reaction solvent) was stirred at room temperature under a hydrogen atmosphere for 2 h in presence either of 3% Pt/C or 10% Pd/C. The reaction mixtures were analysed by TLC and, in the case of 10% Pd/C, showed the consumption of the starting material, whereas the the use of 3% Pt/C resulted in no change. These findings led to the decision to utilise 3% Pt/C.

Reduction via hydrogenation in most cases works at room temperature just above atmospheric pressure, which can be achieved using a hydrogen-filled balloon. Different pressure and temperature conditions might be needed in cases of poor reactivity as in the presence of a highly substituted double bond (172).

Following evaluation of the conditions for the hydrogenation, all the pure products obtained from the different cross metathesis reactions were combined. The reduction of the double bond and removal of the benzyl protecting group was achieved under a hydrogen atmosphere at room temperature, monitoring over 30 h.

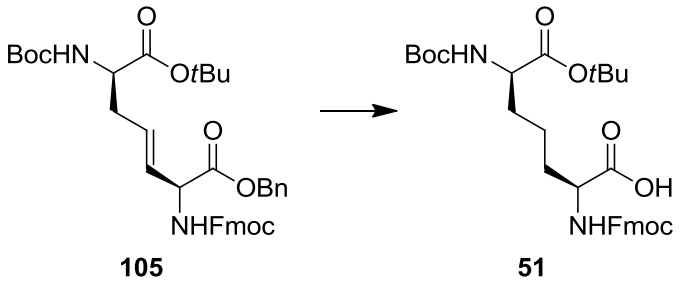

105 **51**

Scheme 2.27 Hydrogenation of the cross-metathesis product
Reagents and conditions: 3% Pt/C, MeOH, H_2O, CH_2Cl_2, H_2, 30 h, 72%.

TLC and HPLC analysis indicated the almost complete consumption of the starting material after 30 h and the appearance of one major compound and two minor compounds, each more polar than the starting material. The product was sufficiently

pure to be used crude for the next step. Any possible side products of the hydrogenation would probably retain the benzyl ester protection, which would prevent loading onto the resin, which requires a free carboxyl group. Alkenes are reduced more promptly than benzyl protecting groups are removed (173), therefore the formation of a free carboxyl-containing by-product retaining the alkene function is highly unlikely.

2.3 Synthesis of the putative Mpl tripeptide substrate H-Ala-D-Glu(*m*DAP-OH)-OH

Following the hydrogenation step and MS and NMR confirmation of the presence of the desired product, the *m*DAP-containing crude product was loaded onto a 2-chlorotrityl chloride derivatised resin (Scheme 2.28) and used for the synthesis of H-Ala-D-Glu(*m*DAP-OH)-OH (**52**).

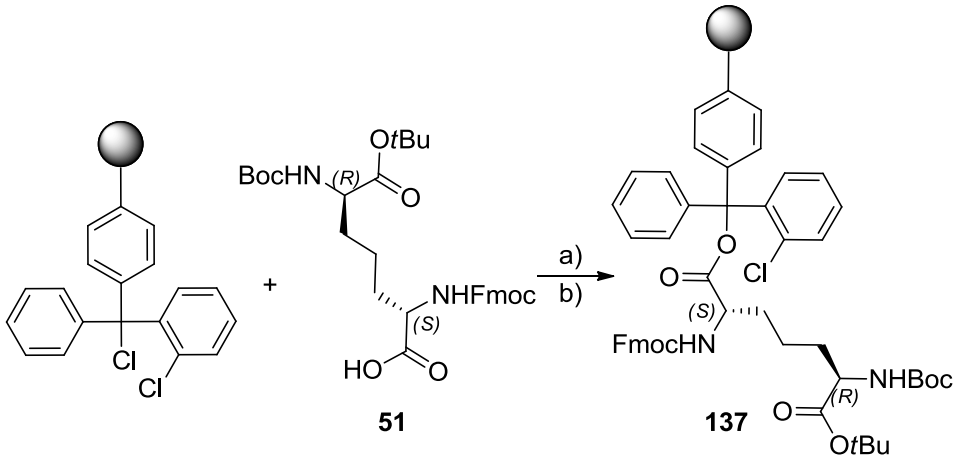

Scheme 2.28 Loading of appropriately-protected *m*DAP onto 2-ClTrt resin
Reagents and conditions: a) dry CH_2Cl_2, DIEA, Ar, 2 h; b) CH_2Cl_2, MeOH, DIEA, 1 h.

Unusually, an excess of 2-chlorotrityl chloride resin (based on manufacturer's substitution) was used to maximise the amount of the *m*DAP building-block that could be successfully loaded. Unreacted 2-chlorotrityl chloride groups were capped after loading using methanol. This loading procedure had been previously validated using Fmoc-Glu(O*t*Bu)-OH followed by deprotection and coupling with Fmoc-Ala-OH. The loading of *m*DAP proceeded as shown in Scheme 2.28.

Manual Fmoc deprotection with 20% piperidine was performed, followed by coupling with Fmoc-D-Glu-O*t*Bu then Fmoc-Ala-OH, using HBTU/HOBt/DIEA-mediated activation as described in Chapter 4.3. Deprotections and couplings were repeated and success monitored using the Kaiser test. Positive Kaiser tests were generally

quite weak, most likely as a consequence of the low loading of the resin, so the initial *m*DAP Fmoc deprotection was performed three times as a precaution. Final cleavage of the tripeptide proceeded as described in Chapter 4.3.

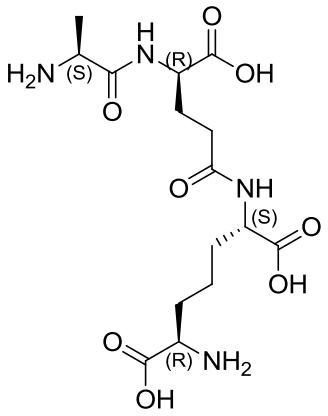

52

HPLC analysis showed closely-eluting components with low retention times. Purification via semi-preparative HPLC led to a product containing two components. Mass spectrometry and NMR confirmed the presence of the desired product but no further purification could be performed due to the small mass of the sample. The main issue was the very early elution of the components, due to their high polarities, giving little opportunity to interact with the stationary phase. Both components eluted together right at the start of the preparative run. MS analysis seems to indicated the presence of M+57, which is characterisitic of the incomplete deprotection of the *t*Bu ester. It could possibly also be an alkylated by-product (the *t*Bu cations produced during cleavage can theoretically react irreversibly with nucleophilic groups like the amino groups). As the NMR spectrum showed little evidence of impurities, HPLC analysis was repeated; interestingly, the chromatogram showed that the concentration of one of the major components had decreased, perhaps suggesting that it had been hydrolysed.

2.3.1 Biological evaluation

2.3.1.1 Target-based evaluation (Mpl overexpression and purification)

The *m*DAP-containing PG fragments were meant to be used for the characterisation of *M. tuberculosis* Rv3712, the putative Mpl. Due to the time required for the synthesis of the suitably-protected *m*DAP building block and the fact that the sample of tripeptide **52** was insufficiently pure, a full evaluation has yet to be performed.

Nonetheless the recombinant enzyme has been heterologously overexpressed in *E.coli* and purified (full experimental details are described in Chapter 4.6).

2.3.1.1.1 Transformation

The plasmid pCDFDuet-1, carrying the gene of interest *rv3712*, the *tig*A insert and streptomycin resistance (a gift from Professor Gabriel Waksmann, see Chapter 4.6.3), was transformed by heat-shock into competent BL21(DE3)pLysS *E. coli* cells, selected for over-expression of Mpl through previous optimisation studies, as described in Chapter 4.6.5.5. The successful transformation was confirmed by the positive growth of colonies in the presence of streptomycin and chloramphenicol, as the competent cells also contained a plasmid conferring chloramphenicol resistance upon them.

2.3.1.1.2 Over-expression of Rv3712 (*M. tuberculosis* Mpl)

The colonies obtained after transformation were used to start small seed cultures (as described in Chapter 4.6.5.6) that were inoculated into an appropriate volume of medium containing streptomycin and chloramphenicol and incubated at 37 °C until the culture reached the appropriate OD. Following the data from a previous optimisation of the over-expression procedure, the culture was induced with IPTG to reach a final concentration of 0.5 mM. One culture was not induced but was kept as a negative control (uninduced). Overnight incubation at 18 °C followed. The cells were harvested as described in Chapter 4.6.5.6. A small sample was not centrifuged after sonication to keep as a control (whole cell protein).

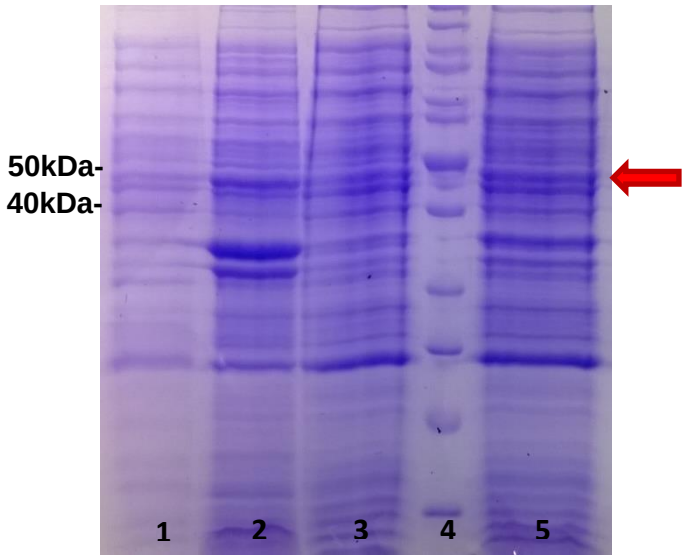

Figure 2.6 Gel electrophoresis showing the successfull overexpression of recombinant Mtb Rv3712 in *E.coli*. The band corresponding to the target protein, which has an estimated molecular weight of 45.3 kDa (174), is highlighted by the red arrow. Lanes: (1) uninduced sample; (2) whole-cell sample; (3) cell pellet; (4) marker; (5) cell lysate

The pellet and the soluble fraction were run on an SDS-PAGE gel, as described in Chapter 4.6.5.9, against the uninduced and whole cell sample (Fig. 2.6).

It can be observed that all of the fractions contain the band corresponding to Rv3712. The band is more distinguishable and intense in the cell lysate sample than in that for the uninduced cells, as expected. It is also noticeable that the cell pellet sample also contains a band consistent with the molecular weight of Rv3712, which may mean that the protein was partially segregated in inclusion bodies, due to possible misfolding.

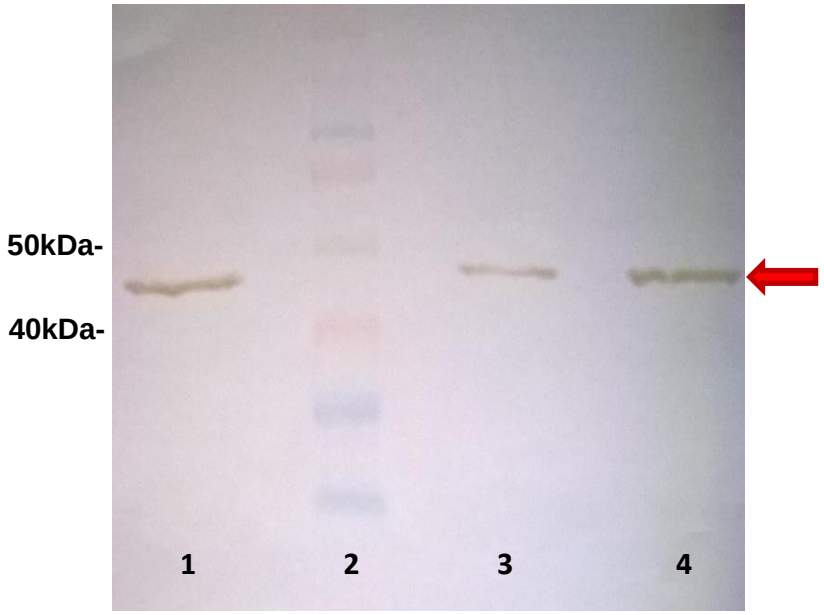

Figure 2.7 Western blot showing the successful overexpression of recombinant Mtb Rv3712 in *E. coli.* The 6x-His epitope tag monoclonal antibodies, used in this method, bind to the 6His-tag on Rv3712 resulting in an orange coloured band (highlighted by the red arrow). Lanes: (1) cell pellet; (2) marker; (3) cell lysate; (4) whole-cell sample.

Another gel was loaded with the cell pellet, cell lysate and whole-cell sample and used for western blotting (Chapter 4.6.5.12). The western blot, which involves the use of antibodies specific to, in this case, a polyhistidine-tag (6His-tag), shows a clear brown-orange band corresponding to the desired protein. The 6His-tagged protein can be seen as present in the whole cell sample, in the cell pellet and in the cell lysate (Fig. 2.7).

2.3.1.1.3 Purification of Rv3712

Following the over-expression of Rv3712 in the BL21(DE3)pLysS competent cells,

isolation and purification of the protein was attempted.

Plasmid pCDFDuet-1Rv3712Tig was designed to contain a sequence for the expression of an *N*-terminal 6His-tag on the target protein; therefore the recombinant protein can be isolated by affinity purification using Ni-NTA resin. Columns were run using 10 to 250 mM imidazole solutions to elute the protein. Ni-NTA has coordinated (chelated) Ni^{2+} cations that bind to the basic nitrogen atoms in the side chain imidazole rings of histidine residues. Imidazole competes for binding with nickel and displaces the histidine.

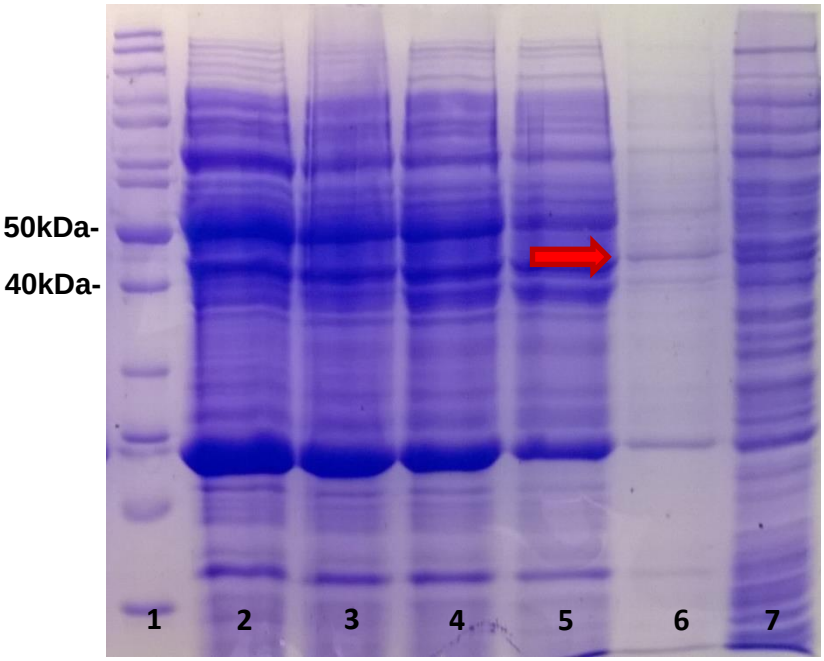

Figure 2.8 Gel electrophoresis of the fractions obtained from the lysate purification on Ni-NTA column. The red arrowhighlights the band corresponding to Rv3712. Lanes: (1) marker; (2) 10 mM imidazole eluate; (3) 50 mM eluate; (4) 100 mM eluate; (5) 150 mM eluate; (6) 200 mM eluate; (7) 250 mM eluate

The fractions obtained were loaded and run on an SDS-PAGE gel (Fig. 2.8). The developed gel shows the Rv3712 protein eluting clearly with the 200 mM imidazole solution. It is also evident that other proteins are eluting together with the target protein, therefore the Ni-NTA purification system needs to be optimised further and the product further purified by gel filtration, using size exclusion to separate the pure protein.

The promising results for the over-expression and purification of Rv3712 will eventually present the opportunity, when a sample with the required purity (>95% in the case of recombinant proteins) has been obtained, for crystallisation trials. Such

trials generally require 10 mg/mL solutions but, in case of proteins larger than 30 kDa, 2-5 mg/mL should prove sufficient. A previous study (174) estimated the weight of Rv3712, including the 6His-tag, to be 45.3 kDa. For now, visual preliminary observations estimate the purity to be around 60% and, as 70-80% is considered sufficient for biochemical assays, the product needs to be subjected to further size-exclusion chromatography.

Considering the need for further purification, the quantities of enzyme obtained after Ni-NTA resin purification (typically 20-50 µg/mL) are currently inadequate to reach the amount required for crystallisation trials.

The observation of the *M. tuberculosis* Mpl band in the cell pellet suggests the presence of the enzyme in inclusion bodies. This is not a rare occurrence when trying to express foreign proteins in a host cell through the use of plasmid expression vectors; furthermore it seems that non-native proteins expressed in *E. coli*, especially if genetically modified, are particularly prone to the formation of inclusion bodies (175).

In the hope of finding out the reason why the expression of pure Mpl didn't reach desirable levels, cultures of different *E.coli* cells were grown and monitored: one culture of BL21(DE3) competent cells containing plasmid pLysS only, one culture of *E. coli* DH5α cells (used for cloning) containing pCDFDuet-1, and two cultures of BL21(DE3)pLysS cells containing the plasmid pCDFDuet-1 carryng *tig*A and *rv*3712 constructs were compared (Fig. 2.9).

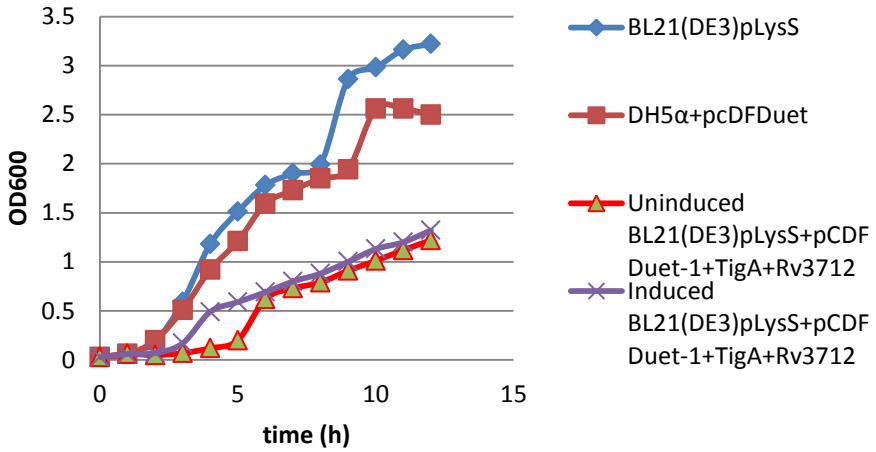

Figure 2.9 Comparison of *E. coli* growth curves for different cultures

The seed cultures were prepared according to the procedure in Chapter 4.6.5.6. The

seed cultures were inoculated as described in Chapter 4.6.5.8, but the first two types of cells (BL21(DE3)pLysS and DH5α+pCDFDuet) were grown at 37 °C continuously, while the cultures carrying the constructs were moved and incubated at 18 °C once they reached OD = 0.5. One of the latter two cultures was induced with IPTG while the other was kept as an uninduced control as described in Chapter 4.6.5.8. The growth curve comparison shows how the cultures incubated at 37 °C grew faster and reached a steady state within 12 hours, while the others significantly slowed their growth after being moved to 18 °C incubation; during exponential growth the curve shape switched from sigmoidal to linear (for what is possible to observe within 12 hours). This could be considered as a direct effect of the temperature. On the other hand, when all four cultures were incubated at 37 °C, a difference in the growth velocity could still be noticed with the cultures carrying the construct growing more slowly. It is also possible to observe that the two identical cultures of BL21(DE3)pLysS+pCDFDuet-1+TigA+*rv*3712, even when treated equally (before OD = 0.5) grew at different velocities. This is suggestive of the variability that can often be encountered when growing cells but further experiments will follow. The behaviour of the cells could be better evaluated by growing three BL21(DE3)pLysS cultures, two with and one without the *M. tuberculosis* Mpl construct, under the same conditions (37 °C until OD = 0.5, then 18 °C) but then only inducing one of the cultures carrying the construct with IPTG. This would provide a clearer negative control.

2.3.1.2 Whole-cell evaluation

Testing *m*DAP-containing fragments on mycobacteria or Gram negative bacteria in a whole-cell assay would be unlikely to provide any useful information, as they would be the desired substrates of the Mur ligases, therefore participating in the normal processes of the cell and not providing any insight as to whether they entered the cell. They could be tested on Gram positive bacteria eventually to see whether they are able to exert any inhibitory activity. As mentioned before, ultimately the real value in having access to the *m*DAP-containing PG fragments is to characterise the activity of the isolated recombinant Mpl, with the ultimate goal of evaluating the effect of inhibitors on this activity.

2.4 Synthesis of lasso peptides with anti-tuberculosis activity[‡]

Lasso peptides are potent cyclic natural products of bacterial origin. They have a knotted structure consisting of a *C*-terminal tail threaded through a loop, which confers upon them extreme stability to enzymatic degradation. They typically possess a variety of different activities, but the lariatins and lassomycin have shown bactericidal activity against *M. tuberculosis*.

2.4.1 Synthesis of lasso peptides and linear precursor analogues using Dmab side chain protection strategy

While the primary goal was to complete the total syntheses of the natural products, we also sought to synthesise their non-cyclised (linear) analogues to examine if they retain any antimycobacterial activity. It was also unknown at this time if the synthesised natural product sequences would spontaneously fold to give the native threaded conformation. If that proved not to be the case, we would also be able to evaluate if the non-threaded structures retained antimycobacterial activity. Taking lariatin A, **31**, as an example, the assembly of the linear sequence would be followed by head-to-side-chain cyclisation reaction, between Gly1 and Glu8. The first strategy adopted involved the use of Dmab (**138**, 4-(*N*-[1-(4,4-dimethyl-2,6-dioxocyclohexylidene)-3-methylbutyl]amino)benzyl) as the side chain protection for the Glu residue involved in this coupling reaction. This protecting group can be removed on resin under mild conditions using 2% hydrazine hydride in DMF and it is stable to piperidine and removal of Fmoc, Boc and trityl (167).

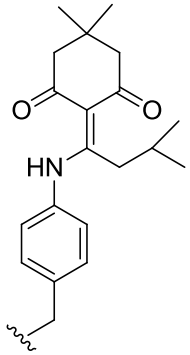

138

Linear lariatin A would be synthesised using standard SPPS before selective removal of the Dmab group, and on-resin cyclisation using DIC and HOAt (Scheme

[‡]Some aspects of this work were contributed to by MPharm and MSc project students Sienna Feguson and Ammar Ahmed, under my supervision

2.29). On-resin cyclisation presents the advantage, compared to cyclisation in solution, of favouring intramolecular reaction over intermolecular reaction and of taking place while the other residues remain protected.

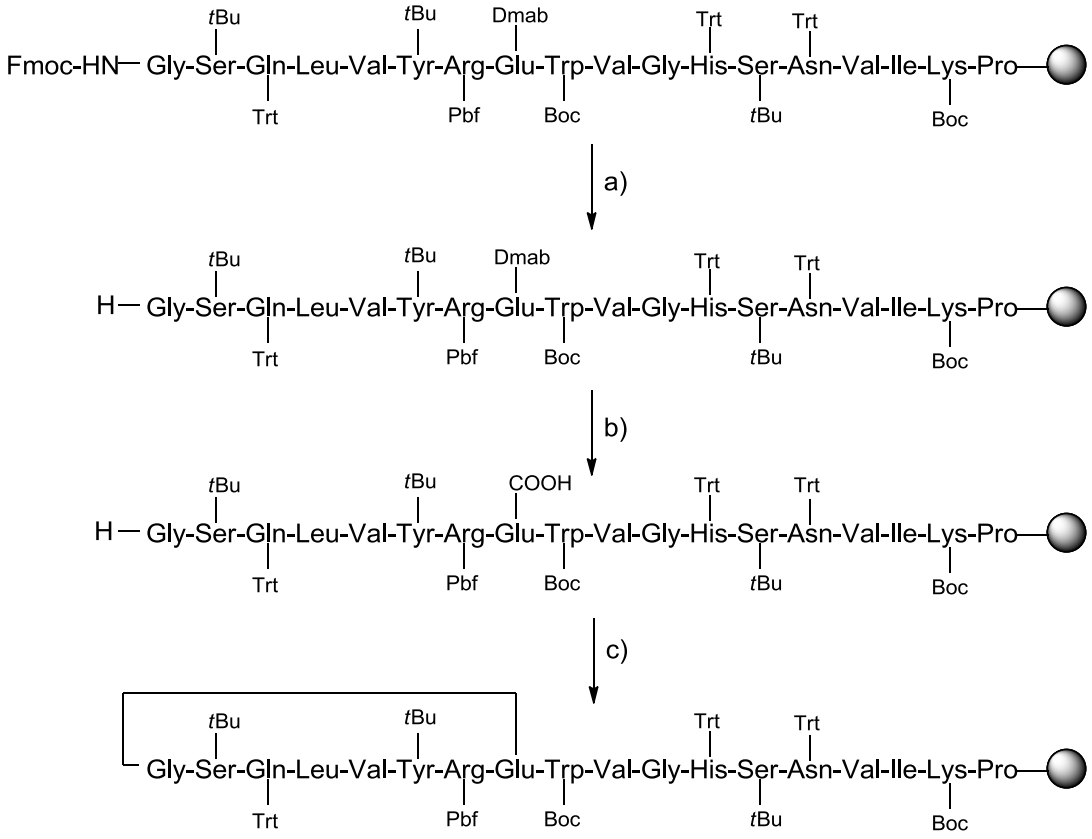

Scheme 2.29 Head-to-side-chain cyclisation of lariatin A linear precursor
Reagents and conditions: a) 20% piperidine in DMF, 2 x 15 min; b) 2% hydrazine monohydride in DMF, 5 x 3 min; c) DIC, HOAt, DMF, 24 h.

2.4.1.1 Synthesis of lariatin A and B

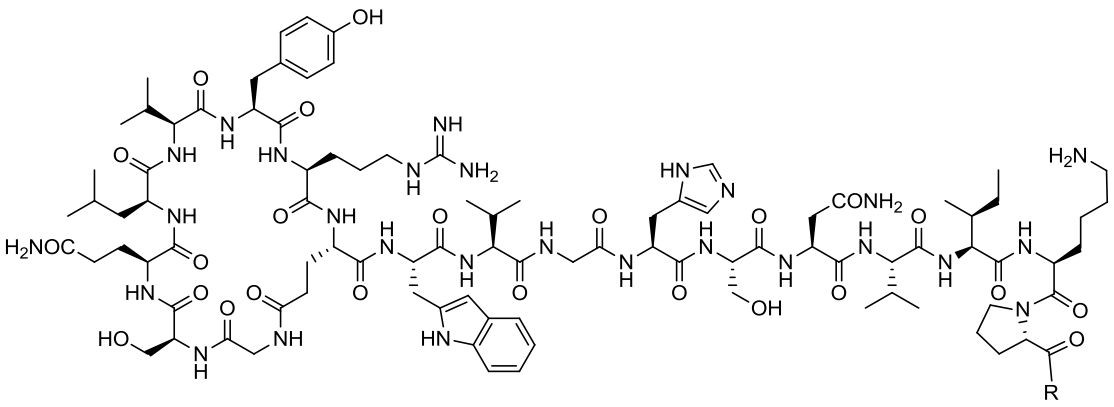

31, Lariatin A, GSQLVYREWVGHSNVIKP, (R = OH)
32, Lariatin B, GSQLVYREWVGHSNVIKPGP, (R = Gly-Pro-OH)

The first attempt at the (automated SPPS) synthesis of lariatin A **31** was conducted starting from H-Pro-2-ClTrt resin. The synthesis of the similar lariatin B **32** was conducted in parallel. The bulky 2-ClTrt resin is preferred over the use of a Wang resin as the latter can result in unwanted DKP formation at the dipeptide stage (see Chapter 1.3.5). Glu8 was incorporated as the side chain Dmab-protected derivative. After completion of the linear sequence and removal of the final Fmoc group, the Dmab group was selectively removed according to the standard protocol (2% hydrazine monohydrate), followed by treatment with 5 mM sodium hydroxide in aqueous methanol to fully remove any residual aminobenzyl ester (176). A Kaiser test at this stage was expected to confirm the presence of the free amino group at the *N*-terminus, but the test was unexpectedly negative. The same problem was seen with the lariatin B sequence. A further piperidine treatment to ensure complete Fmoc removed failed to change the result of the Kaiser test. Consequently cyclisation was not attempted at this stage and the peptide was cleaved from the support and analysed by ESI-MS in order to investigate what had happened.

ESI-MS analysis of the crude lariatin A cleavage product showed signals at *m/z* 1035.6 and 1247.6, which are consistent with the presence of the $[M+2H]^{2+}$ ion of the desired/expected molecule (the deprotected linear precursor of lariatin A, acyclic **31**) and the $[M+H]^{+}$ ion of a truncated pyroglutamyl-peptide (**139**) respectively. The ESI-MS results for the linear lariatin B sample showed signals at *m/z* 1112.5, consistent with $[M+2H]^{2+}$ ion of the desired/expected peptide (the linear precursor of lariatin B, acyclic **32**), and at 1401.7 suggesting similarly the presence of the $[M+H]^{+}$ ion of a truncated pyroglutamyl-peptide (**140**).

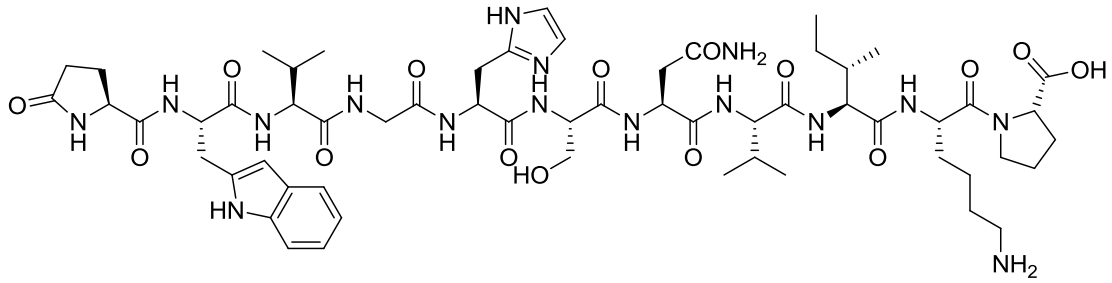

139 (R = OH)
140 (R = Gly-Pro-OH)

The formation of such pyroglutamyl derivatives is due to the reaction of the N^{α}-amino group of Glu (or Gln) with its side chain carboxyl (or carboxamide) to give a lactam ring (Scheme 2.30). If this occurs during chain elongation, there is subsequently no *N*-terminal free amino group, required for further coupling,

generating a truncated peptide. This phenomenon would explain the negative (or at least very weak) Kaiser test results. In the case of Glu, this side reaction seems to be promoted in the presence of a base. Piperidine deprotection therefore provides an environment that might encourage such a reaction to take place. This reaction can also occur when the side chain of Glu has an activated γ-carboxyl group, which could be problematic during cyclisation attempts (177). Furthermore, Dmab deprotection conditions have previously been reported to trigger the production of unacceptable levels of side products (178).

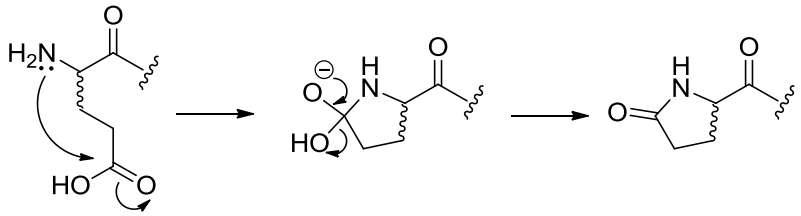

Scheme 2.30 Pyroglutamate formation

The crude products of the attempted lariatin A and B syntheses were not purified, given the high proportion of the pyroglutamyl by-product present and their poor resolution from the linear precursors, therefore no definite quantitative data are available on the degree of pyroglutamate formation. Nonetheless it might be inferred that pyroglutamate formation was sufficiently significant (>50%) to produce an essentially negative Kaiser test. The intramolecular cyclisation leading to pyroglutamate formation and subsequent failed elongation has been previously reported to have taken place using the Dmab protecting group (177).

MS analysis also indicated the absence of any glutamic acid aminobenzyl ester, indicating that complete Dmab removal had been achieved. While this may seem to justify the use of the 5 mM NaOH treatment (176), it is possible that complete removal was achieved using the 2% hydrazine monohydrate treatment alone. There remain, however, some concerns over the stability of the 2-ClTrt linker to these conditions (labile at pH >10), which may lead to premature peptide cleavage (169). There was also concern that the use of the 5 mM NaOH might increase the likelihood of pyroglutamate formation.

The automated synthesis of lariatins A and B was therefore repeated. Dmab removal was achieved as previously using hydrazine monohydrate, but without the additional NaOH treatment to try to minimise any premature cleavage or pyroglutamate formation. This time the Kaiser test (after *N*-terminal Fmoc removal)

was positive and the cyclisation was therefore attempted using DIC and 1-hydroxy-7-azabenzotriazole (HOAt) coupling methodology. The cyclisation step had to be repeated three times, for both lariatin A and B, before a negative Kaiser test was obtained, implying complete reaction of the *N*-terminal amino groups. After cleavage, the crude samples were purified using preparative HPLC and samples were sent for ESI-MS.

HPLC analysis of the crude products for the intended cyclic lariatins A and B indicated the presence, in both cases of one major peak. ESI-MS of the fraction from the lariatin A product isolated via RP-HPLC, showed signals at *m/z* 1291.8 and 1247.8 consistent with the $[M-H+2Na]^+$ and $[M+H]^+$ ions of the truncated pyroglutamyl-peptide. Likewise the pure fraction obtained from purification of the intended lariatin B showed signals at *m/z* 1401.8, 1423.9 and 1447.8 consistent with the $[M+H]^+$, $[M+Na]^+$ and $[M+2Na]^+$ ions of the truncated pyroglutamyl-peptide. This outcome, despite the avoidance of the NaOH treatment, provides further evidence about the unsuitability of Dmab for this synthesis. It seems that the N^{α}-Fmoc deprotection of the Glu(ODmab) residue, possibly as well as subsequent deprotection(s) and/or activation of the Gly γ-carboxyl group are responsible for the pyroglutamate formation and truncation, preventing successful cyclisation. In the chromatograms of the crude products of both attempted lariatin A and B syntheses, a minor peak (poorly resolved) elutes immediately before the truncated pyroglutamyl-peptide. We speculate that these slightly more polar compounds are more likely to be uncyclised linear peptides rather than the successfully cyclised lariatins. Unfortunately it wasn't possible to isolate these compounds in order to verify this hypothesis.

2.4.1.2 Synthesis of linear lariatin A and B analogues

Linear lariatin A and B analogues were synthesised with the aim of evaluating whether their antimycobacterial activity persisted even when uncyclised. They were automatically synthesised starting from preloaded H-Pro-2-ClTrt resin. The naturally-occurring Glu8 residue was substituted with Gln (introduced as the side chain trityl-protected derivative) as the side chain terminal amide is structurally more similar to the amide (lactam) group found in the cyclic peptides, mimicking the amide bond formed with Gly1 (**141**, **142**).

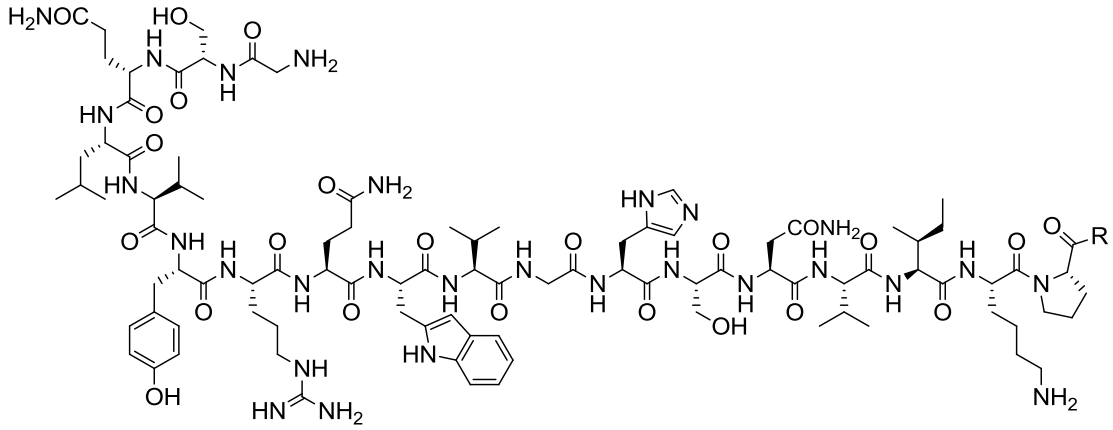

141, GSQLVYRQWVGHSNVIKP (R = OH)
142, GSQLVYRQWVGHSNVIKPGP (R = Gly-Pro-OH)

After cleavage, HPLC analysis of the crude linear analogue of lariatin A showed two major products in an approximately 1:1 ratio. HPLC purification led to isolation of the two compounds and ESI-MS analysis confirmed the presence of the desired product and its pyroglutamate derivative. The desired product was isolated in a 5% overall yield after RP-HPLC purification. The crude product of the automated synthesis of the lariatin B linear analogue showed one single main component in the HPLC chromatogram. Purification via preparative HPLC resulted in its isolation (4% overall yield), and it was confirmed as the desired product by ESI-MS. The apparent absence of pyroglutamate formation in the Gln(Trt)-containing linear lariatin B analogue (and the much-reduced formation in the lariatin A analogue) could suggest that the Glu(ODmab) residue rendered its formation more favourable. This finding has been corroborated previously in the literature: the use of Glu(O*t*Bu) in Fmoc-based peptide synthesis overcame previously noted pyroglutamate formation (177). The same authors also reported that the use of amino acids of varying steric size as residues adjacent to an *N*-terminal Glu(ODmab) residue had little effect on the rate of the undesired reaction (177).

2.4.1.3 Synthesis of lassomycin linear *C*-terminal free acid analogue

Linear analogue **143** was synthesised with the intention of comparing its antitubercular activity with that of the native lassomycin (**33**, pg. 45) and deduce whether cyclisation and methyl esterification at the *C*-terminus are necessary for activity. **143** was synthesised automatically on preloaded Fmoc-Ile-Wang resin. In a similar approach to that used for the lariatins, the side chain residue involved in the head-to-side chain cyclisation, in lassomycin's case Asp8, was substituted with Asn in the linear analogue, as the amide better resembles the peptide bond found between Asp8 and Gly1 in the cyclic molecule. The synthesis was largely

straightforward and the crude product HPLC chromatogram indicated very good purity, with only minor quantities of contaminants. A small portion was purified via preparative HPLC for a final yield of 25%. LC-MS analysis of the pure sample showed signals consistent with the desired product.

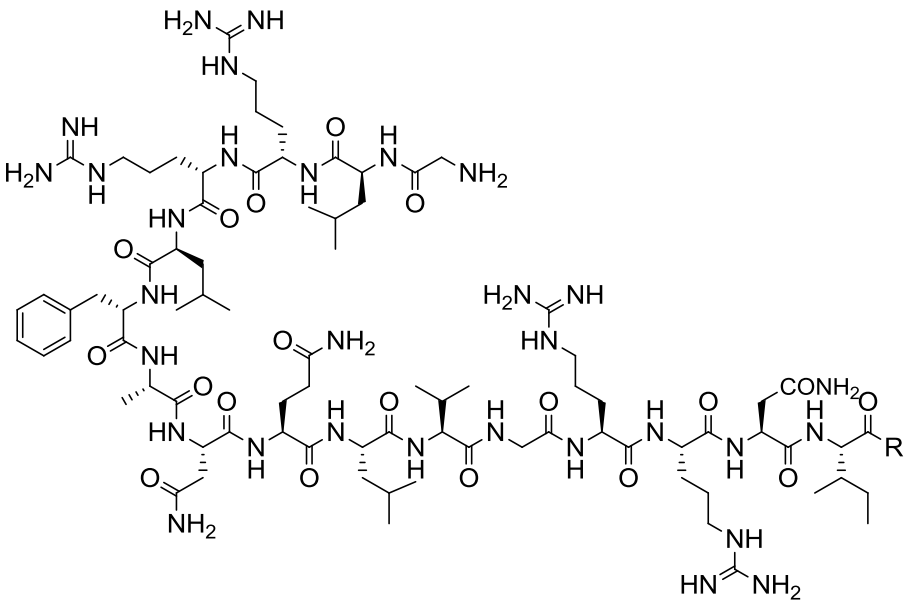

143, GLRRLFANQLVGRRNI (R = OH)
144, GLRRLFANQLVGRRNI (R = OCH_3)

2.4.1.4 *C*-Terminal methyl esterification of lassomycin linear free acid

The purity of the Asn-containing linear analogue was deemed sufficient to use the crude product as the starting material for the Fischer methyl esterification of the *C*-terminus, thus avoiding two HPLC purifications. This synthesis of **144** was attempted to produce a linear analogue structurally closer to lassomycin, as a *C*-terminal methyl ester is found in the natural product. The peptide was dissolved in dry methanol and treated with a solution of HCl in dioxane for 24 h. HPLC analysis of the resulting crude product showed the formation of a single major product with a few minor side products and therefore the sample was purified via preparative HPLC and the fractions containing the major peak (5% yield) analysed via ESI-MS. The results showed signals at *m/z* 475.0 and 479.0 consistent with the $[M+4H]^{4+}$ ion of the target structure and with the $[M+4H]^{4+}$ ion of a possibly doubly methylated by-product. The site of the second methylation is unknown. A possible explanation begins with rearrangement of a carboxamide-containing side chain residue, such as Asn, via a two-step deamidation reaction, and has been previously reported (Scheme 2.31) (179,180).

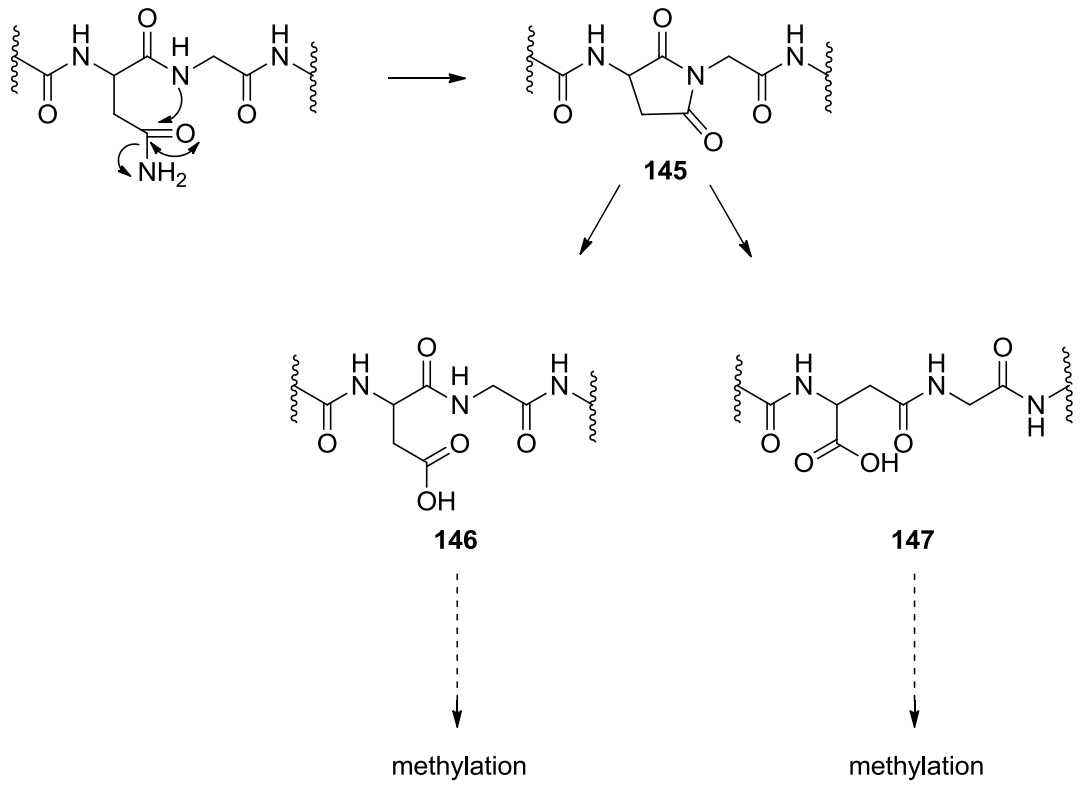

Scheme 2.31 The succinimide can open to an aspartate or an isoaspartate

Nucleophilic attack by the amide nitrogen of the peptide bond with the adjacent residue causes the formation of a succinimide, which can then open in two possible ways: either where the cyclisation occurred, yielding the corresponding aspartate (**146**) or on the other side, causing the formation of isoaspartate (**147**). In both cases a free carboxyl group is generated and would be available for methylation (Scheme 2.31).

The esterification was repeated once more using the purified linear peptide acid, to evaluate if the additional purification step might improve the overall yield. Samples of the reaction mixture were taken every hour and examined via HPLC to monitor the progression of desired (and unwanted) product formation over time. The AUCs were used to calculate the proportional concentrations of each reactant or product in the mixture at each time point. The reaction was stopped after analysis of the reaction mixture at the 4 h time point, at which time the reaction was essentially complete. The mixture was poured into water and diethyl ether and the peptide-containing aqueous phase washed several times with more ether (181). The product was purified to afford the target esterified peptide in 45% yield. The esterification exhibited first-order kinetics with respect to the free carboxylic acid. Fischer

esterification is generally a second-order reaction but in this case the large excess of methanol causes it to follow *pseudo*-first-order kinetics (182).

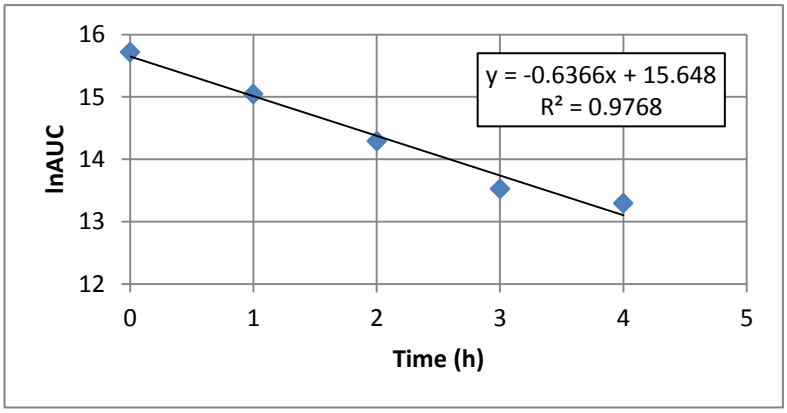

Figure 2.10 Linear plot of ln AUC *vs*. time (h) confirming the pseudo-first-order kinetics of the Fischer esterification reaction performed

As shown in Fig. 2.10 the calculated slope of the line of best fit gives a rate constant of 0.64 h^{-1}. Given this value, the half-life of the reaction was calculated at approximately 1.1 h, fitting with the fact that the concentration of reactant seemed to steadily almost halve at every hourly sampling. As R^2 = 0.98 indicates a strong linear relationship between ln AUC and the reaction time, the data appear to fit closely to a *pseudo*-first-order reaction model.

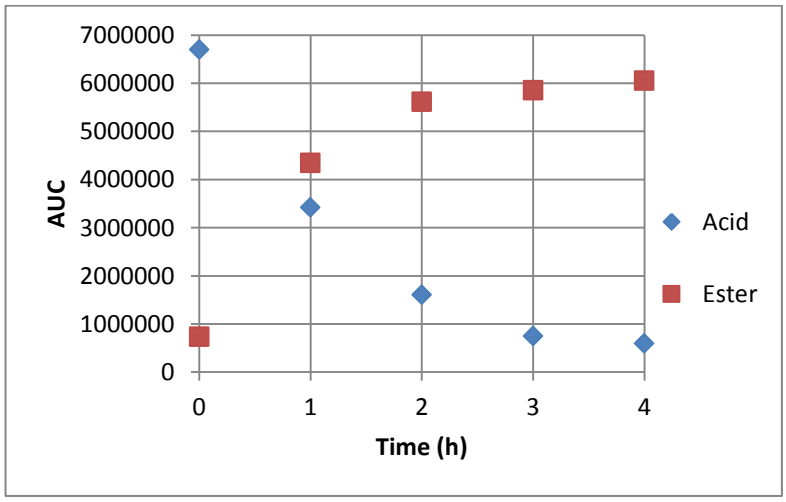

Figure 2.11 Plot of AUC *vs*. time (h) showing the reaction progression in terms of starting material and final product

Monitoring of the reaction progression allowed a suitable time point to be chosen at which to stop it when the conversion of starting material to product was essentially complete and when the levels of by-product formation remained acceptable. Comparison of the HPLC profiles of the collected samples showed how, within the

first hour, starting material and desired product had approximately reached the same concentration (as the line intersection suggests in Fig. 2.11). After 2 h the reaction was approximately 75% complete. Within the subsequent 2 h, consumption of the starting material was observed but the concentration of minor by-products started to become more noticeable, and by 4 h the amount of starting material was negligible, with by-product formation starting to increase further. As highlighted in Fig. 2.9, during the last hour the concentrations of starting and desired final product almost reached a plateau. From these results, it was unsurprising that in this second attempt at esterification, lasting only 4 h instead of 24 h (as done previously and as reported in the literature (181)), the yield of pure product isolated was much higher, as the optimum point in terms of conversion to product and acceptable by-product formation had been reached. It is therefore clear that for this sequence a long reaction time is not recommended.

2.4.1.5 Synthesis of the cyclic lassomycin free acid precursor

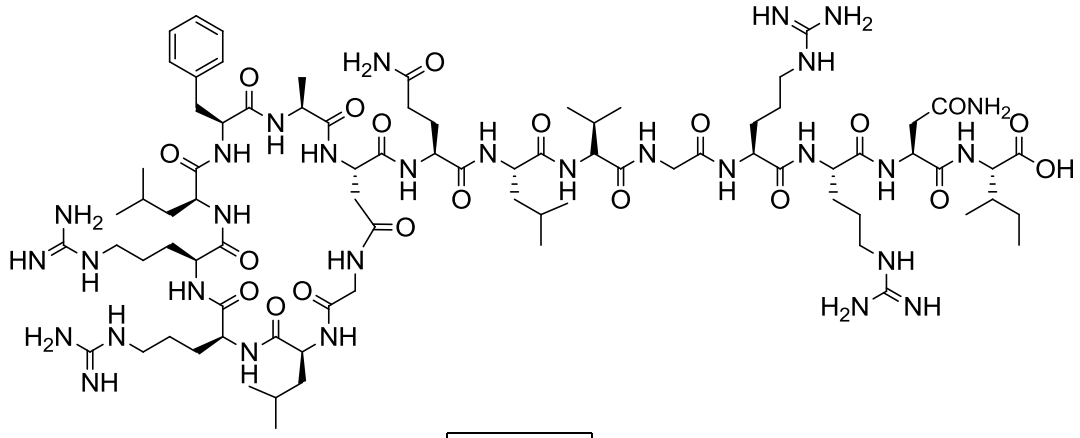

148, GLRRLFADQLVGRRNI

The cyclic lassomycin precursor was synthesised starting from preloaded Fmoc-Ile-Wang resin. The sequence was assembled via SPPS, incorporating Asp8 with side chain ODmab protection. The removal of Dmab (2% hydrazine monohydrate) was followed by on-resin cyclisation using DIC and HOAt. Two cyclisation steps of 24 h failed to give a negative Kaiser test, so the reaction was repeated a third time and a negative result was obtained after 24 h. In a subsequent attempt at the synthesis of **148**, the peptide-resin was treated with 5 mM NaOH for 3 h after the 2% hydrazine monohydrate treatment in order to ensure full removal of the Dmab deprotection prior to the cyclisation. In this attempt, the cyclisation still remained incomplete after two 24 h treatments with DIC/HOAt, but a negative Kaiser test was obtained after 6 h of a third cyclisation step. The HPLC profiles of the crude products from both syntheses showed no significant differences, and as a consequence they were

combined for purification purposes. The desired cyclic peptide was isolated in 1.5% yield. This outcome suggests that the NaOH treatment is apparently unnecessary and perhaps the cyclisation steps could be shorter in duration, while keeping the number of repetitions. A further attempt at the synthesis utilised a different cyclisation strategy; as two cycles of 24 h in DIC/HOAt failed to give a negative Kaiser test two cycles of a 6 h reaction using benzotriazole-1-yl-oxy-tris-pyrrolidinophosphonium hexafluorophosphate (PyBOP) and HOAt in the presence of DIEA were employed. The results of the Kaiser test seemed qualitatively improved, but the crude product had a similar HPLC profile to that of the other attempts. The crude product obtained using the latter cyclisation method was purified and resulted in an improved yield of 3.9%.

The HRMS (ESI) results for the isolated compound confirmed the presence of a signal at *m/z* 622.7047 consistent with the $[M+3H]^{3+}$ ion of the desired cyclic product (1865.1 Da). It should be noted, however, that the theoretical internal aspartimide by-product **149** has exactly the same molecular weight. Formation of aspartimide (Scheme 2.32) can be acid or base catalysed (183) and piperidine is generally the cause of its formation in Fmoc SPPS (184). This by-product has been reported to spontaneously form during elongations of Asn- or Asp-containing sequences (185); the nitrogen from the amide bond with the adjacent residue can attack the side chain carboxyl moiety of Asp. In a side-chain protected amino acid, such as Asp(ODmab), this carboxyl group is masked as an ester and can act as a leaving group in this reaction. Nucleophiles such as piperidine (or water, if present) can attack either one of the carbonyl carbon atoms and open the aspartimide ring (Scheme 2.33) (186). Unfortunately the isolated product has not yet been synthesised in sufficient quantity to allow unequivocal confirmation of the success of cyclisation via NMR. It is therefore not yet possible to realise to exclude the formation of the aspartamyl-peptide.

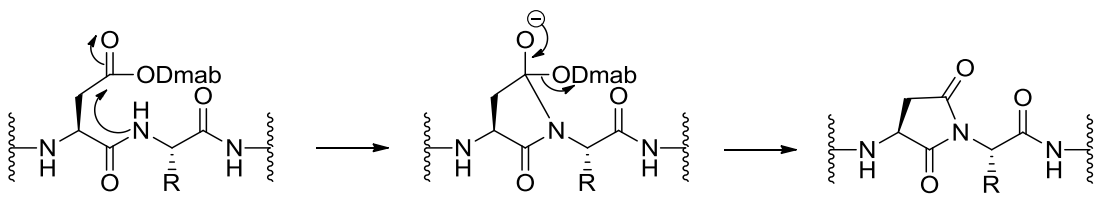

149

Scheme 2.32 Mechanism of aspartimide formation

Interestingly, in these syntheses some fractions were found to contain, according to ESI-MS signals, an unknown product of molecular weight corresponding to 2024.0 Da and products consistent with the α-piperidide of the β-peptide (**150**) or the β-piperidide of the α-peptide (**151**) (1951.0 Da). These molecules can be derived from the aspartimide ring opening mediated by the piperidine nucleophile (Scheme 2.33), or could be due to premature loss of the Dmab group, which might subsequently lead to activation of the Asp carboxylic side chain, which might then react with piperidine.

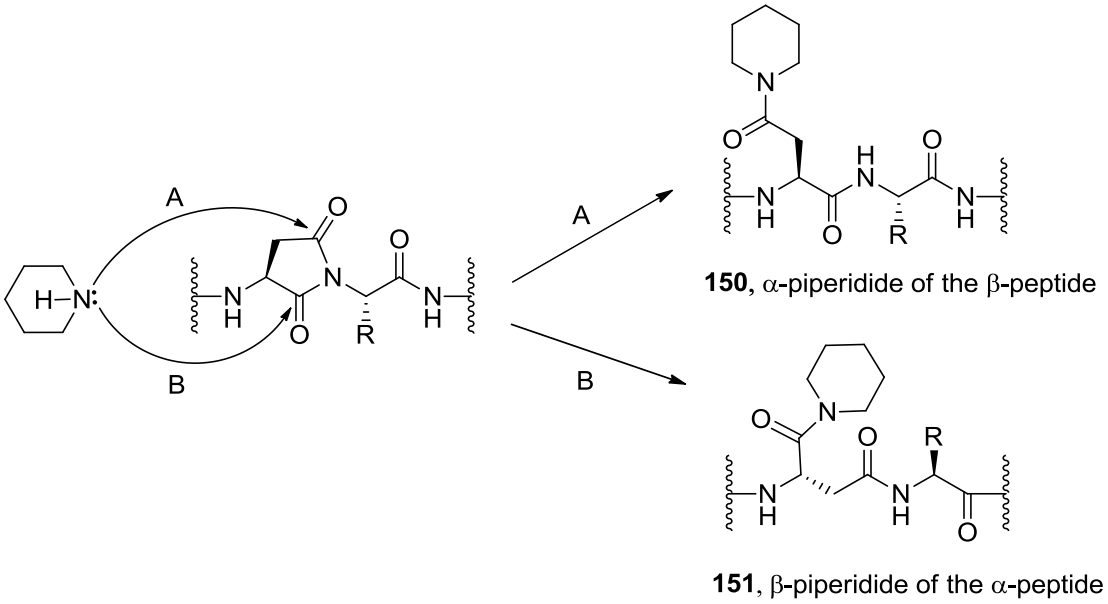

Scheme 2.33 Piperidine nucleophilic attack on the aspartamyl-peptide

2.4.2 Synthesis of lasso peptides and linear analogues using allyl ester side chain protection strategy

Following these findings the further attempts to attain the cyclic lasso peptides featured the use of a different semi-permanent protecting group on the side chain of the residue involved in the cyclisation. The use of the allyl ester (OAll) protecting group strategy has been found to produce high yields of cyclic peptides and fewer side products, when compared to the use of Dmab on the same sequence (177,178). It was therefore chosen as the Glu8 (lariatins) and Asp8 (lassomycin) side chain protecting group even though the moisture-free palladium-catalysed removal of OAll might prove itself more challenging and less convenient than the hydrazinolysis required for Dmab.

2.4.2.1 *O*-Allyl strategy synthesis of cyclic lariatins A and B

The first trial to synthesise lariatin A using allyl side chain protection on Glu8 was attempted manually following the usual manual protocol described in the general methods. The final residue coupling was not followed by Fmoc deprotection (as is typical in the Dmab strategy): the OAll deprotection step is performed first. Allyl ester removal requires anhydrous conditions, which were achieved by sealing the vessel with a rubber septum, followed by removal of air by vacuum and insertion of an Ar balloon. Through use of a syringe dimethylamineborane in dry CH_2Cl_2 was added to the resin, followed by quick addition of tetrakis(triphenylphosphine)palladium(0) catalyst ($Pd(PPh_3)_4$) (187). Deprotection proceeded for 1 h, followed by removal of the solvents using positive pressure of inert gas. After allyl ester removal, the terminal Fmoc group was removed with 20% piperidine and its success confirmed via the Kaiser test. A wash with 5% DIEA in DMF was added to remove any residual piperidine that might react with the free carboxylic acid moiety after its activation. Cyclisation for 24 h with DIC and HOAt was successfully confirmed by a negative Kaiser test, followed by cleavage of the peptide from the resin.
In parallel, a second trial was also attempted using automated SPPS, following the optimised protocol previously identified (two couplings of 30 min each using a 2.5-fold molar excess of activated amino acid). The remaining steps (deprotections, cyclisation and cleavage) following the assembly of the linear sequence were conducted identically as described for the manual synthesis.

Both cleaved crude lariatin A products (217 mg from the manual synthesis and 235 mg from the automated synthesis) were analysed via HPLC and their profiles were extremely similar. Each crude sample was divided into two portions (to avoid exceeding the capacity of the preparative column) and purified by preparative HPLC. The fractions collected, after being analysed via HPLC, were combined according to their identity and purity and sent for LC-MS analysis. The signals at *m/z* 1026.6 and 684.7 are consistent with the $[M+2H]^{2+}$ and $[M+3H]^{3+}$ ions of the desired product, which was isolated in a final yield of 1.5%. Some impure fractions, whose HPLC profiles confirmed the presence of lariatin A as the major component, were combined for a total mass of 22 mg. After evaluation of possible systems that could have allowed the separation of the contaminants, purification of this impure sample was attempted on a semi-preparative HPLC column. The fractions collected, however, were unfortunately still not completely pure.

As the products from the manual and automated syntheses were of very similar quality, the synthesis of lariatin B, incorporating Glu(OAll), was conducted

automatically (for its obvious advantages of time and convenience). The synthesis was also programmed to utilise the standard 2 × 30 min double coupling protocol with 2.5 equivalents of activated amino acid per coupling and all the steps were performed similarly to the synthesis of lariatin A. The crude product HPLC highlighted the presence of two major peaks. Approximately half of the crude sample was subjected to purification; the pure fractions corresponding to the later eluting peak, which added up to a disappointing 3% yield, were analysed by LC-MS and showed signals at *m/z* 1103.5 and 736.1 consistent with the $[M+2H]^{2+}$ and $[M+3H]^{3+}$ ions of the desired cyclic lariatin B product.

2.4.2.2 *O*-Allyl strategy synthesis of cyclic lassomycin free acid precursor

The synthesis of the cyclic lassomycin precursor **148** using Asp(OAll) was attempted automatically. The synthesiser was programmed to follow the same optimised protocol as developed above. As with the lariatin synthesis, the final Fmoc deprotection of the linear peptide was not performed and the resin-bound peptide was transferred to a sealed vessel, under Ar atmosphere, to provide for the required anhydrous conditions of allyl ester deprotection. The removal of the Asp8 side chain protection was followed by Fmoc deprotection prior to the cyclisation step. In the case of lassomycin, as experienced previously, one 24 h treatment with DIC and HOAt did not result in a negative Kaiser test, therefore the cyclisation was repeated a second time which unfortunately failed to lead to any improvement. One possible reason could have been that the allyl deprotection failed or was incomplete, subsequently resulting in the lack of sufficient activated carboxyl component to allow the cyclisation to take place fully. Therefore the peptide-resin was washed thoroughly and the anhydrous conditions under Ar atmosphere re-established. The OAll removal step was repeated, followed by a third attempt at cyclisation for 24 h. Once again the Kaiser test remained positive and no further trials were attempted. The peptide was cleaved and the crude sample analysed: the HPLC chromatogram shows three major peaks; purification lead to the isolation of a compound whose MS analysis showed signals at *m/z* 988.9, 622.8 and 467.4 consistent with the $[M+2H]^{2+}$, $[M+3H]^{3+}$ and $[M+4H]^{4+}$ ions of either the desired product or its aspartimide-derivative (see discussion above). The retention time of the compound isolated was longer (R_t = 9.92 min) than that of the product obtained via the ODmab side chain protection strategy (R_t = 9.10 min). It is likely that one of these two different products is the desired cyclic product and the other is the aspartimide by-product, as both have the same molecular weight, consistent with the mass spectral data. It might be expected that the product with the longer retention time (from the OAll strategy

synthesis) is more likely to be the cyclic product as it lacks a free *N*-terminus and should be lower in polarity.

2.4.3 General discussion of attempted lasso peptide syntheses

The synthesis of the linear analogues of the three lasso peptides has been successfully achieved, as well as the Fischer *C*-terminal esterification of the lassomycin linear analogue. Unthreaded cyclic lariatins A and B have been synthesised for the first time. The SPPS strategy demonstrated itself prone to a number of undesirable side reactions which resulted in poor yield recovery. The main difficulties were encountered while using γ- and β-carboxyl Dmab side chain protection, which has previously been reported to be associated with the problematic formation of pyroglutamate and aspartimide by-products. Asp(ODmab)-containing sequences are particularly prone to the formation of the latter derivatives, while Glu(ODmab) (and Gln) containing sequences can lead to the occurrence of *N*-terminal pyroglutamyl peptides. The pyroglutamyl-peptide was identified in and isolated from the crude products of the attempted lariatin syntheses, while the aspartamyl product has likely been identified among the products of the attempted cyclic lassomycin free acid precursor syntheses, but preliminary MS data cannot unequivocally identify it as the molecular weights of the aspartimide-containing peptide and the desired cyclic peptide are the same (1866.3 Da). In addition, piperidine adducts were isolated from the cyclic lassomycin precursor crude mixture; these are formed by aspartimide ring opening by nucleophilic attack on either of the carbonyl carbon atoms, or by premature loss of Dmab.

The use of γ-carboxyl side chain allyl protection proved to be a better strategy than the employment of Dmab for the synthesis of the lariatins allowing their isolation, even though in very low yields (1.5 and 1.8% respectively). The HPLC profiles enabled the identification of pyroglutamyl-peptides even using this strategy, though present in lower concentrations than seen in the Glu(ODmab) strategy synthesis. Allyl removal is more challenging due to the necessity to maintain dry conditions and there was some suspicion that this may have compromised the outcome of the cyclic lassomycin synthesis, but MS signals are consistent with ions corresponding to the desired product or the aspartimide derivative. In the case of lassomycin the crude product obtained with the OAll strategy, analysed via HPLC, showed the presence of a peak distinct to that from the crude product obtained via the ODmab strategy. Isolation of this peak was achieved and the sample analysed by NMR, with the intention of comparing the spectra of the two products to find differences that

would allow identification of the isolated compounds. Unfortunately the NMR obtained from the latest purification was of poor quality possibly because of the very limited amount available, therefore it was not possible to come to any definitive conclusions. Automated SPPS proved itself a satisfactory method to access the linear precursors. Overall, however, the chosen synthetic strategies still require some optimisation for the synthesis of these cyclic peptide natural products.

2.4.4 Biological evaluation

The lariatins have previously been tested on *M. tuberculosis* and *M. smegmatis* (118,120); lariatin A showed bactericidal activity against both organisms, while lariatin B only against the latter. Lassomycin has been selectively tested only on *M. tuberculosis* against which it shows a minimum inhibitory concentration (MIC) of 0.8-3 mg/mL (depending on the strain used) (115).

2.4.4.1 Target-based evaluation

The mechanism of action of the laritins has not yet been investigated. Under these circumstances it is clear how it would not have been possible to perform a target-based assay. The reported mechanism of lassomycin action is based on the inhibition of the ATP-dependent protease ClpC1P1P2 (115), but the attainment of the target enzyme was beyond the scope of this work.

2.4.4.2 Whole-cell evaluation

Among the lasso peptides, the pure cyclic lariatin B sample was tested on the SPOTi assay on *M. smegmatis*, *M. aurum* and *M. bovis* BCG. The bacteria were cultured as described in Chapter 4.6.5.6. The 2.4 mg of lariatin B available were dissolved in water to a concentration of 50 mg/mL and the dilution plate was prepared as described in Chapter 4.6.5.13. The dilutions were transferred to a 96-well plate and mixed with agar. Once the agar had solidified the bacterial cultures were inoculated and the plates incubated according at 37 °C for 3 days for *M. smegmatis*, 35 °C for 5 days for *M. aurum* and 37 °C for 14 days for *M.bovis* BCG.

The plates showed no inhibition of bacterial proliferation, while the INH positive control performed as expected. This is very likely to be due to the fact that an unthreaded structure will lack the stability to hydrolytic enzymes that is probably one of the main reasons for lasso peptides potency and effectiveness. The threaded conformation may also be crucial for interaction with a specific target, which mediates the antibacterial activity.

The remaining cyclic and linear peptides are still in the process of being evaluated for their activities against mycobacterial strains.

3. CONCLUSIONS

3.1 Synthesis of Lys-containing PG fragments and analogues

The Lys-containing fragments of the peptidoglycan have successfully been assembled both manually and automatically. Comparison of the two synthetic methods showed that, despite the lack of monitoring of coupling completion that is possible during manual synthesis, the automated system gave products with a significantly higher level of purity. Automated solid-phase peptide synthesis has therefore revealed itself to be the ideal methodology in obtaining these short peptide sequences, representing a saving in time, money and workload.

The optimisation of the Syro I system was conducted through testing of a series of protocols. These involved the synthesis of the same peptide (Leu-enkephalin) sequence with different combinations of equivalents of amino acid per coupling, numbers of couplings and durations of couplings. While tentative trends could be seen, the results obtained showed no clearly significant differences in the pure yields, fuelling the doubt that the sample peptide utilised might have been too easy to synthesise, such that the method could not discriminate between the protocols. Consequently ACP 65-74, a well-known challenging sequence, was used to repeat the evaluation of the protocols. The outcomes showed no clearly apparent differences in yield among the various protocols, except for the one involving two 30 min couplings with a 2.5-fold molar excess of activated amino acid, which was subsequently utilised as the standard for the automated synthesis of several analogues of the Lys-containing PG fragments and the lasso peptides. Nonetheless it is possible to observe how increasing the number of couplings and the duration of the reaction, up to 30 min, seems to improve the yield to a certain extent. Swelling of the resin prior to deprotection and HOBt addition did not appear to exert a great influence on the synthetic outcome for this sequence. It is possible that the lack of statistical significance in the observed differences in yield may have been a consequence of the small number of repeats of each trial.

The peptides obtained were evaluated against *M. aurum*, *M. smegmatis* and *M. bovis BCG*, using the SPOTi whole-cell assay, in the hope of detecting their potential as antimycobacterial/anti-TB agents. Unfortunately the compounds did not show any interesting activity. The intention was also to evaluate them as substrates or inhibitors for Mpl, using an enzyme-based assay, but the heterologous expression and purification of *M. tuberculosis* Mpl had not yet been perfected to enable these

studies to be conducted. The Lys-containing fragments and their sequence analogues also failed to show any inhibitory effect against the Gram negative organism *E. coli*.

The Lys-containing PG fragments are now available for characterisation of the activity of different Mur ligases in Gram positive bacteria and to be tested for any inhibitory effect on *M. tuberculosis* Rv3712. The sequence analogues will also be evaluated against Gram positive and negative bacterial Mur ligases to determine if they have any inhibitory activity.

3.2 Synthesis of *m*DAP-containing PG fragments and analogues

The production of protected *m*DAP was successfully achieved via cross-metathesis between olefins D-allylglycine and L-vinylglycine, as suggested by Roychowdury *et al.* (36,147). In order to utilise the product in SPPS for the production of peptide fragments of PG, an appropriate orthogonal protection strategy needed to be followed. The necessary building blocks chosen were N^{α}-Fmoc-protected vinylglycine benzyl ester and N^{α}-Boc D-allylglycine *tert*-butyl ester. Their synthesis was attempted following a variety of methods which led to the successful attainment of the vinylglycine component. Unfortunately, the use of an enzymatic resolution methodology for the large-scale synthesis of D-allylglycine proved unsuitable as the acylase enzyme was not very efficient for hydrolysis of the N^{α}-acetyl-L-allylglycine, resulting in poor enantiomeric purity. Commercially available N^{α}-Boc D-allylglycine was purchased instead and subsequently protected as the *t*Bu ester.

Similar published cross-metathesis reactions prescribed 24 h at room temperature. A preliminary evaluation of times and temperatures seemed to suggest the suitability of a microwave-assisted methodology. This method was pursued and the product successfully obtained at 55 °C within 1 h on a small scale, conveniently followed by preparative HPLC purification. Comparison of the efficiency of two different catalysts – Hoveyda-Grubbs and Grubbs 2nd generation – showed no significant difference, therefore the reaction was repeated using the Grubbs 2nd generation catalyst as suggested by reported methods (36,147). Attempts to conduct the reaction on larger scale were inconsistent and often unsuccessful, so the small scale cross-metathesis reactions were repeated a number of times, combining and purifying the products until sufficient *m*DAP precursor was collected. The successful hydrogenation of the double bond led to the isolation of the suitably-protected *m*DAP, retaining the Fmoc protecting group.

The product was loaded onto a 2-ClTrt resin and the tripeptide H-Ala-D-Glu(*m*DAP-OH)-OH manually assembled. The purification was only partially successful; MS confirmed the presence of the tripeptide in the sample, but the desired product was contaminated by another co-eluting compound of similar R_f. The two compounds eluted very quickly by RP-HPLC even using 100% water as the mobile phase. Unfortunately it was not possible to further purify the product because of the small amount collected and because of time limitations.

While protected *m*DAP can be now synthesised, the methodology requires much optimisation. With more *m*DAP in hand, more tripeptide could be synthesised and purification perhaps attempted using a longer column or different stationary phase. Another possibility could be to couple the *N*-terminal Ala as the Boc-protected derivative, prior to mild cleavage from the 2-ClTrt resin. In this manner, after removal from the solid support, the peptide, and possibly the unwanted product too, will bear a protecting group that will render them less polar. This should make them elute later when the gradient is changing, therefore allowing for a better separation.

The tripeptide will then be available for activity evaluation as a substrate for Mpl or MurE. Furthermore, ready access to *m*DAP will be useful for the preparation of other PG fragments and analogues. The fragments could then be used to evaluate the activity of different Mur ligases in a number of pathogens and analogues could be developed as possible inhibitors that may have value in TB therapy.

The recombinant heterologous expression of Rv3712, *M. tuberculosis* putative Mpl, was successfully achieved in *E. coli* BL21(DE3)pLysS competent cells, using pCDFDuet-1 as a vector. However, its isolation still requires optimisation, especially for the purification step. It will be necessary to consider performing a second purification before utilising the product enzyme in any biological evaluation. That should be sufficient to start testing the enzyme activity. This could be assessed through a colorimetric assay (Scheme 3.1) able to detect the release of inorganic phosphate derived from the hydrolysis of ATP following enzyme activity in the presence of substrates. There is a 1:1 proportion between the enzyme's use of ATP and the molecules of peptide substrate used. This assay was originally developed to characterise the activity of recombinant Mur ligases from *M. tuberculosis* (Mur C, D, E and F) (39,54,61); it uses PiColorLock Gold kit (Innova Biosciences) and requires the enzyme, ATP, UDP-Mur*N*Ac and the investigated peptide.

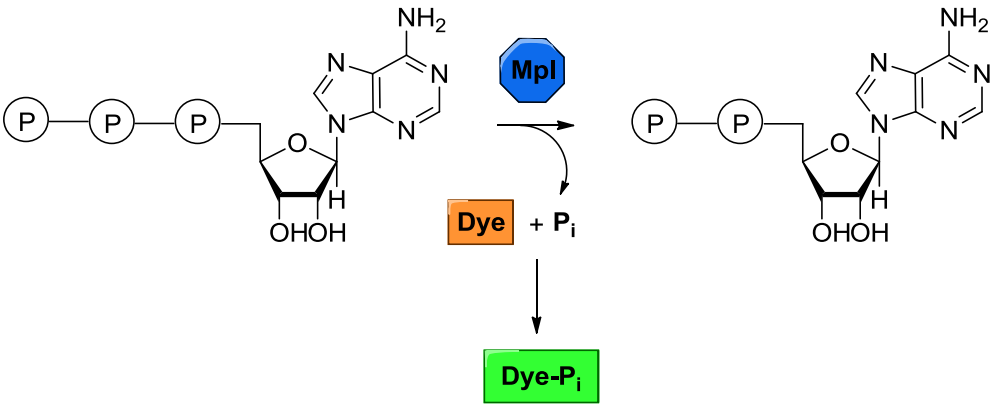

Scheme 3.1 Activity assay: the dye binds to the inorganic phosphate and turns from orange to green.

This assay can be readily used to evaluate enzyme activity using the single amino acid L-Ala, the already synthesised dipeptide (L-Ala-D-Glu, **53**) and the crude *m*DAP-containing tripeptide (Chapter 2.3), even in its impure form, and eventually tetra- and pentapeptides. It will also serve to investigate the substrate analogues/inhibitors and the associated inhibitory kinetic parameters. This information would contribute to the biochemical characterisation of this enzyme in *M. tuberculosis.*

With the purpose of elucidating the structure of the enzyme it is intended to set up crystallisation trials. This would require larger amounts of pure enzyme, as discussed in Chapter 2.3.1.1.3. Improvements in the enzyme yield could be investigated by changing the vector, the surrogate or the cloning strategy.

For this purpose it may be useful to change the surrogate cells used for the protein expression. BL21(DE3)pLysS competent cells were picked after an optimisation study performed by Nukala *et al.* (174), who compared results with those obtained with NEB Express and Rosetta DE3. Munshi *et al.* (54), though, during the study of the *M. tuberculosis* Mur ligases Mur C and Mur F, switched from BL21(DE3)pLysS to *Pseudomonas putida* strain KT2442 and it was found that the latter allowed the isolation of higher amounts of purer enzyme. Therefore the transformation of the construct into this specific strain is currently being considered a viable option to improve the recovery of pure *M. tuberculosis* Mpl.

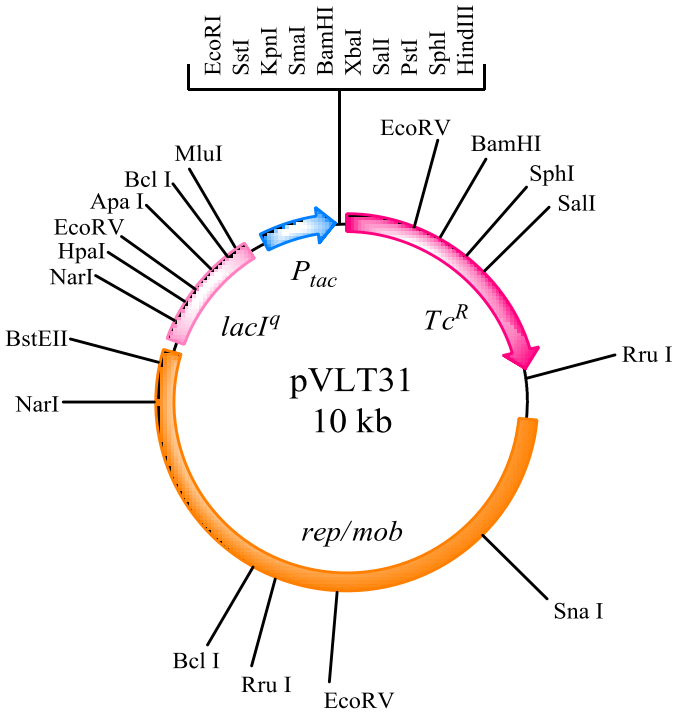

Figure 3.1 Schematic representation of plasmid pVLT31

The *P. putida* cells used by Munshi *et al.* (54) were carrying pVLT31 (Fig. 3.1) as a vector. The Mtb-Mpl construct will need to be cloned into pVLT31 and the clones will be selected in *E. coli* DH5α. The *P. putida* cells will need to be rendered electro-competent before being able to be transformed.

Another option would be to approach an alternative cloning strategy following the work of Usha *et al.* (188). The *M. tuberculosis* genome is highly biased towards C- and G-ending codons. It seems that when using a surrogate this can become an issue; the *M. tuberculosis* gene is being translated by ribosomes belonging to a different organism (*E. coli*) which has a different bias. This causes the ribosome to stall when it encounters alternatively biased codons. This critically reduces the amount of protein produced. In their work, Usha modified only the first 30 nucleotides to match the preferences of the surrogate, without changing the product composition. Their efforts resulted in a dramatic increase in the production of the desired mycobacterial protein.

Substrates to be tested will include L-Ala, the Lys- and *m*DAP-containing pentapeptide (L-Ala-D-Glu(Xaa-D-Ala-D-Ala-OH)) and *N*-terminal truncated di-, tri- and tetrapeptides and their UDP-Mur*N*Ac derivatives. Peptides including isosteres of *m*DAP or of other residues in the chain will also be evaluated.

3.3 Synthesis of anti-TB lasso peptides and linear analogues

The synthesis of the threaded lasso peptides, such as the lariatins, is an intriguing challenge but an objective of this study was to evaluate whether unthreaded or linear peptides with the same sequences might retain a degree of antibacterial activity. Lassomycin was initially reported to have a non-threaded structure, but a later study by Lear *et al*. (116) suggests that its structure is actually threaded.

The linear analogues of both lariatins A and B were successfully synthesised. The syntheses of the lariatins were challenging and complicated by pyroglutamate formation, probably promoted by the basic conditions used during Fmoc deprotection, with subsequent failed elongation of the peptide considerably reducing the yields. Dmab side-chain protection removal seems to further facilitate the formation of pyroglutamate as previously reported. Linear peptides bearing Gln instead of Glu seemed also to be affected by this side reaction. Pyroglutamate formation severely hindered the production of the cyclic lariatins. HPLC analysis of the crude lariatin cyclisation products showed only one major peak in each case, and these were identified through ESI-MS to be the pyroglutamate derivatives. ESI-MS analysis of the crude samples failed to indicate the presence of the desired cyclised peptides.

In the case of lassomycin, the linear analogue with a free *C*-terminal carboxyl group and bearing Asn in position 8, was obtained successfully. Methyl esterification of the *C*-terminus was also successful. HPLC-based analysis of the reaction kinetics helped define a better reaction time (reducing it from 24 h to 4 h) and improved the yield. Lassomycin cyclisation using a Dmab protection strategy produced a product which, according to MS analysis, has a molecular weight corresponding either to the cyclised peptide or the aspartimide derivative. Additional material will be required for the necessary NMR studies to fully elucidate the structure of the product.

Given the problems encountered with the Dmab protection strategy, the syntheses of the cyclic molecules were repeated using an allyl ester side chain protecting group. Using this strategy, pyroglutamate formation proved less problematic, but the conditions required for allyl deprotection are less convenient than those for Dmab removal. The allyl strategy allowed the successful attainment of the cyclised lariatins A and B, even though in disappointingly low yields. The synthesis of the lassomycin free acid using this strategy yielded a compound with a molecular weight consistent with that of either the desired cyclic peptide or its aspartimide derivative.

Overall the synthetic routes examined seemed far from optimal. Of the cyclic peptides successfully synthesised only the lariatin B product was tested against different mycobacterial strains and it failed to show any inhibitory activity. This may be a consequence of the fact that it is very unlikely to be threaded like the natural product as this conformation does not seem to form spontaneously. As expected, the unthreaded conformation does not possess the activity of the threaded one. This may be related to its conformation or increased susceptibility to hydrolytic enzymes as the unusually high stability of the lasso peptides, which may be related to their potency, would be missing.

Lariatin A, the linear lariatin analogues and *C*-terminal free acid and methylated linear lassomycin analogues are in the process of being evaluated against mycobacteria. The products isolated from the synthesis of the cyclic lassomycin free acid with the two different strategies have different retention times and both have a molecular weight consistent with the desired cyclic free acid. It is likely that one is the desired cyclic free acid and the other is the aspartimide. NMR analysis of the pure samples has unfortunately not, at this stage, helped to definitively identify which compound is which, due to the very small amounts available. Additional material will be necessary in order to confirm the structure of these products.

Possible options to improve the outcomes include reduction of the occurrence of aspartimide formation by using milder bases than piperidine (such as piperazine), as reported by Wade *et al*. (189). This might lead to a lower efficiency of deprotection but could possibly be overcome by an increased number of deprotection steps. Addition of 0.1 M HOBt to the piperidine solution has also been suggested to minimise the formation of aspartimide (183).

3.4 General conclusion and future work

The establishment of a successful method for the synthesis of protected *m*DAP provides the opportunity for the production of a number of PG fragments that could be used for the evaluation of Mur ligases from both Gram positive and Gram negative bacteria to aid understanding of the PG synthesis machinery. In the first instance, larger quantities of protected *m*DAP will need to be synthesised to allow incorporation into fragments that will be used for the characterisation of *M. tuberculosis* Rv3712, through the assay mentioned in Chapter 3.2. Furthermore, the availability of protected *m*DAP will allow its incorporation into different peptides designed to inhibit recycling enzymes. Peptides of future interest will also include

UDP-Mur*N*Ac-linked PG fragments, fragments truncated in different positions and fragments modifiec on the *N*- or *C*-terminus.

The heterologous expression of *M. tuberculosis* Rv3712 could be improved by changing the vector and competent cells, as suggested in Chapter 3.2, and if isolated in sufficient quantities could be used for crystallisation trials, alone or in combination with its substrates.

The large-scale synthesis of N^{α}-Boc D-allylglycine *tert*-butyl ester from allyl bromide and diethylacetamidomalonate, followed by enzymatic resolution, still needs to be optimised. Access to a preparative HPLC chiral column may provide an opportunity for more efficient isolation of the desired product.

4. EXPERIMENTAL

4.1 Materials and general methods

All amino acids and resins were purchased from Novabiochem (Merck), Nottingham, UK. $CDCl_3$, D_2O and CD_3OD for NMR spectroscopy were purchased from Cambridge Isotope Laboratories Inc. Peptide synthesis grade DMF was obtained from Rathburn Chemicals, Walkerburn, UK. All other chemicals, solvents and reagents were obtained from Sigma-Aldrich, Fisher Scientific or Tokyo Chemical Industry Co., Ltd. When required, solvents were purchased in the anhydrous form, freshly distilled or dried accordingly to established practices. Merck pre-coated (aluminium-backed) silica gel 60 F_{254} TLC plates were used for monitoring the reactions. TLC plates were either visualised under UV radiation at 254 nm, or stained with ninhydrin (in 95% ethanol and 4.5% acetic acid) or with PMA (phosphomolybdic acid in ethanol, 5% *w/v* solution), followed by heating.

4.2 Spectroscopic methods

NMR characterisation was performed using a Bruker Avance Spectrometer, operating at 400 MHz or 500 MHz frequency. The data collected were processed using Bruker NMR Suite 3.5 and TOPSPIN 3.2 Plot Editor software. The chemical shifts (δ) are expressed in ppm downfield from TMS and calibrated to the residual peak of the deuterated solvent. The peaks have been described as: singlet (s), broad singlet (br s), doublet (d), double doublet (dd), broad doublet (br d), triplet (t), quartet (q) or multiplet (m), coupling constants are stated in Hz. Spectral assignments were assisted using the appropriate 2D experiments, including ^{1}H-^{1}H COSY, HMQC and HMBC. Mass spectrometry data were obtained from a Finnigan Navigator Single Quadrupole Mass Spectrometer (low resolution) or Waters Q-TOF Global Ultima® (high resolution) instrument using electrospray ionisation (ESI). LC-MS data were acquired on a Shimadzu LC-MS 2020 system combined with a LC-20AD Prominence pump (running 10% MeCN for 1 min, then 10-95% MeCN over 7 min and then 95% MeCN for 5 min), a SPD-20A Prominence UV/VIS detector, a CTO-20A Prominence column oven (40 °C), a DGU-20A5 Prominence degasser and a SIL-20ADht Prominence autosampler. Analytical RP-HPLC separation was generally achieved using a 4.6 × 250 mm Waters Atlantis® dC_{18} 5 μm column or (when specified) a Macherey-Nagel EC 4.0 × 200 mm NUCLEODEX βOH chiral column. Both preparative and analytical HPLC used a mixture of solvent A (0.02% *v/v* TFA in water) and solvent B (0.016% *v/v* TFA in 90% aqueous MeCN) as the

mobile phase. A gradient system was generally used for analytical HPLC, running 0% to 100% B over 20 minutes, then 100% B for 5 minutes, then 100% to 0% B over 5 minutes (flow rate 1.2 mL/min) (System A1), or 0% to 50% B over 25 minutes, then 50% to 100% B over 2 minutes, then 100% B for 5 minutes, then finally 100% to 0% B over 3 minutes (flow rate 1.2 mL/min) (System A2). Analytical separations were carried out using System A1 unless otherwise stated. The gradient was controlled with a Waters Alliance e2695 Separations Module and elution was monitored at 214 or 254 nm (except for Marfey's method analyses, which were monitored at 340 nm) using a Waters 2489 dual wavelength detector. Retention times (using System A1 unless otherwise stated) are reported in minutes.

Semi-preparative and preparative RP-HPLC separation were achieved using, respectively, a 10 × 250 mm and a 19 × 250 mm Waters Atlantis® dC_{18} 10 µm column. The preparative gradient was controlled with a Waters 600 Controller and Delta 600 pump and elution was monitored at 214 nm using a Waters 2487 detector. Different gradient systems were used for separation depending on the mixture. A flow rate of 10.4 mL/min was used unless otherwise specified. System P1: 0% to 20% B over 20 minutes, then 20 to 70% B over 50 minutes, then 70% to 100% B over 20 minutes. System P2: 50% to 100% B over 40 minutes, then 100% B for 20 minutes. System P3: 0% B for 10 minutes, then 0 to 30% B over 40 minutes, then 30% to 50% B over 30 minutes and finally 50% B for 20 min. System P4: 10% B over 10 minutes, then 10 to 60% B over 50 minutes, then 60% to 100% B over 20 minutes. System P5: 0% to 20% B over 20 minutes, then 20 to 60% B over 60 minutes, then 60% to 100% B over 20 minutes. System P6: 10% B for 10 minutes, then 10 to 60% B over 30 minutes, then 60% B for 10 minutes and finally 60 to 100% B over 10 min. System P7: 0% to 20% B over 20 minutes, then 20 to 80% B over 80 minutes, then 80% to 100% B over 20 minutes.

4.3 Solid-phase peptide synthesis

Unless otherwise specified, N^{α}-Fmoc-protected amino acids pre-loaded onto Wang resins were used. The resin was washed and swelled in DMF (*ca.* 2 mL) for 1 hour. N^{α}-Fmoc deprotection was performed with 20% *v/v* piperidine in DMF (ca. 4 mL) for 2 × 15 minutes followed by a thorough wash with DMF.

Couplings with Fmoc-protected amino acids were performed using a 2.5-fold excess (over manufacturer's resin substitution) of amino acid, HBTU and HOBt in the presence of a 5-fold excess of $i\text{Pr}_2\text{NEt}$ (DIEA), dissolved in minimal DMF. Each coupling was allowed to proceed for 30 min unless otherwise specified, before

briefly washing the resin and repeating once. The Kaiser test (190) was used to monitor the completion of the coupling. Briefly, a sample (*ca.* 2-3 mg) of resin was removed from the coupling mixture, washed with DMF and 50% *v/v* CH_2Cl_2 in methanol then dried briefly under suction. 80% *m/v* phenol in ethanol (1 drop), 0.04 mg/mL KCN in pyridine (2 drops) and 0.28 M ninhydrin in ethanol (1 drop) were added to the dried resin, followed by heating at 110 °C for *ca.* 3 min. In the case of positive test, the coupling step was repeated until a negative test result was obtained. After a final deprotection step, the resin was washed thoroughly with CH_2Cl_2 then 50% *v/v* CH_2Cl_2 in methanol and finally dried for 2 min under vacuum. The resin was then transferred to a desiccator where it was left to dry under vacuum for at least 3 h (and preferably overnight). Cleavage of the peptides from the resin was performed by acidolysis with TFA. For each 100 mg of resin used, 2 mL of a mixture of 95% TFA, 2.5% water and 2.5% triisopropylsilane (*v/v/v*) was added to the sample and the suspension gently stirred for 2 h. The sample was then filtered under vacuum through a sintered glass funnel and the resin beads washed with fresh TFA. The filtrate was evaporated to near dryness and then cold diethyl ether was added to the residue to precipitate the product. The crude peptide was filtered by gravity and washed with fresh ether before extraction into 95% (*v/v*) aqueous acetic acid. Finally the product was freeze-dried.

The side chain protecting groups used for amino acids were (unless otherwise specified): Pbf for Arg; Boc for Lys, Trp and His; Trt for Asn and Gln; *t*Bu for Ser and Tyr; and O*t*Bu for Asp and Glu.

4.4 Automated solid-phase peptide synthesis

Automated solid phase synthesis was performed using a Syro I single channel automatic peptide synthesiser (BioTage, Sweden).

Prior to the synthesis, the resin was swelled in DMF for 1 h. The synthesiser was programmed to perform deprotection using two different concentrations of piperidine in DMF: a first deprotection cycle of 3 min with 40% *v/v* piperidine in DMF and a second one of 12 min with 20% *v/v* piperidine in DMF solution followed by 6 washes of 1 min with DMF (vortexing for 10s, followed by a 1 min break). Unless otherwise specified, couplings were programmed to use 2.5 molar equivalents (over resin substitution) of amino acid (in DMF) and HBTU and a two-fold excess of DIEA. Stock solutions of 0.5 M HBTU in DMF, 0.5 M protected amino acid in DMF and 2 M DIEA in NMP were freshly prepared and loaded into the synthesiser. The machine

was programmed to perform 2 × 30 minutes couplings for each amino acid, with intermittent vortexing for 15 s, followed by 2 min breaks. Between couplings three washes of 1 min with DMF were performed (vortexing for 10 s, 1 min break). After the final deprotection step the resin was washed with CH_2Cl_2 and finally dried for 2 min under vacuum. The solid phase vessels containing the resin were then transferred to a desiccator where they were dried for at least 3 h.

Cleavage and isolation proceeded as described above for manual synthesis. For protocols involving the use of a centrifuge, cleavage was followed, after TFA removal, by addition of 10 mL cold *tert*-butyl methyl ether. If required, the sample was refrigerated overnight to maximise precipitation of the peptide and was then centrifuged twice at 3500 rpm (4 °C), decanting and replacing the *tert*-butyl methyl ether supernatant at the end of the first run. After the second run, the supernatant ether was discarded and the residue was dissolved in 95% aqueous acetic acid and freeze-dried.

4.5 Advanced Marfey's method: FDAA derivatisation

1-Fluoro-2-4-dinitrophenyl-5-L-alanine amide (FDAA) derivatisation was achieved by dissolving the amino acid in distilled water and adding to it 0.8 equivalents of 1 M aqueous $NaHCO_3$. To the solution, 1.85 molar equivalents of a 1% *m/v* solution of FDAA in acetone was added and the mixture was left to stir 1 h at 45 °C. 1 M HCl was added to quench the reaction and the mixture was transferred to an HPLC vial, making up the volume to 1 mL with Solvent B. The mixture was analysed by RP-HPLC on a chiral column using System A2.

4.6 Biological methods

4.6.1 Chemicals, reagents and solutions

Reagents for molecular biology were obtained from New England BioLabs (UK) Ltd (Hitchin, UK). Protein ladders and DNA purification kits were obtained from Thermo Fisher Scientific (Loughborough, UK). All stock solutions were prepared in double distilled water (ddH_2O) unless otherwise stated. Percentage solutions are described as volume/volume (*v/v*) or as weight/volume (*w/v*).

4.6.2 Bacterial strains

BL21(DE3)pLysS Singles Competent Cells were obtained from Merck Millipore (Watford, UK). These competent cells are highly efficient for protein expression. Protein expression is controlled by the T7 promoter and has a ribosome binding site

(RBS). It is lysogenic for λDE3. It contains the T7 bacteriophage gene encoding T7 RNA polymerase under control of the UV5 promoter. pLysS carries T7 lysozyme, which lowers the background expression level of the target gene under control of the T7 promoter but does not interfere with the level of expression achieved by IPTG induction. The BL21(DE3)pLysS competent cells provide higher control of protein expression and are chloramphenicol-resistant.

4.6.3 Vector

pCDFDuet-1 was a generous gift from Professor Gabriel Waksmann, Birkbeck, University of London, UK. This vector is used for the recombinant expression of two target open reading frames (ORFs). The vector contains two multiple cloning sites (MCS) each of which is preceded by a T7 *lac* promoter and ribosome binding site. The vector also carries *lac I* and a streptomycin resistance gene. Rv3712 was cloned in MCS1 by digesting with *EcoR I* and *Hind III.* The Tig A (Rv2462c) gene from *M. tuberculosis* was cloned in MCS 2 in between *Nde I* and *Xho I* restriction endonuclease sites (Fig. 4.1).

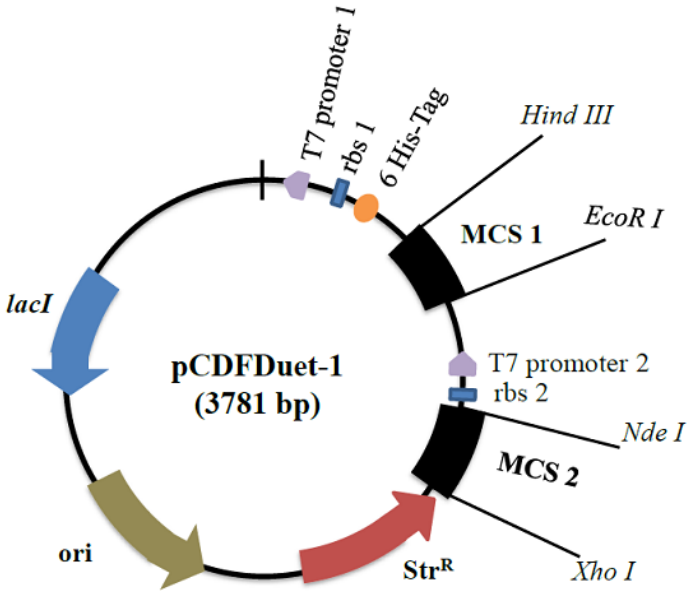

Figure 4.1 Plasmid pCDFDuet-1

4.6.4 Bacterial growth media

25 g of Luria-Bertani broth (LB) was dissolved in 1 L of double distilled water. Prior to use, the broth was sterilised by autoclaving at 121 °C and 1.1 bar pressure for 15 min. Once sterilised the medium was stored in a dry, cool area.

4.6.5 Methods

4.6.5.1 Stock solutions for SDS-Page gel electrophoresis

10X Running Buffer: 30 g of Tris base and 144 g of glycine were dissolved in 1 L of ddH_2O and stored in a dry place.

1X Running Buffer: 100 mL of 10X stock and 10 mL of 10% SDS were made up to 1000 mL with ddH_2O.

Resolving/Separating Gel Buffer (1.5 M Tris-HCl, 0.5% *(w/v)* SDS at pH 8.8):
90.85 g of Tris base and 2.5 g of SDS were dissolved in 350 mL of water and the pH adjusted to 8.8 with 1 N HCl. The volume was made up to 500 mL with ddH_2O and stored in a dry place.

Stacking Gel Buffer (0.5 M Tris-HCl, 0.5% (w/v) SDS at pH 6.8): 30.28 g of Tris base and 2.5 g of SDS were dissolved in 350 mL of water and the pH adjusted to 6.8 with 1 N HCl. The volume was made up to 500 mL with ddH_2O and stored in a dry place.

Acrylamide 40% contains acrylamide and bis-acrylamide in a 29:1 ratio. Acrylamide can autopolymerise when dissolved in water and addition of free radicals speeds up this process. Bis-acrylamide serves as a cross-linking agent for the gel formation.

1% Ammonium Persulphate (APS): 0.1 g of ammonium persulphate was dissolved in 10 mL of sterile dH_2O. It was prepared freshly and stored at 4 °C. It serves as source of free radicals and initiates polymerisation.

Tetramethylethylenediamine (TEMED): 99% TEMED was used to initiate polymerisation.

5X Sample Preparation Buffer contains 10 mL of stacking buffer, 5 mL of glycerol, 2 g of SDS, 5 mg of bromophenol blue and 5 mL of β-mercaptoethanol. The components were dissolved and stored at 4 °C in a dark tube as β-mercaptoethanol is light sensitive.

Gel stain (order of addition): 7.5 g of Coomassie brilliant blue (CBB) R250, 910 mL methanol, 725 mL ddH_2O, 375 mL glacial acetic acid.

Destaining Buffer: 250 mL methanol and 375 mL acetic acid were made up to 5000 mL with ddH_2O.

12% Resolving Gel was prepared by mixing 1.376 mL deionised water, 0.866 mL separating buffer, 1.043 mL acrylamide, 0.188 mL 1% APS and 7.5 µL TEMED.
Stacking Gel was prepared by mixing 0.713 mL deionised water, 0.313 mL stacking buffer, 0.188 acrylamide, 0.038 mL 1% APS and 5 µL TEMED.

4.6.5.2 Buffer solutions for protein expression and purification

1 M Tris-HCl (pH 7.4):
60.57 g of Tris base was dissolved in 400 mL of ddH_2O and adjusted pH to 7.4 with 1 N HCl, then made up the volume with ddH_2O to 500 mL and stored at room temperature in a dry place.
Lysis Buffer consisted of 20 mM Tris-HCl (pH = 8) and 300 mM NaCl.
1 M Imidazole (pH 8): 34.04 g of imidazole was dissolved in 400 mL of ddH_2O, adjusted with 1 N HCl to pH = 8 and made up to 500 mL. The solution was stored in a dry place at room temperature.
Elution Buffer consisted of 20 mM Tris-HCl, 300mM NaCl and 10-250 mM imidazole.
1 M IPTG (isopropylthio-β-D-galactoside): 2.3 g of IPTG in was dissolved in 10 mL of ddH_2O and sterilised by passing it through a 0.20 µm filter (Sartorius Stedim Biotech, Appleton Woods, Birmingham, UK). The solution was dispensed into 1 mL aliquots and stored at -20 °C.
Bovine Serum Albumin (BSA): 2 mg/mL stock concentration was diluted to 0.1 µg/µL with water.

4.6.5.3 Stock solutions

Streptomycin (50 mg/mL): 500 mg streptomycin was dissolved in 10 mL of ddH_2O, sterilised by passing it through a 0.20 µm single use mini start filter (Sartorius Stedim Biotech, Appleton Woods, Birmingham, UK), then dispensed into 1 mL aliquots and stored at -20 °C.
Chloramphenicol (34 mg/mL): 340 mg chloramphenicol was dissolved in 10 mL of 100% ethanol, then dispensed into 1 mL aliquots and stored at -20 °C.
25X EDTA-free Protease Inhibitor: One complete Mini protease inhibitor cocktail tablet (Roche Diagnostics GmBH, Basel, Switzerland) was completely dissolved in 2 mL of sterile water, divided in 500 µL aliquots and stored at -20 °C.
1X EDTA-free Protease Inhibitor: 400 µL of the 25X stock was added to 10 mL of lysis buffer.

4.6.5.4 Western Blot

Transfer Buffer consisted of 24 mM Tris, 192 mM glycine and 20% methanol.

TBST (Tris-Buffered Saline with Tween) consisted of 50 mM Tris HCl pH 7.4, 150 mM NaCl and 0.05% Tween 20.
TBS (Tris-Buffered Saline) consisted of 50 mM Tris HCl pH 7.4, 150 mM NaCl.

4.6.5.5 Bacterial transformation

The competent cells were kept on ice. 50 µL of competent cells and 1 µL of purified plasmid was added into a sterile, ice-cold 12 mL PP-tube (Greiner® Bio-one) and incubated for 10 min on ice. The tube was kept for 40 s in a water bath at 42 °C to provide a heat shock. The cells were then put immediately on ice for an additional 2 min. 900 µL of LB medium was then added to the tubes and the cells incubated at 37 °C for 1 h at 180 rpm. 100 µL of incubated culture was spread on the LB-agar plates containing the appropriate antibiotic (either streptomycin alone or in combination with chloramphenicol). The plates were allowed to dry and incubated at 37 °C for 18 h.

4.6.5.6 Seed cultures

4.6.5.6.1 *E.coli* for heterologous expression

Seed cultures of *E. coli* were prepared in sterile conditions with 10 mL of sterile LB broth in a 50 mL Falcon tube containing the appropriate antibiotic (streptomycin 50 µg/mL and/or chloramphenicol 34 µg/mL), and inoculated with one colony from a solid agar culture or a small amount from a 50% glycerol stock using a sterile disposable loop. The culture was then incubated at 37 °C, 180 rpm for 18 h.

4.6.5.6.2 Mycobacterial species for SPOTi

M. aurum (NC 10437)*, M. smegmatis* mc^2155 and *M. bovis* BCG Pasteur cultures were prepared in sterile conditions with 10 mL Difco Middlebrook 7H9 broth (containing 0.02% glycerol and 0.05% Tween 80) supplemented with 10% ADC and inoculated with a small amount from a 50% glycerol stock. The culture was incubated at 35 °C, for *M. aurum* and *smegmatis*, at 37 °C for *M. bovis* BCG, with 180 rpm shaking.

Growth of cultures was monitored by measuring the turbidity of the culture suspension (as optical density, OD) at 600 nm in a cell density meter (WPA Biowave CO 8000). When the cultures reached mid-exponential phase they were passaged twice into fresh medium. Once OD reached 0.8, dilutions were carried out in fresh medium to obtain 10^{-3} dilutions, (10^{-2} in the case of *M. aurum)*, prior to their use for SPOTi. The undiluted bacterial cultures were cryopreserved as stated in Chapter 4.6.5.9.

4.6.5.6.3 *E.coli* for SPOTi

E. coli DH5α cultures were initiated from glycerol stocks in 10 mL Luria Broth medium using 1% inoculum and grown at 37 °C at 180 rpm overnight. The culture was passaged once before the experiment. Once OD reached 0.8, dilutions were carried out in fresh LB medium to obtain 10^{-3} dilution prior to use for the SPOTi assay.

4.6.5.7 Long-term preservation of bacterial cultures

50 % (*v/v*) glycerol stocks were used for long-term storage of all bacterial cultures. 500 µL of sterile glycerol was mixed in a cryovial (Corning®) with 500 µL of seed culture and the mixture inverted 10 times. The cryovial was stored in a -80 °C freezer.

4.6.5.8 Heterologous expression of proteins in *E. coli*

4 mL of seed culture was inoculated in 400 mL LB medium supplemented with 50 µg/mL of streptomycin and 34 µg/mL of chloramphenicol and incubated at 37 °C at 180 rpm constant rotation until OD_{600} = 0.5.

1 M IPTG was added, reaching a final 0.5 mM concentration, to induce protein expression and the culture was incubated for 18 h at 18 °C with 180 rpm constant rotation. IPTG was not added to one culture that was kept as a control (uninduced).

After incubation the cells were harvested at 4 °C at 9000 rpm for 15 min (Beckmann Coulter® JLA 10.25). The supernatant was discarded, the pellet thoroughly resuspended in ice-chilled lysis buffer containing 1X protease inhibitor (5 mL for each 400 mL culture) and sonicated (Soniprep® 150) at 10 microns amplitude for 5 cycles (30 s active sonication followed by 1 min break) while keeping the tube immersed in a water-ice mixture. A small sample was then kept for the estimation of the whole protein content. A further centrifugation cycle of 45 minutes at 20 000 rpm at 4 °C (Beckmann Coulter® JA 25.5) followed. The supernatant containing the soluble proteins was filtered and divided into 1 mL aliquots. Cell pellet and lysate contents were compared to those of the total protein and uninduced sample through SDS-PAGE gel electrophoresis. The cell lysate was then carried forward to the purification step.

4.6.5.9 SDS-PAGE gel electrophoresis

Unless otherwise specified, all the samples loaded on the SDS-PAGE gels were prepared with 16 µL of sample and 4 µL of 5X sample preparation buffer mixed in an Eppendorf tube by 15 s centrifugation. The samples were then heated to 100 °C for

10 min and centrifuged for 15 s. 18 µL was loaded on the gel, next to a 5 µL load of PageRuler® Ladder or, if preparing for a western blot, with Spectra Multicolor® Ladder. The gel was run at 200 V (Bio-Rad Powerpac 300) for 45-60 min until the dye front ran out of the bottom of the gel. Following the run, the gel was stained in Coomassie staining solution for 5 min, then washed with water for 5 min and destained overnight with destaining solution on a Mini orbital shaker SO5 (Stuart Scientific, Stone, UK).

4.6.5.10 Purification of Rv3712 with Ni-NTA resin

This type of purification uses affinity chromatography columns. In this case, the molecule that needs to be isolated has been designed to express 6 consecutive His residues. The resin consists of nickel-charged nitrilotriacetic acid chelate immobilised on 6% cross-linked agarose. The metal has a high affinity for His.

The procedure involved used a gravity-flow column containing 4 mL of resin. The supernatant containing the soluble proteins was loaded on the column after a 10 column-volume (CV) pre-equilibration with lysis buffer. Fractions containing unbound proteins were collected. Subsequently 10 CV of 10 mM imidazole in elution buffer was loaded and fractions collected. Finally sequential 1 CV of increasing imidazole dilutions was used to elute the protein which was collected in fractions. Recombinant proteins were eluted with 250 mM imidazole. The collected fractions were analysed through 12% SDS-PAGE electrophoresis gels.

Regeneration of the column involved sequential washes with 3 CV of deionised water, 3 CV of 0.5 M NaOH, 2 CV of deionised water and 3 CV of lysis buffer. The column was then stored at 4 °C. In the case of long-term storage, an additional 3 CV wash with 70% ethanolwas required.

4.6.5.11 Bradford Assay

This colorimetric assay is utilised to estimate the concentration of protein in a sample. Bovine serum albumin (BSA) is used as the protein standard dilution of which allows the construction of a calibration curve.

The Bradford reagent essentially consists of Coomassie Blue G-250.

The assay is carried out on a 96-well plate as outlined in Table 3.1. The concentration of each sample was determined by comparison of the measured value with those from the BSA calibration curve. Absorbances were measured using a fluorimeter at 595 nm (Fluostar Optima®, BMG Labtech).

Well	BSA (µL)	Water (µL)	Protein (µL)	Sample Final Concentration (µg/µL)	Bradford Reagent (µL)
A	0	150	-	0.000	150
B	10	140	-	0.007	150
C	20	130	-	0.013	150
D	30	120	-	0.020	150
E	40	110	-	0.027	150
F	50	100	-	0.033	150
G	-	148	2	sample	150

Table 4.1 Bradford assay plate set-up

4.6.5.12 Western blot

A 10% SDS-PAGE gel was prepared and loaded with the appropriate marker, as described in Chapter 4.6.5.9. After the run, the gel was passed briefly in water twice and left for 15 min in transfer buffer.

One nitrocellulose membrane, cut to fit the size of the gel, was immersed for 30 s in methanol, 1 min in ddH_2O and finally left for 15 min in transfer buffer.

Six 3mm Whatman® blotting papers, cut to fit the size of the gel, were left for 15 min in transfer buffer.

The different layers were assembled inside a Bio-Rad® Trans-Blot SD Semi-Dry Transfer Cell in the following order, from bottom to top: 3 filter papers, the membrane, the gel, 3 filter papers. The cell was closed and a 15 V potential difference applied across the system for 1 h.

The membrane was then removed from the cell and immersed in 5% fat-free milk in TBST at -4 °C for 16 h. It was then transferred to 3% fat-free milk in TBST solution three times for 10 min, followed by 1 h immersion in a solution of 6x-HIS Epitope Tag Monoclonal Antibodies in 3% fat-free milk in TBST. The membrane was then washed three times for 10 min in 3% fat-free milk in TBST, then once in TBST for 10 min and once in TBS for 10 min. Finally a SIGMAFAST™ Protease Inhibitor Cocktail Tablet, EDTA-free solution was poured onto the membrane and left until the bands

started appearing. The membrane was then removed and stored in between two filter papers.

4.6.5.13 High-throughput spot culture growth inhibition assay (HT-SPOTi)

HT-SPOTi was a spot culture assay used to screen the antibacterial properties of a compound against a population of bacterial cells (191). The semi-automated assay was conducted in a 96-well plate. The peptides were dissolved in H_2O and diluted to a 50 mg/mL concentration. 20 µL of solution was used to prepare a series of two-fold dilutions, 2 µL of which were then dispensed into each well of a 96-well plate to which 200 µL of agar, kept at 55 °C, was added (Middlebrook 7H10 agar, supplemented with 0.05% (*v/v*) glycerol and 10% (*v/v*) OADC for mycobacteria, LB agar for *E. coli*). The highest concentration used was 500 µg/mL. Wells with no compound (H_2O only) and INH were used as experimental controls. To all the plates, 2 µL of early to mid-log bacterial culture was spotted in the middle of each well and the plates were incubated (*M. aurum* 35 °C for five days, *M. smegmatis* 35 °C for three days, *M. bovis* BCG 37 °C for fourteen days, *E. coli* 37 °C overnight). The assay result was evaluated by direct eye observation of the appearance of spots (191).

4.7 Synthetic methods

H-Ala-D-Glu(Lys-D-Ala-D-Ala-OH)-OH (53). Pentapeptide **53** was synthesised starting from Fmoc-D-Ala-Wang resin. The synthesis was carried out both automatically (0.080 mmol) and manually (0.160 mmol) as described in the general methods. Lys was introduced as its side chain Boc-protected derivative. Fmoc-D-Glu-O*t*Bu was coupled to the Lys α-amino group via its side chain γ-carboxyl group. The two crude samples were combined for purification via RP-HPLC to afford the title compound as an amorphous white solid (50 mg, 43%). ESI-MS ($C_{20}H_{36}N_6O_8$) 488.26 *m/z* (%): 977.40 $[2M+H]^+$ (100). RP-HPLC: R_t = 7.39 min. ^{1}H NMR (H_2O + D_2O): δ = 1.34 (d, 3H, *J* = 7.2, D-Ala CH_3), 1.34-1.47 (m, 2H, Lys δCH_2), 1.39 (d, 3H, *J* = 7.3, D-Ala CH_3), 1.51 (d, 3H, *J* = 7.1, L-Ala CH_3), 1.64 (m, 2H, Lys εCH_2), 1.71-1.79 (m, 2H, D-Glu βCH), 1.97 (m, 1H, Lys βCH_a), 2.16 (m, 1H, Lys βCH_b), 2.36 (m, 2H, Lys γCH_2), 2.95 (t, 2H, *J* = 5.15, D-Glu γCH_2), 4.09 (q, 1H, *J* = 6.95 – 14.0, L-Ala αCH), 4.21 (q, 1H, *J* = 6.7 – 14.1, D-Glu αCH), 4.28-4.34 (m, 3H, Lys and 2 x D-Ala αCH), 8.26 (d, 1H, *J* = 6.0, NH), 8.32 (d, 1H, *J* = 7.3, NH), 8.42 (d, 1H, *J* = 6.5, NH), 8.68 (d, 1H, *J* = 7.4, NH).

H-Ala-D-Glu(Lys-OH)-OH (54) Tripeptide **54** was synthesised automatically on 0.080 mmol scale using Fmoc-Lys(Boc)-Wang resin as described in the general methods. The manual synthesis was conducted on a 0.132 mmol scale as specified in the general methods.

The two crude samples were combined for purification via RP-HPLC to afford the title compound as a white solid (30 mg, 41%). ESI-MS ($C_{14}H_{26}N_4O_6$) 346.19 *m/z* (%): 347.4 $[M+H]^+$ (55). RP-HPLC: R_t = 4.74 min. ^{1}H NMR (H_2O + D_2O): δ = 1.44 (m, 2H, Lys δCH_2) 1.50 (d, 3H, *J* = 6.5, L-Ala CH_3), 1.65 m, 2H, Lys εCH_2), 1.72 (m, 1H, D-Glu βCH_a), 1.86 (m, 1H, D-Glu βCH_b), 2.00 (m, 1H, Lys βCH_a), 2.18 (m, 1H, Lys βCH_b), 2.38 (m, 2H, Lys γCH_2), 2.95 (t, 2H, *J* = 5.65, D-Glu γCH_2), 4.08 (q, 1H, *J* = 7.0 – 14.0, L-Ala αCH), 4.28-4.36 (m, 2H, D-Glu αCH and Lys αCH), 8.32 (d, 1H, *J* = 7.2, NH), 8.70 (d, 1H, *J* = 7.4, NH).

H-Ala-D-Glu(Lys-D-Ala-OH)-OH (55). Tetrapeptide **55** was synthesised starting from Fmoc-D-Ala-Wang resin. The synthesis was carried out both automatically (0.080 mmol) and manually (0.160 mmol) as described in the general methods. Lys and D-Glu were introduced as described for **53**.

The two crude samples were combined for purification via RP-HPLC to afford the title compound as an amorphous white solid (20 mg, 20%). ESI-MS ($C_{17}H_{31}N_2O_7$) 417.19 *m/z* (%): 222.1 $[M+2H+Na]^{2+}$ (55), 417.9 $[M+H]^+$ (20). RP-HPLC: R_t = 7.22 min. ^{1}H NMR (90% H_2O/D_2O): δ = 1.37 (d, 3H, *J* = 7.3, D-Ala CH_3), 1.44 (m, 2H, Lys δCH_2), 1.52 (d, 3H, *J* = 7.0, L-Ala CH_3), 1.65 (m, 2H, Lys εCH_2), 1.72 (m, 1H, D-Glu βCH_a), 1.78 (m, 1H, D-Glu βCH_b), 1.99 (m, 1H, Lys βCH_a), 2.18 (m, 1H, Lys βCH_b), 2.39 (m, 2H, Lys γCH_2), 2.96 (t, 2H, *J* = 5.7, D-Glu γCH_2), 4.09 (q, 1H, *J* = 7.0 - 14.0, L-Ala αCH), 4.28 (q, 1H, *J* = 7.0 – 13.5, D-Glu αCH), 4.33 (q, 2H, *J* = 7.3 – 14.0, Lys and D-Ala αCH), 8.24 (d, 1H, *J* = 6.9, D-Glu NH), 8.37 (d, 1H, *J* = 10.5, Lys NH), 8.67 (d, 1H, *J* = 7.4, D-Ala NH).

H-Ala-D-Glu-OH (56). Both manual and automated syntheses were initially attempted starting from Fmoc-D-Glu(O*t*Bu)-Wang resin on 0.080 mmol scale using the procedures described in the general methods but unfortunately preparative RP-HPLC did not result in the isolation of the desired dipeptide.

Subsequently, Fmoc-D-Glu(O*t*Bu)-OH **59** (0.25 g, 0.60 mmol, 1.1 equiv) was loaded on 2-chlorotrityl chloride resin (0.41 g, 1.33 mmol g^{-1} substitution, 0.54 mmol). Both the resin and the amino acid were dried for 3 days in a desiccator prior to loading. The resin was then allowed to swell in 1 mL of freshly distilled dry CH_2Cl_2 under an N_2 atmosphere. The amino acid was dissolved in a minimal amount of dry CH_2Cl_2

and DIEA (0.41 mL, 2.38 mmol, 4.4 equiv) was added. The mixture was added to the resin and the suspension stirred at room temperature for 2 h. The resin was then transferred to a solid phase reaction vessel and washed 3 times with CH_2Cl_2/MeOH/DIEA (17:2:1), 3 times with CH_2Cl_2, twice with DMF and twice with CH_2Cl_2. It was then drained and dried in a desiccator overnight. The dipeptide sequence was completed using the standard deprotection and coupling (Fmoc-Ala-OH) procedures, followed by cleavage and isolation, described in the general methods, The product was freeze-dried overnight and purified. RP-HPLC yielded the title peptide as an amorphous white solid (77 mg, 47%). ESI-MS ($C_8H_{14}N_2O_5$) 218.09 *m/z* (%): 219.01 $[M+H]^+$ (100). RP-HPLC: R_t = 6.01 min. ^{1}H NMR (H_2O + D_2O): δ = 1.48 (d, 3H, *J* = 7.1, L-Ala CH_3), 1.94 (m, 1H, D-Glu βCH_a), 2.15 (m, 1H, D-Glu βCH_b), 2.40 (t, 2H, *J* = 7.4, D-Glu γCH_2), 4.06 (q, 1H, *J* = 7.1 – 14.1, L-Ala αCH), 4.31 (q, 1H, *J* = 8.1 – 16.1, D-Glu αCH), 8.55 (d, 1H, *J* = 7.5, L-Ala NH).

Leu-enkephalin (61). The sample used for generation of the calibration curve was synthesised manually as described in the general methods, on 0.210 mmol scale starting from Fmoc-Leu-Wang resin. Purification lead to the isolation of the title compound as an amorphous white solid (43 mg, 37%). ESI-MS ($C_{28}H_{37}N_5O_7$) 555.27 *m/z* (%): 1111.50 $[2M+H]^+$ (100), 578.30 $[M+Na]^+$ (50). RP-HPLC: R_t = 13.11 min. The calibration curve (Fig. 4.1) was obtained starting from a stock solution made by dissolving 2 mg of the pure sample in 1 mL of water. Five two-fold serial dilutions of the stock solution were prepared and the six samples analysed in triplicate by HPLC. The mean AUC of the desired peak was plotted for each concentration of standard solution to generate the calibration curve.

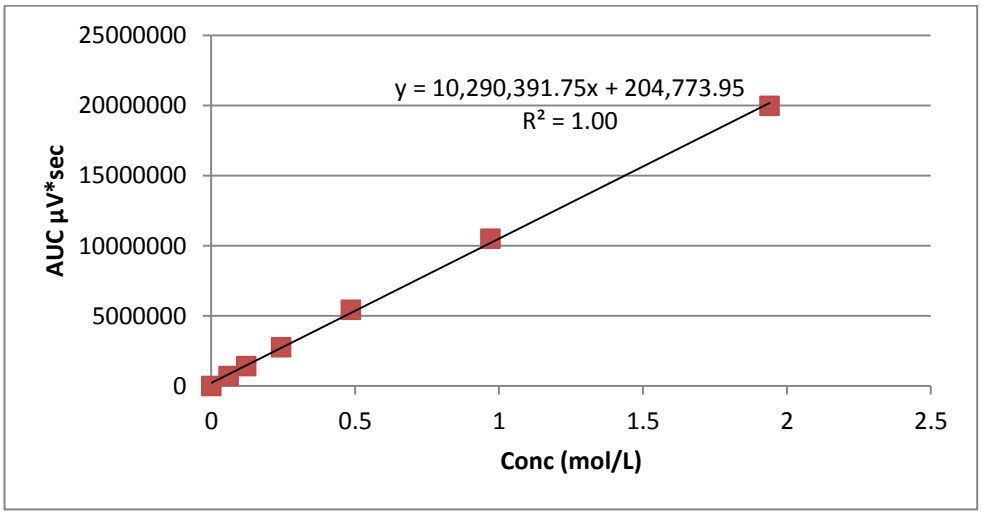

Figure 4.2 Calibration curve for Syro I optimisation using Leu-enkephalin

The syntheses for the automated coupling protocol evaluation using the gravimetric method were carried out in quadruplicate, while those analysed using the calibration curve interpolation were performed in triplicate. The crude samples were obtained starting from 100 mg of Fmoc-Leu-Wang resin (0.069 mmol). SPPS, work-up and cleavage proceeded largely as described in the general methods and according to the protocol being examined (Tables 2.2 and 2.3).

The resin was swelled in 1 mL of DMF for 1 hour (excluding Table 2.3 entry #9, which omitted the swelling step). N^{α}-Fmoc deprotection was achieved as described in the general methods by treatment with 40% piperidine in DMF for 3 min and with 20% piperidine for 12 min, followed by washing with DMF. Automated couplings used variable excesses (refer to Tables 2.2. and 2.3) of amino acid residue, activated using an equimolar amount of HBTU and a two-fold excess (over activated amino acid) of DIEA. Couplings were allowed to proceed for the appropriate amount of time for the selected protocol. The resins were then washed with DMF and the reagents replaced for a second and third coupling if required. After final deprotection and washing (DMF), the resins were finally washed three times with a 1:1 mixture of CH_2Cl_2 and methanol. The resins were placed in a desiccator for 2 h. The peptides were removed from the resins by acidolysis using TFA. The peptide-resin was treated with 0.25% *v/v* TIS and 0.25% *v/v* water in TFA, stirring for 2 h. The mixture was then filtered and the resin beads washed once with TFA. The TFA was removed under a stream of nitrogen gas and the crude peptide precipitated from cold diethyl ether, extracted into 95% aqueous ethanoic acid and lyophilised.

Analysis of the samples was achieved via RP-HPLC. Sample absorbance was recorded at 214 or 254 nm. The crude sample was diluted in 10 mL of Solvent A and 2 mL of Solvent B. The value of the AUC of the peak of interest was taken and substituted into the equation of the line of best fit of the calibration curve. The calculated concentration of the pure peptide present in the crude sample was multiplied by 555.6 g mol^{-1} (molecular weight of Leu-enkephalin) and the mass of the pure peptide present in the entire sample was obtained. These masses were used to calculate the yield of each protocol evaluated. The results were compared and examined for statistical significance using a one-way ANOVA test, performed using GraphPad Prism 7.

ACP 65-74 (62). The peptide was synthesised automatically starting from 400 mg of Fmoc-Gly-Wang (0.78 mmol/g) and cleaved as described in the general synthetic procedure (Chapter 4.3) to yield a crude mass of 0.137 g. 64 mg of the crude

material was purified via preparative HPLC to yield 4.6 mg (1.4% yield) of pure product as an amorphous white solid. ESI-MS ($C_{47}H_{74}N_{12}O_{16}$) 1062.53 *m/z* (%): 1085.55 $[M+Na]^+$ (90). RP-HPLC: R_t = 9.803 min.

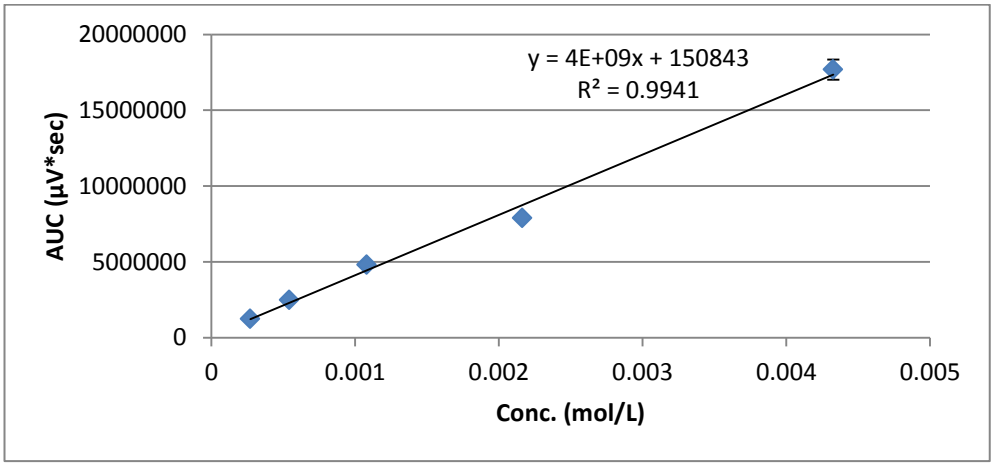

Figure 4.3 Calibration curve for Syro I optimisation using ACP 65-74

The calibration curve (Fig. 4.2) was obtained starting from a stock solution made by dissolving 4.6 mg of pure **62** in 1 mL of water. Four two-fold serial dilutions of the stock solution were prepared and the five samples analysed in triplicate by HPLC. The mean AUC of the desired peak was plotted for each concentration of standard solution to generate the calibration curve.

The syntheses for the automated protocol evaluation were carried out in triplicate starting from 50 mg of Fmoc-Gly-Wang (0.039 mmol). SPPS, work-up and cleavage proceeded as described in the general methods and according to the protocol being examined (Table 2.4).

The resin was swelled in 1 mL of DMF for 1 hour (excluding Table 2.4 entry #9, which omitted the swelling step). N^{α}-Fmoc deprotection was achieved as described in the general methods by treatment with 40% piperidine in DMF for 3 min and with 20% piperidine for 12 min, followed by washing with DMF. Automated couplings used variable excesses (refer to Table 2.4) of amino acid residue, activated using an equimolar amount of HBTU and a two-fold excess (over activated amino acid) of DIEA. For the protocol in Table 2.4 entry #10, 2.5 equiv of HOBt was added to the coupling mixture. Couplings were allowed to proceed for the appropriate amount of time for the selected protocol. The resins were then washed with DMF and the reagents replaced for a second and third coupling if required. After final deprotection and washing (DMF), the resins were finally washed three times with a 1:1 mixture of CH_2Cl_2 and methanol. The resins were placed in a desiccator for 2 h. The peptides

were removed from the resins by acidolysis using TFA. The peptide-resin was treated with 0.25% *v/v* TIS and 0.25% *v/v* water in TFA, stirring for 2 h. The mixture was then filtered and the resin beads washed once with TFA. The TFA was removed under a stream of nitrogen gas and the crude peptide precipitated from cold diethyl ether, extracted into 95% aqueous ethanoic acid and lyophilised.

Analysis of the samples was achieved via RP-HPLC. Sample absorbance was recorded at 214 or 254 nm. The crude sample was diluted in 5 mL of Solvent A and 1 mL of Solvent B. The mean of the AUC values measured for ACP 65-74 peak for each protocol repetition was taken and substituted into the equation of the line of best fit of the calibration curve. The calculated concentration of the pure peptide present in the crude sample was multiplied by 1063.16 g mol^{-1} (molecular weight of ACP 65-74) and the mass of the pure peptide present in the entire sample was determined. These masses were used to calculate the yield of each protocol evaluated

The results were compared and examined for statistical significance using a one-way ANOVA test, performed using GraphPad Prism 7.

H-Val-D-Glu(Lys-OH)-OH (63). Tripeptide **63** was obtained automatically on 0.025 mmol scale, starting from Fmoc-Lys(Boc)-Wang resin, as described in the general methods. HPLC analysis of the crude peptide (white amorphous solid, 7.7 mg, 82%) indicated only a single major product. The crude product was used for biological evaluation without further purification. ESI-MS ($C_{16}H_{30}N_4O_6$) 374.22 *m/z* (%): 373.30 $[M-H]^-$ (100). RP-HPLC: R_t = 7.84 min.

H-Leu-D-Glu(Lys-OH)-OH (64). Tripeptide **64** was obtained automatically on 0.025 mmol scale, starting from Fmoc-Lys(Boc)-Wang resin, as described in the general methods. HPLC analysis of the crude peptide (white amorphous solid, 7.0 mg, 72%) indicated only a single major product. The crude product was used for biological evaluation without further purification.. ESI-MS ($C_{17}H_{32}N_4O_6$) 388.23 *m/z* (%): 411.2 $[M+Na]^+$ (100), 389.20 $[M+H]^+$ (14). RP-HPLC: R_t = 8.39 min.

H-Ile-D-Glu(Lys-OH)-OH (65). Tripeptide **65** was obtained automatically on 0.025 mmol scale, starting from Fmoc-Lys(Boc)-Wang resin, as described in the general methods. HPLC analysis of the crude peptide (white amorphous solid, 7.7 mg, 79%) indicated only a single major product. The crude product was used for biological evaluation without further purification. ESI-MS ($C_{17}H_{32}N_4O_6$) 388.23 *m/z* (%): 411.3 $[M+Na]^+$ (100), 389.20 $[M+H]^+$ (12). RP-HPLC: R_t = 8.38 min.

H-Ala-D-Glu(Arg-OH)-OH (66). Tripeptide **66** was obtained automatically on 0.025 mmol scale, starting from Fmoc-Arg(Pbf)-Wang resin, as described in the general methods. HPLC analysis of the crude peptide (white amorphous solid, 8.1 mg, 86%) indicated only a single major product. The crude product was used for biological evaluation without further purification. ESI-MS ($C_{14}H_{26}N_6O_6$) 374.19 *m/z* (%): 375.20 $[M+H]^+$ (100). RP-HPLC: R_t = 7.51 min.

H-Ala-D-Glu(Lys-Gly-Gly-OH)-OH (67). Pentapeptide **67** was obtained automatically as on 0.025 mmol scale, starting from Fmoc-Gly-Wang resin, described in the general methods. HPLC analysis of the crude peptide (white amorphous solid, 7.8 mg, 68%) indicated only a single major product. The crude product was used for biological evaluation without further purification. ESI-MS ($C_{18}H_{32}N_6O_8$) 460.23 *m/z* (%): 921.40 $[2M+H]^+$ (100), 943.40 $[2M+Na]^+$ (15). RP-HPLC: R_t = 7.35 min.

Diethyl-2-acetamido-2-allylmalonate (108). Sodium metal (5.3 g, 0.230 mol) was dissolved in 250 mL of absolute ethanol and diethylacetamidomalonate (50.0 g, 0.230 mol, 1 equiv) was added in one portion, stirring to ensure complete dissolution. Allyl bromide (28.87 mL, 0.316 mol, 1.4 equiv) was then added and the reaction mixture was stirred under reflux for 48 h at 110 °C. The mixture was cooled to room temperature and the mixture was concentrated under reduced pressure. Water (200 mL) was added to the residue followed by extraction with chloroform (200 mL). The aqueous layer was extracted twice more with 100 mL of fresh chloroform. The combined organic layers were washed with 300 mL of brine, dried with $MgSO_4$, filtered and evaporated to obtain a yellow oil. The product was taken up in 20 mL of ethanol and poured into 300 mL of ice-water, then stirred until a waxy white precipitate formed. The precipitate was filtered and washed several times with ice water, and dried in a desiccator overnight to yield the title compound as a white solid (typically 31-50%). HRMS (ESI) *m/z*: Calcd for $C_{12}H_{20}NO_5$ $[M+H]^+$ 258.1342; found 258.1343. ^{1}H NMR ($CDCl_3$): δ = 1.24 (t, 6H, *J* = 7.1, 2 x $CH_2\mathit{CH_3}$), 2.01 (s, 3H, NHCO$\mathit{CH_3}$), 3.05 (d, 2H, *J* = 7.4, βCH_2), 4.22 (q, 4H, *J* = 7.1, 2 x $\mathit{CH_2}CH_3$), 5.07 (s, 1H, δCH_a), 5.10 (d, 1H, *J* = 3.36, δCH_b), 5.55 (m, 1H, γCH), 6.72 (s, 1H, NH); ^{13}C NMR ($CDCl_3$): δ = 14.1 ($CH_2\mathit{CH_3}$), 23.1 (NHCO$\mathit{CH_3}$), 37.1 (βC), 62.7 ($\mathit{CH_2}CH_3$), 66.3 (αC), 119.9 (δC), 131.4 (γCH), 167.8 ($\mathit{COO}CH_2CH_3$), 169.0 ($\mathit{CO}CH_3$).

2-Acetamidopent-4-enoic acid (113). NaOH (4.19 g, 0.105 mol, 1.1 equiv) was added in one portion to a solution of **108** (24.45 g, 0.095 mol) in 200 mL of 50% *v/v* ethanol in water. The mixture was stirred under reflux for 16 h at a 110 °C. After

cooling the mixture to room temperature, the ethanol was evaporated under reduced pressure and the remaining aqueous solution was washed with an equal volume of diethyl ether. The aqueous layer was acidified with 2 M HCl to pH 1.5 and extracted 3 times with 250 mL of ethyl acetate. The combined organic layers were dried over $MgSO_4$, filtered and evaporated to yield the title compound as a white solid (typically 60-78%). HRMS (ESI) *m/z*: Calcd for $C_7H_{12}NO_3$ $[M+H]^+$ 158.0817; found 158.0816. ^{1}H NMR (CD_3OD): δ = 1.97 (s, 3H, CH_3), 2.44 (m, 1H, βCH_a), 2.59 (m, 1H, βCH_b), 4.45 (m, 1H, αCH), 4.98 (s, 1H, OH), 5.11 (m, 2H, δCH_2), 5.78 (m, 1H, γCH); ^{13}C NMR (CD_3OD): δ = 22.4 (CH_3), 37.0 (βCH_2), 53.5 (αCH), 118.6 (δCH_2), 134.6 (γCH), 173.3 (*CO*CH_3), 174.7 (COOH).

(*S*)-2-Aminopent-4-enoic acid (115) (192)**. 113** (12.00 g, 76.40 mmol) was dissolved in 500 mL of distilled water. The solution was brought to pH 7.5 with 2 M LiOH. Acylase I from *Aspergillus melleus* (440 mg, 8.3 U/mmol of acyl-L-aa) was added and the solution left to stir at room temperature for 7 days maintaining pH 7.5. 2 M HCl was then added to bring the pH to 5 and 1.5 g of activated charcoal was added. The mixture was stirred while heating it to 60 °C, then filtered through a Celite® pad and brought to pH 1.5 with conc. HCl. The filtrate was extracted 4 times with equal volumes of ethyl acetate. The organic phases were combined and reserved for the isolation of **114** (below). The aqueous layer volume was reduced under vacuum and extracted once more with 1.5 volumes of ethyl acetate. The aqueous phase was then evaporated and the residue washed three times with hot ethanol. The ethanol filtrate was evaporated, taken up in water, then freeze dried and stored. FDAA derivatisation (see general methods) and HPLC analysis at 340 nm showed an *R*:*S* enantiomeric ratio of 3:97. R_f = 0.55 (*n*BuOH/CH_3COOH/H_2O 2:1:1). ^{1}H NMR (CD_3OD): δ = 2.58 (m, 1H, βCH_a), 2.69 (m, 1H, βCH_b), 3.61 (m, 1H, αCH), 5.23 (m, 2H, δCH_2), 5.82 (m, 1H, γCH), identical to the NMR spectra reported in literature.

(*R*)-2-Acetamidopent-4-enoic acid (114) (192)**.** The reserved organic phases were dried with MgSO4, filtered and evaporated to give an oil. The oil was dissolved in acetone and evaporated under reduced pressure to give the title compound as white solid (5.11 g, 85%). $[\alpha]_D$ = +20.0° for a 78:22 ratio (similar to what expected given the published $[\alpha]_D$ = +35.0° for the enantiomeric pure molecule (154)). R_f = 0.75 (*n*BuOH/AcOH/H_2O 2:1:1). ^{1}H NMR (CD_3OD): δ = 1.97 (s, 3H, CO*C*H_3), 2.43 (m, 1H, βCH_a), 2.58 (m, 1H, βCH_b), 4.44 (q, 1H, *J* = 5.0, αCH), 5.11 (m, 2H, δCH_2), 5.76 (m, 1H, γCH).

(*R*)-2-Aminopent-4-enoic acid (116) (192)**.** 2.5 M NaOH (101.4 mL, 253.50 mmol) was added to **114** (5.11 g, 32.50 mmol) and the solution stirred under reflux for 24 h at 110 °C. After cooling to room temperature, 5 M HCl was added until pH 7 and precipitation occurred. The precipitate was filtered and washed twice with hot ethanol. The filtrate was then evaporated under reduced pressure to yield the title compound as a white solid (1.02 g, 27%). FDAA derivatisation (see general methods) and HPLC analysis at 340 nm showed an *R*:*S* enantiomeric ratio of 80:20. R_f = 0.56 (*n*BuOH/AcOH/H_2O 2:1:1). ^{1}H NMR (D_2O): δ = 2.73 (m, 2H, βCH_2), 3.98 (q, 1H, *J* = 12.1, αCH), 5.37 (m, 2H, δCH_2), 5.82 (m, 1H, γCH). ^{13}C NMR (D_2O): δ = 34.7 (αCH), 53.6 (βCH*2*), 120.8 (γCH), 131.2 (δCH_2).

(*R*)-2-((*tert*-Butoxycarbonyl)amino)pent-4-enoic acid (119) (193)**.** N^{α}-Boc-D-allylglycine · DCHA (100 mg, 0.25 mmol) was taken up in 10 mL of EtOAc and washed 2 × 10 mL of 0.5 M $KHSO_4$. The organic layer was dried over $MgSO_4$, filtered and evaporated. The free acid was used as required without further purification.

(*R*)-*tert*-Butyl 2-((*tert*-butoxycarbonyl)amino)pent-4-enoate (49) (193)**.** N^{α}-Boc-D-allylglycine (1.00 g, 4.64 mmol) was dissolved in dry CH_2Cl_2 (20 mL) followed by the addition of DIC (0.78 mL, 5.10 mmol, 1.1 equiv), DMAP (0.17 g, 1.39 mmol, 0.3 equiv) and *tert*-butanol (2.22 mL, 23.2 mmol, 5 equiv). The reaction mixture was allowed to stir at room temperature under an argon atmosphere for 18 h. The mixture was then filtered and the residue washed with CH_2Cl_2 (2 × 25 mL). The filtrate was washed with 0.5 M $KHSO_4$ (2 × 25 mL) and the organic layer dried over $MgSO_4$, filtered and evaporated. The resulting crude oil was subjected to flash chromatography (petroleum ether/EtOAc 19:1) to yield the title product as a white solid (0.74 g, 60%). RP-HPLC: R_t = 19.82 min. ^{1}H NMR ($CDCl_3$): δ = 1.43 (s, 9H, 3 x *t*Bu CH_3), 1.45 (s, 9H, 3 x Boc CH_3), 2.48 (m, 2H, βCH_2), 4.24 (q, 1H, *J* = 6.4, αCH), 5.03 (d, 1H, *J* = 4.8, NH), 5.11 (m, 2H, δCH_2), 5.67 (m, 1H, γCH) identical to the NMR spectra reported in literature. ^{13}C NMR ($CDCl_3$): δ = 28.0 (*t*Bu 3 x CH_3), 28.3 (Boc 3 x CH_3), 37.0 (βCH_2), 53.3 (αCH), 79.4 (tBu *C*CH_3), 82.5 (Boc *C*CH_3), 118.8 (δCH_2), 132.5 (γCH), 155.7 (*C*O*C*OCH_3), 171.9 (*C*O*C*OCH_3).**(*S*)-1-Benzyl 5-*tert*-butyl 2-((((9*H*-fluoren-9-yl)methoxy)carbonyl)amino) pentanedioate (126).** A solution of **125** (6 g, 14.10 mmol) in methanol (120 mL) was cooled to 0 °C. A solution of Cs_2CO_3 (2.30 g, 7.06 mmol, 0.5 equiv) in methanol was added dropwise, while keeping the temperature constant at 0 °C. The mixture was allowed to stir at 25 °C for 20 min, then was evaporated to dryness and co-evaporated sequentially with toluene, benzene and hexane. The residue was taken up in dry DMF (30 mL),

benzyl bromide (2 mL, 16.92 mmol, 1.2 equiv) was added and the solution was allowed to stir at room temperature for 18 h under an argon atmosphere. The volume was reduced under reduced pressure and the residue taken up in $CHCl_3$ and washed with water (1*10 mL) and 0.5 M $KHSO_4$ (10 mL). The combined organic layers were dried over $MgSO_4$, filtered and evaporated to yield the title compound as a white solid (6.73 g, 93%). R_f = 0.48 (hexane/EtOAc 2:1). ESI-MS ($C_{31}H_{33}NO_6$) 515.23 *m/z* (%): 538.10 $[M+Na]^+$ (100), 1054.40 [2M+Na]+ (95). ^{1}H NMR ($CDCl_3$): δ = 1.44 (s, 9H, 3 x CH_3), 1.97 (m, 1H, βCH_a), 2.19 (m, 1H, βCH_b), 2.31 (m, 2H, γCH_2), 4.21 (t, 1H, *J* = 13.9, Fmoc CH), 4.34-4.47 (m, 3H, αCH and Fmoc CH), 5.19 (s, 2H, OCH_2Ph), 5.49 (d, 1H, *J* = 8.0, NH), 7.29-7.42 (m, 9H, Fmoc and benzyl CHAr), 7.59 (d, 2H, *J* = 7.3, Fmoc CHAr), 7.76 (d, 2H, *J* = 7.5, Fmoc CHAr). ^{13}C NMR ($CDCl_3$): δ = 27.5 (βCH_2), 28.1 (3 x CH_3), 31.4 (γCH_2), 47.2 (Fmoc CH), 53.6 (αCH), 67.1 (OCH_2Ph), 67.3 (Fmoc CH_2), 120.0 (Fmoc CHAr), 125.1 (Fmoc CHAr), 127.1-128.6 (Fmoc and benzyl CHAr).

(*S*)-4-((((9*H*-Fluoren-9-yl)methoxy)carbonyl)amino)-5-(benzyloxy)-5-oxopentanoic acid (124). A solution of **126** (2.62 g, 5.08 mmol) in 50% *v/v* TFA in CH_2Cl_2 (25 mL) was allowed to stir for 2 h under an argon atmosphere and then evaporated. The residue was taken up in ethyl acetate and washed with sat. aq. $NaHCO_3$ (20 mL), 5% HCl (20 mL), sat. aq. NaCl (20 mL). The organic layer was dried over $MgSO_4$, filtered and evaporated to yield the title compound as a colourless oil (2.02 g, 87%).R_f = 0.12 (hexane/EtOAc 2:1). ^{1}H NMR ($CDCl_3$): δ = 1.98 (m, 1H, βCH_{2a}), 2.23 (m, 1H, βCH_{2b}), 2.41 (m, 2H, γCH_2), 4.20 (t, 1H, *J* = 13.4, Fmoc CH), 4.41 (d, 2H, *J* = 7.2, Fmoc CH_2), 4.46 (m, 1H, αCH), 5.18 (s, 2H, OCH_2Ph), 5.45 (d, 1H, *J* = 7.8, NH), 7.28-7.41 (m, 9H, Fmoc and benzyl CHAr), 7.58 (d, 2H, *J* = 7.2, Fmoc CHAr), 7.75 (d, 2H, *J* = 2.5, Fmoc CHAr). ^{13}C NMR ($CDCl_3$): δ = 27.5 (βCH_2), 29.7 (γCH_2), 47.2 (Fmoc CH), 53.3 (αCH), 67.1 (OCH_2Ph), 67.5 (Fmoc CH_2), 120.0 (Fmoc CHAr), 125.1 (Fmoc CHAr), 127.1-128.7 (Fmoc and benzyl CHAr), 135.0 (PhC), 141.3 (*C*OOCH_2Ph), 143.7 (Fmoc C$_a$), 143.8 (Fmoc C$_b$), 156.0 (CONH), 177.31 (COOH).

(*S*)-Benzyl 2-((((9*H*-fluoren-9-yl)methoxy)carbonyl)amino)but-3-enoate (50).

Method A: Fmoc-Glu-OBn (2.0 g, 4.35 mmol) was suspended in benzene (100 mL). Copper (II) acetate monohydrate (0.22 g, 1.10 mmol, 0.25 equivl) was added and the mixture was stirred under argon for 1 h at room temperature. Lead tetraacetate (3.86 g, 8.70 mmol, 2 equiv) was added to the suspension and the mixture stirred under argon for 1 h at room temperature, before refluxing at 85 °C for 42 h. The

mixture was filtered through a Celite® pad, the filtrate diluted with ethyl acetate, then washed three times with water and once with brine. The organic phase was dried over $MgSO_4$, filtered and evaporated to yield a yellow syrup. The crude product was purified via flash column chromatography (petroleum ether/EtOAc 19:1) to yield the title compound as a white solid (4.1 mg, 2%). R_f = 0.58 (petroleum ether/EtOAc 1:1). ESI-MS ($C_{26}H_{23}NO_4$) 413.16 m/z (%): 621.05 $[M+Pb]^+$ (100). ^1H NMR ($CDCl_3$): δ = 4.16 (t, 1H, *J* = 6.8, Fmoc CH), 4.34 (d, 2H, *J* = 6.8, Fmoc CH_2), 4.92 (t, 1H, *J* = 4.4, αCH), 5.13 (s, 2H, benzyl CH_2), 5.23 (m, 2H, γCH_2), 5.41 (d, 1H, *J* = 7.3, NH), 5.85 (m, 1H, βCH), 7.19-7.38 (m, 9H, Fmoc and benzyl CHAr), 7.52 (d, 2H, *J* = 7.2, Fmoc CHAr), 7.69 (d, 2H, *J* = 7.5, Fmoc CHAr). ^{13}C NMR ($CDCl_3$): δ = 47.2 (Fmoc CH), 56.2 (αCH), 67.2 Fmoc CH_2), 67.5 (OCH_2Ph), 117.9 (γCH_2), 120.0 (Fmoc CHAr), 125.1 (Fmoc CHAr), 128.6-127.1 (Fmoc and benzyl CHAr), 132.3 (βCH).

Method B: A solution of Fmoc-hSer-OBn (**133**) (1.46 g, 3.39 mmol) and *o*NO_2SeCN (0.65 g, 3.73 mmol, 1.1 equiv) in dry THF (17 mL) was cooled to 0 °C. PBu_3 (0.94 mL, 3.73 mmol, 1.1 equiv) was added dropwise over 20 min and the solution was stirred 2 h at 25 °C. H_2O_2 (1.92 mL, 30%) was added at 0 °C and the reaction was left to stir for 16 h at 25 °C. The mixture was poured onto sat. aq. NaCl (25 mL) and extracted with ethyl acetate (3 × 25 mL). The organic layers were combined, washed with fresh sat. aq. NaCl (25 mL), dried over $MgSO_4$, filtered and evaporated to give a brown oil. The crude product was purified by flash chromatography (petroleum ether/EtOAc 17:3) to yield the title compound as a yellow solid (0.64 g, 45%). R_f = 0.61 (hexane/EtOAc 1:1). ESI-MS ($C_{26}H_{23}NO_4$) 413.16 *m/z* (%): 436.1 $[M+Na]^+$ (100). RP-HPLC: R_t = 21.51 min. ^1H NMR ($CDCl_3$): δ = 4.23 (t, 1H, *J* = 6.8, Fmoc CH), 4.43 (d, 2H, *J* = 6.8, Fmoc CH_2), 5.01 (t, 1H, *J* = 4.3, αCH), 5.21 (s, 2H, benzyl CH_2), 5.30 (m, 2H, γCH_2), 5.52 (d, 1H, *J* = 7.2, NH), 5.94 (m, 1H, βCH), 7.29-7.49 (m, 9H, Fmoc and benzyl CHAr), 7.60 (d, 2H, *J* = 7.2, Fmoc CHAr), 7.77 (d, 2H, *J* = 7.3, Fmoc CHAr).

(*S*)-4-*tert*-Butyl 1-phenyl 2-((((9H-fluoren-9-yl)methoxy)carbonyl)amino) succinate (131). A solution of Fmoc-Asp(O*t*Bu)-OH (**130**) (5.00 g, 12.1 mmol) in methanol (100 mL) was cooled to 0 °C. A solution of Cs_2CO_3 (1.97 g, 6.05 mmol, 0.5 equiv) in methanol (40 mL) was added dropwise and stirred for 20 min at 25 °C. The volume was reduced by vacuum and the solution co-evaporated once with toluene,once with benzene and once with hexane. The residue was taken up in dry DMF (25 mL) and benzyl bromide (1.72 mL, 14.5 mmol, 1.2 equiv) was added and stirred overnight under argon atmosphere, at 25 °C. The volume was reduced under reduced pressure, the residue taken up in $CHCl_3$ and washed once with H_2O and

once with 0.5 M $KHSO_4$. The organic phase was dried over $MgSO_4$, filtered and evaporated to give the title compound as a white solid (6.01 g, 99%). R_f = 0.62 (hexane/EtOAc 2:1). ESI-MS ($C_{30}H_{31}NO_6$) 501.22 *m/z* (%): 1025.35 $[2M+Na]^+$ (100), 524.25 $[M+Na]^+$ (25). ^1H NMR ($CDCl_3$): δ = 1.42 (s, 9H, 3 x CH_3), 2.79 (d, 1H, *J* = 17.2, βCH_a), 2.98 (d, 1H, *J* = 16.9, βCH_b), 4.23 (t, 1H, *J* = 7.2, Fmoc CH), 4.37 (m, 2H, Fmoc CH_2), 4.65 (m, 1H, αCH), 5.21 (m, 2H, OCH_2Ph), 5.84 (d, 1H, *J* = 8.5, NH), 7.28-7.42 (m, 9H, Fmoc and benzyl CHAr), 7.59 (d, 2H, *J* = 7.3, Fmoc CHAr), 7.76 (d, 2H, *J* = 7.5, Fmoc CHAr). ^{13}C NMR ($CDCl_3$): δ = 28.0 (3xCH_3 *t*Bu), 37.8 (βCH_2), 47.1 (Fmoc CH), 50.7 (αCH), 67.3 (Fmoc CH_2), 67.4 (OCH_2Ph), 119.9 (Fmoc CHAr), 125.2 (Fmoc CHAr), 128.5-127.1 (Fmoc and benzyl CHAr).

(*S*)-3-((((9*H*-Fluoren-9-yl)methoxy)carbonyl)amino)-4-oxo-4-phenoxybutanoic acid (132). A solution of **131** (6.01 g, 12.00 mmol) in 50% CH_2Cl_2 in TFA (50 mL) was stirred for 2 h under argon atmosphere and then evaporated to give a yellow oil. The residue was taken up in ethyl acetate and washed with sat. aq. $NaHCO_3$ (40 mL), 5% HCl (40 mL) and sat. aq. NaCl (40 mL). The organic layer was dried over $MgSO_4$, filtered and evaporated to give the title compound as a white solid (5.05 g, 94%). R_f = 0.16 (hexane/EtOAc 2:1). ESI-MS ($C_{26}H_{23}NO_6$) 445.15 *m/z* (%): 443.80 $[M-H]^-$ (90).

(*S*)-Benzyl 2-((((9*H*-fluoren-9-yl)methoxy)carbonyl)amino)-4-hydroxybutanoate (133). A solution of **132** (2.43 g, 5.46 mmol) in dry THF (15 mL) was cooled to -10 °C, treated with *N*-methylmorpholine (634 µL, 5.77 mmol, 1.05 equiv) and stirred for 5 min under argon atmosphere at -10 °C. Isobutyl chloroformate (754 µL, 5.77 mmol, 1.05 equiv) was added dropwise and the mixture stirred for 30 min under an argon atmosphere at -10 °C. The mixture was filtered through a Celite® pad, washing thoroughly with THF, and the filtrate was collected and cooled to -10 °C. $NaBH_4$ (0.312 g, 8.25 mmol, 1.5 equiv), pre-dissolved in H_2O (4 mL), was added dropwise. The mixture was then stirred for 1 h at 0 °C and 1 h at 25 °C. The suspension was diluted with EtOAc and washed once with 1 M $KHSO_4$, once with sat. aq. $NaHCO_3$ and once with sat. aq. NaCl. The organic layer was dried over $MgSO_4$, filtered and evaporated and the crude product was purified by flash chromatography (petroleum ether/EtOAc 1:1) to yield the title compound as a white solid (1.16 g, 50%). R_f = 0.25 (petroleum ether/EtOAc 1:1). ESI-MS ($C_{26}H_{25}NO_5$) 431.17 *m/z* (%): 430.70 $[M-H]^-$ (25), 296.10 (100). ^1H NMR ($CDCl_3$): δ = 1.73 (m, 1H, βCH_{2a}), 2.18 (m, 1H, βCH_{2b}), 2.71 (m, 1H, OH), 3.56-3.72 (m, 2H, γCH_2), 4.22 (t, 1H, *J* = 6.28, Fmoc CH), 4.43 (m, 2H, Fmoc CH_2), 4.59 (m, 1H, αCH), 5.20 (dd, 2H, *J* = 12.24, 16.36, OCH_2Ph), 5.70 (d, 1H, *J* = 7.8, NH), 7.41-7.29 (m, 9H, Fmoc and

benzyl CHAr), 7.59 (d, 2H, *J* = 7.4, Fmoc CHAr), 7.76 (d, 2H, *J* = 7.5, Fmoc CHAr). ^{13}C NMR ($CDCl_3$): δ = 35.6 (βCH_2), 47.2 Fmoc CH), 51.3 (αCH), 58.3 (γCH_2), 62.1 (Fmoc CH_2), 67.3 (OCH_2Ph), 120.0 Fmoc CHAr), 125.0 (Fmoc CHAr), 12.7-127.1 (Fmoc and benzyl CHAr).

(2*R*,7*R*)-Di-*tert*-butyl 2,7-bis((*tert*-butoxycarbonyl)amino)oct-4-enedioate (136). 10 mg (0.037 mmol) of N^{α}-Boc D-allylglycine *tert*-butyl ester (**49**) and 1.56 mg (0.002 mmol, 5 mol %) of Grubbs 2nd generation catalyst were transferred and sealed into a microwave vial. Using a needle the vial was evacuated and then filled with N_2. 300 µL of dry CH_2Cl_2 was injected into the vial and the mixture stirred for 30 s before placing the vial in the microwave. The sample was irradiated for 10 min at a target temperature of 40 °C, then 10 min at 65 °C, 10 min at 120 °C and 10 min at 130 °C. Each time a TLC sample was taken for comparison. R_f = 0.13 (petroleum ether/EtOAc 9:1).

(2*S*,6*R*)-1-Benzyl 7-*tert*-butyl 2-((((9*H*-fluoren-9-yl)methoxy)carbonyl)amino)-6-((*tert*-butoxycarbonyl)amino)hept-3-enedioate (105). 0.024 g (0.088 mmol) of N^{α}-Boc D-allylglycine *tert*-butyl ester (**49**), 0.065 g (0.157 mmol, 1.8 equiv) of N^{α}-Fmoc vinylglycine benzyl ester **50** and 3.64 mg (4.28 µmol, 5%) of Grubbs 2nd generation catalyst were transferred and sealed into a microwave vial. Using a needle the vial was evacuated and then filled with N_2. 1.95 mL of dry CH_2Cl_2 was injected into the vial and the mixture stirred for 30 s before placing the vial in the microwave. The sample was irradiated for 1 h at a target temperature of 55 °C. The sample was evaporated to dryness to yield a brown liquid (0.082 g). The crude product was purified via preparative HPLC (System P2) to give the title compound as a white solid (4.7 mg, 8%). ESI-MS ($C_{38}H_{44}N_2O_8$) 656.31 *m/z* (%): 679.4 $[M+Na]^+$ (100). RP-HPLC: R_t = 23.62 min. ^{1}H NMR ($CDCl_3$) δ = 1.44 (s, 18H, Boc 3 x CH_3, *t*Bu 3 x CH_3), 2.44-2.55 (m, 2H, δCH_2), 4.22-4.25 (m, 2H, εCH and Fmoc CH), 4.37-4.46 (m, 2H, Fmoc CH_2), 4.95 (m, 1H, αCH), 5.19 (d, 1H, *J* = 6.0, Boc NH), 5.24 (m, 2H, Bn CH_2), 5.51 (t, 1H, *J* = 8.4, Fmoc NH), 5.63-5.71 (m, 2H, βCH and γCH), 7.31-7.44 (m, 9H, Fmoc and Bn CHAr), 7.62 (2H, d, *J* = 7.2, Fmoc CHAr), 7.78 (2H, d, *J* = 7.6, Fmoc CHAr) identical to the NMR spectra reported in literature (147). ^{13}C NMR ($CDCl_3$): δ = 28.0-28.3 (2 x C(*C*H_3)$_3$), 35.7 (δCH_2), 47.12 (εCH and Fmoc CH), 55.5 (αCH), 67.2-67.6 (Fmoc CH_2), 82.2 (*t*Bu *C*(CH_3)$_3$), 120.0-128.0 (Fmoc and Bn CHAr), 128.3 (γCH), 128.6 (βCH) 135.0 (Bn CAr), 141.3 (Fmoc 2 x CAr), 143.7 (Fmoc 2 x Car *ortho*).

(2S,6R)-2-((((9H-Fluoren-9-yl)methoxy)carbonyl)amino)-7-(tert-butoxy)-6-((tert-butoxycarbon-yl)amino)-7-oxoheptanoic acid (51). 40 mg (0.062 mmol) of alkene **105** was dissolved in 11 mL of 9:1:1 mixture of MeOH, H_2O and CH_2Cl_2 and 3% dry Pt/C (0.020 g) was added. The mixture was stirred under a hydrogen atmosphere (balloons) at room temperature, monitoring the reaction via TLC. The reaction was complete after 30 h and the mixture was then filtered through a Celite® pad, washed with MeOH and evaporated to dryness. The residue was taken up with hexane and evaporated three times, followed by the addition of MeCN and freeze-drying to yield the title compound as an amorphous white solid (35.0 mg, 72%). HRMS (ESI) *m/z.* Calcd for $C_{31}H_{40}N_2NaO_8$ $[M+Na]^+$ 591.2682; found 591.2673. RP-HPLC: R_t = 20.11 min. ^{1}H NMR (CD_3OD): δ = 1.32-1.35 (m, 20 H, 3xCH_3 Boc, 3xCH_3 *t*Bu, γCH_2), 1.47-1.75 (m, 4H, βCH_2 δCH_2), 3.85 (m, 1H, εCH), 4.04 (m, 1H, αCH), 4.13 (t, 1H, *J* = 6.8, Fmoc CH), 4.26 (m, 2H, Fmoc CH_2), 7.21 (t, 2H, *J* = 7.6, Fmoc CHAr),-7.29 (t, 2H, *J* = 7.2, Fmoc CHAr), 7.58 (t, 2H, *J* = 6.4, Fmoc CHAr), 7,69 (d, 2H, *J* = 7.2, Fmoc CHAr). ^{13}C NMR (CD_3OD): δ = 28.3-28.7 (Boc CH_3 and *t*Bu CH_3), 32.4 (γCH_2), 48.0 (Fmoc CH), 55.0 (αCH), 55.8 (εCH), 68.0 (Fmoc CH_2) 80.1, 82.6 (Boc *C*$(CH_3)_3$ and *t*Bu *C*$(CH_3)_3$), 120.09 (Fmoc CHAr), 126.3 (Fmoc CHAr), 128.2 (Fmoc CHAr), 128.8 (Fmoc CHAr), 142,6 (Fmoc CAr), 145.4 (Fmoc CAr *ortho*).

H-Ala-D-Glu(*m*DAP-OH)-OH (52). 0.044 g of 2-ClTrt resin (0.072 mmol) was left to swell in dry CH_2Cl_2 in a sealed vessel under Ar atmosphere for 30 min. 0.020 g of Fmoc-*m*DAP(Boc,O*t*Bu)-OH (**51**) (0.043 mmol, 0.6 equiv based on the manufacturer's resin substitution) was dissolved in 0.44 mL (10 mL per g of resin) of dry CH_2Cl_2 in a sealed vessel under an Ar atmosphere, followed by the addition of 0.029 mL (0.172 mmol, 4 equiv) of DIEA. The *m*DAP-containing solution was then transferred by syringe into the flask containing the resin and the mixture allowed to shake for 2 h. The resin was drained and washed three times with dry CH_2Cl_2, three times with 17:2:1 (*v/v/v*) CH_2Cl_2:MeOH:DIEA and shaken for 1 h in the same mixture. Finally the resin was washed three times with CH_2Cl_2 and three times with DMF.

52 was manually synthesised, cleaved and isolated as described in the general methods. Purification via RP-HPLC (System P3) led to the isolation of the desired peptide (contaminated by a closely-eluting by-product) as an amorphous white solid (4.7 mg, 28%). ESI-MS ($C_{15}H_{26}N_4O_8$) 390.18 *m/z* (%): 389.14 $[M-H]^-$ (100), 412.1 $[M-H+Na]^-$ (75), 445.1 $[M+tBu-H]^-$ (60), 467.0 $[M+tBu-2H+Na]^{2-}$ (35). RP-HPLC: R_t = 2.61 min (by-product R_t = 3.72 min). ^{1}H NMR (D_2O+H_2O): δ = 1.32 (m, 2H, *m*DAP

γCH_2), 1.42 (d, 3H, *J* = 7.5, Ala βCH_3), 1.61 (m, 1H, *m*DAP βCH_a), 1.69-1.84 (m, 3H, *m*DAP βCH_b and δCH_2), 1.90 (m, 1H, Glu βCH_a), 2.04 (m, 1H, Glu βCH_b), 2.26 (t, 2H, *J* = 8.0, Glu γCH_2), 4.01 (q, 1H, *J* = 7.5, 15.0, Ala αCH), 4.06 (m, 1H, *m*DAP αCH), 4.11 (q, 1H, *J* = 5.5, 15.0, Glu αCH), 3.63 (t, 1H, J = 7.0, *m*DAP εCH), 7.86 (d, 1H, *J* = 7.5, *m*DAP NH), 8.37 (d, 1H, *J* = 7.0, Glu NH).

Linear lariatin A analogue (141). 100 mg (0.085 mmol) of H-Pro-2-ClTrt resin (0.85 mmol/g) was used for the automated synthesis of the lariatin A sequence, in which Glu8 was replaced with Gln8, as described in the general methods. The resin-bound peptide was washed thoroughly with DMF and three times with CH_2Cl_2:MeOH (1:1), dried and desiccated overnight. The peptide was cleaved and isolated according to the procedure described in the general methods. Purification via RP-HPLC (System P4) afforded the title compound as an amorphous white solid (2.8 mg, 5%). ESI-MS ($C_{94}H_{146}N_{28}O_{25}$) 2068.7 *m/z* (%): 1034.9 $[M+2H]^{2+}$ (40), 273.3 (100), 294.9 (97). RP-HPLC: R_t = 9.65 min.

Linear lariatin B analogue (142). 100 mg (0.085 mmol) of H-Pro-2-ClTrt resin (0.85 mmol/g) was used for the automated synthesis of the lariatin B sequence, in which Glu8 was replaced by Gln8, as described in the general methods. The resin-bound peptide was washed thoroughly with DMF and three times with CH_2Cl_2:MeOH (1:1), dried and desiccated overnight. The peptide was cleaved and isolated according to the procedure described in the general methods. Purification via RP-HPLC (System P4) afforded the title compound as a white solid (8.1 mg, 4%). ESI-MS ($C_{101}H_{156}N_{30}O_{27}$) 2222.4 *m/z* (%): 1145.2 $[M+H+3Na]^{2+}$ (100), 1134.9 $[M+2Na]^{2+}$ (77), 1112.1 $[M+2H]^{2+}$ (58). RP-HPLC: R_t = 9.59 min.

***N*-Terminally truncated pyroglutamate derivative of lariatin A (via ODmab side chain protection strategy) (139).** 100 mg (0.085 mmol) of H-Pro-2-ClTrt resin (0.85 mmol/g) was used for the attempted automated synthesis of the cyclic lariatin A peptide sequence as described in the general methods. Glu8 was coupled as its ODmab side chain protected derivative. After the final Fmoc deprotection and thorough washing with DMF, the resin was transferred to SPPS a vessel for the manual cyclisation. This step was preceded by Dmab removal. 2% hydrazine monohydrate in DMF (*ca.* 2 mL) was added to the resin and the mixture shaken for 3 min, followed by draining and washing with DMF. This deprotection step was repeated four more times. The resin was then treated with solution of 5% *v/v* DIEA in DMF (3 × 2 min). After a positive Kaiser test, the resin was washed thoroughly with DMF. The cyclisation was attempted by adding a solution of 34.71 mg HOAt (3

equiv, 0.255 mmol) and 39.5 µL DIC (3 equiv, 0.255 mmol) in DMF to the resin, followed by shaking for 24 h. This step was repeated three times until the Kaiser test provided a negative result. The resin-bound peptide was then thoroughly washed with DMF, washed three times with CH_2Cl_2:MeOH (1:1), dried and desiccated overnight. The peptide was cleaved and isolated according to the protocol described in the general methods to afford a crude mass of 0.072 g. Purification via RP-HPLC (System P4) resulted in the isolation of a single compound as an amorphous white solid (1.9 mg, 1.8%) consistent with the truncated pyroglutamyl-peptide. ESI-MS ($C_{58}H_{86}N_{16}O_{15}$) 1246.69 *m/z* (%): 1291.8 $[M-H+2Na]^+$ (100), 1247.8 $[M+H]^+$ (70). RP-HPLC: R_t = 10.08 min.

***N*-Terminally truncated pyroglutamate derivative of lariatin B (via ODmab side chain protection strategy) (140).** 100 mg (0.085 mmol) of H-Pro-ClTrt resin (0.85 mmol/g) was used for the attempted automated synthesis of the cyclic lariatin B peptide sequence as described in the general methods. Glu8 was coupled as its ODmab side chain protected derivative. After the final Fmoc deprotection and following thorough washing with DMF, the resin was transferred to a vessel for the manual cyclisation. This step was preceded by Dmab removal: 2% hydrazine monohydrate in DMF (*ca*. 2 mL) was added to the resin and the mixture shaken for 3 min, followed by draining and washing with DMF. This deprotection step was repeated four more times. The resin was then treated with a solution of 5% DIEA in DMF (3 × 2 min). After a positive result of the Kaiser test, the resin was washed thoroughly with DMF. The cyclisation was attempted by adding a solution of 34.7 mg HOAt (3 equiv, 0.255 mmol) and 39.5 µL DIC (3 equiv, 0.255 mmol) in DMF to the resin, followed by shaking for 24 h. This step was repeated three times, until the Kaiser test provided a negative result. The resin-bound peptide was then thoroughly washed with DMF, washed three times with CH_2Cl_2:MeOH (1:1), dried and desiccated overnight. The peptide was cleaved and isolated according to the protocol described in the general methods to afford a crude mass of 0.055 g. Purification via RP-HPLC (system P4) resulted in the isolation of a single compound as an amorphous white solid (3.7 mg, 3%) consistent with the truncated pyroglutamyl-peptide. ESI-MS ($C_{65}H_{96}N_{18}O_{17}$) 1440.7 *m/z* (%): 1423.9 $[M+Na]^+$ (75), 1401.8 $[M+H]^+$ (70), 1447.8 $[M+2H+2Na]^{2+}$ (5). RP-HPLC: R_t = 10.03 min.

Linear Asn8 free acid lassomycin analogue (143). 200 mg (0.138 mmol) of Fmoc-Ile-Wang (0.69 mmol/g) was used for the automated synthesis of the lassomycin sequence, in which Asp8 was replaced with Asn8, as described in the general methods. The resin-bound peptide was thoroughly washed with DMF and

three times with CH_2Cl_2:MeOH (1:1), then dried and desiccated overnight. The peptide was cleaved and isolated according to the procedure described in the general methods to yield a crude mass of 0.225 g. 90 mg of crude product was subjected to purification via RP-HPLC (System P5) to afford the title peptide as an amorphous white solid (23.0 mg, 25%). ESI-MS ($C_{82}H_{143}N_{31}O_{20}$) 1882.1 *m/z* (%): 942.6 $[M+2H]^{2+}$ (100), 472.0 $[M+3H]^{3+}$ (82), 628.8 $[M+4H]^{4+}$ (21). RP-HPLC: R_t = 9.60 min.

Linear Asn8 lassomycin methyl ester analogue (144). To 10 mg (5.00 μmol) of **143** were added 1 mL of MeOH and 1 mL of 4 M HCl in dioxane. The mixture was stirred at room temperature for 4 h, monitoring the reaction by HPLC. The mixture was poured into a mixture of 4 mL of water and 3 mL of diethyl ether. The organic layer was washed three times with 2 mL of water and the aqueous phases combined and freeze-dried. The crude product was purified using semi-preparative HPLC (System P6) to afford the title compound as an amorphous white solid (5.0 mg, 45%). ESI-MS ($C_{83}H_{145}N_{31}O_{20}$) 1896.1 *m/z* (%): 475.4 $[M+4H]^{4+}$ (100), 949.4 $[M+2H]^{2+}$ (16). RP-HPLC: R_t = 10.02 min.

Cyclic lassomycin synthesis (via ODmab side chain protection strategy) (148). First attempt: 200 mg (0.138 mmol) of Fmoc-Ile-Wang (0.69 mmol/g) was used for the automated synthesis of the peptide following the protocol of two couplings with 2.5 equiv of activated amino acid for 30 min each time. Asp8 was coupled as its side chain ODmab protected derivative. The final residue was not Fmoc deprotected. The resin-bound peptide was thoroughly washed with DMF and three times with CH_2Cl_2:MeOH (1:1) then was transferred to a manual synthesis vessel and washed thoroughly with DMF. Five treatments of 3 min with 2% hydrazine monohydrate in DMF were performed followed by five washes with DMF. The product was treated three times for 2 min with 5% DIEA in DMF and then washed five times with DMF. After a positive Kaiser test result, a 24 h cyclisation was attempted using 64 μL (3 equiv, 0.414 mmol) of DIC and 56.4 mg (3 equiv, 0.414 mmol) of HOAt dissolved in minimal DMF. The following Kaiser test was positive, therefore this step was repeated. After a further positive result, cyclisation of 6 h duration was attempted twice, using a mixture of 0.359 g (5 equiv, 0.690 mmol) of PyBOP and 0.094 g (5 equiv, 0.690 mmol) of HOAt dissolved in DMF, and 235 μL (10 equiv, 1.38 mmol) of DIEA. After these treatment the Kaiser test result improved, therefore the resin was washed thoroughly in DMF, and three times with CH_2Cl_2:MeOH (1:1) and desiccated overnight. The resin was then cleaved and the product isolated as described in the general methods to yield a crude mass of 0.181 g. The crude product was subjected

to purification via RP-HPLC (system P7) to afford a product consistent with the molecular weight of the desired product (or the aspartimide adduct of the linear sequence, see Discussion) as a white solid (10.0 mg, 3.9%).

Second attempt: the synthesis was repeated starting from 80 mg (0.055 mmol) of Fmoc-Ile-Wang (0.69 mmol/g) and the steps were carried out as described for the earlier attempt. As before, 24 h cyclisation with DIC and HOAt failed to give a negative Kaiser test therefore the peptide was treated with 5 mM NaOH in MeOH:H_2O (1:1) for 3 h. The Kaiser test result was once more positive therefore the cyclisation step was repeated. After a further positive result, the same cyclisation reaction was attempted once again for 6 h. After this treatment the Kaiser test result improved, therefore the resin was washed thoroughly in DMF, and three times with CH_2Cl_2:MeOH (1:1) and desiccated overnight. The resin was then cleaved and the product isolated as described in the general methods to yield a crude mass of 0.081 g.

Third attempt: an analogous synthesis starting from 80 mg of resin was also performed, omitting the NaOH treatment and performing 3 DIC/HOAt cyclisation's reactions of 24 h each, finally obtaining a negative Kaiser test. The crude product obtained (0.074 g) was combined with that of the previous attempt and subjected to purification via RP-HPLC (system P7) to afford a product consistent with the molecular weight of the desired product (or the aspartimide adduct of the linear sequence, see Discussion, as an amorphous white solid (3.0 mg, 1.5%). HRMS (ESI) *m/z*. Calcd for $C_{82}H_{140}N_{30}O_{20}$ $[M+3H]^{3+}$ 622.7032; found 622.7047. RP-HPLC: R_t = 9.10 min.

Cyclic lariatin A (via OAll side chain protection strategy) (31).

Manual SPPS

200 mg (0.164 mmol) of H-Pro-ClTrt resin (0.82 mmol/g) was used for the manual synthesis of the peptide as described in the general methods. Glu8 was coupled as its side chain OAll protected derivative. The final residue coupled was not Fmoc deprotected. The peptide-resin was thoroughly washed with DMF, washed three times with CH_2Cl_2:MeOH (1:1), dried briefly under suction and desiccated overnight. The SPPS vessel was then sealed with a septum, the air removed and replaced with Ar using a balloon to maintain dry conditions. Dry CH_2Cl_2 was added using a syringe and the resin left to swell for 30 min. After removal of the CH_2Cl_2 via positive pressure of Ar, 0.019 g (2 equiv, 0.328 mmol) of dimethylamineborane, previously dissolved in dry CH_2Cl_2 (4 mL), was added to the resin in the sealed vessel and

allowed to stand for 30 min. Afterwards 0.189 g (1 equiv, 0.164 mmol) of $Pd(PPh_3)_4$ was quickly and carefully added and the vessel was shaken for 1 h. The resin was washed four times with CH_2Cl_2 and four times with DMF, followed by two Fmoc deprotection steps of 15 min with 20% piperidine in DMF. After confirmation of the Fmoc removal using the Kaiser test, the resin-bound peptide was washed once with 5% DIEA in DMF to remove any residual piperidine, followed by a thorough wash with DMF. One 24 h cyclisation step was performed, using 0.076 mL of DIC (3 equiv, 0.492 mmol) and 0.067 g of HOAt (3 equiv, 0.492 mmol) in minimal DMF. Following a negative Kaiser test, the peptide-bound resin was thoroughly washed with DMF, washed three times with CH_2Cl_2:MeOH (1:1), dried and desiccated overnight. The peptide was cleaved and isolated according to the procedure described in the general methods to afford a crude mass of 0.217 g.

Automated

200 mg (0.164 mmol) of H-Pro-ClTrt resin (0.82 mmol/g) was used for the automated synthesis of the peptide following the protocol of two couplings with 2.5 equiv of activated amino acid for 30 min each time. Glu8 was coupled as its side chain OAll protected derivative.The final residue was not Fmoc deprotected. The resin-bound peptide was thoroughly washed with DMF, washed three times with CH_2Cl_2:MeOH (1:1), dried briefly under suction and desiccated overnight. The resin was then transferred to a manual SPPS vessel. OAll deprotection, Fmoc deprotection and cyclisation were carried out as described for the manual procedure above. The resin-bound peptide was thoroughly washed with DMF, washed three times with CH_2Cl_2:MeOH (1:1), dried and desiccated overnight. The resin was cleaved isolated according to the procedure described in the general methods, to afford a crude mass of 0.235 g.

The crude products of the manual and automated syntheses were combined and purified by RP-HPLC (System P4) to yield the desired lariatin A as an amorphous white solid (9.0 mg; 1.5%). ESI-MS ($C_{94}H_{143}N_{27}O_{25}$) 2051.2 *m/z* (%): 1026.6 $[M+2H]^{2+}$ (100), 684.7 $[M+3H]^{3+}$ (70). RP-HPLC: R_t = 10.58 min.

Cyclic lariatin B (via OAll side chain protection strategy) (32). 200 mg (0.164 mmol) of H-Pro-ClTrt resin (0.82 mmol/g) was used for the automated synthesis of the peptide following the protocol of two couplings with 2.5 equiv of activated amino acid for 30 min each time. Glu8 was coupled as its side chain OAll protected derivative. The final residue was not Fmoc deprotected. The resin-bound peptide

was thoroughly washed with DMF, washed three times with CH_2Cl_2:MeOH (1:1), dried briefly under suction and desiccated overnight. The resin was then transferred to a manual SPPS vessel which was sealed with a septum and maintained under an Ar atmosphere using a balloon. Dry CH_2Cl_2 was added using a syringe and the resin left to swell for 1 h. After removal of the CH_2Cl_2 via positive pressure of Ar, OAll removal was achieved using the method described above for **31** above. After confirmation of the Fmoc removal using the Kaiser test, the resin-bound peptide was washed once with 5% DIEA in DMF to remove any residual piperidine, followed by a thorough wash with DMF. One 24 h cyclisation step was performed, using 0.076 mL of DIC (3 equiv, 0.492 mmol) and 0.067 g of HOAt (3 equiv, 0.492 mmol) in minimal DMF. Following a negative Kaiser test, the peptide-bound resin was thoroughly washed with DMF, washed three times with CH_2Cl_2:MeOH (1:1), dried and desiccated overnight. The resin was cleaved and isolated as described in the general methods to afford a crude mass of 0.210 g. 0.100 g of crude product was purified via RP-HPLC (System P4) and, after combination of the fractions, resulted in the isolation of a single compound as an amorphous white solid (3.1 mg, 1.8%) consistent with the desired product. ESI-MS ($C_{101}H_{153}N_{29}O_{27}$) 2205.2 *m/z* (%): 736.1 $[M+3H]^{3+}$ (100), 1103.1 $[M+2H]^{2+}$ (15). RP-HPLC: R_t =10.40 min.

Cyclic free acid lassomycin (via OAll side chain protection strategy) (148). 236 mg (0.164 mmol) of Fmoc-Ile-Wang resin (0.69 mmol/g) was used for the automated synthesis of the peptide following the protocol of two couplings with 2.5 equiv of amino acid for 30 min each time. Asp8 was coupled as its side chain OAll protected derivative. The final residue was not Fmoc deprotected and the resin-bound peptide was thoroughly washed in DMF, washed three times with CH_2Cl_2:MeOH (1:1), dried briefly and desiccated overnight. The resin was then transferred to a manual SPPS vessel which was sealed with a septum then mantained under an Ar atmosphere using a balloon. Dry CH_2Cl_2 was added using a syringe and the resin left to swell the resin for 30 min. After removal of CH_2Cl_2 via positive pressure of Ar, 0.019 g (2 equiv, 0.328 mmol) of dimethylamineborane, previously dissolved in dry CH_2Cl_2 (4mL), was added to the resin in the sealed vessel and allowed to stand for 30 min. Afterwards 0.189 g (1 equiv, 0.164 mmol) of $Pd(PPh_3)_4$ was quickly and carefully added and the vessel was shaken for 1 h. The resin was washed four times with CH_2Cl_2 and four times with DMF, followed by two Fmoc deprotection steps of 15 min with 20% piperidine in DMF. After confirmation of the Fmoc removal, using the Kaiser test, the resin-bound peptide was washed once with 5% DIEA in DMF to remove any residual piperidine, followed by a thorough wash with DMF.. A 24 h cyclisation step was performed, using 0.076 mL of DIC (3 equiv, 0.492 mmol) and

0.067 g of HOAt (3 equiv, 0.492 mmol) dissolved in minimal DMF. After a positive Kaiser test, the resin was washed in DMF and the 24 h cyclisation was repeated twice more. Unfortunately the Kaiser test remained weakly positive. The peptide-bound resin was thoroughly washed with DMF, washed three times with CH_2Cl_2:MeOH (1:1) dried briefly under suction and then desiccated overnight. The resin was cleaved and the resulting peptide processed as described in the general methods, to afford a crude mass of 0.28 g. 70 mg of crude product were purified via RP-HPLC and, after combination of the fractions, resulted in the isolation of a single compound as an amorphous white solid (3.0 mg, 3.9%) consistent with the molecular weight of the desired product (or the aspartimide adduct of the linear sequence, see Discussion). ESI-MS ($C_{82}H_{140}N_{30}O_{20}$) 1865.1 *m/z* (%): 933.9 $[M+2H]^{2+}$ (100), 622.8 $[M+3H]^{3+}$ (95), 467.45 $[M+4H]^{4+}$ (20). RP-HPLC: Rt = 9.92 min.

4.7.1 List of compounds

Below is a table which shows the compound number in bold and where it appears in the experimental section.

5. REFERENCES

1. Pendleton JN, Gorman SP, Gilmore BF. Clinical relevance of the ESKAPE pathogens. *Expert Rev Anti Infect Ther*. 2013;11(3):297–308.

2. Boucher HW, Talbot GH, Bradley JS, Edwards JE, Gilbert D, Rice LB, et al. Bad bugs, no drugs: no ESKAPE! An update from the Infectious Diseases Society of America. *Clin Infect Dis*. 2009;48(1):1–12.

3. World Health Organization. Global Tuberculosis Report. WHO Press. 2015;(20th Edition).

4. de Kantor IN, LoBue P, Thoen CO, Int JTLD. Human tuberculosis caused by Mycobacterium bovis in the United States, Latin America and the Caribbean. *Int J Tuberc Lung Dis*. 2010;14(11):1369–73.

5. Russell DG. Mycobacterium tuberculosis and the intimate discourse of a chronic infection. *Immunol Rev*. 2011;240(1):252–68.

6. Flynn JL, Chan J. Tuberculosis: latency and reactivation. *Infect Immun*. 2001;69(7):4195–201.

7. Gupta A, Kaul A, Tsolaki AG, Kishore U, Bhakta S. Mycobacterium tuberculosis: immune evasion, latency and reactivation. *Immunobiology*. 2012;217(3):363–74.

8. Lin PL, Flynn JL. Understanding Latent Tuberculosis: A Moving Target. *J Immunol*. 2010;185(1):15–22.

9. Tufariello JM, Chan J, Flynn JL. Latent tuberculosis: mechanisms of host and bacillus that contribute to persistent infection. *Lancet Infect Dis.* 2003;3(9):578–90.

10. Belanger AE, Besra GS, Ford ME, Mikusová K, Belisle JT, Brennan PJ, et al. The embAB genes of Mycobacterium avium encode an arabinosyl transferase involved in cell wall arabinan biosynthesis that is the target for the antimycobacterial drug ethambutol. *Proc Natl Acad Sci U S A*. 1996;93(21):11919–24.

11. Hartmann GR, Heinrich P, Kollenda MC, Skrobranek B, Tropschug M, Weiß W. Molecular Mechanism of Action of the Antibiotic Rifampicin. *Angew. Chem. Int. Ed. Engl.* 1985:1009–14.

12. Almeida Da Silva PE, Palomino JC. Molecular basis and mechanisms of drug resistance in Mycobacterium tuberculosis: classical and new drugs. *J Antimicrob Chemother*. 2011;66(7):1417–30.

13. Zhang Y, Shi W, Zhang W, Mitchison D. Mechanisms of Pyrazinamide Action and Resistance. *Microbiol Spectr*. 2014;2(4):2-0023-2013.

14. Singh P, Mishra AK, Malonia SK, Chauhan DS, Sharma VD, Venkatesan K, et al. The paradox of pyrazinamide: an update on the molecular mechanisms of pyrazinamide resistance in Mycobacteria. *J Commun Dis*. 2006;38(3):288–98.

15. Zhang Y, Scorpio A, Nikaido H, Sun Z. Role of acid pH and deficient efflux of pyrazinoic acid in unique susceptibility of Mycobacterium tuberculosis to pyrazinamide. *J Bacteri*ol. 1999;181(7):2044–9.

16. Sulis G, Roggi A, Matteelli A, Raviglione MC. Tuberculosis: Epidemiology and Control. *Mediterr J Hematol Infect Dis*. 2014;6(1):e2014070.

17. National Institute of Allergy and Infectious Diseases. [accessed 2012 Dec 1]. Available from: http://www.niaid.nih.gov/topics/tuberculosis/understanding/whatistb/scientificillustrations/pages/multidrugresistantillustration.aspx

18. Lehmann J. Para-aminosalicylic acid in the treatment of tuberculosis. *Lancet*. 1946;1(6384):15–6.

19. Shim TS, Jo K-W. Medical Treatment of Pulmonary Multidrug-Resistant Tuberculosis. *Infect Chemother*. 2013;45(4):367–74.

20. Ji B, Lounis N, Truffot-Pernot C, Grosset J. In vitro and in vivo activities of levofloxacin against *Mycobacterium tuberculosis*. *Antimicrob Agents Chemoter*. 1995;39(6):1341–4.

21. Richeldi L, Covi M, Ferrara G, Franco F, Vailati P, Meschiari E, Fabbri LM, *et al*. Clinical use of Levofloxacin in the long-term treatment of drug resistant tuberculosis. *Monardi Arch Chest Dis*. 2002;57(1):39–43.

22. Rastogi N, Labrousse V, Goh KS. In vitro activities of fourteen antimicrobial agents against drug susceptible and resistant clinical isolates of Mycobacterium tuberculosis and comparative intracellular activities against

the virulent H37Rv strain in human macrophages. *Curr Microbiol*. 1996;33(3):167–75.

23. Rodriguez JC, Ruiz M, Lopez M, Royo G. In vitro activity of moxifloxacin, levofloxacin, gatifloxacin and linezolid against Mycobacterium tuberculosis. *Int J Antimicrob Agents*. 2002;20(6):464–7.

24. Amyes SGB. Magic bullets, lost horizons : the rise and fall of antibiotics. London: Taylor & Francis; 2001.

25. Flores AR, Parsons LM, Pavelka Jr. MS. Genetic analysis of the beta-lactamases of Mycobacterium tuberculosis and Mycobacterium smegmatis and susceptibility to beta-lactam antibiotics. *Microbiology.* 2005;151(Pt 2):521–32.

26. Danilchanka O, Pavlenok M, Niederweis M. Role of porins for uptake of antibiotics by Mycobacterium smegmatis. *Antimicrob Agents Chemother*.. 2008;52(9):3127–34.

27. Alcaide F, Pfyffer GE, Telenti A. Role of embB in natural and acquired resistance to ethambutol in mycobacteria. *Antimicrob Agents Chemother*.. 1997;41(10):2270–3.

28. Meacci F, Orru G, Iona E, Giannoni F, Piersimoni C, Pozzi G, *et al*. Drug resistance evolution of a Mycobacterium tuberculosis strain from a noncompliant patient. *J Clin Microbiol.* 2005;43(7):3114–20.

29. Udwadia ZF, Amale RA, Ajbani KK, Rodrigues C. Totally drug-resistant tuberculosis in India. *Clin Infect Dis*; 2012: 579–81.

30. Migliori GB, De Iaco G, Besozzi G, Centis R, Cirillo DM. First tuberculosis cases in Italy resistant to all tested drugs. *Euro Surveill*. 2007;12(5):E070517.1.

31. Velayati AA, Masjedi MR, Farnia P, Tabarsi P, Ghanavi J, Ziazarifi AH, *et al*. Emergence of new forms of totally drug-resistant tuberculosis bacilli: super extensively drug-resistant tuberculosis or totally drug-resistant strains in iran. *Chest*. 2009;136(2):420–5.

32. Velayati AA, Farnia P, Masjedi MR. The totally drug resistant tuberculosis (TDR-TB). *Int J Clin Exp Med*. 2013;6(4):307–9.

33. Brennan PJ. Structure, function, and biogenesis of the cell wall of Mycobacterium tuberculosis. *Tuberc*.. 2003;83(1–3):91–7.

34. Chen J. Identifying Biosynthetic Pathways for Mycobacterial Cell Wall Components Using Transposon Mutagenesis [Thesis]. School of Biosciences, University of Birmingham; 2010.

35. Royet J, Dziarski R. Peptidoglycan recognition proteins: pleiotropic sensors and effectors of antimicrobial defences. *Nat Rev Micro*. 2007;5(4):264–77.

36. RoyChowdhury A, Boons GJ. The synthesis of diaminopimelic acid containing peptidoglycan fragments using metathesis cross coupling. *Tetrahedron Lett*. 2005;46(10):1675–8.

37. Smith CA. Structure, Function and Dynamics in the mur Family of Bacterial Cell Wall Ligases. *J Mol Biol*. 2006;362(4):640–55.

38. Meroueh SO, Bencze KZ, Hesek D, Lee M, Fisher JF, Stemmler TL, *et al*. Three-dimensional structure of the bacterial cell wall peptidoglycan. *Proc Natl Acad Sci U S A*. 2006;103(12):4404–9.

39. Basavannacharya C, Moody PR, Munshi T, Cronin N, Keep NH, Bhakta S. Essential residues for the enzyme activity of ATP-dependent MurE ligase from Mycobacterium tuberculosis. *Protein Cell*. 2010;1(11):1011–22.

40. Marrakchi H, Lanéelle M-A, Daffé M. Mycolic Acids: Structures, Biosynthesis, and Beyond. *Chem Biol*. 2014;21(1):67–85.

41. Hett EC, Rubin EJ. Bacterial growth and cell division: a mycobacterial perspective. *Microbiol Mol Biol Rev*; 2008:126–56.

42. Wietzerbin J, Das BC, Petit JF, Lederer E, Leyh-Bouille M, Ghuysen JM. Occurrence of D-alanyl-(D)-*meso*-diaminopimelic acid and *meso*-diaminopimelyl-*meso*-diaminopimelic acid interpeptide linkages in the peptidoglycan of Mycobacteria. *Biochemistry*. 1974;13(17):3471–6.

43. Goffin C, Ghuysen JM. Multimodular penicillin-binding proteins: an enigmatic family of orthologs and paralogs. *Microbiol Mol Biol Rev*. 1998;62(4):1079–93.

44. Both D, Steiner EM, Stadler D, Lindqvist Y, Schnell R, Schneider G. Structure of LdtMt2, an L,D-transpeptidase from *Mycobacterium tuberculosis*. *Acta Crystallogr D Biol Crystallogr*. 2013;69(Pt 3):432–41.

45. Templin MF, Ursinus A, Höltje J-V. A defect in cell wall recycling triggers autolysis during the stationary growth phase of Escherichia coli. *EMBO J.* 1999;18(15):4108–17.

46. Kumar P, Arora K, Lloyd JR, Lee IY, Nair V, Fischer E, *et al.* Meropenem inhibits D,D-carboxypeptidase activity in *Mycobacterium tuberculosis*. *Mol Microbiol*. 2012;86(2):367–81.

47. Lavollay M, Arthur M, Fourgeaud M, Dubost L, Marie A, Veziris N, et al. The Peptidoglycan of Stationary-Phase *Mycobacterium tuberculosis* Predominantly Contains Cross-Links Generated by L,D-Transpeptidation. *J Bacteriol*. 2008;190(12):4360–6.

48. Mahapatra S, Crick DC, Brennan PJ. Comparison of the UDP-N-acetylmuramate:L-alanine ligase enzymes from *Mycobacterium tuberculosis* and *Mycobacterium leprae*. *J Bacteriol*. 2000;182(23):6827–30.

49. Shanmugam A, Natarajan J. Computational genome analyses of metabolic enzymes in *Mycobacterium leprae* for drug target identification. *Bioinformation*.. 2010;4(9):392–5.

50. Patin D, Bostock J, Chopra I, Mengin-Lecreulx D, Blanot D. Biochemical characterisation of the chlamydial MurF ligase, and possible sequence of the chlamydial peptidoglycan pentapeptide stem. *Arch Microbiol*. 2012;194(6):505–12.

51. Han SG, Lee WK, Jin BS, Lee KI, Lee HH, Yu YG. Identification of novel irreversible inhibitors of UDP-*N*-acetylglucosamine enolpyruvyl transferase (MurA) from *Haemophilus influenzae*. *J Microbiol Biotechnol.* 2013;23(3):329–34.

52. Barreteau H, Sosič I, Turk S, Humljan J, Tomašić T, Zidar N, *et al*. MurD enzymes from different bacteria: Evaluation of inhibitors. *Biochem Pharmacol*. 2012;84(5):625–32.

53. Barreteau H, Kovac A, Boniface A, Sova M, Gobec S, Blanot D. Cytoplasmic steps of peptidoglycan biosynthesis. *FEMS Microbiol Rev*. 2008;32(2):168–207.

54. Munshi T, Gupta A, Evangelopoulos D, Guzman JD, Gibbons S, Keep NH, *et al.* Characterisation of ATP-Dependent Mur Ligases Involved in the

Biogenesis of Cell Wall Peptidoglycan in *Mycobacterium tuberculosis. PLoS One.* 2013;8(3): e60143.

55. Bertrand JA, Auger G, Martin L, Fanchon E, Blanot D, Le Beller D, *et al*. Determination of the MurD mechanism through crystallographic analysis of enzyme complexes. *J Mol Biol*. 1999;289(3):579—90.

56. Fiuza M, Canova MJ, Patin D, Letek M, Zanella-Cleon I, Becchi M, *et al*. The MurC ligase essential for peptidoglycan biosynthesis is regulated by the serine/threonine protein kinase PknA in *Corynebacterium glutamicum. J Biol Chem*. 2008 Dec;283(52):36553–63.

57. Sink R, Barreteau H, Patin D, Mengin-Lecreulx D, Gobec S, Blanot D. MurD enzymes: some recent developments. *Biomol Concepts*. 2013;4(6):539–56.

58. Walsh AW, Falk PJ, Thanassi J, Discotto L, Pucci MJ, Ho HT. Comparison of the D-glutamate-adding enzymes from selected gram-positive and gram-negative bacteria. *J Bacteriol.* 1999;181(17):5395–401.

59. Mengin-Lecreulx D, Falla T, Blanot D, van Heijenoort J, Adams DJ, Chopra I. Expression of the *Staphylococcus aureus* UDP-*N*-acetylmuramoyl- L-alanyl-D-glutamate:L-lysine ligase in *Escherichia coli* and effects on peptidoglycan biosynthesis and cell growth. *J Bacteriol*. 1999;181(19):5909–14.

60. Kouidmi I, Levesque RC, Paradis-Bleau C. The biology of Mur ligases as an antibacterial target. *Mol Microbiol*. 2014;94(2):242–53.

61. Basavannacharya C, Robertson G, Munshi T, Keep NH, Bhakta S. ATP-dependent MurE ligase in *Mycobacterium tuberculosis*: Biochemical and structural characterisation. *Tuberculosis*. 2009;90(1):16–24.

62. Patin D, Boniface A, Kovac A, Herve M, Dementin S, Barreteau H, *et al.* Purification and biochemical characterization of Mur ligases from *Staphylococcus aureus. Biochimie*. 2010;92(12):1793–800.

63. Usha V, Dover LG, Roper DI, Futterer K, Besra GS. Structure of the diaminopimelate epimerase DapF from *Mycobacterium tuberculosis*. *Acta Crystallogr D Biol Crystallogr.* 2009;65(Pt 4):383–7.

64. van Heijenoort J. Recent advances in the formation of the bacterial peptidoglycan monomer unit. *Nat Prod Rep.* 2001;18(5):503–19.

65. Mohammadi T, van Dam V, Sijbrandi R, Vernet T, Zapun A, Bouhss A, *et al.* Identification of FtsW as a transporter of lipid-linked cell wall precursors across the membrane. *EMBO J.* 2011;30(8):1425–32.

66. Sieger B, Schubert K, Donovan C, Bramkamp M. The lipid II flippase RodA determines morphology and growth in *Corynebacterium glutamicum. Mol Microbiol*. 2013;90(5):966–82.

67. Gupta R, Lavollay M, Mainardi JL, Arthur M, Bishai WR, Lamichhane G. The *Mycobacterium tuberculosis* gene, ldtMt2, encodes a non-classical transpeptidase required for virulence and resistance to amoxicillin. *Nat Med.* 2010;16(4):466–9.

68. Park JT, Uehara T. How Bacteria Consume Their Own Exoskeletons (Turnover and Recycling of Cell Wall Peptidoglycan)†. *Microbiol Mol Biol Rev*. 2008;72(2):211–27.

69. Herve M, Boniface A, Gobec S, Blanot D, Mengin-Lecreulx D. Biochemical characterization and physiological properties of *Escherichia coli* UDP-*N*-acetylmuramate:L-alanyl-gamma-D-glutamyl-*meso*-diaminopimelate ligase. *J Bacteriol*. 2007;189(11):3987–95.

70. Das D, Herve M, Feuerhelm J, Farr CL, Chiu HJ, Elsliger MA, *et al*. Structure and function of the first full-length murein peptide ligase (Mpl) cell wall recycling protein. *PLoS One*. 2011;6(3):e17624.

71. UniProt Knowledgebase. UniProtKB - C0Q6I7 (C0Q6I7_SALPC). [accessed 2016 Apr 1].
Available from: http://www.uniprot.org/uniprot/C0Q6I7

72. Liger D, Masson A, Blanot D, van Heijenoort J, Parquet C. Over-production, purification and properties of the uridine-diphosphate-*N*-acetylmuramate:L-alanine ligase from *Escherichia coli. Eur J Biochem*. 1995;230(1):80–7.

73. Mengin-Lecreulx D, van Heijenoort J, Park JT. Identification of the mpl gene encoding UDP-*N*-acetylmuramate: L-alanyl-gamma-D-glutamyl-*meso*-diaminopimelate ligase in *Escherichia coli* and its role in recycling of cell wall peptidoglycan. *J Bacteriol*. 1996;178(18):5347–52.

74. Johnson JW, Fisher JF, Mobashery S. Bacterial cell-wall recycling. *Ann N Y Acad Sci*. 2013;1277:54–75.

75. Reith J, Mayer C. Peptidoglycan turnover and recycling in Gram-positive bacteria. *Appl Microbiol Biotechnol*. 2011;92(1):1–11.

76. Litzinger S, Duckworth A, Nitzsche K, Risinger C, Wittmann V, Mayer C. Muropeptide rescue in *Bacillus subtilis* involves sequential hydrolysis by beta-*N*-acetylglucosaminidase and *N*-acetylmuramyl-L-alanine amidase. *J Bacteriol*. 2010;192(12):3132–43.

77. Borisova M, Gisin J, Mayer C. Blocking Peptidoglycan Recycling in *Pseudomonas aeruginosa* Attenuates Intrinsic Resistance to Fosfomycin. *Microb Drug Resis*t. 2014;20(3):231–7.

78. Gomez MJ, Neyfakh AA. Genes involved in intrinsic antibiotic resistance of *Acinetobacter baylyi. Antimicrob Agents Chemother*. 2006;50(11):3562–7.

79. Gisin J, Schneider A, Nägele B, Borisova M, Mayer C. A cell wall recycling shortcut that bypasses peptidoglycan de novo biosynthesis. *Nat Chem Biol*. 2013;9(8):491–3.

80. Arnison PG, Bibb MJ, Bierbaum G, Bowers AA, Bugni TS, Bulaj G, *et al*. Ribosomally synthesized and post-translationally modified peptide natural products: overview and recommendations for a universal nomenclature. *Nat Prod Rep*. 2013;30(1):108–60.

81. Fleming A. On the Antibacterial Action of Cultures of a Penicillium, with Special Reference to their Use in the Isolation of *B. influenzæ*. *Br J Exp Pathol*. 1929;10(3):226–36.

82. Wang F, Cassidy C, Sacchettini JC. Crystal structure and activity studies of the *Mycobacterium tuberculosis* beta-lactamase reveal its critical role in resistance to beta-lactam antibiotics. *Antimicrob Agents Chemother*. 2006;50(8):2762–71.

83. Wivagg CN, Bhattacharyya RP, Hung DT. Mechanisms of beta-lactam killing and resistance in the context of *Mycobacterium tuberculosis. J Antibiot.* 2014;67(9):645–54.

84. Hugonnet JE, Tremblay LW, Boshoff HI, Barry 3rd CE, Blanchard JS. Meropenem-clavulanate is effective against extensively drug-resistant *Mycobacterium tuberculosis*. *Science.* 2009;323(5918):1215–8.

85. Kurz SG, Wolff KA, Hazra S, Bethel CR, Hujer AM, Smith KM, *et al*. Can inhibitor-resistant substitutions in the Mycobacterium tuberculosis beta-Lactamase BlaC lead to clavulanate resistance?: a biochemical rationale for the use of beta-lactam-beta-lactamase inhibitor combinations. *Antimicrob Agents Chemother*. 2013;57(12):6085–96.

86. Segura C, Salvado M, Collado I, Chaves J, Coira A. Contribution of beta-lactamases to beta-lactam susceptibilities of susceptible and multidrug-resistant *Mycobacterium tuberculosis* clinical isolates. *Antimicrob Agents Chemother*. 1998;42(6):1524–6.

87. Li W-J, Li D-F, Hu Y-L, Zhang X-E, Bi L-J, Wang D-C. Crystal structure of L,D-transpeptidase LdtMt2 in complex with meropenem reveals the mechanism of carbapenem against *Mycobacterium tuberculosis. Cell Res*. 2013;23(5):728–31.

88. Wallace BA. Structure of gramicidin A. *Biophys J*. 1986;49(1):295–306.

89. Burkhart BM, Gassman RM, Langs DA, Pangborn WA, Duax WL, Pletnev V. Gramicidin D conformation, dynamics and membrane ion transport. *Biopolymers*. 1999;51(2):129–44.

90. Liou J-W, Hung Y-J, Yang C-H, Chen Y-C. The antimicrobial activity of gramicidin A is associated with hydroxyl radical formation. *PLoS One*. 2015;10(1):e0117065.

91. Joint Formulary Committee. British National Formulary (online). London: BMJ Group and Pharmaceutical Press. [accessed 2016 Jun 1].
Available from: http://www.medicinescomplete.com

92. Knox JR, Pratt RF. Different modes of vancomycin and D-alanyl-D-alanine peptidase binding to cell wall peptide and a possible role for the vancomycin resistance protein. *Antimicrob Agents Chemother*. 1990;34(7):1342–7.

93. Watanakunakorn C. Mode of action and in-vitro activity of vancomycin. *J Antimicrob Chemother*. 1984;14 Suppl D:7–18.

94. Somma S, Gastaldo L, Corti A. Teicoplanin, a new antibiotic from *Actinoplanes teichomyceticus nov.* sp. *Antimicrob Agents Chemother.* 1984;26(6):917—923.

95. Wilson AP, Gruneberg RN. Use of teicoplanin in community medicine. *Eur J Clin Microbiol Infect Dis*. 1994;13(9):701–10.

96. Fox JL. Antimicrobial peptides stage a comeback. *Nat Biotech.* 2013;31(5):379–82.

97. Lamb HM, Wiseman LR. Pexiganan acetate. *Drugs*. 1998;56(6):1044–7.

98. Dipexium Pharmaceuticals Inc. Dipexium Receives European Medicines Agency Scientific Advice on Clinical and Regulatory Pathway for Locilex. 2015 [accessed 2016 Jul 1].
Available from: https://www.drugs.com/nda/locilex_150602.html

99. Stone KJ, Strominger JL. Mechanism of action of bacitracin: complexation with metal ion and C 55 -isoprenyl pyrophosphate. *Proc Natl Acad Sci U S A.* 1971;68(12):3223–7.

100. Economou NJ, Cocklin S, Loll PJ. High-resolution crystal structure reveals molecular details of target recognition by bacitracin. *Proc Natl Acad Sci U S A.* 2013;110(35):14207–12.

101. Accessdata.fda.gov. Drugs@FDA: FDA Approved Drug Products. 2016 [accessed 2016 Jun 1].

Available from:
http://www.accessdata.fda.gov/scripts/cder/drugsatfda/index.cfm?fuseaction=Search.Overview&DrugName=BACITRACIN

102. Raaijmakers JM, De Bruijn I, Nybroe O, Ongena M. Natural functions of lipopeptides from *Bacillus* and *Pseudomonas*: more than surfactants and antibiotics. *FEMS Microbiol Rev*. 2010;34(6):1037–62.

103. Bender CL, Alarcón-Chaidez F, Gross DC. *Pseudomonas syringae* Phytotoxins: Mode of Action, Regulation, and Biosynthesis by Peptide and Polyketide Synthetases. *Microbiol Mol Biol Rev*. 1999;63(2):266–92.

104. Baltz RH. Daptomycin: mechanisms of action and resistance, and biosynthetic engineering. *Curr Opin Chem Biol*. 2009;13(2):144–51.

105. Asaduzzaman SM, Sonomoto K. Lantibiotics: Diverse activities and unique modes of action. *J Biosci Bioeng*. 2009;107(5):475–87.

106. Willey JM, van der Donk WA. Lantibiotics: peptides of diverse structure and function. *Annu Rev Microbiol*. 2007;61:477–501.

107. Maksimov MO, Pan SJ, James Link A. Lasso peptides: structure, function, biosynthesis, and engineering. *Nat Prod Rep*. 2012;29(9):996–1006.

108. Rebuffat S, Blond A, Destoumieux-Garzon D, Goulard C, Peduzzi J. Microcin J25, from the macrocyclic to the lasso structure: implications for biosynthetic, evolutionary and biotechnological perspectives. *Curr Protein Pept Sci*.. 2004;5(5):383–91.

109. Gould A, Ji Y, Aboye TL, Camarero JA. Cyclotides, a novel ultrastable polypeptide scaffold for drug discovery. *Curr Pharm Des*. 2011;17(38):4294–307.

110. Smith AB, Daly NL, Craik DJ. Cyclotides: a patent review. *Expert Opin Ther Pat*. 2011;21(11):1657–72.

111. Ling LL, Schneider T, Peoples AJ, Spoering AL, Engels I, Conlon BP, *et al*. A new antibiotic kills pathogens without detectable resistance. *Nature*. 2015; 22;517(7535):455–9.

112. Stanley RE, Blaha G, Grodzicki RL, Strickler MD, Steitz TA. The structures of the anti-tuberculosis antibiotics viomycin and capreomycin bound to the 70S ribosome. *Nat Struct Mol Biol*. 2010;17(3):289–93.

113. Maus CE, Plikaytis BB, Shinnick TM. Mutation of tlyA confers capreomycin resistance in *Mycobacterium tuberculosis. Antimicrob Agents Chemother.* 2005;49(2):571–7.

114. Li Y, Zyrah S, Rebuffat S. Lasso Peptides: Bacterial Strategies to Make and Mantain Bioactive Entangled Scaffolds. *Springer Briefs in Microbiology*. Springer; 2015.

115. Gavrish E, Sit CS, Cao S, Kandror O, Spoering A, Peoples A, *et al*. Lassomycin, a ribosomally synthesized cyclic peptide, kills *Mycobacterium tuberculosis* by targeting the ATP-dependent protease ClpC1P1P2. *Chem Biol*. 2014;21(4):509–18.

116. Lear S, Munshi T, Hudson AS, Hatton C, Clardy J, Mosely JA, *et al*. Total chemical synthesis of lassomycin and lassomycin-amide. *Org Biomol Chem*.

2016;14(19):4534–41.

117. Zhao N, Pan Y, Cheng Z, Liu H. Lasso peptide, a highly stable structure and designable multifunctional backbone. *Amino Acids*. 2016;48(6):1347–56.

118. Iwatsuki M, Tomoda H, Uchida R, Gouda H, Hirono S, Omura S. Lariatins, antimycobacterial peptides produced by *Rhodococcus* sp. K01-B0171, have a lasso structure. *J Am Chem Soc*. 2006;128(23):7486–91.

119. Iwatsuki M, Koizumi Y, Gouda H, Hirono S, Tomoda H, Omura S. Lys17 in the “lasso” peptide lariatin A is responsible for anti-mycobacterial activity. *Bioorg Med Chem Lett*. 2009;19(10):2888–90.

120. Iwatsuki M, Uchida R, Takakusagi Y, Matsumoto A, Jiang CL, Takahashi Y, *et al*. Lariatins, novel anti-mycobacterial peptides with a lasso structure, produced by *Rhodococcus jostii* K01-B0171. *J Antibiot*. 2007;60(6):357–63.

121. Jones JA. Amino acid and peptide synthesis. 2nd ed. Oxford: Oxford University Press; 2002.

122. Anderson GW, McGregor AC. *t*-Butyloxycarbonylamino Acids and Their Use in Peptide Synthesis. *J Am Chem Soc*. 1957;79(23):6180–3.

123. Kimmerlin T, Seebach D. “100 years of peptide synthesis”: ligation methods for peptide and protein synthesis with applications to beta-peptide assemblies. *J Pept Res.* 2005. 229–60.

124. Sigler GF, Fuller WD, Chaturvedi NC, Goodman M, Verlander M. Formation of oligopeptides during the synthesis of 9-fluorenylmethyloxycarbonyl amino acid derivatives. *Biopolymers.* 1983;22(10):2157–62.

125. Hughes AB. Amino Acids, Peptides and Proteins in Organic Chemistry, Protection Reactions, Medicinal Chemistry, Combinatorial Synthesis. Vol. 4. WILEY-VCH Verlag GmbH & Co. KGaA, Weinheim; 2011.

126. Chan WC, White PD. Fmoc solid phase peptide synthesis : a practical approach. Oxford: Oxford University Press; 2000.

127. Sheehan JC, Hess GP. A New Method of Forming Peptide Bonds. *J Am Chem Soc*. 1955;77(4):1067–8.

128. Gross E, Meienhofer J. Peptides: Analysis, Synthesis, Biology. Rich DH,

Singh J, editors. Vol. 1, The carbodiimide method. Academic press, New York; 1979. 241-261.

129. Dourtoglou V, Ziegler J-C, Gross B. L'hexafluorophosphate de O-benzotriazolyl-N,N-tetramethyluronium: Un reactif de couplage peptidique nouveau et efficace. *Tetrahedron Lett*. 1978;19(15):1269–72.

130. Abdelmoty I, Albericio F, Carpino LA, Foxman BM, Kates SA. Structural studies of reagents for peptide bond formation: Crystal and molecular structures of HBTU and HATU. *Lett Pept Sci*. 1994;1(2):57–67.

131. Mitchell AR. Bruce Merrifield and solid-phase peptide synthesis: a historical assessment. *Biopolymers*. 2008;90(3):175–84.

132. Kaiser E, Colescott RL, Bossinger CD, Cook PI. Color test for detection of free terminal amino groups in the solid-phase synthesis of peptides. *Anal Biochem*. 1970;34(2):595–8.

133. Howl J. Peptide synthesis and applications. Totowa, N.J.: Humana Press; 2005.

134. Pedroso E, Grandas A, de las Heras X, Eritja R, Giralt E. Diketopiperazine formation in solid phase peptide synthesis using p-alkoxybenzyl ester resins and Fmoc-amino acids. *Tetrahedron Lett*. 1986;27(6):743–6.

135. Bodanszky M. Side Reactions in Peptide Synthesis. In: Principles of Peptide Synthesis. Springer Berlin Heidelberg. 1993. 169–214.

136. Chiva C, Vilaseca M, Giralt E, Albericio F. An HPLC-ESMS study on the solid-phase assembly of C-terminal proline peptides. *J Pept Sci*. 1999;5(3):131–40.

137. Fields CG, Lloyd Dh, Macdonald RL, Otteson KM, Noble RL. HBTU activation for automated Fmoc solid-phase peptide synthesis. *Pept Res*. 1991;4(2):95–101.

138. Arunan C, Rajasekharan Pillai VN. Synthesis of Acyl Carrier Protein Fragment 65–74 on a Flexible Cross-linked Polystyrene Support: Comparison with Merrifield Resin. *Tetrahedron*. 2000;56(19):3005–11.

139. Hancock WS, Prescott DJ, Vagelos PR, Marshall GR. Solvation of the polymer matrix. Source of truncated and failure sequences in solid phase

synthesis. *J Org Chem.* 1973;38(4):774–81.

140. Gupta A, Bhakta S, Chemother JA. An integrated surrogate model for screening of drugs against *Mycobacterium tuberculosis*. *J Antimicrob Chemother*. 2012;67 (6):1380–91.

141. Hervé M, Kovač A, Cardoso C, Patin D, Brus B, Barreteau H, *et al*. Synthetic tripeptides as alternate substrates of murein peptide ligase (Mpl). *Biochimie.* 2013;95(6):1120–6.

142. Gao Y, Lane-Bell P, Vederas JC. Stereoselective synthesis of *meso*-2,6-diaminopimelic acid and its selectively protected derivatives. *J Org Chem.* 1998;(63):2133–43.

143. Hasegawa M, Kawasaki A, Yang K, Fujimoto Y, Masumoto J, Breukink E, Nunez G, *et al*. A role of lipophilic peptidoglycan-related molecules in induction of Nod1-mediated immune responses. *J Biol Chem*. 2007;282:11757–64.

144. Fujimoto Y, Inamura S, Kawasaki A, Shiokawa Z, Shimoyama A, Hashimoto T, *et al*. Chemical synthesis of peptidoglycan fragments for elucidation of the immunostimulating mechanism. *J Endotoxin Res*. 2007;13(3):189–96.

145. Kawasaki A, Karasudani Y, Otsuka Y, Hasegawa M, Inohara N, Fujimoto Y, *et al*. Synthesis of diaminopimelic acid containing peptidoglycan fragments and tracheal cytotoxin (TCT) and investigation of their biological functions. *Chem a Eur J*. 2008;14(33):10318–30.

146. Saito Y, Yoshimura Y, Wakamatsu H, Takahata H. A Facile Synthesis of Fully Protected meso-Diaminopimelic Acid (DAP) and Its Application to the Preparation of Lipophilic N-Acyl iE-DAP. *Molecules*. 2013;18(1):1162–73.

147. Roychowdhury A, Wolfert MA, Boons GJ. Synthesis and proinflammatory properties of muramyl tripeptides containing lysine and diaminopimelic acid moieties. *Chembiochem*. 2005;6(11):2088–97.

148. Pellicciari R, Natalini B, Marinozzi M. L-Vinylglycine from L-Homoserine. *Synth Commun*. 1988;(18(14)):1715–21.

149. Salituro GM, Townsend CA. Total syntheses of (−)-nocardicins A−G: a biogenetic approach. *J Am Chem Soc*. 1990;112(2):760–70.

150. Bommarius AS, Drauz K, Klenk H, Wandrey C. Operational stability of enzymes. Acylase-catalyzed resolution of *N*-acetyl amino acids to enantiomerically pure L-amino acids. *Ann N Y Acad Sci*. 1992;672:126–36.

151. Young DD, Torres-Kolbus J, Deiters A. Microwave-assisted synthesis of unnatural amino acids. *Bioorg Med Chem Lett*. 2008;18(20):5478–80.

152. Lin YA, Chalker JM, Floyd N, Bernardes GJL, Davis BG. Allyl Sulfides Are Privileged Substrates in Aqueous Cross-Metathesis: Application to Site-Selective Protein Modification. *J Am Chem Soc*. 2008;130(30):9642–3.

153. Bhushan R, Brückner H. Marfey's reagent for chiral amino acid analysis: A review. *Amino Acids*. 2004;27(3):231–47.

154. Cook GR, Kargbo RB. Stereoselective Indium-Mediated Allylation Reactions. *Current Organic Chemistry*. 2007; Vol.11:1287–309.

155. Wuts P, Greene T. Greene's protective groups in organic synthesis. 5th ed. New York: Wiley; 2014: p. 108-110.

156. Neises B, Steglich W. Simple Method for the Esterification of Carboxylic Acids. *Angew Chemie Int Ed English*. 1978;17(7):522–4.

157. Konda Y, Takahashi Y, Arima S, Sato N, Takeda K, Dobashi K, *et al*. First total synthesis of Mer-N5075A and a diastereomeric mixture of α and β-MAPI, new HIV-I protease inhibitors from a species of *Streptomyces*. *Tetrahedron.* 2001;57(20):4311–21.

158. Rees DO, Bushby N, Cox RJ, Harding JR, Simpson TJ, Willis CL. Synthesis of [1,2-$^{13}C_2$, ^{15}N]-L-homoserine and its incorporation by the PKS-NRPS system of *Fusarium moniliforme* into the mycotoxin fusarin C. *Chembiochem.* 2007;8(1):46–50.

159. Hanessian S, Sahoo SP. A novel and efficient synthesis of L-vinylglycine. *Tetrahedron Lett*. 1984;25(14):1425–8.

160. Afzali-Ardakani A, Rapoport H. L-Vinylglycine. *J Org Chem.* 1980;45(24):4817–20.

161. Dalton DR. Foundations of organic chemistry : unity and diversity of structures, pathways, and reactions. Oxford: Wiley-Blackwell; 2011: p. 675.

162. Lehman Jr SE, Schwendeman JE, O'Donnell PM, Wagener KB. Olefin isomerization promoted by olefin metathesis catalysts. *Inorganica Chim Acta*. 2003;345:190–8.

163. Lamborelle N, Simon JF, Luxen A, Monbaliu J-CM. Continuous-flow thermolysis for the preparation of vinylglycine derivatives. *Org Biomol Chem.* 2015;13(48):11602–6.

164. Stille JK, Groh BL. Stereospecific cross-coupling of vinyl halides with vinyl tin reagents catalyzed by palladium. *J Am Chem Soc.* 1987;109(3):813–7.

165. Smith AB 3rd, Adams CM, Kozmin SA, Paone D V. Total synthesis of (-)-cylindrocyclophanes A and F exploiting the reversible nature of the olefin cross metathesis reaction. *J Am Chem Soc*. 2001;123(25):5925–37.

166. Kastrinsky D, Kumar P, Marriner G, Barry CE. A Convergent Synthesis of Chiral Diaminopimelic Acid Derived Substrates for Mycobacterial L,D-Transpeptidases. *Synthesis*. 2012;44:3043–8.

167. Isidro-Llobet A, Alvarez M, Albericio F. Amino acid-protecting groups. *Chem Rev*. 2009;109(6):2455–504.

168. Maegawa T, Fujiwara Y, Ikawa T, Hisashi H, Monguchi Y, Sajiki H. Novel deprotection method of Fmoc group under neutral hydrogenation conditions. *Amino Acids*. 2009;36(3):493–9.

169. Atherton E, Bury C, Sheppard RC, Williams BJ. Stability of fluorenylemthoxycarbonylamino groups in peptide synthesis. Cleavage by hydrogenolysis and by dipolar aprotic solvents. *Tetrahedron Lett*. 1979;20(32):3041–2.

170. Carpino LA, Han GY. 9-Fluorenylmethoxycarbonyl function, a new base-sensitive amino-protecting group. *J Am Chem Soc*. 1970;92(19):5748–9.

171. Kelly RC, Gebhard I, Wicnienski N. Synthesis of (R)- and (S)-(glu)thz and the corresponding bisthiazole dipeptide of dolastatin 3. *J Org Chem*. 1986;51(24):4590–4.

172. Smith MB. March's Advanced Organic Chemistry: Reactions, Mechanisms, and Structure. Wiley-Blackwell; 2013.

173. Smith MB, March J. March's Advanced Organic Chemistry: Reactions,

Mechanisms, and Structure. Wiley-Interscience; 2001: p. 1545.

174. Nukala S. Overexpression and purification of murein peptide ligase (Mpl) from *M. tuberculosis*. Birkbeck College, London; 2012.

175. Krueger JK, Kulke MH, Schutt CE, Stock J. Protein inclusion body formation and purification. *Biopharm Manuf*. 1989;2(3):40–5.

176. Conroy T, Jolliffe KA, Payne RJ. Efficient use of the Dmab protecting group: applications for the solid-phase synthesis of N-linked glycopeptides. *Org Biomol Chem*. 2009;7(11):2255–8.

177. Johnson T, Liley M, Cheeseright TJ, Begum F. Problems in the synthesis of cyclic peptides through use of the Dmab protecting group. *J Chem Soc Perkin Trans 1*. 2000;(16):2811–20.

178. Coleman DR th, Ren Z, Mandal PK, Cameron AG, Dyer GA, Muranjan S, et al. Investigation of the binding determinants of phosphopeptides targeted to the SRC homology 2 domain of the signal transducer and activator of transcription 3. Development of a high-affinity peptide inhibitor. *J Med Chem*. 2005;48(21):6661–70.

179. Geiger T, Clarke S. Deamidation, isomerization, and racemization at asparaginyl and aspartyl residues in peptides. Succinimide-linked reactions that contribute to protein degradation. *J Biol Chem*. 1987;262(2):785–94.

180. Ma M, Kutz-Naber KK, Li L. Methyl esterification assisted MALDI FTMS characterization of the orcokinin neuropeptide family. *Anal Chem*. 2007;79(2):673–81.

181. Gimenez D, Andreu C, del Olmo M, Varea T, Diaz D, Asensio G. The introduction of fluorine atoms or trifluoromethyl groups in short cationic peptides enhances their antimicrobial activity. *Bioorg Med Chem*. 2006;14(20):6971–8.

182. Corbett JF. Pseudo first-order kinetics. *J Chem Educ*. 1972;49(10):663.

183. Lauer JL, Fields CG, Fields GB. Sequence dependence of aspartimide formation during 9-fluorenylmethoxycarbonyl solid-phase peptide synthesis. *Lett Pept Sci*. 1995;1(4):197–205.

184. Flora D, Mo H, Mayer JP, Khan MA, Yan LZ. Detection and control of

aspartimide formation in the synthesis of cyclic peptides. *Bioorg Med Chem Lett*. 2005;15(4):1065–8.

185. Subirós-Funosas R, El-Faham A, Albericio F. Aspartimide formation in peptide chemistry: occurrence, prevention strategies and the role of N-hydroxylamines. *Tetrahedron*. 2011;67(45):8595–606.

186. Stathopoulos P, Papas S, Kostidis S, Tsikaris V. Alpha- and beta- aspartyl peptide ester formation via aspartimide ring opening. *J Pept Sci*. 2005;11(10):658–64.

187. Biotage. Automated Synthesis of Cyclic Peptides on Biotage Initiator+Alstra. 2014. [Accessed on 2016 Sept 21].
Available from: http://www.biotage.com/product-page/biotage-initiator-alstra

188. Usha V, Dover LG, Roper DL, Lloyd AJ, Besra GS. Use of a codon alteration strategy in a novel approach to cloning the Mycobacterium tuberculosis diaminopimelic acid epimerase. *FEMS Microbiol Lett*. 2006;262(1):39–47.

189. Wade JD, Mathieu MN, Macris M, Tregear GW. Base-induced side reactions in Fmoc-solid phase peptide synthesis: Minimization by use of piperazine as Nα-deprotection reagent. *Lett Pept Sci*. 2000;7(2):107–12.

190. Coin I, Beyermann M, Bienert M. Solid-phase peptide synthesis: from standard procedures to the synthesis of difficult sequences. Nat Protoc. 2007;2(12):3247-56.

191. Evangelopoulos D, Bhakta S. Rapid methods for testing inhibitors of mycobacterial growth. *Methods Mol Biol*. 2010;642:193–201.

192. Krishnamurthy S, Arai T, Nakanishi K, Nishino N. Epoxy amino acids produced from allylglycines intramolecularly cyclised to yield four stereoisomers of 4-hydroxyproline derivatives. *RSC Adv*. 2014;4(5):2482–90.

193. C. G. Biagini S, E. GibsoneThomas S, P. Keen S. Cross-metathesis of unsaturated [small alpha]-amino acid derivatives. *J Chem Soc Perkin Trans 1*. 1998;(16):2485–500.